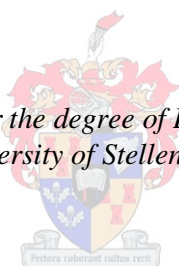


# **Comprehensive multidimensional gas chromatography for the analysis of Fischer–Tropsch products**

by  
Katriena Elizabet van der Westhuizen

*Dissertation presented for the degree of Doctor of Philosophy at the  
University of Stellenbosch*



Promoter: Prof. Pat Sandra  
Co-promoter: Dr. André de Villiers  
Faculty of Science  
Department of Chemistry and Polymer Science

December 2011

## Declaration

I, the undersigned, hereby declare that the work contained in this dissertation is my own original work and that I have not previously in its entirety or in part submitted it at any university for a degree

Signature: \_\_\_\_\_

Date: \_\_\_\_\_

Copyright© 2011 Stellenbosch University  
All rights reserved

## ABSTRACT

The analysis of Fischer–Tropsch–derived (FT–derived) synthetic crude and derived products is very challenging because of the highly complex nature of these products. In this study, the use of comprehensive multidimensional gas chromatography (GCxGC) with time-of-flight mass spectrometry (TOF-MS) and flame ionisation detection (FID) was investigated for the analysis of these products and the technique was found to be invaluable for the analysis of these complex mixtures.

The compositions of FT synthetic crude, produced at low temperature (LT–FT) and high temperature (HT–FT) processes were compared and the effect that changes in FT reaction temperature has on product formation was investigated. Results for conventional one-dimensional GC (1D-GC) and GCxGC were compared. It was found that conventional 1D–GC does not have sufficient peak capacity to separate the thousands of compounds in the HT–FT products. GCxGC provides a huge peak capacity of tens-of-thousands to separate highly complex mixtures. Structured chromatograms, where groups of compounds with similar properties are grouped together, aid in peak identification. Moreover, sensitivity at low microgram per milliliter levels is obtained. These attributes enabled accurate analysis of various complex feed and product streams in the FT refinery, and also various final fuel products.

The use of GCxGC alone was demonstrated, and also combined with high performance liquid chromatography (HPLC), supercritical fluid chromatography (SFC) and nuclear magnetic resonance (NMR) when even more separation power was needed. HPLC–GCxGC enabled the separation of alkene and cyclic alkane compound classes in oligomerisation products. These compound classes have similar mass spectra, elute in adjacent regions and co-elute even to some extent on the GCxGC contour plot, making differentiation difficult. SFC is a good replacement for HPLC for these applications because it does not use solvents as mobile phases. CO<sub>2</sub> is easily evaporated after the separation and does not interfere with the GCxGC separation of the analytes. SFC is also a very good technique to separate the compound classes of alkanes, alkenes, aromatics and oxygenates, and is therefore highly complementary to GCxGC.

The combination of GCxGC with NMR data was also found to be very valuable for the identification of branched alkane isomers in LT–FT diesels. GCxGC provides excellent separation of individual compounds but the identification of isomers (except for mono–methyl branching) is difficult because the mass spectra of most of these isomers are similar and not all compounds are in the mass spectral libraries. NMR, on the other hand, is able to distinguish between the individual types of branched isomers but has limited separation power for the complex mixtures. By combining the two techniques, the best of both was obtained.

The study found GCxGC to be invaluable for the analysis of the highly complex FT–derived products, while its combination with other techniques such as HPLC, SFC and NMR provided even more separation power.

## Opsomming

Die hoogs komplekse samestelling van sintetiese ru-olie en afgeleide produkte, afkomstig van Fischer-Tropsch (FT) sintese, bied groot uitdagings aan die analis. Die studie het die gebruik van GCxGC met 'n TOF-MS en FID bestudeer vir die analise van FT produkte en het bevind dat die tegniek van onskatbare waarde is vir die analise van die hoogs komplekse mengsels.

Die samestellings van produkte van lae- en hoë-temperatuur FT prosesse is vergelyk en die effek van 'n verhoging in die reaksie-temperatuur op die produk samestelling is ondersoek. Resultate vir 1D-GC and GCxGC is vergelyk en dit was duidelik dat 1D-GC nie naastenby voldoende piekkapasiteit het om al die komponente van die produkte wat tydens die hoë-temperatuur proses gevorm word, te kan skei nie. Die GCxGC se piekkapasiteit daarteenoor is in die orde van tienduisende wat die skeiding van hoogs komplekse mengsels moontlik maak terwyl die tegniek hoogs gestruktureerde kontoerplotte verskaf wat help met identifikasie van komponente. Die tegniek is verder ook baie sensitief en kan komponente op lae  $\mu\text{g/mL}$  vlakke waarneem. Hierdie eienskappe het akkurate analise van verskeie FT produkstrome moontlik gemaak.

Die kombinasie van GCxGC met HPLC, SFC en KMR het selfs meer skeidingskrag verskaf waar nodig. HPLC-GCxGC het die skeiding van alkene en sikliese alkane moontlik gemaak. Hierdie komponent klasse se massaspektra is feitlik dieselfde en terselfdertyd elueer die twee groepe reg langs mekaar, en oorvleuel soms selfs tot 'n mate, op die GCxGC kontoerplot, sodat dit moeilik is om daartussen te onderskei. SFC is 'n goeie alternatief vir HPLC in meeste toepassings aangesien die tegniek net  $\text{CO}_2$  gebruik, wat maklik verdamp by kamertemperatuur en nie oplosmiddels gebruik wat se pieke steur met die van die lae-kookpunt komponente op die GCxGC kontoerplot nie. Skeidings van die komponentgroepe alkane, alkene, aromate en oksigenate is moontlik met SFC en daarom komplimenteer dit die GCxGC skeiding goed aan.

Die kombinasie van GCxGC met kern-magnetiese resonansie (KMR) is van waarde gevind om die verskillende tipes vertakkings in 'n lae-temperatuur FT diesel te identifiseer.

GCxGC verskaf uitstekende skeiding van individuele komponente maar die identifikasie van die verskillende isomere, behalwe vir die mono-metiel vertakkings, is moeilik aangesien die massaspektra van baie van die komponente soortgelyk is en die komponente nie in die massa spektrum-biblioteke voorkom nie. KMR, aan die ander kant, kan tussen die individuele vertakkings onderskei maar het beperkte skeidingskrag vir komplekse mensels. Deur die twee tegnieke te kombineer is die beste van albei tegnieke bekom.

Die studie het bevind dat GCxGC van onskatbare waarde is vir die analise van die komplekse sintetiese FT produkte terwyl die kombinasie met ander tegnieke soos HPLC, SFC and KMR selfs meer skeidingskrag verskaf.

## Acknowledgements

I would such as to express my sincere gratitude to the following people and organisations for their contributions throughout this study:

My study supervisors, Prof. Pat Sandra and Dr. André de Villiers, for their expert guidance, patience and sheer hard work in assisting me with the preparation of this manuscript and publications;

Sasol Technology R&D, for providing me with many challenging opportunities and for supporting my studies financially; my line manager, Dr. Riaan Bekker; and our department manager, Dr. Bongani Nkosi, for their expert guidance and support; and my colleagues, Hein Potgieter, Piet de Coning, Mariam Ajam, Sibusiso Mtongana, Nico Prinsloo and Renier Crous, for their technical contributions and support;

My husband, Eben, for his unconditional love and support, without which this study would not have been possible; my three children, two granddaughters and soon-to-be-born grandson, Ziegfried, Adèle, Alicia, Carla, Skyla and Xander, who are my inspiration and my pride and joy; my mother, Marie Hardy, who loves me unconditionally and who is always there when I need her. Thanks also to my two sons-in-law and daughter-in-law, Bernard, Rudi and Seugnet, who take such excellent care of the people I love most in the world;

Above all, to our dear Lord, Jesus Christ: I trust in You with all my heart and You lead me and clear the road for me to follow. How great You are!

# Table of Contents

<b>List of publications</b>	<b>i</b>
<b>Abbreviations</b>	<b>iii</b>
<b>1. Introduction and Objectives</b>	<b>1</b>
<b>2. Fundamental Aspects of GCxGC</b>	<b>7</b>
<b>2.1 Basic principles</b>	<b>8</b>
<b>2.2 Modulators</b>	<b>9</b>
<b>2.3 Column considerations</b>	<b>11</b>
<b>2.4 Temperature and pressure considerations</b>	<b>13</b>
<b>2.5 Detectors commonly used in petrochemical applications</b>	<b>18</b>
2.5.1 Universal detectors	19
2.5.1.1 Flame ionisation detector	19
2.5.1.2 Time-of-flight mass spectrometer	19
2.5.1.3 Quadrupole mass spectrometer	20
2.5.2 Selective detectors	21
2.5.2.1 Sulphur chemiluminescence detector	21
2.5.2.2 Nitrogen chemiluminescence detector	22
2.5.2.3 Atomic emission detector	22
2.5.3 Other detectors used in combination with GCxGC	22

<b>2.6</b>	<b>Complementary techniques and hyphenation with GCxGC</b>	<b>23</b>
2.6.1	High performance liquid chromatography	24
2.6.2	Supercritical fluid chromatography	25
2.6.3	Nuclear magnetic resonance	26
<b>2.7</b>	<b>References</b>	<b>27</b>
<b>3.</b>	<b>GCxGC for Fischer–Tropsch Product Analysis</b>	<b>31</b>
<b>3.1</b>	<b>Introduction to Fischer–Tropsch technology (Literature study)</b>	<b>32</b>
<b>3.2</b>	<b>Comprehensive two–dimensional gas chromatograph for the analysis of Fischer–Tropsch oil products</b>	<b>38</b>
3.2.1	Introduction	38
3.2.2	Experimental	41
3.2.2.1	Samples and reactor experiments	41
3.2.2.2	Analytical conditions	41
3.2.3	Results and discussion	42
3.2.3.1	1D–GC and GCxGC analysis of Fischer–Tropsch oils	42
3.2.3.2	Comparison of quantitative results of 1D–GC and GCxGC for HT–FT oil	45
3.2.3.3	Application of GCxGC to follow primary and secondary product formation in HT–FT products	48
3.2.4	Conclusions	52
<b>3.3</b>	<b>References</b>	<b>54</b>

<b>4. GCxGC in Fischer–Tropsch Refining</b>	<b>56</b>
<b>4.1 Introduction</b>	<b>57</b>
<b>4.2 Experimental</b>	<b>60</b>
<b>4.3 Results and discussion</b>	<b>61</b>
4.3.1 Analysis of Superflex™ catalytic cracking	62
4.3.2 Dehydration	64
4.3.3 Oligomerisation of 1–hexene using solid phosphoric acid (SPA) catalyst	66
4.3.4 GCxGC inlet hydrogenation	69
4.3.5 PAH compounds in HT–FT diesel	72
<b>4.4 Conclusion</b>	<b>76</b>
<b>4.5 References</b>	<b>77</b>
<b>5. Applications of GCxGC for Fuel Analysis</b>	<b>78</b>
<b>5.1 GCxGC to investigate the relation between composition and     physical properties of Fischer–Tropsch–derived fuels and blends</b>	<b>79</b>
5.1.1 Introduction	79
5.1.2 Experimental	80
5.1.2.1 Comprehensive multidimensional GC analysis	80
5.1.2.2 <sup>13</sup> C NMR experiment acquisition	80
5.1.3 Results and discussion	81
5.1.3.1 Distillation range	83
5.1.3.2 Cold flow properties	85
5.1.3.3 Combining GCxGC and NMR data to evaluate branching in fuels	89

5.1.3.4 Density	92
5.1.3.5 Octane and cetane numbers	96
5.1.4 Conclusions	99
5.1.5 References	101
<b>5.2 Fractionation by HPLC combined with GCxGC–TOF–MS for analysis of cyclics in oligomerisation products of Fischer–Tropsch-derived light alkenes</b>	<b>102</b>
5.2.1 Introduction	102
5.2.2 Experimental	105
5.2.2.1 Oligomerisation reactions	105
5.2.2.2 Bromination	106
5.2.2.3 LC fractionation	106
5.2.2.4 GCxGC–TOF–MS and FID analysis	108
5.2.3 Results and discussion	108
5.2.3.1 Optimisation of the LC fractionation procedure	108
5.2.3.2 LC fractionation combined with GCxGC–TOF–MS analysis of the final oligomerisation product	109
5.2.3.3 Determination of the cyclic/alkene distribution in oligomerisation products	115
5.2.3.4 Comparison of the alkene composition in oligomerisation products versus in conventional FT products	117
5.2.4 Conclusions	119
5.2.5 References	120
<b>5.3 The use of GCxGC with time–of–flight mass spectrometry to investigate dienes and Diels–Alder polymerisation products in high temperature Fischer–Tropsch based fuel</b>	<b>122</b>
5.3.1 Introduction	122
5.3.2 Experimental	124
5.3.2.1 Samples	124
5.3.2.2 Instrumentation	124
5.3.3 Results and discussion	125

5.3.4 Conclusion	132
5.3.5 References	133
<b>5.4 Application of GCxGC using a polar × non–polar column combination for the analysis of synthetic jet fuel</b>	<b>134</b>
5.4.1 Introduction	134
5.4.2 Experimental	136
5.4.2.1 Samples	136
5.4.2.2 Chromatographic conditions	137
5.4.2.3 Analytical procedure	138
5.4.2.4 Stability tests	139
5.4.3 Results and discussion	140
5.4.3.1 GCxGC optimisation	140
5.4.3.2 Chemical composition of fully synthetic and crude–derived jet fuels.	145
5.4.3.2 Fuel stability	150
5.4.4 Conclusions	151
5.4.5 References	154
<b>6. Current Projects and Future Challenges</b>	<b>157</b>
<b>6.1 On–line GCxGC for the analysis of HT–FT products</b>	<b>158</b>
6.1.1 Introduction	158
6.1.2 Experimental	160
6.1.2.1 Sampling system	160
6.1.2.2 Analytical system and conditions	160
6.1.2.3 Identification and quantification	162
6.1.3 Results and discussion	163
6.1.4 Summary	168

<b>6.2 On-line SFC–GCxGC for the analysis of FT products</b>	<b>168</b>
6.2.1 Introduction	168
6.2.2 Experimental	169
6.2.3 Initial results and future work	170
6.2.4 Summary	173
<b>6.3 GCxGC–SCD, GCxGC–NCD</b>	<b>174</b>
6.3.1 Introduction	174
<b>6.4 Further challenges</b>	<b>175</b>
<b>6.5 References</b>	<b>176</b>
<b>7. Conclusions</b>	<b>178</b>

## **Note**

This dissertation has been written on the style required for the Journal of Chromatography A. It is presented as a compilation of manuscripts already published and submitted for publication. Each manuscript is a chapter of an individual entity and some repetition between chapters has therefore been unavoidable.

## List of publications

- [1] R. Van der Westhuizen, R. Crous, A. De Villiers, P. Sandra,  
Title: Comprehensive two-dimensional gas chromatography for the analysis of Fischer-Tropsch oil products  
J. Chromatogr. A 1217 (2010) 8334.
- [2] R. van der Westhuizen, H. Potgieter, N. Prinsloo, A. de Villiers, P. Sandra,  
Title: Fractionation by liquid chromatography combined with comprehensive two-dimensional gas chromatography-mass spectrometry for analysis of cyclics in oligomerisation products of Fischer-Tropsch derived light alkenes  
J. Chromatogr. A 1218 (2011) 3173.
- [3] R. Van der Westhuizen, A. Crouch, P. Sandra,  
Titel: The use of GCxGC with time-of-flight mass spectrometry to investigate dienes and Diels-Alder polymerisation products in high temperature Fischer-Tropsch based fuels  
J. Sep. Sci. 31 (2008) 3423.
- [4] R. Van der Westhuizen, M. Ajam, P. De Coning, J. Beens, A. de Villiers, P. Sandra,  
Title: Comprehensive two-dimensional gas chromatography for the analysis of synthetic and crude-derived jet fuels  
J. Chromatogr. A 1218 (2011) 4478.

## Papers in preparation

- [1] Chapter 4.3.4  
Comprehensive two-dimensional gas chromatography with on-line hydrogenation in the analysis of Fischer-Tropsch-derived fuels.
- [2] Chapter 5.1  
Comprehensive two-dimensional gas chromatography to investigate the relation between composition and physical properties of Fischer-Tropsch-derived fuels and blends.

[3] Chapter 6.1

On-line comprehensive two-dimensional gas chromatography for the analysis of high temperature Fischer–Tropsch products.

## Abbreviations

1D–GC	Conventional one–dimensional gas chromatography
AED	Atomic emission detector
ASF	Anderson–Schulz–Flory
CAD	Corona charged aerosol detector
CatPoly	Catalytic polymerisation
CDU	Crude oil distillation
CDF	crude-derived fuel
CFPP	Cold filter plugging point
CGC	Capillary gas chromatography
CTL	Coal– to– liquids
CN	Cetane number
DEPT	Distortionless enhancement by polarization transfer
ECD	Electron capture detector
EIC	Extracted ion chromatogram
FAME	Fatty acid methyl ester
FCC	Fluid catalytic cracking
FIA	Fluorescent indicator absorption
FID	Flame ionisation detection
FPD	Flame photometric detector
FSJF	Fully synthetic jet fuel
FT	Fischer–Tropsch
GB	Gigabyte
GC	Gas chromatography

GC–MS	Gas chromatography–mass spectrometry
GCxGC	Comprehensive two–dimensional GC
GTL	Gas- to-liquids
HAD	Hydroisomerisation
HDN	Hydrodenitrogenation
HDO	Hydrodeoxygenation
HDS	Hydrodesulphurisation
HPLC	High performance liquid chromatography
HT–FT	High temperature Fischer–Tropsch
i.d.	Internal diameter
$K_{sp}$	solubility product constant
LMCS	Longitudinally modulating cryogenic system
LT–FT	Low temperature Fischer–Tropsch
MB	Megabyte
MDGC	Multidimensional gas chromatography
MEK	Methyl-ethyl-ketone
MS	Mass spectrometry
MTBE	Methyl tertiary butyl ether
m/z	mass to charge ratio
n: i ratio	Normal alkane to branched alkane ratio
NCD	Nitrogen chemiluminescence
NMR	Nuclear magnetic resonance spectroscopy
NPD	Nitrogen–phosphorus detector
PAH/s	Polycyclic aromatic hydrocarbon/s
PFPD	Pulsed flame photometric detector

PVA	Poly(vinyl alcohol)
qMS	Quadrupole mass spectrometer
SCC	Superflex™ Catalytic Cracking
SCD	Sulphur chemiluminescence detector
SFC	Supercritical fluid chromatography
SIM	Selected ion monitoring mode
SLO	Stabilised light oil
SPA	Solid phosphoric acid
SPE	Solid phase extraction
SPK	Synthetic paraffinic kerosene
SSJF	Semi-synthetic jet fuel
TCD	Thermal conductivity detector
TDR	Tube deposit ratio
TIC	Total ion chromatogram
TOF-MS	Time-of-flight mass spectrometer
ULO	Unstabilised light oil

# **Chapter 1**

## **Introduction and Objectives**

## Chapter 1: Introduction and Objectives

Sasol is a world leader in the production of synthetic fuels and chemicals, converting coal and natural gas into liquid fuels, fuel components and chemicals through its proprietary Fischer–Tropsch (FT) technologies. Based in South Africa, the company has substantial and growing interests world–wide. While fuels are the main product, the group’s chemical portfolio also includes polymers, co–monomers, solvents, surfactants, waxes, phenols and specialty organic and inorganic chemicals.

From an analytical chemistry viewpoint this wide portfolio creates huge challenges. Synthetic crude products derived from Fischer–Tropsch (FT) technologies are highly complex and their analyses require a great amount of skill. Unlike conventional crude–derived products that contain mainly alkanes and aromatics, synthetic crude also contains significant amounts of alkenes and oxygenates. Sub–classes of the alkenes are the 1–alkenes, internal alkenes and dienes, all of which can contain linear, branched or cyclic compounds. Oxygenate classes include alcohols, ketones, aldehydes, acids and esters, and these can also be linear, branched or cyclic.

The development of comprehensive two–dimensional gas chromatography (GCxGC) for the analysis of volatile organic chemicals in highly complex matrices has been one of the greatest developments in analytical chemistry. While GCxGC has been used for a number of years already in some petrochemical laboratories abroad, such as Shell and BP, for a number of years already, it is a relatively new addition to the Sasol Technology Research and Development analytical laboratory. The technique has provided a much better understanding of FT products in a relatively short time and has become an invaluable tool in the laboratory.

This study was focused on the evaluation of GCxGC for FT applications. GCxGC was found to be an essential analytical tool for the analysis of highly complex synthetic crude, feed and products of various processes in refining and also the final fuels and chemicals. It would have been an enormous task to investigate all of the hundreds of Sasol processes, so a few applications were selected to highlight the value of this technique.

## Chapter 1: Introduction and Aim

---

The study mainly investigated products of the high temperature Fischer–Tropsch (HT–FT) process because of the higher complexity of these products, compared to low temperature Fischer–Tropsch (LT–FT) products. Conventional one–dimensional GC (1D–GC) has been used extensively in the past and is still used in almost all of the Sasol laboratories, while the use of GCxGC is currently mainly limited to the research and development laboratories. The composition of FT products was therefore investigated using both 1D–GC and GCxGC. Results demonstrated that 1D–GC does not provide sufficient separation power for the analysis of the complex synthetic crude products. Differences in results are attributed to the high degree of peak overlap caused by the limited peak capacity of the 1D–GC. The effect of increasing the FT reaction temperature on the formation of secondary products was investigated and valuable information that was not previously available was obtained about compounds present at trace levels, for example, the formation of aromatic precursors and subclasses and trends in oxygenate and cyclics formation at increasing FT reaction temperatures.

A number of applications showed that this technique is also of great value in the FT refinery. The feed and products after selective hydrogenation of dienes to mono–alkenes, of oxygenate dehydration to mono–alkenes and the oligomerisation of 1–hexene were a few applications that were investigated. It was further shown that valuable information could be obtained by performing hydrogenation in the GCxGC inlet liner prior to GCxGC analysis and that this information could help to distinguish between cyclic and non–cyclic alkenic compound classes. This approach was found to be especially valuable when only small amounts of sample were available. The increase in the polycyclic aromatic hydrocarbons (PAHs) content of a HT–FT fuel after addition of a tar fraction was investigated and it was found that the PAH content of the fuel did not change significantly but that the density of the fuel increased considerably.

About two thirds of Sasol’s products are fuels and hence the greatest part of this study was dedicated to fuel analysis, especially jet fuels and diesels, for which the present demand is the highest. The global industry is familiar with crude–derived fuels but still slightly skeptical about synthetic fuels.

## Chapter 1: Introduction and Aim

---

As part of this study, comparison of results obtained by GCxGC for synthetic fuels and their crude-derived counterparts showed that the synthetic fuels are environmentally more friendly and do not contain any polar compounds that may be harmful to a vehicle or to the environment. GCxGC further enabled us to draw correlations between a fuel's composition and its physical and chemical properties such as cetane number, cold flow properties, density, etc. Valuable information could also be obtained on the degree of branching in FT fuels by combining nuclear magnetic resonance spectroscopy (NMR) and GCxGC, such as the effect of the degree of branching on the cold flow properties of the fuel.

Even though the GCxGC provides exceptionally high peak capacities (in the region of tens of thousands), compound co-elution still occurs, for example for oligomerisation products. In these cases a high performance liquid chromatography (HPLC) or supercritical fluid chromatography (SFC) fractionation step prior to GCxGC analysis is of great assistance to help distinguish between compound classes. HPLC was combined with GCxGC to show that cyclic compounds are indeed formed during the oligomerisation reaction of 1-butene. It was possible to distinguish between alkene and cyclic alkane distributions in fuel products derived from the oligomerisation reaction. We further showed that the alkenic oligomerisation product contained mainly compounds with internal double bonds.

Gum formation in gasoline was investigated and it was shown that Diels-Alder adduct formation contributed towards gum formation in fuels. Several Diels-Alder dimers and trimers were identified by using GCxGC with time-of-flight mass spectrometer (TOF-MS). This information contributes to the understanding of the ageing process that gasoline is subjected to during storage and of its stability.

Sasol is the first company worldwide to obtain international approval for commercial use of its fully synthetic jet fuel (FSJF). Numerous studies were performed on the jet fuel to ensure that it is conforming to international specifications. GCxGC was most useful in these studies. A quantitative method was developed for the analysis of the jet fuel and comparisons were done with a commercial crude-derived jet fuel. It was found that the fuels had very similar hydrocarbon composition, although compounds were present in different ratios.

## Chapter 1: Introduction and Aim

---

This implied that synthetic jet fuels do not introduce any molecules into aircraft's fuel systems that might negatively affect the fuel's properties.

The presence of trace-levels of hetero-atomic species, linked to environmental pollution, was confirmed in the crude-derived fuel, and their absence in the FSJF demonstrated. Stability tests confirmed that the synthetic fuel has much higher stability, probably because of the absence of hetero-atomic species.

A number of projects employing GCxGC are still in progress at Sasol. An on-line GCxGC system was connected to laboratory-scale microreactors in one of the research laboratories to evaluate and develop optimal reaction conditions for the industrial HT-FT plant in Secunda and also for planning future FT plants. The purpose of the on-line system is to eliminate errors resulting from product sampling, while investigating optimal plant parameters. HT-FT products are distributed between the gas and oil phases, with some oxygenates also present in the reaction water. In the past, samples were taken off-line, the phases separated and analysed individually and finally results combined. The combined data indicated relatively large errors, mainly resulting from evaporation of light material during off-line sampling and cooling. With the on-line GCxGC, in contrast, a diluted gaseous sample is injected and more accurate results are obtained without loss of volatile material. Future plans include the development of a multipoint gas calibration system for accurate quantification and a possible improvement of the steam-heated sample lines to electrically heated sample lines to reach higher temperatures and eliminate the possibility of condensation of heavy components.

An exiting new project is the on-line coupling of SFC to GCxGC. SFC is valuable for the separation of compound classes such as oxygenates, alkanes, alkenes and aromatics. By combining SFC on-line with GCxGC, the separation of highly complex mixtures is further enhanced. Moreover, SFC has the advantage that, unlike HPLC, only CO<sub>2</sub> is used as mobile phase. Solvents used in HPLC are not environmentally friendly; they obscure low boiling compounds on the GCxGC contour plot and decrease the sensitivity of the analysis. On the other hand, CO<sub>2</sub> evaporates in the GC inlet liner without loss of the volatile analytes and there is no interference with analyte peaks on the GCxGC plot.

## Chapter 1: Introduction and Aim

---

Other future projects include the addition of sulphur and nitrogen chemiluminescence detectors in GCxGC. These detectors will enable the accurate quantification of sulphur and nitrogen containing species, or their lack thereof, in FT and crude-derived products.

This study found GCxGC to be an invaluable technique for the analysis of all FT products and streams because of its exceptionally high peak capacity, highly structured separations and high sensitivity. GCxGC can also be hyphenated, or combined with various other techniques such as HPLC, SFC and NMR, to further improve the separations, and coupled to a number of non-selective and selective detectors. GCxGC should replace conventional 1D-GC in all petrochemical laboratories where highly complex samples need to be analysed.

# **Chapter 2**

# **Fundamental Aspects of GCxGC**

## Chapter 2: Fundamental Aspects of GCxGC

### 2.1 Basic principles

Comprehensive two-dimensional GC (GCxGC) is one of the most powerful analytical techniques available today for the analysis of complex volatile mixtures. In 1984 Giddings proposed the idea of subjecting a sample to multiple types of separations to achieve improved separation power [1], but GCxGC was only successfully implemented by John Phillips in 1991 [2]. The technique involves the coupling of two independent columns by an interface or modulator. The modulator periodically collects small fractions of eluent from the first dimension column and pulses it to the second column where analysis is completed before the next pulse is received. Sampling is done in such a way that the separation obtained in the first dimension is preserved, and all compounds in the sample are subjected to both separation dimensions.

The main advantage of GCxGC is the large increase in peak capacity, which relates to an equivalent increase in separation power. For conventional GC, where the peak capacity is limited to the number of peaks that can (theoretically) be separated by a single GC column, the peak capacity is in the order of a few hundred. For GCxGC on the other hand, the peak capacity is the product of the peak capacities of two columns of different selectivities and is in the order of tens-of-thousands. The GCxGC separation space is a two-dimensional plane compared to the straight line separation space of conventional 1D-GC. This often leads to highly ordered GCxGC plots, where peaks belonging to homologous series are positioned along straight lines on the retention plane. A roof-tile effect is obtained where groups of compounds, consisting of structurally related compounds, are piled upon each other just such as roof-tiles. Compounds in a single roof-tile have the same carbon number but different structural arrangement. This allows unequivocal chemical compound and group-type classification and identification [3,4]. An increase in sensitivity compared to what can be achieved with conventional GC is an added bonus. A very fast separation is achieved in the second dimension column that minimises peak broadening and effectively increases the signal-to-noise ratio, and therefore the sensitivity, by a factor of up to ten times compared to conventional GC [5,6].

## Chapter 2: Fundamental Aspects of GCxGC

---

### 2.2 Modulators

The purpose of the modulator is to trap a small fraction of eluent from the first column, refocus it, and pulse it into the second–dimension column [7], where the narrow fraction is fully analysed before the next fraction arrives. Preservation of the first dimension separation is achieved through the choice of modulator sampling frequency or modulation period. Each first dimension peak should be sampled at least three times [8]. The modulation period is consistent with the second column separation time, which is typically around 2–8 s and therefore basically isothermal. It is possible that a compound has a retention time in the second dimension that is longer than the modulation period. This peak will then elute or “wrap–around” with peaks of the next modulation. Provided wrap–around does not interfere with the ordered nature of the chromatogram, it does not pose any problems.

Modulator designs have improved much recent years. The “sweeper” used a rotating slotted heater to rapidly move over a thick–film capillary, but this approach was time–consuming to optimise and had a restricted application range. A major improvement was the longitudinally modulating cryogenic system (LMCS) that used liquid CO<sub>2</sub> to trap and refocus analytes at the beginning of the secondary column. The trap was moved rapidly to an upstream position to expose the analyte–containing zone to the GC oven for refocussing and injection [9].

Currently, jet–based thermal modulators are dominating the field. These modulators produce narrow second dimension peaks to deliver high peak capacities and have the added advantage that there are no moving parts. Single jet and dual–jet modulators using CO<sub>2</sub> for cooling provide satisfactory results and a robust interface with relatively narrow peak widths (45–95 ms). For more volatile components, the use of liquid nitrogen is mandatory to extend the application range from –100 to about –160°C [10]. Dedicated hot jets may be used to provide fast heating rates, although some modulators use the GC oven temperature for this purpose with good results.

Gaines and Frysinger [11] evaluated temperature requirements for thermal modulation. They determined that hot jet duty cycles of 300 ms produced optimum modulation.

## Chapter 2: Fundamental Aspects of GCxGC

---

Although the hot jet heater block temperature was set at 100°C above the oven temperature, the maximum temperature achieved at the modulator column was only 40°C above the oven temperature. This heating condition ensured rapid peak desorption and narrow modulated peaks. The cold spot temperature had to be 120–140°C colder than the eluent temperature to trap the target compounds. These authors evaluated peak shapes as a diagnostic tool to determine whether the cold jet temperature was sufficient to trap the target compound. For satisfactory results, the modulation must produce sharp, symmetrical peaks, where the signal returns to the baseline within two peak widths and where the peaks exhibit no breakthrough. When the trapping temperature is too high, the modulated peak is tailed and may not return to the baseline. If too low, compounds may not be completely desorbed by the hot jet, resulting in peak broadening and degrading of both first and second dimension resolution.

Much research is currently being carried out on valve-based modulators. These modulators are often used to prevent breakthrough of highly volatile analytes or to enable a more flexible second-dimension operation [12, 13]. Multi-port valve systems are simple, robust and low-cost alternatives to thermal modulation, requiring no cryogenic solvents. In 1998, Synovec and coworkers [14] introduced a high-speed multi-port valve system to divert small portions of primary column effluent to the head of the secondary column. Bueno and Seeley [12] collected primary effluent in a sample loop and operated under differential flow conditions that employed a high secondary column flow to flush the sample loop in a fraction of the fill time. This permitted a greater portion of the primary column eluent to be sampled. A flow-switching device was developed by Janssen et al. [15] that mitigated the disadvantages of the valve-based systems.

Tranchida et al. [16] recently developed a very promising flexible chip-based pneumatic modulator consisting of a metallic disk or chip with internal channels, which is located inside the GC oven but apart from the two dimensions. The disk is linked to an auxiliary pressure unit and is characterised by an interchangeable sample loop. The valve part of the modulator is located outside the GC oven and therefore does not have to adhere to column temperature restrictions.

## Chapter 2: Fundamental Aspects of GCxGC

---

While cryogenic modulation is generally preferred, valve-based modulation systems are ideal for field applications where the use of cooling gases is not practical.

### 2.3 Column considerations

Giddings [17] defined the following criteria for a truly multidimensional separation: (1) the components in a mixture have to be subjected to two or more separation steps in which their displacements are dependent on different factors; and (2) when two or more components are substantially separated in any single step, they should remain separated until completion of the total operation. This prescribes that the distribution of components in one dimension should not be related to their distribution in the other dimension. Such a separation is then regarded as orthogonal.

Non-orthogonal set-ups have also been reported to provide excellent and highly structured separations with superior within- and between-group separations [18, 19]. A more important target than orthogonality should be to obtain the separation of the target compounds from the matrix interference.

The first dimension columns are the same high-resolution columns that are used for conventional 1D-GC, while the secondary columns are designed for fast analysis. In order to preserve first dimension separation, at least three to four modulations are required across a first dimension peak. For peak widths in the order of 10–30 s, the modulation period should be in the order of 2–8 s. Second dimension separation should therefore also be completed in 2–8 s to prevent wrap-around. Very short (0.5–2 m), narrow bore ( $\approx 0.1$ – $0.18$  mm) columns with small film thickness (0.05– $0.18$   $\mu\text{m}$ ) are generally selected as secondary columns for most applications. Peak widths at the baseline of such columns range from 50 – 500 ms.

In principle, all kinds of stationary phases can be used in the first dimension of GCxGC, but non-polar phases, (primarily dispersive van der Waals interactions) are generally preferred. Separation on these columns is based on volatility, to produce a boiling point separation. All of the analytes eluting in a narrow fraction will therefore have similar volatilities.

## Chapter 2: Fundamental Aspects of GCxGC

---

As the second dimension separation is essentially isothermal, the separation obtained by any other type of column in the second dimension should be governed by specific interactions with the stationary phase, and not by volatility. This then provides a true orthogonal separation and the entire plane of the GCxGC chromatogram is used. Polar columns (for which dispersive van der Waals forces,  $\pi$ - $\pi$ , dipole-dipole and dipole-induced interactions are all strong) are preferred as second dimension columns.

Oxygenates such as fatty acid methyl esters (FAME) are often not completely separated from hydrocarbons, and separation according to the number of double bonds in FAME cannot be achieved if a non-polar x polar column set is used [20]. Much improved chromatographic behaviour is obtained in the reversed set-up.

Seeley et al. [21] developed a GCx2GC system that splits the primary column effluent into two secondary columns in order to obtain a pair of chromatograms for each run. The dual secondary column configuration greatly facilitated compound identification and increased the separation efficiency for mixtures containing organic compounds with polar functional groups such as alcohols, ketones, esters, etc.

Column overloading is a common problem in GCxGC. Broader first dimension peaks help to produce smaller second dimension fractions that reduce the chance of secondary column overloading. For analyses where analyte concentrations vary a lot and high resolution is required, thicker-phase primary columns and larger-diameter secondary columns are better, though at the cost of analysis time. In general, 0.25 and 0.5  $\mu\text{m}$  film primary columns and 150  $\mu\text{m}$  I.D. secondary columns are good choices [22].

## Chapter 2: Fundamental Aspects of GCxGC

---

### 2.4. Temperature and pressure considerations

Temperature programming in GCxGC is generally slower than used for conventional 1D–GC in order to meet modulation criteria. Typical temperature rates are 1–3°C/min. As mentioned, the fast separation in the second dimension is essentially isothermal. In some GCxGC systems (such as the Leco Pegasus 4), the second dimension column is housed in a secondary oven to allow flexible and independent temperature programming. The maximum temperature limit of the polar column is often the limiting temperature factor for GCxGC operation.

The maximum temperature for a polyethylene glycol (wax) column is around 260°C, and for a cyanopropyl column around 280°C. These temperatures are too low to elute all the compounds in heavier diesels. To enable GCxGC analysis of higher carbon numbers, the polar column is often substituted for a mid–polarity column such as a 50% phenylpolysilphenylene–siloxane (BPX–50) that has a higher maximum temperature limit of around 370°C. By combining this column with a high temperature non–polar column in the first dimension (e.g. dimethylpolysiloxane (DB1–HT)) with a maximum temperature of around 430°C), successful separation of hydrocarbons up to C<sub>60</sub> can be obtained [23]. As the separation on the non–polar (boiling point separation)/mid–polarity (both boiling point and polarity separation) column set is not completely independent, the separations are not completely orthogonal and less of the <sup>2</sup>D separation space is used. The advantage of this column set in detecting higher carbon numbers should therefore be measured against the need to obtain optimal resolution.

It is crucial to know the flow rates in the GCxGC column set in order to optimise pressure settings, but in practice it is difficult to predict the velocities when the columns have different diameters. The average linear velocity through the system can be determined through the total system dead time, but that does not say anything about the velocities in the individual columns. Harynuk and co-workers developed a flow model that predicts the pressure settings required to generate specific flow rates in different segments of the GCxGC columns [22]. The model can also predict the length of the delay loop for use with loop–type modulators.

## Chapter 2: Fundamental Aspects of GCxGC

---

Beens et al. used calculations to demonstrate that one column can be operated close to optimal flow conditions and a sub-optimum separation can then be accepted on the other column [24]. These authors developed a computer program to assist in the process of selecting column dimensions and to optimise flow rates for all types of columns. The program requires column dimensions and carrier gas type as input parameters, and calculates parameters of the GCxGC separation using flow rate and plate height equations. These calculations are discussed below.

One of the conditions for a truly multidimensional separation is to have at least three to four second-dimension cuts over the width of a first-dimension peak [17]. For four second-dimension cuts over the width of a first-dimension peak with a peak width at baseline equal to  $6\sigma$ , the following equation is valid:

$${}^2t_r \leq 1.5 \times {}^1\sigma \quad (1)$$

$$\text{or } {}^2t_0(1+{}^2k) \leq 1.5 \times {}^1\sigma \quad (2)$$

According to nomenclature proposed by Schoenmakers et al. [25],  ${}^2t_0$ ,  ${}^2t_r$  and  ${}^2k$  are dead-time, retention time and retention factor in the second-dimension column and  ${}^1\sigma$  is the standard deviation of a peak eluting from the first-dimension column. From (1) the modulation criterion which has to be fulfilled for a two-dimensional separation is defined as  ${}^2t_r / {}^1\sigma \leq 1.5$ .

A full mathematical treatment is only possible for isothermal operation, which is hardly ever applied in a routine GCxGC environment. For temperature programming, broadening can only be estimated. However, Schutjes et al. [26] showed that the general conclusions regarding the influence of pressure, column dimensions, flow rates, etc. on band width in programmed operation are identical to those in isothermal operation.

## Chapter 2: Fundamental Aspects of GCxGC

---

The widths of the bands eluting from the first–dimension column,  ${}^1\sigma$ , if operated under isothermal conditions, is given by :

$${}^1\sigma = \sqrt{\frac{{}^1H {}^1t_r^2}{{}^1L}} \quad (3)$$

where  ${}^1H$  is the plate height and  ${}^1L$  is the length of the first–dimension column and  ${}^1t_r$  is the first–dimension retention time.

${}^1H$  can be written as [27]:

$${}^1H = \frac{1}{{}^1CE} \left( \left( \frac{2 {}^1D_{m,o}}{{}^1u_o} + \frac{f({}^1k) {}^1d_c^2}{{}^1D_{m,0}} \right) {}^1f_1 + \frac{g({}^1k) {}^1d_f^2}{{}^1D_s} {}^1f_2 \right) \quad (4)$$

where  ${}^1D_{m,o}$  is the analyte diffusion coefficient in the mobile phase in the first–dimension column under column outlet conditions, i.e. at the modulator;  ${}^1u_o$  is the outlet linear velocity of the first column, i.e. the velocity at the modulator pressure;  ${}^1d_c$  is the diameter of the first column;  ${}^1d_f$  is the stationary phase film thickness of the first–dimension column;  ${}^1D_s$  the analyte diffusion coefficient in the first–dimension column stationary phase;  ${}^1CE$  is the coating efficiency of the first column.

$f({}^1k)$  and  $g({}^1k)$  are functions of the retention factor:

$$f({}^1k) = \frac{(1+6{}^1k+11{}^1k^2)}{96(1+{}^1k)^2} \quad (5)$$

$$g({}^1k) = \frac{2{}^1k}{3(1+{}^1k)^2} \quad (6)$$

${}^1f_1$  and  ${}^1f_2$  are pressure correction factors [28]:

$${}^1f_1 = \frac{9({}^1p_o^4 - 1)({}^1p_o^2 - 1)}{8({}^1p_o^3 - 1)^2} \quad (7)$$

## Chapter 2: Fundamental Aspects of GCxGC

---

$$\text{and } {}^1f_2 = \frac{3({}^1p_o^2 - 1)}{2({}^1p_o^3 - 1)} \quad (8)$$

$$\text{where } {}^1p_o = \frac{{}^1p_{in}}{{}^1p_{out}} \quad (9)$$

${}^1p_{in}$  and  ${}^1p_{out}$  are the inlet and outlet pressures of the first–dimension column. The equations describing band width and plate height for the second–dimension column are analogous.

All parameters in equations (1)–(9) are relatively easy to obtain, with the exception of  ${}^1p_{out}$  (which is identical to  ${}^2p_{in}$ ). These parameters represent the midpoint pressure, the pressure in the modulator. Knowledge of this pressure is crucial to describe the flows in both columns. Because it could not be measured or calculated, a detailed insight into the gas flow in GCxGC columns was, however, lacking. Beens et al. [24] calculated this pressure indirectly from the inlet and outlet pressures of the column combination using the Poiseuille equation and the fact that the mass flow through both columns is the same (the columns are coupled in series). According to the Poiseuille equation, the volumetric flow rate through the first–dimension column is equal to:

$${}^1F = \left( \frac{\pi^1 d_c^4}{256\eta^1 L} \right) \left( \frac{{}^1p_{in}^2 - {}^1p_{out}^2}{{}^1p_{out}} \right) \left( \frac{T_{mod}}{{}^1T} \right) \quad (10)$$

where  ${}^1F$  is the volumetric flow through the first–dimension column under modulator conditions,  $\eta$  is the dynamic viscosity of the carrier gas, and  $T_{mod}$  and  ${}^1T$  are the temperatures in the modulator and first–dimension column.

The equation is slightly different for the second–dimension column:

$${}^2F = \left( \frac{\pi^2 d_c^4}{256\eta^2 L} \right) \left( \frac{{}^2p_{in}^2 - {}^2p_{out}^2}{{}^2p_{out}} \right) \left( \frac{T_{mod}}{{}^2T} \right) \left( \frac{{}^2p_{out}}{{}^1p_{out}} \right) \quad (11)$$

## Chapter 2: Fundamental Aspects of GCxGC

---

The term  $({}^2p_{out}/{}^1p_{out})$  is needed to convert the velocity in the second–dimension column to modulator conditions. Under steady–state conditions  ${}^1F$  is equal to  ${}^2F$ . If it is further assumed that the temperatures in the two columns and the modulator are the same, equations (10) and (11) can be combined to give:

$$\left(\frac{{}^1d_c^4}{{}^1L}\right)\left(\frac{{}^1p_{in}^2 - {}^1p_{out}^2}{{}^1p_{out}}\right) = \left(\frac{{}^2d_c^4}{{}^2L}\right)\left(\frac{{}^2p_{in}^2 - {}^2p_{out}^2}{{}^2p_{out}}\right)\left(\frac{{}^2p_{out}}{{}^1p_{out}}\right) \quad (12)$$

Rewriting this equation gives:

$${}^1p_{out}^2 = \frac{{}^1d_c^4 {}^2L {}^1p_{in}^2 + {}^2d_c^4 {}^1L {}^2p_{out}^2}{{}^2d_c^4 {}^1L + {}^1d_c^4 {}^2L} \quad (13)$$

The input and output pressures of both columns are now known, and the average linear velocities and residence times can be calculated from:

$${}^1u_o = \frac{{}^1F}{(\pi/4){}^1d_c^2} \quad (14)$$

$$\text{to be } {}^1\bar{u} = {}^1u_o {}^1f_2 \quad (15)$$

$$\text{and } {}^1t_r = \frac{{}^1L(1+{}^1k)}{{}^1\bar{u}} \quad (16)$$

where  ${}^1\bar{u}$  is the average linear velocity in the first–dimension column.

Identical equations hold for the second–dimension column.

From these equations, the plate height curves and band widths could be calculated.

The required viscosities were calculated from the equations given by Ettre [29]. Stationary–phase diffusion coefficients can be calculated from [30]:

## Chapter 2: Fundamental Aspects of GCxGC

---

$$D_s = \frac{D_m}{50000} \quad (17)$$

${}^1D_{m,o}$  is calculated from:

$${}^1D_{m,o} = \frac{{}^2D_{m,o} {}^2P_{out}}{{}^1P_{out}} \quad (18)$$

Here,  ${}^2D_{m,o}$  the analyte diffusion coefficient, is obtained from the models proposed by Fuller et al. [31]. Using this approach, the pressure settings needed for optimal resolution can be calculated.

In this study, it was preferred to maintain a constant mass flow of carrier gas throughout a GCxGC run rather than to define the column pressure settings for the start and end of the GCxGC run. It was found that a constant carrier gas flow provided similar resolution and peak capacity, and also accurate quantification. Higher alkanes eluted at similar second-dimension retention times for a constant carrier gas flow and it was easily to optimise the two-dimensional separation space to obtain the highest orthogonality and therefore obtain optimal use of the two-dimensional separation space.

### 2.5 Detectors commonly used in petrochemical applications

The very fast separation in the second dimension column produces very narrow peaks with widths of about 50–100 ms at the baseline. These peaks require detectors to be very fast, with data acquisition rates in the order of at least 100 Hz and negligible internal volume to achieve proper reconstruction of second-dimension chromatograms. The capacity of a detector to track the rapidly changing peak profiles depends on the design of the electronics, flow paths and make-up gas introduction, the type of detector response mechanism and the chemistry of the response [32].

## Chapter 2: Fundamental Aspects of GCxGC

---

### 2.5.1 Universal detectors

#### 2.5.1.1 Flame ionisation detector

The flame ionisation detector (FID) was the first detector applied to GCxGC because it was the only available universal detector at the time that was capable of providing a suitable data acquisition rate [33–34]. This detector is still used extensively today in petrochemical applications. The FID produces ions in a flame when burning carbon compounds. The resulting ion current is proportional to the amount of carbon present in the compound. The FID does not provide a response for heteroatomic species. Where organic compounds contain heteroatoms, these compounds can still be analysed with the help of FID response factors to compensate for the detector's lack of response [35]. FID detectors have fast data acquisition rates (up to 300 Hz), good sensitivity and good quantitative capabilities over a wide linear range [36–38]. Although the FID does not provide structural information, the highly structured separations provided by GCxGC are often sufficient to identify most compounds in a complex hydrocarbon matrix.

#### 2.5.1.2 Time-of-flight mass spectrometer

Time-of-flight mass spectrometer (TOF-MS) systems are the preferred detectors for GCxGC because they provide structural information which is essential for peak identification and have data acquisition rates of up to 500 spectra per second. The high scanning rates prevent spectral skewing and deconvolution becomes very powerful. The Pegasus software package from Leco Corporation (USA) contains deconvolution algorithms that can locate and identify mass spectra of closely eluting compounds based on unique ions.

Ions are formed in the TOF-MS source as a discrete ion packet and are pulsed via acceleration slits into the flight tube. Ions will have a distribution of masses and essentially constant kinetic energy, while their velocities will be inversely proportional to the square root of the mass-to-charge ratio ( $m/z$ ) of the ions.

## Chapter 2: Fundamental Aspects of GCxGC

---

Their arrival times at the detector will be distributed according to the square root of their  $m/z$  [39]. The heavier the ion is, the longer is its time-of-flight.

Small differences in kinetic energy affect the mass resolution of the mass spectrometer and to reduce this, a reflectron or ion mirror is placed in the drift region. The reflectron uses a constant electrostatic field to reflect the ion beam toward the detector. The more energetic ions penetrate deeper into the reflectron, and take a slightly longer path to the detector. Less energetic ions of the same mass-to-charge ratio penetrate a shorter distance into the reflectron and, correspondingly, take a shorter path to the detector.

TOF-MS data files are very large. For a GCxGC-TOF-MS analysis of 90 min and a data acquisition rate of 100 spectra/s, 540,000 mass spectra will be recorded. Data files become very large (0.5–2 GB) and powerful computers are necessary to process data and to display results. Data processing of a single GCxGC-TOF-MS file may take an hour or longer, depending on the computer resources. For this reason, GCxGC-TOF-MS and GCxGC-FID are often combined for routine analyses in the petrochemical laboratory. The same peak distribution patterns are obtained for the two systems and because FID data files are relatively small, data processing is completed within a few seconds. TOF-MS is used initially to identify peaks in a typical sample and peak identifications are then applied to FID for fast routine analysis and quantification.

### 2.5.1.3 Quadrupole mass spectrometer

Quadrupole MS (qMS) systems typically have relatively low scanning speeds ( $\approx 20$  scans/s), which are sufficient for identification purposes but not for quantification in GCxGC because the narrow peaks are not sufficiently defined. Recently, rapid-scanning instruments have become commercially available and allow scanning rates of up to 10 000 Da/s [40,41]. Data acquisition rates of up to 90 Hz can be used in selected ion monitoring (SIM) mode. For applications in a limited mass range (100–300 Da) rapid-scanning qMS is adequate. However, for analysis over a broad mass range, for example when searching for unknowns, TOF-MS becomes necessary.

## Chapter 2: Fundamental Aspects of GCxGC

---

In qMS, ions are produced in the ion source and accelerated into the mass analyser with a small spread of kinetic energies. A quadrupole field is formed by four electrically conducting parallel rods, of which opposite pairs of electrodes are electronically connected. Two opposite rods have an applied potential of  $(U+V\cos(\omega t))$  and the other two rods have a potential of  $-(U+V\cos(\omega t))$ , where  $U$  is a DC voltage and  $V\cos(\omega t)$  is an AC voltage. The applied voltages affect the trajectory of ions traveling down the flight path centered between the four rods. For given DC and AC voltages, only ions of a certain mass-to-charge ratio ( $m/z$ ) pass through the quadrupole filter and all other ions are thrown out of their original path. A mass spectrum is obtained by monitoring the ions passing through the quadrupole filter as the voltages on the rods are varied.

### 2.5.2 Selective detectors

There is an increasing demand for selective detectors because they help to reduce the interferences from co-eluting compounds and generally improve response detectability and detection sensitivity. Selective detectors are most often used to address specific application problems, for example for heteroatom analysis in petrochemical products.

#### 2.5.2.1 Sulphur chemiluminescence detectors

The sulphur chemiluminescence detector (SCD) converts sulphur-species to their respective chemiluminescent ion species. Sulphur-containing molecules are combusted in a hydrogen-rich environment to form  $\text{SO}$ , which is then reacted with ozone to produce  $\text{SO}_2$  and  $\text{O}_2$ . Light emitted as the  $\text{SO}_2$  returns to the ground state is detected by a photomultiplier tube. The SCD has a linear and equimolar response to sulphur components, an absence of quenching effects and excellent selectivity and sensitivity.

SCD detectors have found wide application in petrochemical product analysis. Sulphur is present in coal and natural gas as well as in crude-derived petrochemical feedstock. SCD and nitrogen chemiluminescence (NCD) detectors have to be adapted for proper detection of the narrow GCxGC peaks [45].

## Chapter 2: Fundamental Aspects of GCxGC

---

The main limitation in combining GCxGC with a SCD is the speed of the electronics used in the commercial system [44]. Hua et al. [42,43] obtained a data acquisition rate of 100 Hz when combining SCD with a GCxGC, but reported increased peak widths as a result of the larger cell volume of the SCD.

### 2.5.2.2 Nitrogen chemiluminescence detector

The NCD detector works in a similar fashion to the SCD detector but with NO as intermediate and NO<sub>2</sub> as final product. Light is emitted in the red and infrared regions of the spectrum and detected by a photomultiplier tube. The NCD has an equimolar response towards N-compounds, has a high sensitivity and does not suffer from quenching as a result of matrix effects. The NCD also has many applications in petrochemical analysis [46–48].

### 2.5.5.3 Atomic emission detector

The atomic emission detector (AED) is a multi-element detector that can measure up to 23 different elements, including sulphur, nitrogen, oxygen, silicon, etc. [49]. In the AED, compounds are introduced into a microwave-energised helium plasma that is coupled to a diode array optical emission spectrometer. Elements are atomised and excited to generate characteristic atomic emission spectra. The emitted light is separated into individual lines by a diffraction grating and detected via a photodiode array. The maximum acquisition rate of the AED (10 scans/s) makes it too slow for quantification in GCxGC, but this detector can still provide valuable qualitative information.

### 2.5.5.4 Other detectors used in combination with GCxGC

Nitrogen phosphorus detectors (NPDs) convert sample molecules into negative ions by extracting electrons from a hot solid surface. The beads used for this purpose are electrically heated thermionic sources consisting of an alkali salt in an inorganic ceramic cement matrix. The exact mechanisms are not fully understood, although presumably the alkali atoms catalyse the electron transfer taking place on the bead surface [50–53].

## Chapter 2: Fundamental Aspects of GCxGC

---

Gas flows needs to be optimised to obtain the best conditions with respect to peak magnitude and asymmetry. The NPD provides data acquisition rates of up to 200 Hz.

The electron capture detector (ECD) can deliver data at acquisition rates of up to 50 Hz, but has a large cell volume which gives rise to peak broadening. The ECD is not capable of reproducing peak widths narrower than 300 ms [45].

Flame photometric detection (FPD) has been used successfully as an element-specific detector for GCxGC [54]. The FPD is used primarily for the determination of volatile sulphur or phosphorus compounds, but can also be used for detection of chromium, iron, rhodium, titanium, arsenic, zirconium, molybdenum, tungsten, tin, aluminum and carbon, using selective or non-selective modes of operation. Phosphorus forms HPO species that emit radiation at 510 and 526 nm. Sulphur compounds form a S<sub>2</sub>-species that emits a series of radiation bands around 394 nm. The detector has a linear response for phosphorus but the sulphur response depends on the square of the concentration. The pulsed flame photometric detector (PFPD) has a higher sensitivity and improved selectivity compared to conventional FPD.

### 2.6 Complementary techniques and hyphenation with GCxGC

Even with the high separation power of GCxGC, co-elution still occurs to some degree for certain applications, even when employing various column combinations and optimal temperature programs [55–57]. Peak co-elution leads to inaccurate quantification. Combining TOF-MS with GCxGC can be of great help to separate co-eluting component classes. The high data acquisition rates of TOF-MS (up to 500 Hz) ensure that sufficient data points are obtained across all peaks to make deconvolution of overlapping peaks possible [58–60].

Certain hydrocarbon groups, however, have very similar mass spectra and the same molecular ions, e.g. a C<sub>10</sub> alkene and a C<sub>10</sub> cyclic alkane are seldom distinguishable based on their mass spectra. Similarly, is it almost impossible to distinguish between the mass spectra of dienes, cyclic alkenes and bicyclic alkanes of the same carbon number.

## Chapter 2: Fundamental Aspects of GCxGC

---

For these cases, TOF–MS (or any other mass spectrometric method, including high resolution MS) is not of much help.

Applying a fractionation step prior to GCxGC may therefore be necessary for certain applications. Various authors have used column fractionation to obtain separation of different chemical classes [61, 62]. Breakthrough of some components into different classes was often observed. The breakthrough is mainly due to insufficient separation power of flash–column fractionation. Breakthrough is only noticed during analysis because no detection system is used during fractionation. Vandeuve et al. coupled a silver–based alkene trap to GCxGC to obtain a detailed analysis of hydrocarbons in the C<sub>8</sub>–C<sub>14</sub> range, but observed isomerisation of alkenes due to the high temperatures used for desorption [57].

### 2.6.1 High performance liquid chromatography (HPLC)

A more accurate way to achieve fractionation prior to GC analysis is by using high performance liquid chromatography (HPLC). The technique has high separation power and especially high selectivity, and can be used in combination with a number of detectors. Detection is essential for control of the fractionation step. Off–line liquid chromatography followed by GC analysis of a selected fraction (LC–GC) is frequently used but it does have disadvantages, such as the possibility of sample loss and contamination. The latter risk can be avoided by using on–line LC–GC.

Automated on–line LCxGC was studied by de Koning et al. [63]. These authors developed two interfaces, utilising either a six–port switching valve or a dual side–port syringe for comprehensive transfer of LC eluent to the GC. The LC eluent flow was split after solvent evaporation in the hot split injector of the GC to prevent overloading of the GC columns. They obtained excellent performance in terms of reliability, repeatability and ease of use for both interfaces. Edam et al. combined off–line normal–phase LC on an amino–bonded silica column in combination with GCxGC–FID to obtain group–type separation of saturated, monocyclic and dicyclic aromatic classes [56].

## Chapter 2: Fundamental Aspects of GCxGC

---

The method is unfortunately not suited for the separation of PAHs due to their late elution from the amino-bonded column. Sciarrone et al. similarly combined off-line LC-GCxGC with rapid scanning qMS to separate classes of saturated hydrocarbons, mono-, bi-, tri- and tetracyclic aromatics [64]. These authors used an amino LC column in combination with GCxGC with a large injection volume.

The separation of alkenes is often neglected because of their low presence in petrochemical products. De Koning et al. used the comprehensive coupling of silver-phase LCxGC to separate triglycerides according to carbon number and number of double bonds [63]. Mao et al. combined HPLC, also with a silver modified column, with GCxGC to obtain separation of alkanes, cycloalkanes, alkenes and aromatic groups of oils and oil-polluted soils [65].

One of the major disadvantages of off-line HPLC-GCxGC is the requirement of relatively large volumes of solvents that are used for HPLC separations. Evaporation of solvents, prior to analysis, may lead to loss of volatile analytes. If solvents are not evaporated, they may interfere with analyte peaks and lead to a decrease in sensitivity. This limits the application of HPLC-GCxGC to samples that do not contain highly volatile components.

### 2.6.2 Supercritical fluid chromatography

In recent years interest in supercritical fluids as unique solvent has become more prominent [66]. The hyphenation of SFC to GCxGC looks a very promising technique. SFC provides high separation performance in short analysis times. The absence of large volumes of solvents makes SFC more attractive than HPLC as a fractionation technique for GCxGC. CO<sub>2</sub> is easily evaporated from samples after fractionation, minimising the loss of volatile sample material during solvent evaporation and also the interference of solvent peaks during the GCxGC analysis. The same mobile phase can be used with different stationary phases.

Normal phase SFC on silica, with CO<sub>2</sub> as mobile phase, has become an established method for the separation of aromatic and aliphatic groups in petrochemical samples [67].

## Chapter 2: Fundamental Aspects of GCxGC

---

Norris and Rawdon used a silver–modified HPLC column to obtain separation of aliphatic component classes into alkanes and alkenes but at that time these columns were costly and unstable and required replacement every 6–8 weeks [68]. Venter et al. combined SFC with GC and used sulphur hexafluoride (SF<sub>6</sub>) as alternative mobile phase for the group–type separation of alkane, alkene, aromatic and oxygenate component classes by SFC [69].

### 2.6.3 Nuclear magnetic resonance spectroscopy

By combining GC and nuclear magnetic resonance (NMR), more information can be obtained for structural isomers that have identical mass spectra. Even though structural isomer peaks may be completely separated from each other by GCxGC, these compounds cannot be distinguished by their mass spectra or position on the GCxGC plot only, and confirmation by NMR or another analytical technique is required. Structural isomers can readily be distinguished by using <sup>1</sup>H NMR, but the compounds first have to be isolated and purified.

On–line hyphenation of GC with NMR is not feasible and therefore these analyses need to be performed off–line. Marriott and co–workers combined NMR with microscale–preparative multidimensional GC (MDGC or heart–cutting GC–GC) to isolate pure methylnaphthalenes from crude oils in sufficient quantities for NMR identification [70]. Collection times for the two isomers were ≈16 and ≈15 hours, respectively.

## Chapter 2: Fundamental Aspects of GCxGC

---

### 2.7 References

- [1] J.C. Giddings, *Anal. Chem.* 6 (1984) 1258.
- [2] J.B. Phillips, Z. Liu, *J. Chromatogr. Sci.* 29 (1991) 227.
- [3] J. Beens, J. Blomberg, P.J. Schoenmakers. *J. High Resolut. Chromatogr.* 23 (2000) 182.
- [4] J. Beens, P.J. Schoenmakers, U.A.Th. Brinkman, *J. Chromatogr. A* 972 (2002) 137.
- [5] J. Dalluge, J. Beens, U.A.Th. Brinkman, *J. Chromatogr. A* 1000 (2003) 69.
- [6] P.J. Marriott, R. Shellie, *TrAC*, 21 (2002) 573.
- [7] W. Khummueng, J. Harynuk, P.J. Marriott, *Anal. Chem.* 78 (2006) 4578.
- [8] R. Murphy, M. Schure, J. Foley, *Anal. Chem.* 70 (1998) 1585.
- [9] P.J. Marriott, R.M. Kinghorn, R. Ong, P. Morrison, P. Haglund, M. Harju, *J. High Resolut. Chromatogr.* 23 (2000) 253.
- [10] E.M. Kristenson, P. Korytár, C. Danielson, M. Kalio, M. Brandt, J. Mäkelä, R.J.J. Vreuls, J. Beens, U.A.Th. Brinkman, *J. Chromatogr. A* 1019 (2003) 65.
- [11] R.B. Gaines, G.S. Frysinger, *J. Sep. Sci.* 27 (2004) 380.
- [12] P.A. Bueno Jr., J.V. Seeley, *J. Chromatogr. A* 1027 (2004) 3.
- [13] J. Harynuk, T. Górecki, *J. Sep. Sci.* 27 (2004) 431.
- [14] A.E. Sinha, B.J. Prazen, C.G. Fraga, R.E. Synovec, *J. Chromatogr. A* 1019 (2003) 78.
- [15] H.-G. Janssen, W. Boers, H. Steenberger, R. Horsten, E. Flöter, *J. Chromatogr. A* 1000 (2003) 385.
- [16] P.Q. Tranchida, G. Purcaro, P. Dugo, G. Dugo, P. Dawes, L. Mondello, Development of a chip-based pneumatic modulator for comprehensive two-dimensional gas chromatography, Presented at the 34<sup>th</sup> International Symposium on Capillary Chromatography and the 7<sup>th</sup> GCxGC Symposium, Riva del Garda, Italy, June 2010.
- [17] J.C. Giddings, *J. High Resolut. Chromatogr.*, 10 (1987) 319.
- [18] M. Adahchour, J. Beens, U.A.Th. Brinkman, *J. Chromatogr. A* 1186 (2008) 67.
- [19] M. Adahchour, J. Beens, R.J.J. Vreuls, A.M. Badenburger, U.A.Th. Brinkman, *J. Chromatogr. A* 1054 (2004) 47.
- [20] F. Adam, F. Bertoncini, V. Coupard, N. Charon, D. Thiébaud, D. Espinat, M-C. Hennion, *J. Chromatogr. A* 1186 (2008) 236.
- [21] J.V. Seeley, F.J. Kramp, K.S. Sharpe, S.K. Seeley, *J. Sep. Sci.* 25 (2002) 53.

## Chapter 2: Fundamental Aspects of GCxGC

---

- [22] Z. Zhu, J. Harynuk, T. Górecki, *J. Chromatogr. A* 1105 (2006) 17.
- [23] T. Dutriez, M. Courtiade, D. Thiébaud, H. Dulot, F. Bertoncini, J. Vial, M.-C. Hennion, *J. Chromatogr. A* 1216 (2009) 2905.
- [24] J. Beens, H.-G. Janssen, M. Adahchour, U.A.Th. Brinkman, *J. Chromatogr. A* 1086 (2005) 141.
- [25] P. Schoenmakers, P. Marriott, J. Beens, *LC–GC Eur.* 16 (2003) 335.
- [26] C.P.M. Schutjies, E.A. Vermeer, J.A. Rijks, C.A. Cramers, *J. Chromatogr.* 253 (1982) 1.
- [27] M.J.E. Golay, in: D.H. Desty (Ed.), *Gas Chromatography*, Butterworths, London, UK, 1958. p.36.
- [28] J.C. Giddings, *Dynamics of Chromatography, Part 1, Principles and Theory*, Marcel Dekker, New York, 1965.
- [29] L.S. Ettre, *Chromatographia* 18 (1984) 243.
- [30] A.E. Scheidegger, *The Physics of Flow Through Porous Media*, University of Toronto Press, Toronto, 1960.
- [31] E.N. Fuller, P.D. Schettler, J.C. Giddings, *Ind. Eng. Chem.* 58 (1966) 19.
- [32] F.C.–Y. Wang, *The applications of comprehensive two–dimensional gas chromatography in the petroleum industry*, Presented at the 1st Symposium on Comprehensive Two–Dimensional Gas Chromatography, Volendam, The Netherlands, 2003.
- [33] T.J. Holm, *J. Chromatogr. A* 842 (1999), 221.
- [34] R. Shellie, P.J. Marriott, C.W. Huie, *J. Sep. Sci.* 26 (2003) 1185.
- [35] D.J. David, *Gas Chromatographic Detectors*, John Wiley & sons, New York, 1974.
- [36] J. Beens, H. Boelens, R. Tijssen, J. Blomberg, *J. High Resolut. Chromatogr.* 21 (1998) 47.
- [37] J. Beens, U.A.Th. Brinkman, *Analyst* 130 (2005) 123.
- [38] E.M. Kristenson, P. Korytár, C. Danielson, M. Kallio, M. Brandt, J. Mäkelä, R.J.J. Vreuls, J. Beens, U.A.Th. Brinkman, *J. Chromatogr. A* 1019 (2003) 65.
- [39] M. Guilhaus, *J. Mass Spectrom.* 30 (1995) 1519.
- [40] P. Korytár, J. Parera, P.E.G. Leanards, J. de Boer, U.A.Th. Brinkman, *J. Chromatogr. A* 1067 (2005) 255.
- [41] M. Adahchour, M. Brand, H.–U. Baier, R.J.J. Vreuls, A.M. Batenburg, U.A.Th. Brinkman, *J. Chromatogr. A* 1067 (2005) 245.

**Chapter 2: Fundamental Aspects of GCxGC**

---

- [42] R. Hua, Y. Li, W. Liu, J. Zheng, H. Wei, J. Wang, X. Lu, H. Kong, G. Xu, *J. Chromatogr. A* 1019 (2003) 101.
- [43] R. Hua, J. Wang, H. Kong, J. Liu, X. Lu, G. Xu, *J. Sep. Sci.* 27 (2004) 691.
- [44] J. Blomberg, T. Riemersma, M. van Zuilen, H. Chaabani, *J. Chromatogr. A* 1050 (2004) 77.
- [45] R. Ong, P. Marriott, P. Haglund, *J. Chromatogr. A* 962 (2002) 135.
- [46] B.J. Chawla, *J. Chromatogr. Sci.* 35 (1997) 97.
- [47] C. Y. Wing, D.H. Fine, K.S. Chiu, K. Biemann, *Anal. Chem.* 56 (1984) 1158.
- [48] F.C–Y. Wang, W.K. Robbins, M.A. Greaney, *J. Sep. Sci.* 27 (2004) 468.
- [49] B.D. Quimby, V. Giarrocco, *Application Note: Gas Chromatography*, Hewlett–Packard, California, USA (1997) 1–11.
- [50] H. Carlsson, G. Robertsson, A. Colmsjö, *Anal. Chem.* 73 (2001) 5698.
- [51] P.L. Patterson, *J. Chromatogr. Sci.* 24 (1986) 41.
- [52] P.L. Patterson, *J. Chromatogr.* 167 (1978) 381.
- [53] K. Olah, A. Szoke, Zs. Vajta, *J. Chromatogr. Sci.* 17 (1979) 497.
- [54] R. Shellie, L. Mondello, P.J. Marriott, G. Dugo, *J. Chromatogr. A* 970 (2002) 225.
- [55] P.J. Schoenmakers, J.L.M.M. Oomen, J. Blomberg, W. Genuit, G. Van Velzen, *J. Chromatogr. A* 892 (2000) 29.
- [56] R. Edam, J. Blomberg, H.–G. Janssen, P.J. Schoenmakers, *J. Chromatogr. A* 1086 (2005) 12.
- [57] C. Vendeuvre, F. Bertoncini, D. Espinat, D. Thiebaut, M.–C. Hennion, *J. Chromatogr. A* 1090 (2005) 116.
- [58] Dallüge, J. Beens, U.A.Th. Brinkman, *J. Chromatogr. A* 1000 (2003) 69.
- [59] M. van Deursen, J. Beens, J. Reijenga, P. Lipman, C. Cramers, J. Blomberg, *J. High Resolut. Chromatogr.* 23 (2000) 507.
- [60] X. Lu, J. Wu, H. Kong, R. Hua, W. Tao, J. Gu, G. Zu Chin. *J. Chromatogr. A* 1034 (2004) 199.
- [61] G.S. Frysinger, R.B. Gaines, L. Xu, C.M. Reddy, *Environ. Sci. Technol.* 37 (2003) 165.
- [62] C.M. Reddy, R.K. Nelson, S.P. Sylva, L. Xu, E.A. Peacock, B. Raghuraman, O.C. Mullins, *J. Chromatogr. A* 1148 (2007) 100.

## Chapter 2: Fundamental Aspects of GCxGC

---

- [63] S. de Koning, H.–G. Janssen, M. van Deursen, U.A.Th. Brinkman, *J. Chromatogr. A* 1058 (2004) 217.
- [64] D. Sciarrone, P.Q. Tranchida, R. Costa, P. Donato, C. Ragonese, P. Dugo, G. Dugo, L.J. Mondello, *J. Sep. Sci.* 31 (2008) 3329.
- [65] D. Mao, H. v.d. Weghe, L. Diels, N. De Brucker, R. Lookman, G. Vanermen, *J. Chromatogr. A* 1179 (2008) 33.
- [66] R.M. Smith, *J. Chromatogr. A* 856 (1999) 83.
- [67] ASTM D5186–03(2009), Standard test method for determination of aromatic content and polynuclear aromatic content of diesel fuels and aviation turbine fuels by supercritical fluid chromatography, American Society for Testing Materials, Philadelphia, PA (2009).
- [68] T.A. Norris, M.G. Rawdon, *Anal. Chem.* 56 (1984) 1767.
- [69] A. Venter, E.R. Rohwer, A.E. Laubscher, *J. Chromatogr. A* 847 (1999) 309.
- [70] G.T. Eyres, S. Urban, P.D. Morrison, P.J. Marriott, *J. Chromatogr. A* 1215 (2008) 168.

## **Chapter 3**

# **GCxGC for Fischer–Tropsch Product Analysis**

## Chapter 3: GCxGC for Fischer–Tropsch Product Analysis

### 3.1 Introduction to Fischer–Tropsch technology

Sasol, the South African coal, oil and gas company, is a global energy and chemicals company that has pioneered world-leading technologies to produce quality synthetic fuels and petrochemicals from coal and natural gas. Based in South Africa, Sasol is pursuing international opportunities to commercialise coal-to-liquids (CTL) and gas-to-liquids (GTL) expertise using proprietary Fischer–Tropsch (FT) technology. The company has industrial plants in Sasolburg and Secunda and started their first international GTL venture, Oryx GTL, in Qatar in the Persian Gulf, in 2007, in partnership with Qatar Petroleum. The company is also developing a GTL plant in Nigeria with Chevron and the Nigerian International Petroleum Corporation, and is further exploring GTL opportunities together with joint venture partners in Africa, Australia and the Middle East.

Sasol mines coal in South Africa and converts it, along with Mozambican natural gas, into liquid fuels and chemical feedstock through three distinct types of FT processes. The low temperature (LT–FT) cobalt process is used for Oryx GTL fuels production. The LT–FT iron process is used in Sasolburg for production of waxes and chemicals, and the high temperature (HT–FT) iron process in Secunda is used to produce fuels and chemicals. Sasol's energy cluster focuses on the manufacturing, refining and marketing of automotive fuels, oils and gases, while the chemical cluster produces more than 200 chemicals that are distributed in 110 countries worldwide. These products include waxes, fertilisers, solvents, polymers, surfactants, etc [1]. The solvent product range includes alcohols, ketones, acids, esters, fine chemicals and co-monomers including hexene, octene, pentene and detergent alcohols as well as mining chemicals. FT-derived chemicals are used in several industries, including printing, packaging, plastics, pharmaceuticals, aerosol paints, adhesives, etc.

The FT process can be roughly divided into three basic steps, namely: preparation of the synthesis gas, FT synthesis and product work-up [2]. Synthesis gas is produced either by methane reforming of natural gas or coal gasification.

### Chapter 3: GCxGC for Fischer–Tropsch Product Analysis

---

During the synthesis gas production, the feedstock reacts with steam and oxygen to produce hydrogen, carbon monoxide and carbon dioxide.

Much less carbon dioxide is formed during methane reforming than during coal gasification and future FT plants will therefore preferably be based on cobalt–based LT-FT technology with natural gas as feedstock.

FT synthesis entails the catalytic conversion of synthesis gas to hydrocarbons and water in a surface polymerisation reaction. Fischer–Tropsch chemistry is very complex, but can be simplified into the following four basic reactions:

*Methane formation:*



*Heavier hydrocarbon formation:*



*Alcohol formation:*



*Water gas shift reaction:*



Only four metals, namely iron, cobalt, nickel and ruthenium, have been found to be sufficiently active for FT synthesis. Nickel has a high selectivity for methane, which is an unwanted FT product. Ruthenium, although most active, is scarce and very expensive. This only leaves iron and cobalt as practical catalysts for industrial use. Cobalt catalysts are much more active than iron but are also much more expensive. Because it is difficult to prevent coal derived catalyst poisons from reaching the catalyst, iron catalysts are better suited for use with coal–derived synthesis gas.

### Chapter 3: GCxGC for Fischer–Tropsch Product Analysis

---

It is generally relatively easy to remove potential FT catalyst poisons from natural gas prior to reforming, and for this reason cobalt is used with natural gas–derived synthesis gas. Iron catalysts, on the other hand, are inexpensive, more robust and less sensitive to catalysts poisons, and can be used with both natural gas and coal feed stocks. Cobalt catalysts are more active for hydrogenation reactions than iron, and the products obtained with cobalt catalysts are therefore more saturated.

Alkali promoters such as  $K_2O$ , may be used with iron catalysts to enhance catalyst activity and selectivity while structural promoters such as  $MgO$  and  $Al_2O_3$  may also be used to enhance the surface area of the catalyst. The choice of promoters are important in producing a catalyst with a low selectivity for methane and a high selectivity towards heavier hydrocarbon products with the desired alkene and oxygenate content in the products. Excessive promoter levels have a negative effect on catalyst activity hence optimum levels need to be maintained. High alkali levels are desirable to decrease methane selectivity but lead to operational problems in fluidised bed reactors due to the formation of heavy hydrocarbons, increased carbon formation and increased levels of organic acids. High carbon formation rates result in increased catalyst consumption, while organic acids cause corrosion problems [2]. Cobalt-based catalysts do not appear to be very sensitive to the chemical nature of promoters or supports. Because of the high cost of cobalt, it is important that cobalt be supported on a suitable high area, porous material, under conditions that yield well–dispersed, small cobalt crystals, resulting in a large exposed surface area of the metal.

The design of a reactor is linked to the technology selected to provide synthesis gas to the reactor. The most common reactor systems used with Fe catalysts are high temperature fluidised bed reactors. For precipitated Fe or supported Co catalysts, low temperature slurry reactors are preferred.

FT synthesis always produces a wide range of hydrocarbon and oxygenated hydrocarbon products, whatever the operating conditions. The spread in carbon numbers can be varied by altering the operating temperature, the type of catalyst, the amount and type of promoters in the catalysts, feed gas composition, operating pressure, or the type of reactor used.

### Chapter 3: GCxGC for Fischer–Tropsch Product Analysis

---

Whatever the process conditions, there is always a clear interrelationship between the products formed [2].

The synthetic crude produced during FT synthesis is not the final product and it has to be refined through various processes for chemical and fuel production. Product workup firstly involves the removal of light hydrocarbons and dissolved gases to make the hydrocarbons suitable for atmospheric storage. Valuable chemical feedstock is removed in a second step. Alkenes may be removed by fractionation or extractive distillation and subjected to various processes such as oligomerisation, alkylation, hydroformylation, etc. For LT–FT processes, the alkene content may not be high enough to justify alkene extraction, and the product upgrading typically only involves hydroprocessing and separation. Oxygenates are removed from the FT product by liquid–liquid extraction. Some of the lighter oxygenated products are dissolved in the reaction water and are separated from the bulk of the water by distillation.

After removal of valuable chemicals, the remaining product is further upgraded. Hydrotreatment is the mainstay of refining and is often used as a feed pre–treatment step for refinery operations that are sensitive to impurities, for example, the selective hydrogenation of dienes to mono–alkenes to reduce gum formation during alkylation. Hydrotreatment involves hydrogen addition and is often classified in terms of its function, e.g. hydrogenation of alkenes (HYD), hydrodeoxygenation (HDO), hydrodearomatisation, etc. [3].

Hydroisomerisation (HAD) is used in the refinery to increase the degree of branching of alkanes by rearrangement of the carbon chain. This process can be used to produce isobutane for use in aliphatic alkylation, for C<sub>5</sub>/C<sub>6</sub> HAD to improve the octane number of naphtha, and for the HAD of waxy alkanes for lubricating oil production.

Hydrocracking is used to convert heavy residues with boiling points >360°C into products in the distillate and naphtha boiling ranges. Hydrocracking removes heteroatoms by hydrotreating, cracks heavy material to lighter material, and reduces the aromatic content, especially PAHs, to meet final product specifications.

### Chapter 3: GCxGC for Fischer–Tropsch Product Analysis

---

Distillation is used extensively in all petrochemical plants. It is used to separate mixtures based on volatility differences where the boiling points of the compounds to be separated differ by more than 25°C. Fractional distillation is a special type of distillation used to separate components with boiling points differing by less than 25°C. It is performed by repeating vaporisation–condensation cycles within a packed fractionation column (successive distillations). For mixtures in which compounds evaporate at nearly the same temperature and at the same rate, extractive distillation becomes necessary.

Extractive distillation is a specialised distillation process that uses a miscible, high–boiling and relatively non–volatile solvent, which does not form azeotropes with other compounds in the mixture, to separate these close–boiling species.

Fluid catalytic cracking (FCC) is the most important conversion process used in petroleum refineries to convert high–boiling, high molecular weight hydrocarbon fractions of petroleum crude oils to more valuable gasoline, alkenic gases such as propylene, and other products. It is often the main source of short-chain alkenes in a crude–oil refinery and is focused on motor–gasoline production. The FCC process vaporizes and breaks the long-chain molecules of high–boiling hydrocarbon liquids into much shorter molecules by using a fluidised powdered catalyst. Catalytic cracking produces more gasoline with a higher octane rating than thermal cracking. The small amount of HT–FT residue (slurry oil) is too little to justify FCC, but in principal, this technology can be used for the conversion of the oxygenate–rich FT feed to light alkenes. A KBr Superflex™ Catalytic Cracking (SCC) technology [3] unit has been commissioned at Sasol. This technology differs from standard FCC mainly in terms of operating temperature, which is 50–80°C higher. During this process the oxygenate–rich C<sub>6</sub>–C<sub>7</sub> HT–FT naphtha is converted into ethylene, propylene, and high octane motor–gasoline.

Some oxygenates deactivate catalysts used in alkylation and hydroformylation processes and have to be removed. Dehydration may be used to convert oxygenates in these feeds to alkenes. Dehydration is an acid–catalysed endothermic reaction that aims to convert oxygenates to alkenes by rejection of water from the molecules [4].

### **Chapter 3: GCxGC for Fischer–Tropsch Product Analysis**

---

Alcohol dehydration may occur via direct monomolecular dehydration of the alcohol to an alkene or by the bimolecular dehydration to the ether. Methanol cannot be dehydrated because it only contains one carbon atom; it can only be converted to the ether by bimolecular dehydration. The opposite reaction, the hydration of alkenes to alcohols, is also valuable in FT refining, for example, in the hydration of ethylene to ethanol.

Alkene oligomerisation, the polymerisation of two to ten monomers, is used in HT–FT plants to convert gaseous alkenes into the liquid phase. Short–chain hydrocarbons have relatively good octane numbers but their presence in gasoline is limited by the specification on the vapor pressure of the fuel. Different commercial oligomerisation processes are available.

The catalytic polymerisation (CatPoly) technology of Universal Oil Products (UOP) uses a solid phosphoric acid catalyst supported on an inactive silica support [5,6]. The operating temperature and amount of water in the feed determines the ratios of the different phosphoric acid species in the catalyst, which in turn determines its activity and selectivity behaviour [7,8]. At least some of the alkenic gasoline produced by this process has to be hydrogenated to meet the alkene specification of gasoline.

---

## Chapter 3: GCxGC for Fischer–Tropsch Product Analysis

---

### 3.2 Comprehensive two–dimensional gas chromatography for the analysis of Fischer–Tropsch oil products<sup>1</sup>

#### 3.2.1 Introduction

The Fischer–Tropsch (FT) process is a polymerisation reaction that produces a vast number of compounds over a wide carbon number range. During product work–up, more than 200 industrial chemicals are produced in addition to various grades of fuels (petrol, diesel, jet fuel, etc.) [1]. The fuels are practically free of sulphur– and nitrogen–containing compounds, which make them environmental friendly compared to crude oil derivatives. FT products are distributed over a number of phases. For high temperature processes (HT–FT, with reactor temperatures between 300 °C–380 °C), products are spread over gas, oil and water phases with only small amounts of wax formed. For low temperature processes (LT–FT, reactor temperatures between 200 °C and 250 °C), the average chain length of the product is higher and more waxes are produced. The analysis of any one of these phases is very challenging. This study addresses the analysis of the complex oil products.

The FT product spectrum is dependent on reaction variables such as the reactor system used, temperature, pressure, catalyst formulation, etc. LT–FT processes result in a relatively un–complicated product spectrum with comparatively high average carbon numbers (up to around C<sub>120</sub>) and mostly linear primary FT products. For HT–FT a more complex product is obtained. At elevated reaction temperatures the reaction rate increases and the average chain length of the molecules is reduced with a corresponding increase in methane formation. Secondary product formation (a result of primary FT products that re–adsorb on the catalyst surface and undergo further reaction) is enhanced, resulting in much higher complexity due to the presence of thousands of secondary reaction products at trace levels.

---

<sup>1</sup> R. van der Westhuizen, R. Crous, A. de Villiers, P. Sandra, J. Chromatogr. A 1217 (2010) 8334.

### Chapter 3: GCxGC for Fischer–Tropsch Product Analysis

---

Fundamental studies are aimed at understanding the reactions that take place at the catalyst surface with the ultimate goal of optimizing FT processes. Predictive models were developed to estimate consumption of reactants and the distribution of products with variables such as temperature, partial pressures, catalyst promoter content, etc.

Kinetic models are used to predict the consumption of reactants, whereas selectivity modelling is used to describe the product distribution [2].

Complete predictive models for FT product distributions are not available. The Anderson–Schulz–Flory (ASF) model is a mathematical model for homogeneous polymerisation that has been formulated by Schulz [9] and Flory [10] and extended for chain branching by Friedel and Anderson [11]. This model is often used to characterise FT products and several studies have shown that the FT product spectrum approximately follows this model, although with some deviations [12–14]. According to this model, product distributions can be described by a single parameter namely the chain growth probability  $\alpha$ :

$$\frac{S_n}{n} = \alpha^n \frac{(1-\alpha)^2}{\alpha} \quad (1)$$

$$\ln\left(\frac{S_n}{n}\right) = n \ln \alpha + \ln \frac{(1-\alpha)^2}{\alpha} \quad (2)$$

Where  $S_n$  is the mass (weight) fraction of products with carbon number  $n$ . The chain growth probability factor  $\alpha$  reflects the probability that a molecule will continue reacting to form a longer chain.  $\alpha$  is largely determined by the catalyst and the specific process conditions. A logarithmic plot of the mass fraction per carbon number versus the carbon number will give a straight line. The  $\alpha$ -values are determined from the slopes of the plots and can vary between 0 and 1. In an ideal polymerisation reaction  $\alpha$  will be constant and independent of the carbon number. The majority of ASF plots for Fischer–Tropsch products show a nearly straight line in the region from  $C_4$  and  $C_{12}$ . A break in the ASF trend line in the region  $C_{12} - C_{13}$  has been observed with either higher or lower  $\alpha$ -values for longer chain products.

### Chapter 3: GCxGC for Fischer–Tropsch Product Analysis

---

In addition, deviations from linearity have also been noted in the  $C_1$ – $C_3$  range i.e. methane levels are normally higher and  $C_2$  compounds lower than predicted. Various studies aiming to explain these deviations are often contradictory [12–24].

Until now, one–dimensional GC (1D–GC) was exclusively used in studies of FT selectivity models and their deviations [8,19,20,22,23,25–27]. A number of authors have questioned the accuracy of the GC results used, although no systematic investigation of this aspect has been reported. 1D–GC, even using the most recent high–efficiency capillary columns, provides peak capacities in the order of ~500–600 [28]. For highly complex samples such as HT–FT products, with components present at low ppm (mg/kg) levels, the data used for these studies (and the accuracy of the models themselves) are therefore questionable. Comprehensive two–dimensional GC (GCxGC) provides a number of advantages compared to 1D–GC. Peak capacities for GCxGC are in the order of tens of thousands (the product of the peak capacities of two columns of different selectivity). Moreover, peaks are often arranged in highly ordered and structured plots, where peaks belonging to homologous series are positioned along straight lines on the retention plane. GCxGC is therefore extensively used to characterise petroleum fractions [29–32]. High peak capacity and ordered plots should result in much better quantification compared to 1D–GC to construct ASF selectivity models. To the best of our knowledge, a comparison of 1D–GC and GCxGC in this respect has not yet been reported.

An additional benefit of GCxGC is an increase in sensitivity (up to ten–fold) compared to 1D–GC. This is a result of the very fast separation achieved in the second dimension column that minimises peak broadening and effectively increases the signal–to–noise ratio [31,33]. The sensitivity issue is of less of importance for LT–FT product characterization as the oils consist of only a few hundred, mainly linear primary FT components at percentage levels. On the other hand, sensitivity is of utmost importance for the analysis of HT–FT oils where the highly complex product spectrum contains thousands of primary and secondary components. Moreover, several components or compound classes are only present at trace levels but their presence and quantities are extremely important to optimise and fine–tune the FT process and to study their formation (primary or secondary FT product).

## Chapter 3: GCxGC for Fischer–Tropsch Product Analysis

---

In a Chapter 5.3, we described the characterization of dienes in an HT–FT derived product by GCxGC–TOF–MS. Dienes are prone to polymerisation by Diels–Alder reactions and dimers and trimers were detected in the 2–D plot by operating the MS in the ion extraction mode [34]. Polymerisation is thought to be partially responsible for gum formation in HT–FT–derived products. The analyses of aromatic precursors and aromatic sub–classes and of oxygenates in HT–FT products by GCxGC are presented. Both classes could not be studied in the past because of a high degree of peak overlap in 1D–GC.

Lab–scale micro–FT–reactor experiments are described to illustrate the use of GCxGC to monitor the formation of both classes in function of the temperature.

### 3.2.2 Experimental

#### 3.2.2.1 Samples and reactor experiments

The LT– and HT–FT samples were experimental samples from Sasol Technology R&D, Sasolburg, South Africa. Laboratory–scale micro–FT–reactor experiments were performed at constant pressure and feed gas ratios. Experiments were performed at reaction temperatures of 320 °C, 350 °C and 380 °C. Samples of the oils were taken offline from heated knock–out pots.

#### 3.2.2.2 Analytical conditions

1D–GC analyses were performed on a 7890A Gas Chromatograph equipped with a 5975 inert mass selective detector (MS) and a flame ionisation detector (FID) from Agilent Technologies (Little Falls, DE, USA). The MS was used for identification purposes and the FID for quantification. A 30 m x 250  $\mu\text{m}$  ID x 1  $\mu\text{m}$   $d_f$  HP–1 (Agilent Technologies) was used with a temperature program of 40 °C (0.2 min), ramped at 2 °C/min to 350 °C. A constant helium gas flow of 1.2 mL/min was maintained with a split ratio of 100:1. The injection volume was 0.1  $\mu\text{L}$ .

## Chapter 3: GCxGC for Fischer–Tropsch Product Analysis

---

GCxGC was performed using a Pegasus 4D instrument equipped with a time-of-flight mass spectrometer (TOF–MS) and an FID detector (Leco Corporation, St. Joseph, MI, USA).

The first dimension column was a 30 m x 250  $\mu\text{m}$  x 0.25  $\mu\text{m}$  RTX–Wax (Restek, Bellefonte, PA, USA) with a temperature program of 40°C (0.2 min), ramped at 3°C/min to 245°C. The second dimension column was a 1.8 m x 100  $\mu\text{m}$  x 0.1  $\mu\text{m}$  RTX–5 (Restek), and the second oven followed the first oven with a lead of 25°C. The modulation period was 7 s. The carrier gas was helium at a constant flow of 1.2 mL/min. Injection volume was 0.1  $\mu\text{L}$  with a split ratio of 400:1. TOF–MS was used for identification of compounds or selective ion extraction while the FID was used for quantification. TOF–MS and FID data were collected at 100 spectra (points)/s. To enable direct comparison of GCxGC and 1D–GC results, quantification was performed by normalization of peak areas.

Relevant response factors were used for oxygenated compounds while a response factor of unity was assumed for hydrocarbons. Quantification using GCxGC–FID data were performed using ChromaTOF software (Leco, v4.21).

### 3.2.3 Results and discussion

#### 3.2.3.1 1D–GC and GCxGC analysis of Fischer–Tropsch oils

Petrochemical products are amongst the most complex products. Blomberg et al. [29] estimated the number of compounds in a crude oil–derived middle distillate to be more than  $10^6$ . FT product streams contain alkanes and aromatics, such as in crude–derived products, but additionally contain alkenes and oxygenates in significant amounts, but not S– and N–containing compounds.

LT–FT oils are relatively simple and composed of mainly primary linear molecules present at percentage levels and very little secondary reaction products. However, a high degree of component co–elution is already observed in 1D–GC analysis. The co–elution is not necessarily the result of the limited peak capacity of the column but rather of a shared physical property.

### Chapter 3: GCxGC for Fischer–Tropsch Product Analysis

---

For instance, if the volatility of two compounds is very close and the polarity different, they may co-elute on a column in which separation is based on volatility only, even though the total number of peaks in the sample may be much lower than the peak capacity of the column. Moreover, selectivity of a column for specific classes decreases in function of the temperature and temperature program rate. An example is shown for the analysis of a LT–FT oil on the non-polar (boiling point separation) RTX–5 column under common GC conditions (Figure 1).

For the C<sub>10</sub>–group, the 1-alkene elutes before the n-alkane followed by the cis-internal alkene and the trans-internal alkene. The cis-2-internal alkene peaks elute closer to the n-alkane peaks with increasing carbon number and from C<sub>12</sub> onwards they are completely obscured. This results in an overestimation of the alkanes and an underestimation of the internal alkenes. Branched isomers of alkanes, alkenes and oxygenates also elute in the same area of the GC chromatogram. To distinguish between these classes, it is necessary to identify each of the peaks in the chromatogram and sum them.

Especially ketones, aldehydes and acids are not easily identified because these low-level peaks also elute in the same region as branched isomers.

Co-elution of peaks occurs to an even larger extent when 1D–GC is performed on a polar column (e.g. RTX–Wax). Alkanes and alkenes elute early from these columns because of their non-polar nature and as a result their resolution is worse than obtained on a non-polar column. While the internal alkenes are separated from the n-alkanes on this column, they co-elute with the branched isomers and oxygenates. This results in overestimation of internal alkenes and underestimation of branched isomers and oxygenates. Thus even for a product containing relatively few compounds, quantitative results may differ significantly between two columns of different selectivities. In contrast, by combining the two selectivities, GCxGC provides complete separation of the different compound classes and even branched and linear isomers are separated (Figure 2). Separation in the two-dimensional separation plane occurs according to both boiling point and polarity differences, resulting in group-type separation of the different classes of compounds.

### Chapter 3: GCxGC for Fischer–Tropsch Product Analysis

GCxGC profiling of fuels is commonly performed on what is called the normal phase GCxGC mode i.e. a non-polar column in the first dimension and a polar column in the second dimension.

The reversed GCxGC mode i.e. a polar column (BPX50) in the first dimension and a non-polar column in the second dimension was used by Vendeuvre et al. [35] for better characterisation of the aromatic fraction of petroleum middle-distillates. For FT-products the highest orthogonality and by far the best class separation of alkenes, aromatics and oxygenates is obtained with a WAX column as first column as obvious from Figure 2.

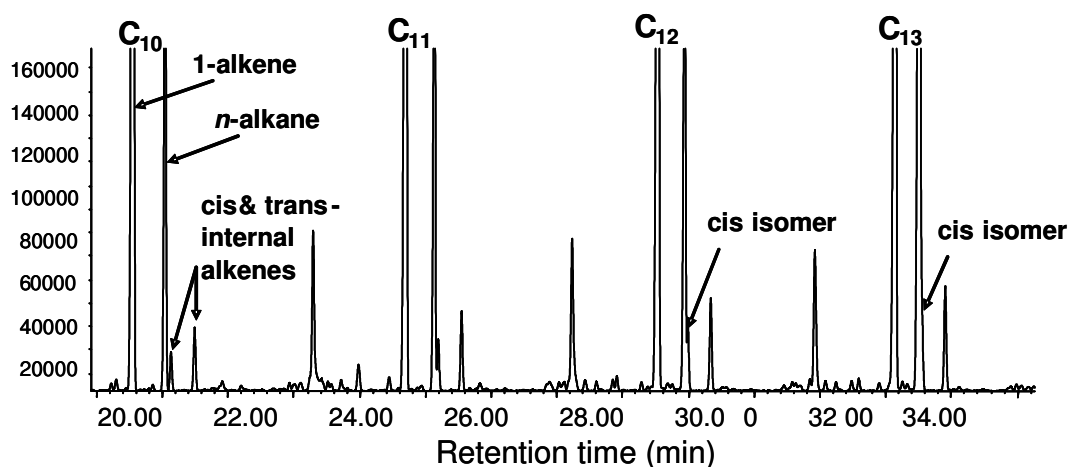


Figure 1. Part of the 1D-GC chromatogram for a LT-FT oil.

## Chapter 3: GCxGC for Fischer–Tropsch Product Analysis

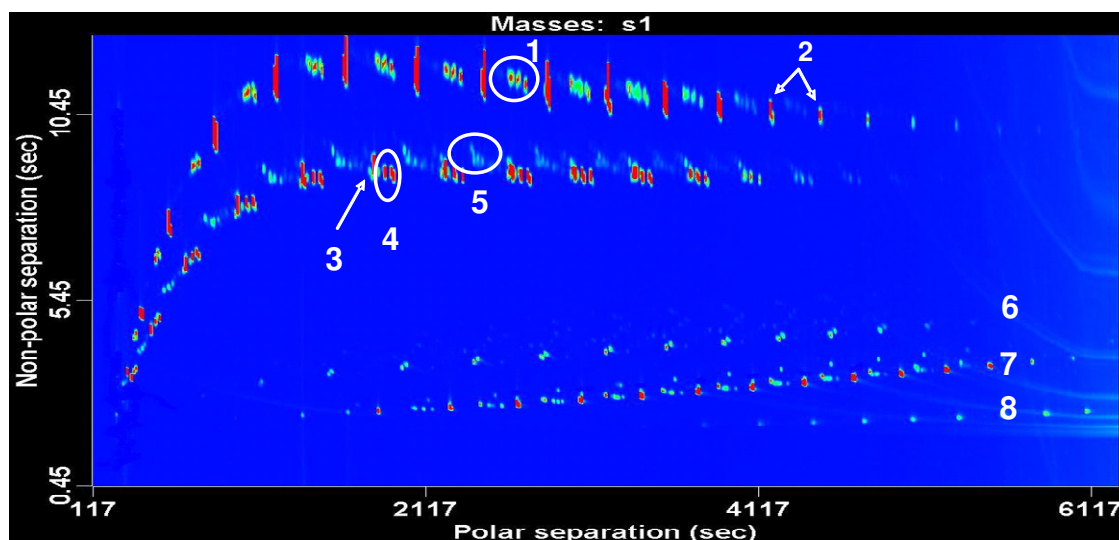


Figure 2. GCxGC–FID analysis of a LT–FT oil. Numbering: 1) branched alkanes, 2) *n*-alkanes, 3) 1–alkenes, 4) 2–alkenes, 5) branched alkenes, 6) linear and branched ketones and aldehydes, 7) linear and branched alcohols and 8) linear and branched acids.

Peak identification and accurate quantification are drastically improved by using GCxGC compared to 1D–GC because peak co–elution is significantly reduced even for relatively simple mixtures such as LT–FT oils. For HT–FT oils, more than 650 compounds can be detected by 1D–GC analysis on a 60 m non–polar capillary column but this is completely insufficient to unravel its complexity. By using a long polar column in the first dimension and a 1.8 m non–polar column in the second dimension, the peak capacity is ca. 15.000 (600 x 25) and the complete 2D separation space is utilised. The different classes of alkanes, alkenes, cyclics, aromatics, alcohols and acids are ordered as illustrated for C<sub>12</sub> in Figure 3.

### 3.2.3.2 Comparison of quantitative results of 1D–GC and GCxGC for HT–FT oil.

In 1D–GC co–eluting peaks of different carbon numbers are grouped together giving incorrect carbon number distributions. As an example, on a non–polar column separation in the region between the C<sub>7</sub> and C<sub>8</sub> *n*-alkanes, one would also find C<sub>8</sub> branched alkane and alkene compounds, C<sub>7</sub> and C<sub>8</sub> cyclic aliphatics, C<sub>5</sub> alcohols, C<sub>6</sub> ketones and aldehydes, C<sub>4</sub> acids and C<sub>7</sub> aromatic molecules.

### Chapter 3: GCxGC for Fischer–Tropsch Product Analysis

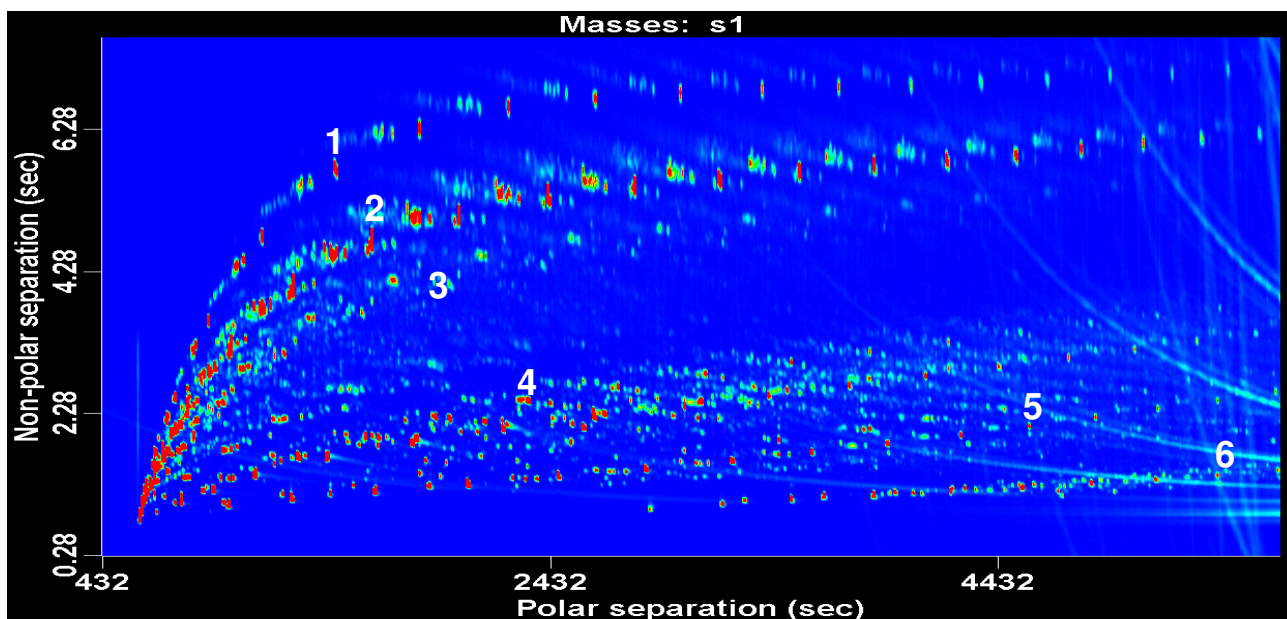


Figure 3. GCxGC–FID analysis of a HT–FT oil. Numbering: 1)  $C_{12}$  alkanes, 2)  $C_{12}$  alkenes, 3)  $C_{12}$  cyclic aliphatics, 4)  $C_{12}$  aromatics, 5)  $C_{12}$  alcohols and 6)  $C_{12}$  acids.

These peaks would be quantified together as  $C_8$  branched compounds. As a result, the total amount for a specific carbon number is either overestimated or underestimated. In contrast, in GCxGC the individual chemical classes and their branched and cyclic isomers are all separated in two dimensions and accurate carbon numbers can be assigned. A comparison of the carbon number distributions for 1–alkenes and for the total product distribution obtained by 1D–GC and GCxGC of a HT–FT oil shows a huge overestimation of  $C_5$ – $C_7$  compounds and an underestimation for higher boiling compounds by 1–D GC (Figure 4).

These quantitative differences have a strong influence on the ASF plots. Figure 5 compares the ASF plots for the 1–alkene and total product carbon distributions for 1–D GC and GCxGC data. The deviation from linearity in the  $C_1$ – $C_6$  region is because only the oil phase of the HT–FT product was analysed and the contribution of gaseous fraction excluded.

A nearly straight line is observed from  $C_7$  to  $C_{20}$  for the 1–alkenes for both methods, but with a slight offset between the two graphs. A larger deviation is noted in the lower carbon number region as a result of the overestimation of 1–alkenes by 1–D GC.

### Chapter 3: GCxGC for Fischer–Tropsch Product Analysis

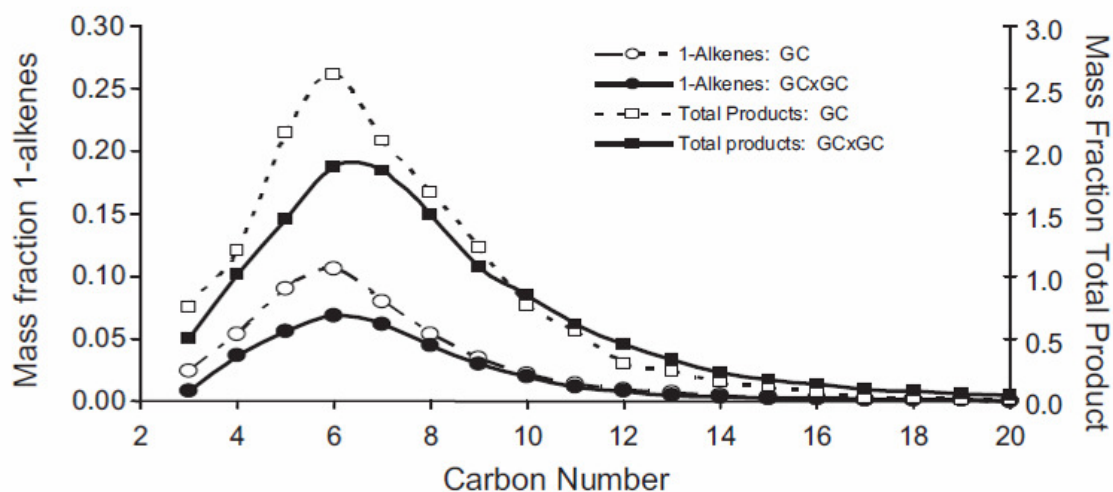


Figure 4. Comparison of the carbon distributions of the total HT–FT product and 1–alkenes obtained by 1D–GC and GCxGC.

This deviation is much clearer for the carbon distribution of the total product, where the plot shows a significant downward trend in the region  $C_7 - C_{20}$  for the 1–D GC data. Accordingly, the slopes of these graphs, which represent  $\alpha$ -values, also differ. The  $\alpha$ -value from the GCxGC analysis is 0.7458. The equation for the straight part of the line (from  $C_7 - C_{20}$ ) was  $y = -0.2933x + 2.7030$  with a  $R^2$ -value of 0.9985. The 1D–GC–data gave an  $\alpha$ -value of 0.6577 with  $y = -0.419x + 3.8942$  and  $R^2=0.9923$ .

It can be concluded that the  $\alpha$ -values traditionally used for HT–FT selectivity models and based on 1D–GC results are inaccurate. Deviations from linearity of ASF plots previously reported by various authors [12–16], can therefore at least in part be attributed to analytical error caused by the high degree of peak co–elution in the 1–D GC methods exclusively used in the past to construct ASF plots.

### Chapter 3: GCxGC for Fischer–Tropsch Product Analysis

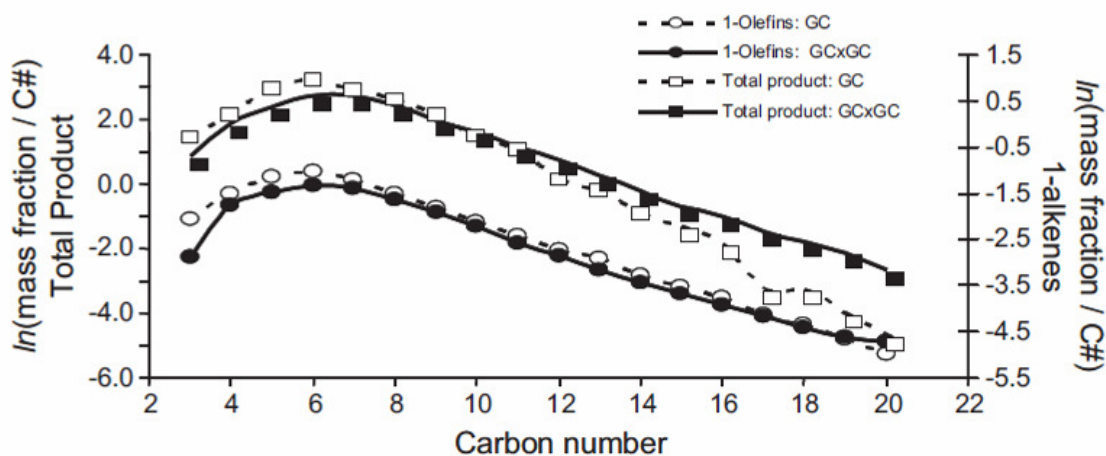


Figure 5. Comparison of ASF plots of the total HT–FT product and 1–alkenes obtained by 1D–GC and GCxGC.

#### 3.2.3.3 Application of GCxGC to follow primary and secondary product formation in HT–FT products

Primary and secondary FT product formation is of utmost importance to optimise FT processes and has been studied by a number of authors [8,13]. By using shorter residence times (removing products from the reactor before secondary reactions can take place) and low space velocities (the relation between volumetric flow and reactor volume), secondary reactions can be suppressed and primary FT products elucidated. In this manner, linear 1–alkenes and *n*–alkanes were identified as primary FT products, while the formation of branched hydrocarbons is believed to proceed via both primary and secondary routes. Linear alcohols and aldehydes are generally regarded as primary FT products, whereas the formation of acids and ketones are thought to be either primary or secondary reactions [2]. Alkene co–feeding studies have indicated that alkenes can act as chain initiators and that double bond shifts of 1–alkenes can occur [36–41]. Alkenes can re–adsorb on the catalyst surface and undergo secondary reactions such as hydrogenation, hydroformylation, hydrogenolysis, etc.

### Chapter 3: GCxGC for Fischer–Tropsch Product Analysis

---

Such as the alkenes, alcohols can re-adsorb on the catalyst surface and undergo secondary reactions. Alkanes and alkenes are dehydrogenated to form aromatics in secondary reactions at the severe conditions of the HT–FT process [2]. Very little information is available in the literature regarding the nature and formation of aromatics and oxygenates.

The general trend in FT processes is that with increasing reaction temperature, an increase in degree of branching, cyclization and formation of aromatics, is observed with a corresponding decrease in total aliphatic content. At HT–FT reaction conditions, more than half the product spectrum can be of a secondary nature. GCxGC in combination with a lab-scale micro reactor is particularly useful to monitor the evolution of secondary products as a function of reaction conditions, since this cannot be done accurately using conventional 1–D GC methods.

Valuable new information was obtained from GCxGC data regarding aromatics in HT–FT products. The aromatic pre-cursor groups of cyclic alkenes, dienes and cyclic dienes, as well as aromatic sub-classes of mononuclear and binuclear aromatics are separated by GCxGC. Higher polyaromatic hydrocarbons are not present in FT products in significant amounts.

The procedure to analyze aromatic precursors and the corresponding formed aromatic compound is illustrated with C<sub>7</sub> (Figure 6A). An ion extracted chromatogram is constructed using m/z 96 for the C<sub>7</sub>–cyclic alkenes and C<sub>7</sub>–dienes (note that both classes are separated in reversed mode GCxGC), m/z 94 for the C<sub>7</sub>–cyclic dienes and m/z 92 for the formed aromatic compound, toluene. The mass fractions in function of temperature are presented in Figure 6B. As expected, the precursors decrease and the aromatics increase in function of temperature.

The same procedure was used to elucidate all aromatic substances in HT–FT oil and on constructing the distribution curve for total mononuclear aromatics, an interesting observation was made that would not have been possible without the help of GCxGC. As opposed to the normal distribution usually found for all other component classes in FT products, two maxima were noted in the distribution curve.

### Chapter 3: GCxGC for Fischer–Tropsch Product Analysis

Figure 7 shows the curves for the total aromatic mass fraction together with the curves for the most abundant classes i.e. the alkyl benzenes, the cyclic alkyl benzenes and the alkenyl benzenes.

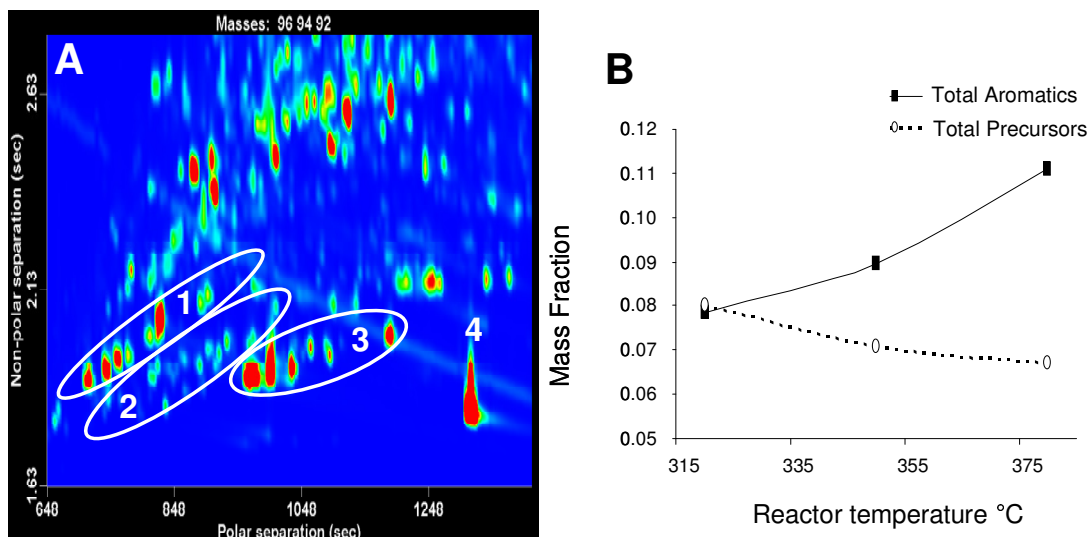


Figure 6. A. Extracted ion contour plot for the C7 aromatic precursors (1, 2 and 3) and toluene(4); B. Evolution of total aromatics and aromatic precursors as a function of reaction temperature.

Further investigation showed that aromatic sub-classes each display unique carbon number distributions, and that these are responsible for the two maxima observed in the total aromatic distribution. The first maximum is due to the alkylbenzenes and the second mainly to the cyclic alkylbenzenes and alkenylbenzenes. Such detailed information on aromatics is particularly valuable for fuels where the aromatic structure influences fuel properties such as density, cetane number, cold flow properties, etc.

In 1D-GC, low level oxygenate peaks are hidden underneath the complex hydrocarbon primary level peaks resulting in an underestimation of their mass fraction. Reversed mode GCxGC is ideally suited to separate low level oxygenated species and to study the correlation of their formation with increasing reaction temperature.

### Chapter 3: GCxGC for Fischer–Tropsch Product Analysis

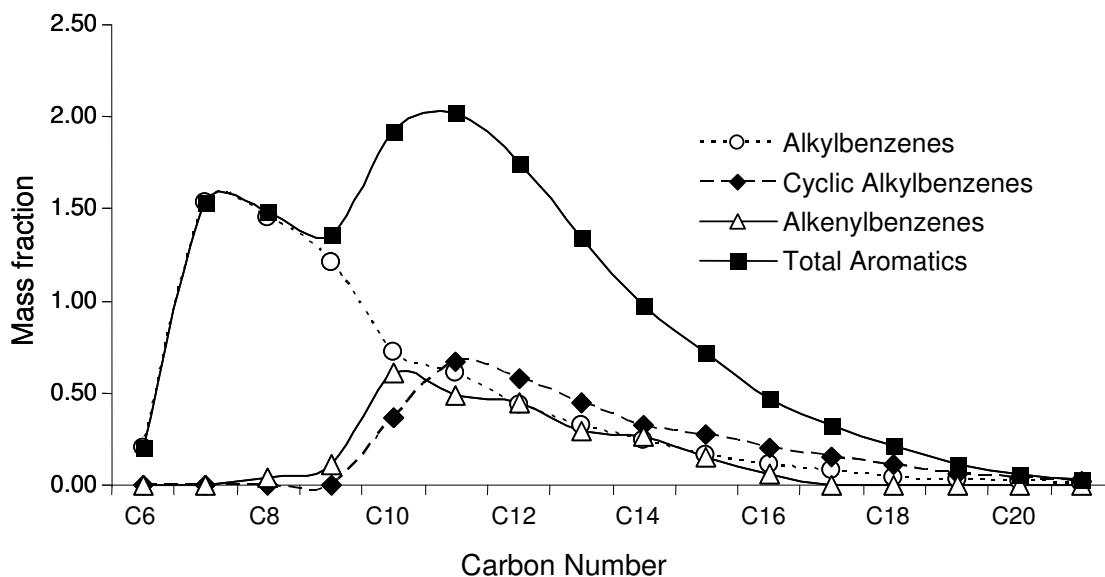


Figure 7. The mononuclear aromatic distribution of an HT-FT oil.

Figure 8A shows the complexity of the relevant part of the HT-FT contour plot for the alcohols, aldehydes and ketones with elucidation of the primary, branched, cyclic and secondary alcohols. For most oxygenates, such as with the aliphatic hydrocarbons, there is an increase in secondary product formation and a corresponding decrease in primary FT products with increasing temperature. Figure 8B shows the effect of reaction temperature in the range of 320 to 380°C on the alcohol fraction. The primary FT 1-alcohols and cyclic alcohols decrease in concentration while the branched and secondary alcohols increase with temperature. The observed decrease in cyclic alcohols is due to their conversion to phenols and other aromatic alcohols.

Similar trends were observed for other oxygenates. As expected, primary aldehydes decrease with increasing temperature while ketones, which are secondary reaction products, increase in concentration with increasing temperature. An increase in the formation of branched and cyclic carbonyls was also observed. Note that although the primary oxygenated products decrease with increasing temperature, the total amount of oxygenates increases.

## Chapter 3: GCxGC for Fischer–Tropsch Product Analysis

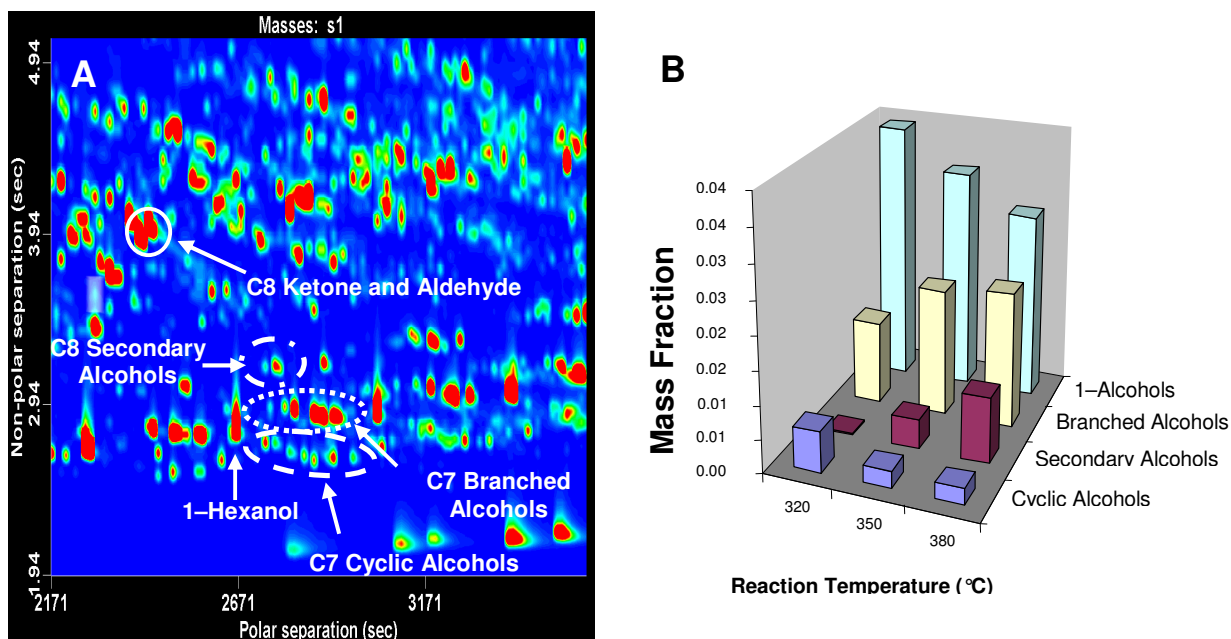


Figure 8. A. Part of the FID contour plot with the aldehydes, ketones and alcohols. B. Changes in levels of alcohols in function of temperature.

The trends for acid formation are more difficult to understand. There is an increase in the formation of branched acids with increasing temperature, but cyclic acids were not observed. Other experimental factors such as the type(s) and levels of alkali promoter as well as ageing of the catalyst are known to affect acid formation [2].

### 3.2.4 Conclusions

GCxGC in the reversed mode provides valuable information about FT products that has not previously been available. The complete two-dimensional separation plane is utilized and the different compound classes and sub-classes are separated based on both volatility and polarity differences. Quantitative data from GCxGC analysis showed that deviations from linearity in ASF plots in the region from C<sub>7</sub>–C<sub>20</sub> are based on co-elution when 1D-GC is applied.

### **Chapter 3: GCxGC for Fischer–Tropsch Product Analysis**

---

The formation of secondary reaction compounds such as aromatics could be studied by evaluating the trends in the formation of aromatic precursors and sub–classes with increasing reaction temperatures.

Two maxima in the total aromatic distribution have been detected for the first time as a result of sub–group distributions that are formed within the mononuclear aromatic class.

This would have been impossible to detect without the high peak capacity of GCxGC. Moreover, by the high sensitivity of GCxGC compounds present at trace level such as the oxygenates could be studied. The information deduced from GCxGC analyses allows the optimisation of plant conditions to produce more high–value fuels and chemicals.

## Chapter 3: GCxGC for Fischer–Tropsch Product Analysis

---

### 3.3 References

- [1] J. Collings. *Mind over Matter – The Sasol Story. A Half-century of Technology Innovation*, Johannesburg, South Africa (2002) Sasol, p 4.
- [2] A. Steynberg, M.E. Dry, *Stud. Surf. Sci. Catal.* 152 (2004) 406.
- [3] A. de Klerk, “Fischer–Tropsch Refining”, Ph.D. Thesis, University of Pretoria, 2008.
- [4] R. J. Nel, A. de Klerk, *Ind. Eng. Chem. Res.* 46 (2007) 3558.
- [5] V.N. Ipatieff, G. Egloff, *Oil Gas J.* 33 (1953) 31.
- [6] V.N. Ipatieff, B.B. Corson, *Ind. Eng. Chem. Res.* 27 (1935) 1077.
- [7] A. de Klerk, D. Leckel, N.M. Prinsloo, *Ind. Eng. Chem. Res.* 45 (2006) 6127.
- [8] A. de Klerk, Mechanism of cracking in the Synfuels catalytic cracker (SCC); Sasol internal communication. FTRC report 447/05, 2005.
- [9] G.V. Schulz, *Z. Physik. Chem.* B30 (1935) 379.
- [10] P. Flory, *J. Am. Chem. Soc.* 58 (1936) 1877.
- [11] R.A. Friedel, R.B. Anderson, *J. Am. Chem. Soc.* 72 (1950) 2307.
- [12] I. Puskas, R.S. Hurlburt, *Catal. Today* 84 (2003) 99.
- [13] H. Schulz, M. Claeys, *Appl. Catal.* 186 (1999) 71.
- [14] J. Patzlaff, Y. Liu, C. Graffmann, J. Graube, *Catal. Today* 71 (2002) 381.
- [15] R. Snel, *Catal. Lett.* 1 (1988) 327.
- [16] Y. Yang, S. Pen, B. Zhong, Q. Wang, *Catal. Lett.* 19 (1993) 351.
- [17] G. P. van der Laan, A.C. M. Beenackers, *Ind. Eng. Chem. Res.* 38 (1999) 1277.
- [18] X. Zhan, B. H. Davis, *Petrol. Sci. Technol.* 18 (2000) 1037.
- [19] Y.Ji, H. Xiang, J. Yang, Y. Xu, Y. Li, B. Zhong, *Appl. Catal. A* 214 (2001) 77.
- [20] G.P. Van der Laan, *Kinetics, Selectivity and Scale Up of the Fischer–Tropsch Synthesis*, Ph.D. Thesis, Rijksuniversiteit Groningen, 1999.
- [21] B. Shi, B. Davis, *Appl. Catal. A* 277 (2004) 61.
- [22] H. Schulz, M. Claeys, *Appl. Catal.* 186 (1999) 71.
- [23] I. Puskas, R.S. Hurlburt, *Catal. Today* 84 (2003) 99.
- [24] B. Shi, B. Davis, *Appl. Catal. A* 277 (2004) 61.
- [25] E.W. Kuipers, C. Scheper, J.H. Wilson, I.H. Vinkenburg, H. Oosterbeek, *J. Catal.* 158 (1996) 288.

### Chapter 3: GCxGC for Fischer–Tropsch Product Analysis

---

- [26] G.A. Huff, C.N. Satterfield, *J. Catal.* 85 (1984) 370.
- [27] H.G. Strenger, *J. Catal.* 92 (1985) 426.
- [28] L.M. Blumberg, W.H. Wilson, M.S. Klee, *J. Chromatogr. A* 894 (1999) 15
- [29] J. Blomberg, P.J. Schoenmakers, J. Beens, R. Tijssen, *J. High Resolut. Chromatogr.* 20 (1997) 539.
- [30] J. Beens, H. Boelens, R. Tijssen, J. Blomberg, *J. High Resolut. Chromatogr.* 21 (1998) 47.
- [31] J. Dalluge, J. Beens, U.A.Th. Brinkman, *J. Chromatogr. A* 1000 (2003) 69.
- [32] M. Adahchour, J. Beens, R.J.J. Vreuls, U.A.Th. Brinkman, *TrAC*. 25 (2006) 726.
- [33] P.J. Marriott, R. Shellie, *TrAC* 21 (2002) 573.
- [34] R. Van der Westhuizen, A. Crouch, P. Sandra, *J. Sep. Sci.* 31 (2008) 3423.
- [35] C. Vendeuvre, R. Ruiz–Guerrero, F. Bertoncini, L. Duval, D. Thiebaut, M–C. Hennion, *J. Chromatogr. A*. 1086 (2005) 21.
- [36] O. Johnston, R. Joyner, *Stud. Surf. Sci. Catal.* 75 (1993) 165.
- [37] E. Iglesia, S.C. Reyes, R.J. Madon, S.L. Soled, *Adv. Catal.* 39, 2 (1993) 221.
- [38] H. Schulz, M. Claeys, *Appl. Catal. A: Gen.* 186 (1999) 71.
- [39] J.H. Boelee, J.M.G. Custers, K. van der Wiele, *Appl. Catal.* 53 (1999) 1.
- [40] K. Fujimoto, *Topics in Catalysis* 2 (1995) 259.
- [41] H. Schulz, Zh. Nie, *Stud. Surf. Sci. Catal.* 136 (2001) 159.

# **Chapter 4**

# **GCxGC in Fischer–Tropsch Refining**

## Chapter 4: GCxGC in Fischer–Tropsch Refining

### 4.1 Introduction

The synthetic crude oil (syncrude) obtained from Fischer–Tropsch (FT) synthesis is not a final product. It has to be refined to produce useful chemicals and transportation fuels. The syncrude refining process is complex, and conventional crude oil refining technologies need to be adapted to deal with FT products. The differences in refining technologies are mostly defined by the differences between the syncrude and crude oil composition [1]. Furthermore, a distinction has to be made between FT products produced at low temperatures (LT–FT, 200°C–220°C) and high temperatures (HT–FT, 300°C–380°C) because differences in their product spectra indicates the need for different refining processes. The majority of the HT–FT product is in the gaseous, oil and aqueous phases and is distributed over lower carbon numbers ( $C_1$ – $\approx C_{30}$ ), compared to the LT–FT product, which is heavier and also contains a wax phase with carbon numbers up to  $\approx C_{100}$ . About a third of the HT–FT product is used for chemicals production; the rest is used for fuel production. The heavier LT–FT product may be cracked to provide diesel, naphtha or kerosene, or it may be processed to form high quality lubricant base oils. The waxy product may also be used to make specialty wax products.

FT product upgrading mainly involves separation and hydroprocessing. Alkenes are the main compound class in HT–FT syncrude. The LT–FT product contains less alkenes, although still significant amounts and crude oil contains no or very little alkenes. Alkenes are very valuable products and may be removed from the HT–FT synthesised light oil by fractionation or extractive distillation. For LT–FT processes, the alkene content may not be high enough to justify extraction or processing and the upgrading may then only involve hydroprocessing and separation [2]. The high alkene content of the HT–FT product is highly beneficial in chemicals production, for example, for use as intermediates in the production of detergents, synthetic lubricants, polymers, etc. Alkenes may be oligomerised, alkylated, hydroformylated, etc. Alkenes also have higher octane numbers than alkanes [3] and are therefore valuable in gasoline production, although they have lower cetane numbers and do not present an advantage over alkanes in diesel production.

## Chapter 4: GCxGC in Fischer–Tropsch Refining

---

Alkenes are reactive molecules, and especially dienes have been shown to contribute to gum formation and engine deposits [4–6] and they are therefore hydrogenated to alkanes or selectively hydrogenated to mono-alkenes during fuel production. Dienes are only formed during secondary reactions at the elevated temperatures of the HT–FT process [7]. Dienes are aromatic precursors which can be linear, branched and/or contain cyclic structures.

Significant amounts of oxygenates are formed during FT synthesis, including alcohols, carboxylic acids, ketones, aldehydes, etc. These compounds are partitioned between the oil phase and the reaction water. Only trace levels of oxygenates are found in crude oil and, except for carboxylic acids, these have little impact on transportation fuel quality or the refining process. However, oxygenates may be poisonous to the catalysts used in chemical refining processes and therefore have to be removed from the product streams. This is conventionally done by extraction or dehydration [8]. Oxygenate refining, such as alkene refining, is therefore very important in syncrude refining, while not really considered in crude oil refining [1]. Oxygenates in the reaction water are removed by distillation and extraction, and from the oil phase mainly by using liquid–liquid extraction. Valuable oxygenates are separated and processed to produce a wide range of chemicals [2], including solvents such as acetone, methyl ethyl ketone, acetic acid, etc. The rest are converted to hydrocarbons during hydrotreatment and used in fuel production.

Crude oil has a higher aromatic content than HT–FT syncrude, while LT–FT does not contain any aromatics. Benzene is carcinogenic and needs to be converted or removed from both crude oil and HT–FT products. This can be done by different means, such as benzene extraction, hydrogenation or alkylation [1]. Heavier aromatics may be responsible for engine deposit formation and increased emissions. The HT–FT product contains mainly mononuclear aromatics, with a small amount of binuclear aromatics and only traces of polynuclear aromatics. The heavy aromatic content of a fuel can be controlled by various methods, for example, by decreasing the upper boiling point (by distillation), by hydrocracking to form lower carbon number molecules, hydrogenation, etc.

## Chapter 4: GCxGC in Fischer–Tropsch Refining

---

Various sulphur and nitrogen species are present in crude oil but are removed from the fuels because they are responsible for serious environmental pollution and do not offer any advantages in terms of fuel properties. Nevertheless, trace levels of these compounds are still present in crude–derived fuels. FT products have the advantage that these heteroatoms are removed from the synthesis gas prior to FT synthesis and syncrude is therefore virtually free of sulphur– and nitrogen–containing compounds [1,2].

After the valuable chemicals have been removed, the remaining FT product is hydrogenated to remove alkenes, alkenylbenzenes and remaining oxygenates, and then fractionated into the various distillation fractions, including gasoline, kerosene, naphtha, diesel, etc. These fractions may be further upgraded using conventional refining processes.

Additional processes are also typically found in the FT refinery: Superflex™ Catalytic Cracking (SCC), where oxygenate–rich HT–FT naphtha is converted to ethylene, propylene and high–octane gasoline; alkene oligomerisation, which involves the polymerisation of two to ten monomers of C<sub>3</sub>–C<sub>5</sub> HT–FT alkenes to heavier products; and various others.

Accurate analysis of feeds and products of all of these processes is essential in order to follow the efficiency and completion of the reactions and to make adjustments to plant conditions in order to optimise the processes. These analyses can be very challenging for the highly complex FT sample mixtures. Comprehensive two–dimensional GC (GCxGC) is a valuable aid in this context because of its very high separation power and the group–type separations that can be achieved with this technique.

In this chapter, the value contributed by GCxGC in the FT refinery is illustrated by a few examples of the analysis of feeds and products of various processes. These include the investigation of the composition of gasoline formed during the SCC process and monitoring of the selective hydrogenation of the dienes formed during the process to mono–alkenes. The LT–FT feed and products of the dehydration of oxygenates to alkenes as well as the products formed during oligomerisation of a pure 1–hexene feed were also investigated.

## Chapter 4: GCxGC in Fischer–Tropsch Refining

---

A useful method by which to carry out hydrogenation in the GCxGC inlet liner, which enables quantification of alkenic compound classes that are otherwise difficult to separate, will also be discussed. Finally, GCxGC results are used to show that HT–FT diesel contains only traces of PAHs and that the addition of a 10% tar fraction increases the density of the fuel without significantly affecting the PAH content.

### 4.2 Experimental

GCxGC was performed using a Pegasus 4D instrument equipped with a time–of–flight mass spectrometer (TOF–MS) and an FID detector (Leco Corporation, St. Joseph, MI, USA). All analyses were performed using the following experimental conditions unless otherwise stipulated. The first dimension column was a 30 m x 250  $\mu\text{m}$  x 0.25  $\mu\text{m}$  RTX–Wax (Restek, Bellefonte, PA, USA) with a temperature program of 40°C (0.2 min), ramped at 3°C/min to 245°C. The second dimension column was a 2.0 m x 100  $\mu\text{m}$  x 0.1  $\mu\text{m}$  RTX–5 (Restek), and the second oven followed the first oven with a lead of 15°C. The modulation period was 10 s. The carrier gas was helium at a constant flow of 1.2 mL/min. The injection volume was 0.1  $\mu\text{L}$ , with a split ratio of 400:1. TOF–MS and selective ion extraction were used for identification of compounds while the FID was used for quantification. TOF–MS and FID data were collected at 100 spectra (points)/s.

For the inlet hydrogenation, 0.1 g of platinum IV chloride (Aldrich  $\geq$  99.99%, Sigma–Aldrich, Johannesburg, SA) was dissolved in a minimum volume of water, Five grams of Chromosorb<sup>®</sup> W AW (80–100 mesh, Supelco, Johannesburg, SA) was added. The water was removed using a rotary evaporator and the catalyst was dried under vacuum for 5 h at 120°C. Eighty milligrams of the catalyst was placed in a glass insert with a glass wool plug at either side. The insert was placed inside the GC and heated overnight at 200°C in a stream of hydrogen. An internal standard of 2.0% (m/v) 1–tert–butyl–1–cyclohexene ( $\geq$ 80%, Fluka) was used to evaluate the completeness of the hydrogenation reaction. Hydrogen was used as carrier gas for both GCxGC–TOF–MS and FID analysis. (The Leco Corporation and other experts were first consulted to ensure that hydrogen can safely be used in the TOF–MS). TOF–MS using

## Chapter 4: GCxGC in Fischer–Tropsch Refining

---

extracted ion chromatography was used to identify compound classes and the separation patterns were then transferred to the FID data for identification and quantification.

PAH analyses were performed using a method similar to that described by Cavagnino et al. [9]. A 30 m x 250  $\mu\text{m}$  x 0.25  $\mu\text{m}$  BPX50 column (SGE International, Melbourne, Australia) was used as first–dimension column with a temperature program of 80°C (0.2 min), ramped at 6°C/min to 340°C. A 1.5 m x 100  $\mu\text{m}$  x 0.10  $\mu\text{m}$  ZB–1HT Inferno column (Aschaffenburg, Phenomenex, Germany) was used in the second dimension. The second oven followed the first oven with a lead of 15°C. The modulation period was 14 s. A split ratio of 100:1 was used, and 0.5  $\mu\text{L}$  was injected. A solvent vent of 300 s was used. A 10% tar fraction from the HT–FT tar plant in Secunda, distilled between 120°C and 360°C, was added to a HT–FT diesel to investigate the effect of the addition on the PAH content of the fuel. A standard test mixture (PAH Mix 3, supplied by Sigma–Aldrich, Supelco catalog no 861291) was used for quantification. An mass of 0.1307 g of the standard was diluted to 25 mL with *m*–xylene ( $\geq 99\%$ , Sigma–Aldrich).

### 4.3 Results and discussion

The FT product spectrum is highly complex, and unlike crude oil that consists of predominantly of alkanes and aromatics, syncrude also contains large amounts of alkenes and oxygenates, which complicate analysis to a large extent. About 75–95% of FT products are aliphatic hydrocarbons, (depending on process conditions). The analysis of alkenes in the presence of alkanes in the highly complex HT–FT products is very challenging because of the large number of isomers that are possible. Alkenes may be linear, branched, or have mono– or multiple cyclic structures. While for most alkenes in FT product streams the single double bond is in the  $\alpha$  position, the double bond may also shift to internal positions and multiple double bonds may be present in some molecules, especially after some refining processes such as oligomerisation and SCC. Mass spectrometry is not always of much help to simplify analysis because it is not possible to distinguish between the mass spectra of some of these compounds. For example, cyclic alkanes and alkenes have the same molar masses and the mass fragmentation patterns are very similar.

## Chapter 4: GCxGC in Fischer–Tropsch Refining

The same applies for the cyclic alkenes and dienes, and also for the bicyclic alkenes and cyclic dienes. The excellent group–type separation obtained by GCxGC is of great help in this regard. Selected applications of GCxGC in FT refining are presented in the following sections.

### 4.3.1 Analysis of Superflex™ catalytic cracking

The Superflex catalytic cracking process (SCC) converts oxygenate–rich C<sub>6</sub>–C<sub>7</sub> HT–FT naphtha into ethylene, propylene and high–octane motor–gasoline. The aliphatic and aromatic hydrocarbons and their sub–groups in the SCC gasoline product are successfully separated on the polar x non–polar two–dimensional GCxGC separation plane (Figure 1). Aliphatics ranged in carbon numbers from C<sub>4</sub> to about C<sub>8</sub> and aromatics from C<sub>7</sub> to C<sub>10</sub>. Of interest was that some diene dimerisation had occurred. The dimers were separated from the rest of the aliphatic hydrocarbons because they are of higher carbon numbers. The dimers were predominantly formed from C<sub>5</sub> and C<sub>6</sub> conjugated and cyclic dienes. Refer to Chapter 5.3 for more information on dienes and Diels–Alder polymerisation in SCC products.

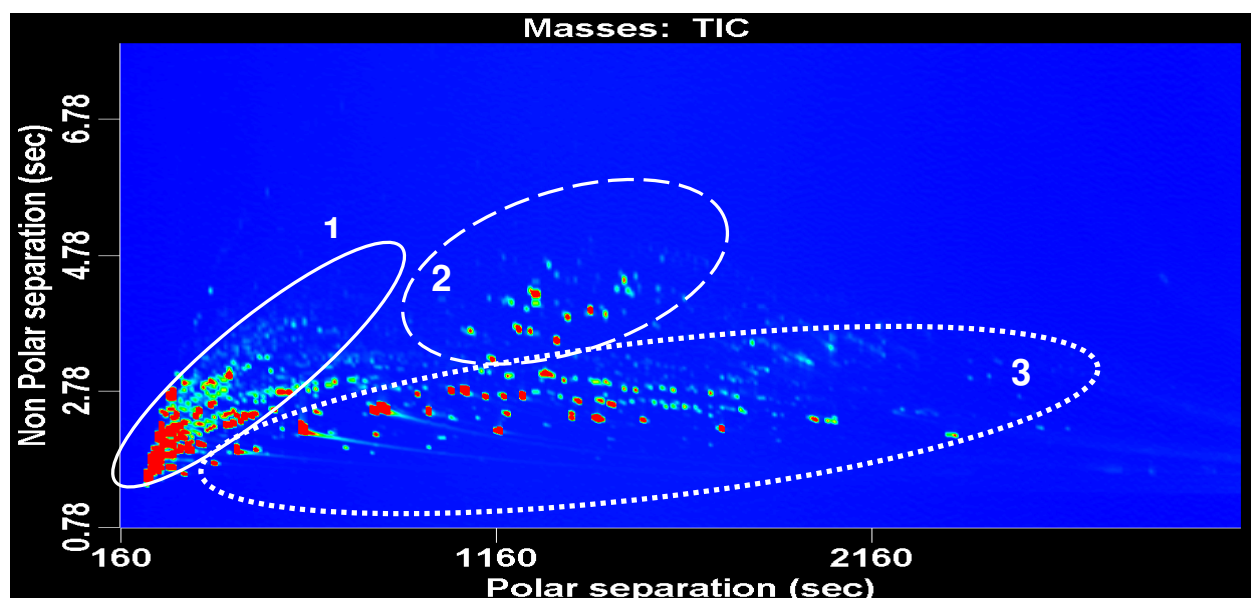


Figure 1. The GCxGC–TOF–MS contour plot shows the group–type separations obtained for the SCC product. The aliphatic hydrocarbons (1+2) are separated from the aromatics (3). Diene dimers (2) were also observed in this sample.

## Chapter 4: GCxGC in Fischer–Tropsch Refining

The excellent group–type separation obtained by GCxGC for the C<sub>4</sub>–C<sub>8</sub> alkanes, alkenes, cyclic alkenes, dienes and the cyclic dienes on the polar x non–polar 2D GCxGC separation plane proved invaluable in the investigation of the selective hydrogenation of dienes to mono–alkenes in the relatively light-boiling SCC gasoline. The effectiveness of the selective hydrogenation can be seen from the extracted ion contour plots in Figure 2.

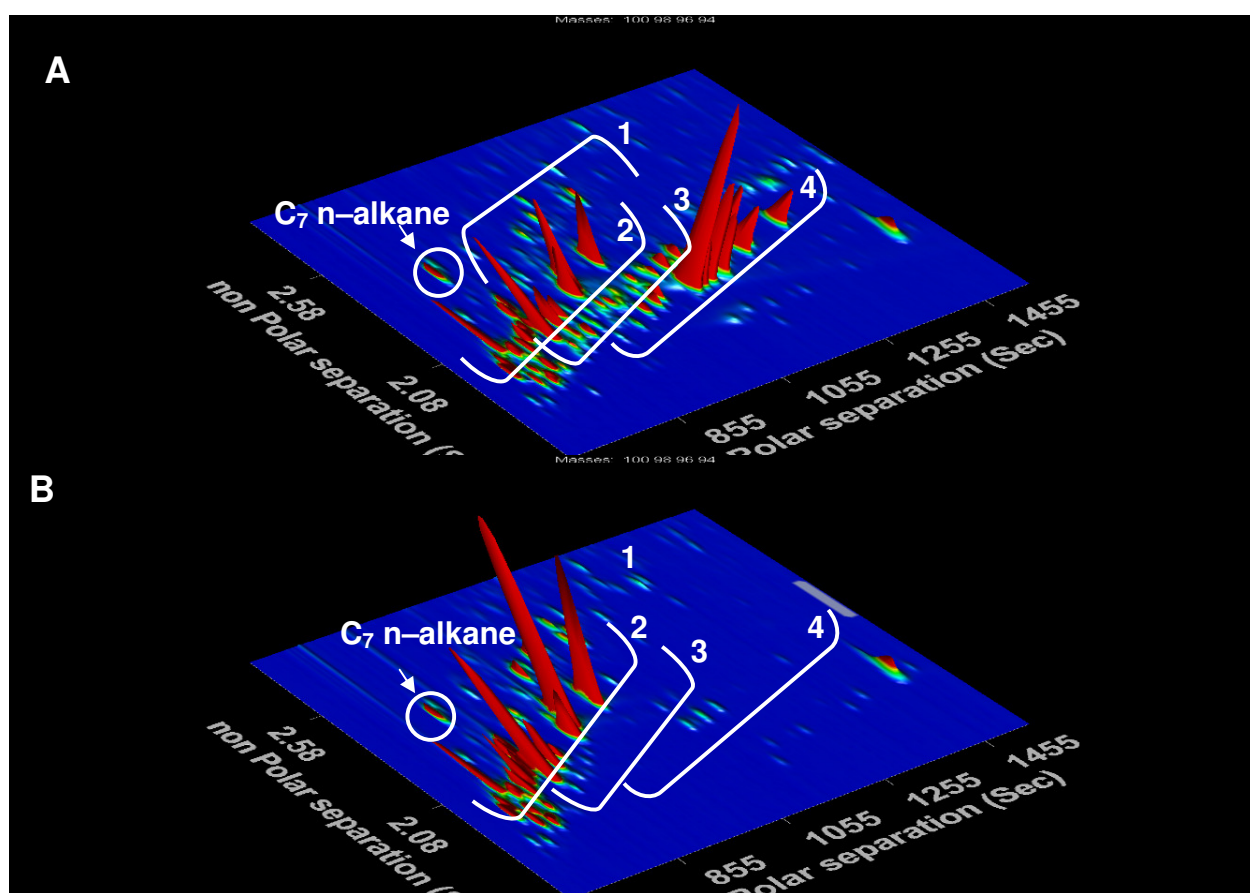


Figure 2. Extracted ion contour plots showing the efficiency of the selective hydrogenation of dienes to alkenes and cyclic dienes to cyclic alkenes. Most of the C<sub>7</sub> dienes with  $m/z$  96 (3) and cyclic dienes with  $m/z$  94 (4) in A were converted to alkenes with  $m/z$  98 (1) and cyclic alkenes with  $m/z$  96 (2) in B.

Only traces of C<sub>7</sub> dienes ( $m/z$  96) and cyclic dienes ( $m/z$  94) were still observed after hydrogenation and could be quantified.

## Chapter 4: GCxGC in Fischer–Tropsch Refining

---

This analysis provided valuable information that enabled the optimisation of plant conditions, as it allowed calculation of the temperature increase required to obtain complete hydrogenation of dienes and cyclic dienes to alkenes, while simultaneously preventing the conversion to alkanes.

### 4.3.2 Dehydration

Dehydration involves the conversion of oxygenates to alkenes by the rejection of water from the molecules. The effectiveness of the dehydration of a C<sub>10</sub>–C<sub>13</sub> LT–FT distillation cut was investigated using GCxGC. Contour plots (Figure 3) show the condensate before and after dehydration. All oxygenates were converted to alkenes, with the exception of trace levels of acids that remained in the product.

A degree of alkene dimerisation was also observed, while the 1–alkene content was found to have decreased. GCxGC results also showed that the most of the alkenic product produced by the dehydration contained internal double bonds (see Figure 4). Also of interest is that the oxygenates in the C<sub>10</sub>–C<sub>13</sub> (alkane) distillation cut were of lower carbon numbers; for example, one may find C<sub>7</sub>–C<sub>10</sub> alcohols, C<sub>8</sub>–C<sub>11</sub> ketones and aldehydes, and C<sub>6</sub>–C<sub>9</sub> acids in a C<sub>10</sub>–C<sub>13</sub> aliphatic hydrocarbon distillation cut. After dehydration, the carbon number of the alkene produced will correspond to that of the oxygenate precursor. This is evident from the increase in alkenes lighter than C<sub>10</sub> (Figure 3B).

## Chapter 4: GCxGC in Fischer–Tropsch Refining

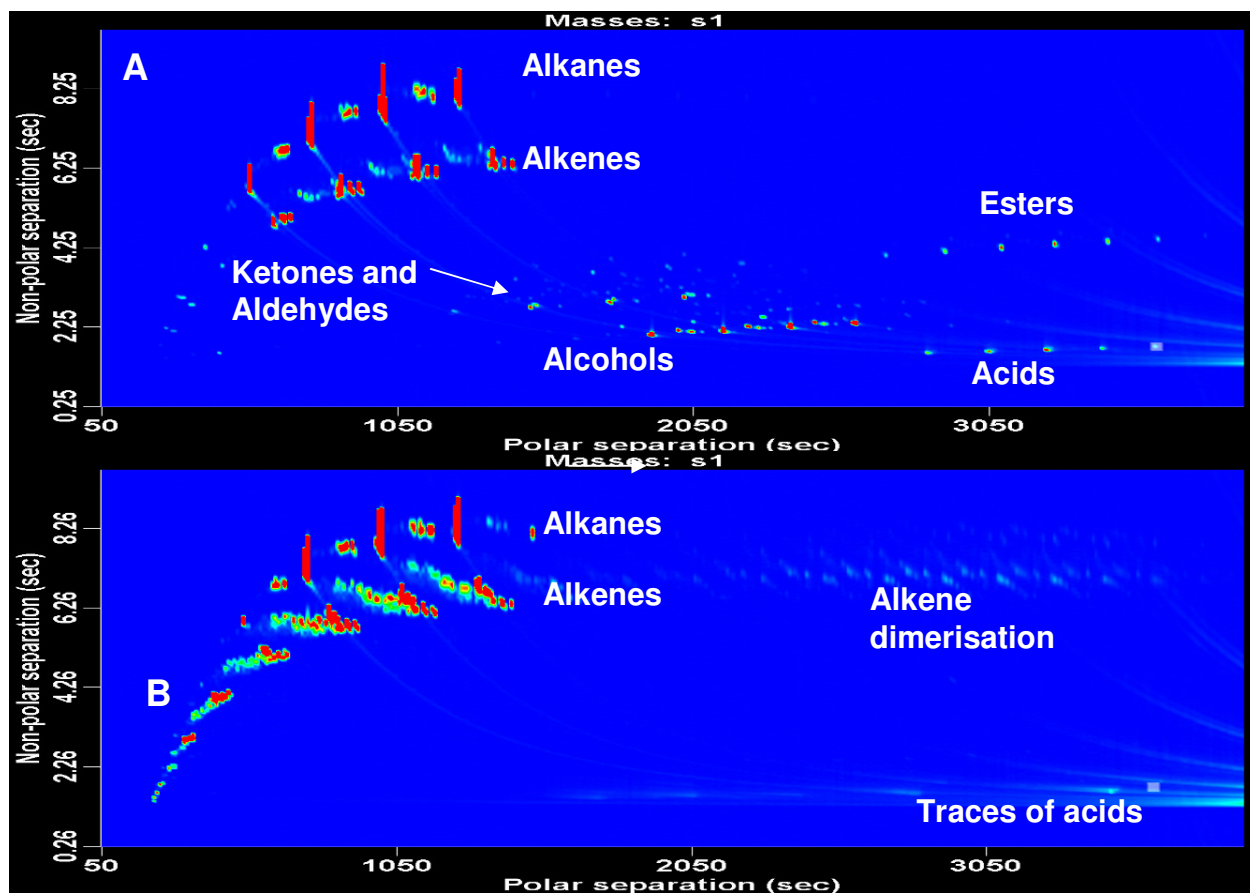


Figure 3. GCxGC–FID contour plots of the  $C_{10}$ – $C_{13}$  distillation cut of a LT–FT oil: A) before and B) after dehydration. [All oxygenates were converted to alkenes except for traces of acids.]

## Chapter 4: GCxGC in Fischer–Tropsch Refining

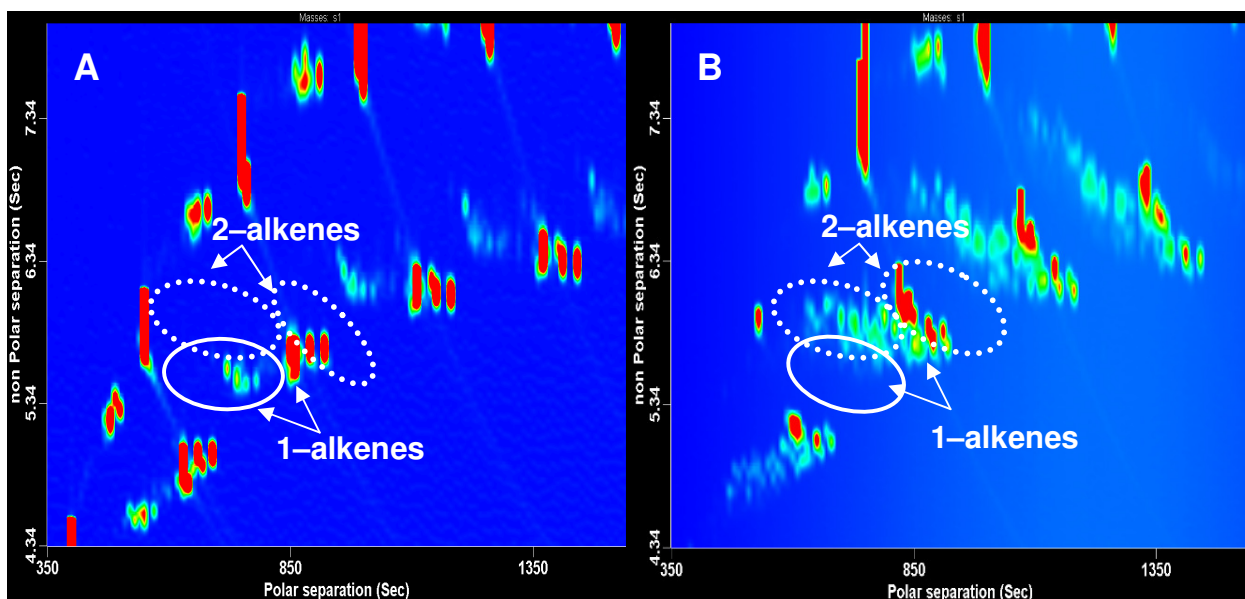


Figure 4. The LT–FT oil (A) contains branched 1–alkenes. Following dehydration of the oxygenates (B), the branched alkenes are mainly 2–alkenes.

### 4.3.3 Oligomerisation of 1-hexene using a solid phosphoric acid catalyst

Sasol uses solid phosphoric acid (SPA) oligomerisation of light alkenes ( $\approx C_3$ – $C_5$ ) to produce a highly branched aliphatic product containing higher molecular weight oligomers. The oligomerisation products are highly complex and are not sufficiently separated on a conventional GC to enable identification. Chapter 5.2 provides detailed information on the oligomerisation products of  $C_3$ – $C_5$  alkenes. This work showed that even GCxGC could not provide clear separation of the various compound classes, and an HPLC fractionation procedure was required prior to GCxGC analysis to separate the compound classes in the complex mixture. The presence of cyclic compounds in the  $C_3$ – $C_5$  alkene oligomerisation product was unexpected. As the kerosene cut (hydrogenated) of this product is a component of fully synthetic jet fuel, it was important to further investigate the source of the cyclic compounds. Questions were raised as to whether the cyclics were the result of the oligomerisation reaction temperature or some trace level contamination in the HT–FT feed.

## Chapter 4: GCxGC in Fischer–Tropsch Refining

---

Experiments were therefore performed to investigate the oligomerisation reaction of pure 1–hexene on the solid phosphoric acid catalyst at reaction temperatures of 100°C and 250°C. GCxGC results clearly show that the complexity of the oligomerisation product increases with increasing reaction temperature. At 100°C reaction temperature, mainly C<sub>12</sub> alkenic dimers were formed, in addition to C<sub>18</sub> trimeric and traces of the C<sub>24</sub> tetrameric species which were also observed. Some fragmentation of the polymers occurred and compounds ranging in carbon numbers from C<sub>10</sub> to C<sub>14</sub> and again from C<sub>16</sub> to C<sub>19</sub> were also identified. A small amount of C<sub>12</sub> cyclic alkenes and/or dienes (these compounds could not be distinguished since they have identical mass spectra, see Chapter 5.2) and also some aromatics were formed. At the higher reaction temperature of 250°C a wider distribution of products was observed; there were more cyclics/dienes and aromatics, and an increase in fragmentation. Products were distributed over more than twelve carbon numbers, with a relatively large amount of aromatics. The GCxGC contour plots in Figure 5 compare the diesel fractions of the oligomerisation products obtained from pure 1–hexene at reaction temperatures of 100°C and 250°C, respectively. While the dimers have molecular masses of 168 mass units, the GCxGC extracted ion plot for the product at reaction temperature 250°C also showed the presence of compounds with masses of 166 and also small amounts of 164 dalton molecules. These masses correspond with the presence of C<sub>12</sub> mono–alkenes (m/z 168), cyclic alkenes or dienes (m/z 166), and also bicyclic alkenes or cyclic dienes (m/z 164).

## Chapter 4: GCxGC in Fischer–Tropsch Refining

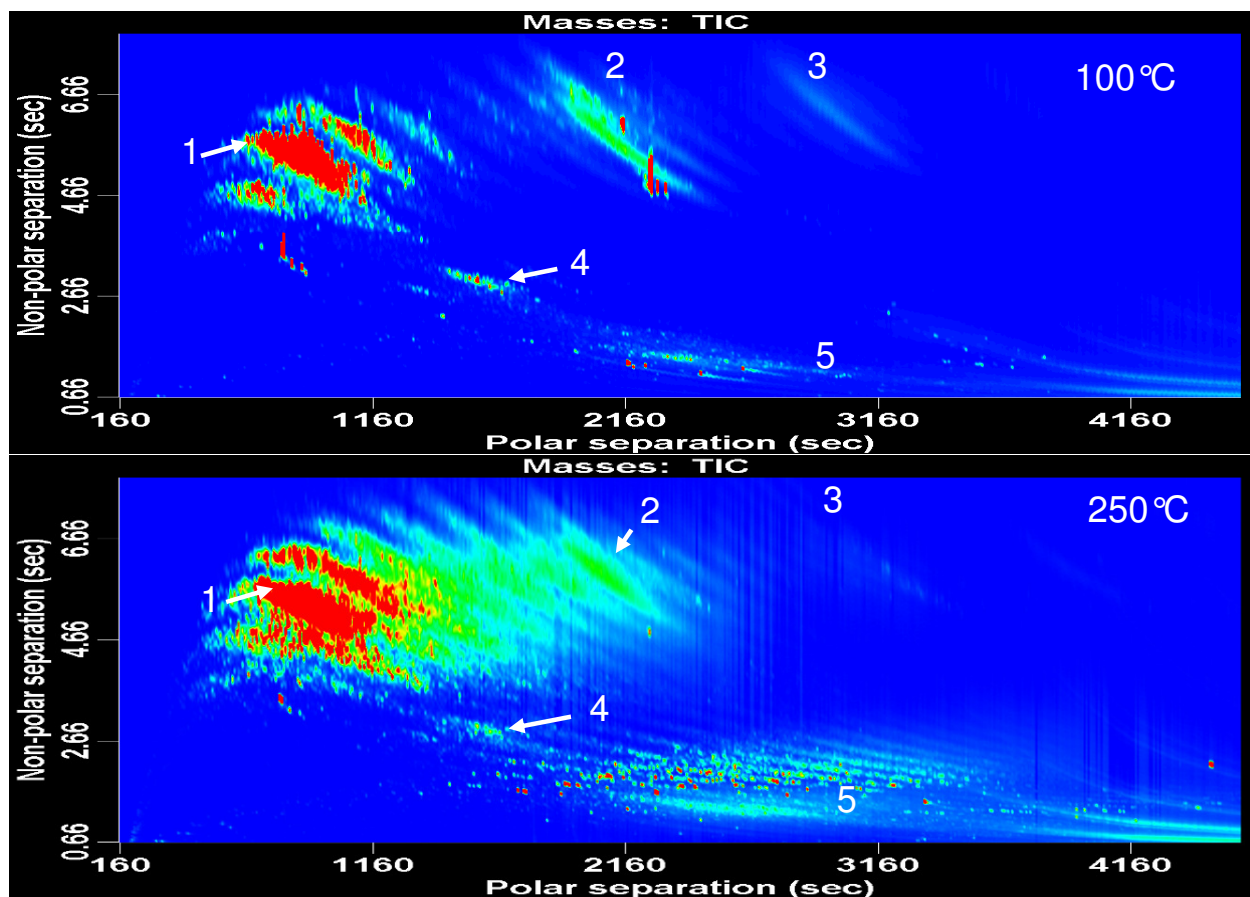


Figure 5. GCxGC–TOF–MS contour plots obtained for the analysis of diesel fractions of oligomerisation products of 1–hexene formed at 100 °C and 250 °C. The principal products are  $C_{12}$  dimers (1), but with increasing temperature a wider distribution of products was observed. An increase in cyclics (4) and aromatic (5) formation occurred at 250 °C, while  $C_{18}$  trimers (2) and  $C_{24}$  tetramers (3) were formed at lower concentrations.

## Chapter 4: GCxGC in Fischer–Tropsch Refining

---

### 4.3.4 GCxGC inlet hydrogenation

In cases where the distinction between aliphatic compound classes is not very clear from the GCxGC contour plot, and the amount of sample is too small for fractionation, it may be useful to fully hydrogenate the compounds to form the corresponding alkane isomers. Subsequent comparison of results before and after hydrogenation allows elucidation of the exact chemical profile of the sample. It is, however, impractical to hydrogenate samples on plant-scale for the purpose of a few analyses only, especially when the reactions were performed in the laboratory and only small amounts of sample are available. A valuable method was developed to perform hydrogenation in a GC inlet liner [10] and this method was applied to the GCxGC separation. Hydrogenation in the GC inlet has the advantage that only the injected volume is hydrogenated. Only a very small amount of sample is therefore needed, the sample in the GC vial does not change and can be used repeatedly. This method was applied to the 1-hexene oligomerisation samples to aid with the distinction between cyclic alkene and diene compound classes.

The hydrogenation reactivity decreases in the order dienes > mono-alkenes > cyclic alkenes > aromatics. It can therefore be assumed that after all the aromatics have been hydrogenated, the hydrogenation reaction was complete. For this reason, a C<sub>10</sub> cyclic alkene was added as internal standard to each sample to measure the completeness of the hydrogenation reaction. The internal standard, 1-tert-butyl-1-cyclohexene (≥80% purity) also contained some C<sub>10</sub> cyclic alkene isomers as impurities which showed as multiple peaks on the GCxGC contour plot (Figures 5 and 6). Identification of compounds had to be done by extracted ion chromatography (EIC) because the complexity of the products was such that the separation between compound groups could not be clearly distinguished on the two-dimensional separation plane. The separation pattern observed for the TOF-MS separation was then transferred for identification of the FID data and subsequent quantification. The alkenic oligomerisation products contained mono-alkenes, dienes/cyclic alkenes, bicyclic alkenes/cyclic dienes (negligible amounts) and aromatics: these groups were quantified by GCxGC-FID analysis of the product before hydrogenation (bh).

## Chapter 4: GCxGC in Fischer–Tropsch Refining

After hydrogenation (ah), the mono-alkenes and non-cyclic dienes were converted to alkanes while the cyclic alkenes, cyclic dienes and aromatics were converted to cyclic alkanes (Figure 6). The non-cyclic diene content was then calculated by subtracting the mono-alkene content from the total alkane content of the hydrogenated product, while the sum of the cyclic alkene and cyclic diene content was determined by subtracting the aromatic content from the total amount of cyclic alkanes in the hydrogenated product. (The negligible amount of cyclic dienes could not be distinguished from the cyclic alkenes in the hydrogenated product because both compound classes were converted to cyclic alkanes.)

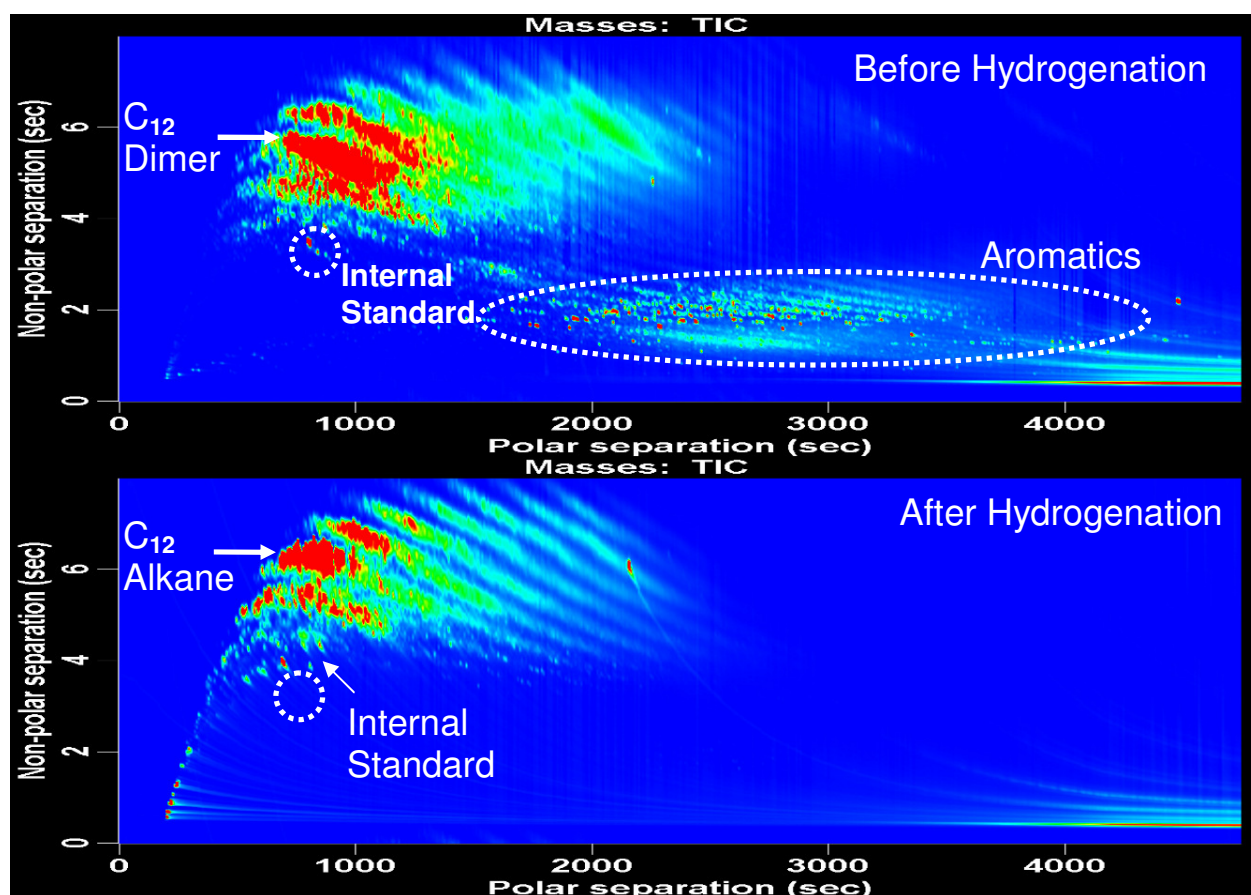


Figure 6. GCxGC–TOF–MS contour plots of the SPA–catalysed 1–hexene product oligomerised at 250 °C before and after hydrogenation demonstrating the complete hydrogenation of the aromatics and cyclic internal standard in the GC inlet liner. The multiple peaks for the internal standard are from the hydrogenation of cyclic alkene impurities to cyclic alkanes.

## Chapter 4: GCxGC in Fischer–Tropsch Refining

---

The completeness of the hydrogenation reaction was demonstrated by the absence of aromatics and the complete conversion of the internal standard to the corresponding cyclic alkane in the hydrogenated product. Normalised results are tabulated in Table 1. It is clear that cyclics formation is a function of reaction temperature and that more cyclics are formed at higher reaction temperatures.

**Table 1: Normalised results obtained by GCxGC–FID, using GC inlet hydrogenation, for the composition of oligomerisation products of 1–hexene over a SPA catalyst at reaction temperatures of 100 °C and 250 °C**

Reaction temperature	Mono-alkenes (bh)	Non-cyclic dienes	Cyclic alkenes and cyclic dienes (negligible)	Aromatics	Light material (residual hexene feed)	Total
		Calculated: total alkanes (ah) – mono-alkenes (bh)	Calculated: cyclic alkanes (ah)–aromatics (bh)	Calculated: (bh)	Material < C7	
°C	Mass %	Mass %	Mass %	Mass %	Mass %	Mass %
100	86.21	6.52	1.32	4.48	1.48	100.00
250	57.86	9.46	16.14	14.78	1.77	100.00

## Chapter 4: GCxGC in Fischer–Tropsch Refining

---

### 4.3.5 PAH compounds in HT–FT diesel

Aromatics are the compound class that contributes most to fuel density. Higher fuel density increases the power output of a vehicle's engine per unit of diesel fuel consumed. However, certain aromatics, especially some polycyclic aromatic hydrocarbons (PAHs), are carcinogenic and contribute to particulate emissions that are harmful to the environment. In South Africa, the PAH content in diesel is controlled through distillation parameters such as distillation temperatures, T85 and T95 (the temperatures at which 85% and 95% of the diesel evaporates, respectively). The European specification EN590 on PAH content in diesel fuels is currently set at 11% m/m, although this will probably be reduced to 8% in the near future. It is important to maintain a balance between optimal engine performance and the lowest possible environmental risk.

The aromatic content of FT products is dependent on reaction conditions, such as the catalyst used and the reaction temperature. In general, an increase in aromatic content is observed with increasing FT reaction temperature. No aromatics are formed during LT–FT synthesis, but for HT–FT synthetic crude the aromatic content may be in the range between 8–12%, of which only trace levels are PAHs.

Because diesel derived from the synthetic crude has a lower aromatic content compared to crude-derived diesel, these fuels sometimes struggle to meet the diesel density specification. The density can be increased by various methods, for example, by blending with a fuel of higher density, by aromatisation processes, or by addition of a heavy fraction such as a tar distillate.

Tar is a residue product of coal gasification and is rich in aromatics that could improve the density of the FT diesel. In this study, the effect of the addition of a 10% tar fraction (120°C–350°C) on the PAH content of a HT–FT diesel was investigated.

The choice of a GCxGC column set for an application is dependent on the nature of the analytes that have to be determined.

## Chapter 4: GCxGC in Fischer–Tropsch Refining

---

While a polar x non-polar column combination provides the largest separation space on the GCxGC separation plane for aliphatic hydrocarbons, a non-polar x polar column combination provides improved separation of PAHs.

To enable the elution of the high molecular mass PAHs in the diesel blends and the PAH standard it was necessary to use columns that could withstand higher temperatures. The maximum temperature limit for the polar column in any GCxGC column set is normally the limiting upper temperature that can be used. Maximum temperatures for polar columns are typically limited to  $\approx 260^\circ\text{C}$  for polyethylene glycol columns and  $\approx 280^\circ\text{C}$  for cyanopropyl columns. For this reason, a polar column is often substituted by a mid-polarity column that can withstand temperatures up to  $\approx 370^\circ\text{C}$  [9]. However, the separations obtained on a mid-polarity column (based on both boiling point and polarity) and a non-polar (boiling point separation) columns are no longer independent, and therefore not orthogonal. Thus the orthogonality is sacrificed to obtain separation of higher carbon numbers.

To analyse higher carbon numbers, shorter first-dimension columns are typically used. Dutriez et al. [11] combined a 10 m DB1-HT column (J&W Scientific) with a 1 m BPX-50 (SGE) mid-polarity column and were able to separate hydrocarbons up to  $\text{C}_{60}$  in vacuum gas oil. There is a trade-off, however: the longer the  $^1\text{D}$  column (for the same  $^2\text{D}$  column), the more theoretical plates and the better the resolution. Therefore, longer  $^1\text{D}$  columns are required to improve resolution, while for the analysis of higher carbon numbers shorter columns are required. Our goal was to obtain maximum resolution for the analysis of carbon numbers up to about  $\text{C}_{40}$ . We therefore combined a 30 m BPX-50 column with a 1 m non-polar ZB-1HT Inferno column and achieved excellent separation of the aliphatic hydrocarbons up to  $\approx \text{C}_{40}$ . GCxGC contour plots comparing the PAH content for a HT-FT diesel, the 90% HT-FT-diesel, 10% tar fraction, and the commercial PAH standard are compared in Figure 7.

Following addition of the tar fraction to the HT-FT diesel, the density of the fuel increased by 0.03 kg/L, while the PAH content increased from 20  $\mu\text{g}/\text{mL}$  to 30  $\mu\text{g}/\text{mL}$ .

## Chapter 4: GCxGC in Fischer–Tropsch Refining

---

This is still well below the PAH content of most crude–derived diesels. Figure 7 shows the main PAHs that were introduced to the diesel were phenanthrene and anthracene.

Although these two compounds are also suspected to be harmful to the environment, none of the known carcinogens benzo(a)anthracene ( $m/z$  228), benzo(a)pyrene ( $m/z$  252), benzo(b)fluoranthene ( $m/z$  252), benzo(k)fluoranthene ( $m/z$  252), chrysene ( $m/z$  228), dibenzo (a,h) anthracene ( $m/z$  287), and indeno (1,2,3–cd) pyrene ( $m/z$  276) were found in the diesel blend. Thus, even though the PAH content of the HT–FT diesel increased with the addition of a 10% tar fraction, it was still well below all fuel specifications, while the density of the blend increased significantly.

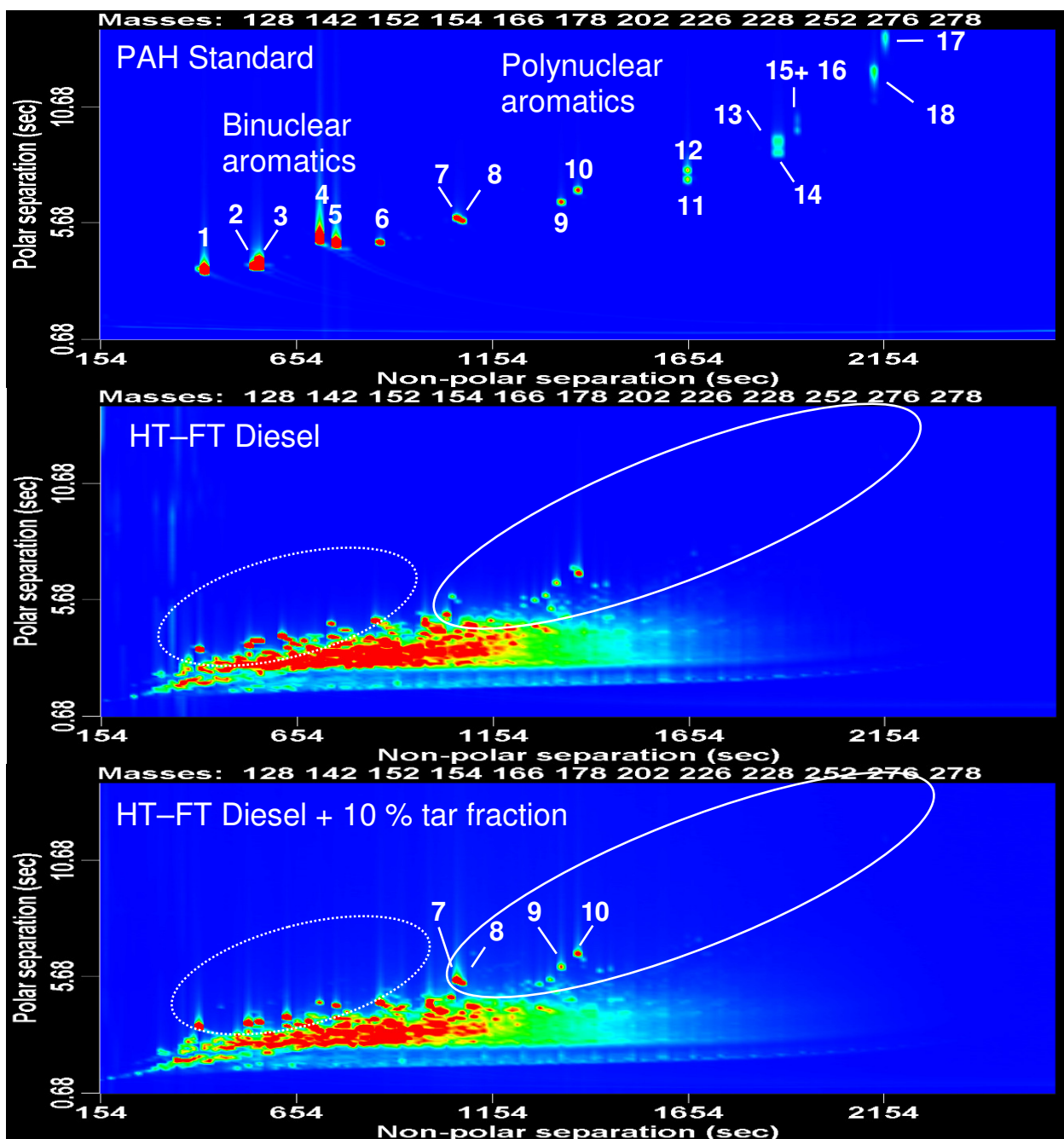


Figure 7. Extracted ion GCxGC-TOF-MS contour plots for the analysis of PAHs in HT-FT diesel, a diesel/10% tar blend and a standard test mixture containing (1) naphthalene, (2) 1-methylnaphthalene, (3) 2-methylnaphthalene, (4) acenaphthylene, (5) acenaphthene, (6) fluorene, (7) phenanthrene, (8) anthracene, (9) fluoranthene, (10) pyrene, (11) benzo(a)anthracene, (12) chrysene, (13) benzo(b)fluoranthene, (14) benzo(k)fluoranthene, (15) benzo(a)pyrene, (16) benzofluoranthene, (17) indeno(1,2,3-cd)pyrene, (18) dibenzo(a,h)anthracene.

## Chapter 5: Applications of GCxGC for Fuel Analysis

---

### 4.4 Conclusion

GCxGC is an essential analytical tool for the analysis of the complex feedstock and products in the FT refinery. Most of the refinery feed and products streams are highly complex, and the high GCxGC peak capacity is therefore essential to enable the separation of most of these compounds.

The selective hydrogenation of SCC products and the inlet hydrogenation of oligomerisation products demonstrate how the highly structured 2D separations obtained with this technique aids identification of compounds. On the other hand, the analysis of trace levels ( $\mu\text{g/mL}$  and sub- $\mu\text{g/mL}$ ) of PAHs in a complex FT diesel demonstrates the high sensitivity and selectivity of the technique. Valuable information was also be obtained from hydrogenation of oligomerisation products in the GC inlet liner. This enabled the analysis of compounds that are difficult to distinguish based their mass spectra and for which only small amounts of product are available.

## Chapter 4: GCxGC in Fischer–Tropsch Refining

---

### 4.5 References

- [1] A. de Klerk, Fischer–Tropsch Refining, PhD. Thesis, University of Pretoria, 2008.
- [2] A. Steynberg, M.E. Dry, *Stud. Surf. Sci. Catal.* 152 (2004) 406.
- [3] Standard test method: ASTM DS 4B, Physical constants of hydrocarbons and non-hydrocarbons, 2<sup>nd</sup> ed.; ASTM International, Philadelphia, PA, 1991.
- [4] J.M. Nagpal, G.C. Joshi, J. Singh, *Fuel Sci. Technol. Int.* 12 (1994) 873.
- [5] J.M. Nagpal, G.C. Joshi, S.N. Rastogi, *Fuel* 74 (1995) 714.
- [6] J.M. Nagpal, G.C. Joshi, S.N. Rastogi, *Fuel* 74 (1995) 720.
- [7] R. Van der Westhuizen, R. Crous, A. de Villiers, P. Sandra, *J. Chromatogr. A* 1217 (2010) 8334.
- [8] R.J. Nel, A. de Klerk, *Ind. Eng. Chem. Res.* 46 (2007) 3558.
- [9] D. Cavagnino, P. Magni, G. Zilioli, S. Trestianu, *J. Chromatogr. A* 1019 (2003) 211.
- [10] M. Kirk, I. Laubscher, The use of a hydrogenating inlet system for the GC quantification of co-eluting alkenes, Poster presentation, Analitika, Stellenbosch, South Africa, 1994.
- [11] T. Dutriez, M. Courtiade, D. Thiébaud, H. Dulot, F. Bertoncini, J. Vial, M–C. Hennion, *J. Chromatogr. A* 1216 (2009) 2905.

# **Chapter 5**

## **Applications of GCxGC for Fuel Analysis**

## Chapter 5: Applications of GCxGC for Fuel Analysis

---

### 5.1 The application of GCxGC to investigate the relationship between composition and physical properties of Fischer–Tropsch–derived fuels and blends

#### 5.1.1. Introduction

Fischer–Tropsch (FT) fuels and FT–crude–derived fuel blends have been used commercially in South Africa for many decades. FT fuels are ideal for blending with crude–derived fuels because their high aliphatic content, low aromatic content and the virtual absence of sulphur and nitrogen compounds increases the cetane number, reduces the density and improves the environmental impact of crude–derived fuels. In addition, the increase in volatility and improvement in cetane number improves combustion properties, which in turn manifests in improved vehicle acceleration times.

FT fuels are produced by the hydroconversion of FT synthetic crude [1,2], which usually involves a range of processes such as hydrogenation, hydrocracking, isomerisation and distillation. To tune the gasoline/kerosene/diesel ratio according to market requirements, processes to increase the chain length of the light fractions, such as oligomerisation to convert light alkenes to heavier alkenes, are also used. A distinction has to be made between FT fuels derived from low temperature (LT–FT) and high temperature (HT–FT) processes for refining purposes. LT–FT fuels, mainly kerosene and diesel [1], contain predominantly linear and branched alkanes. HT–FT fuels, such as gasoline, kerosene and diesel, have more complex compositions that are closer to those of crude–derived fuels, which also contain cyclics and aromatics.

The physical properties of a fuel can be directly linked to its chemical composition. Different compounds affect fuel properties in different ways and a very delicate balance needs to be maintained in terms of chemical composition to ensure that a fuel performs optimally for its intended application. International fuel specifications are reviewed constantly to keep up with developments in engine technology, innovations in fuel refining, changes in fuel standards, and concerns about environmental and health effects.

## Chapter 5: Applications of GCxGC for Fuel Analysis

---

The distillation range, cold flow properties, density, octane– and cetane numbers and aromatic content are a few of the important specifications targeted for regulation.

Comprehensive multidimensional GC (GCxGC) is a valuable tool to obtain detailed information of compounds at molecular level for highly complex petrochemicals mixtures [3–6]. This study focuses on the application of GCxGC to investigate the relationship between fuel chemical composition and physical properties such as density, cetane number, cold flow properties, etc.

### 5.1.2 Experimental

#### 5.1.2.1 Comprehensive multidimensional GC analyses

GCxGC analyses were performed using a Pegasus 4D instrument equipped with time–of–flight mass spectrometer (TOF–MS) and FID detector from Leco Corporation (St. Joseph, MI, USA). TOF–MS was used for the identification of peaks and FID for quantification. Quantification was done by normalisation. The first dimension column was a 30 m x 250  $\mu\text{m}$  x 0.25  $\mu\text{m}$  RTX–Wax (Restek) with a temperature program of 40°C (0.2 min), ramped at 2°C/min to 245°C. The second dimension column was a 1.5 m x 100  $\mu\text{m}$  x 0.1  $\mu\text{m}$  Rxi–5 (Restek). This column followed the first oven temperature with a lead of 40°C. The modulation period was 7 seconds. A constant helium carrier gas flow of 1.2 mL/min was maintained. For injection, the split ratio was 400:1, and the injection volume 0.1  $\mu\text{L}$ . TOF–MS and FID data were collected at 100 spectra (points)/s.

#### 5.1.2.2 $^{13}\text{C}$ NMR experiments

$^{13}\text{C}$  NMR experiments were performed on a Varian UNITY INOVA 600 MHz spectrometer equipped with a switchable 5 mm PFG probe, operating at 150 MHz and at a temperature of 30°C. The operating parameters are a 90° pulse of about 7.125 s with 30  $\mu\text{s}$  delay between each pulse and an acquisition time of 1.3 s. The number of transients (scans) was set to 1724.

## Chapter 5: The use of GCxGC for fuel analysis

---

The sample was dissolved in a small volume of deuterated benzene, which acted as a lock solvent. This allowed a reasonable amount of diesel to be in large excess with regards to the solvent, therefore facilitating collection of quantitative spectra. The  $^{13}\text{C}$  NMR spectrum was run under quantitative conditions, with the decoupler mode set as 'nny'. The distortionless enhancement by polarisation transfer (DEPT) spectrum was run for 2 h, with a delay of 2 s and the total number of scans was 584.

### 5.1.3 Results and discussion

To study the composition of FT fuels and their crude-derived blends at trace levels, a powerful separation technique is essential. The large peak capacity and the structured chemical class separations obtained with GCxGC in the 2D separation plane, especially in the reversed column set-up used here, enables analysis of individual compounds and compound classes, while the inherently high sensitivity of the technique enables analysis of compounds at levels as low as 5 mg/L.

LT-FT fuels are less complex than HT-FT or crude-derived fuels (they consist of linear and branched alkanes only) and valuable information can be gained by analysis of the products that could not be obtained for more complex products. For example, the lack of cyclics and aromatics in the LT-FT fuel enabled us to correlate the effect of the degree of branching and distillation cut on cold flow properties and cetane number of the fuel. The branched alkane peaks of a particular carbon number elute in the same region as up to three lower carbon numbers for highly isomerised fuels, and we were able to distinguish the mono-methyl branched alkanes from the alkanes with two or more branches on a chain (Figure 1). The type of branching on a molecule is an important factor that affects a number of fuel properties such as octane number, cetane number, cold flow properties, density, etc. On the other hand, HT-FT and crude-derived fuels are highly complex mixtures that consist of alkanes and aromatics with subclasses of linear and branched, non-cyclic, monocyclic, bicyclic and possibly higher cyclic hydrocarbons. Aromatics include mononuclear, binuclear or polynuclear classes.

## Chapter 5: The use of GCxGC for fuel analysis

Because of the complex nature of fuel, it is impossible to list all of the thousands of components and evaluate their effects on fuel properties. Compounds with similar properties are therefore grouped together into compound classes and their collective effects on the fuel properties studied. Here, GCxGC is the ideal analytical technique as it naturally groups chemical classes together during the separation process. The differences in composition between synthetic and crude-derived diesels are evident by comparison of the contour plots (Figure 2). The FT fuel has more n-alkanes compared to a higher degree of branching for the crude-derived fuel. We further observed more bi- and polycyclic aliphatics and more cyclic alkylbenzenes in the FT fuel compared to more alkylbenzenes and bi- and polynuclear aromatics in the crude fuel. The application of GCxGC to study various physical properties will be discussed in the following sections.

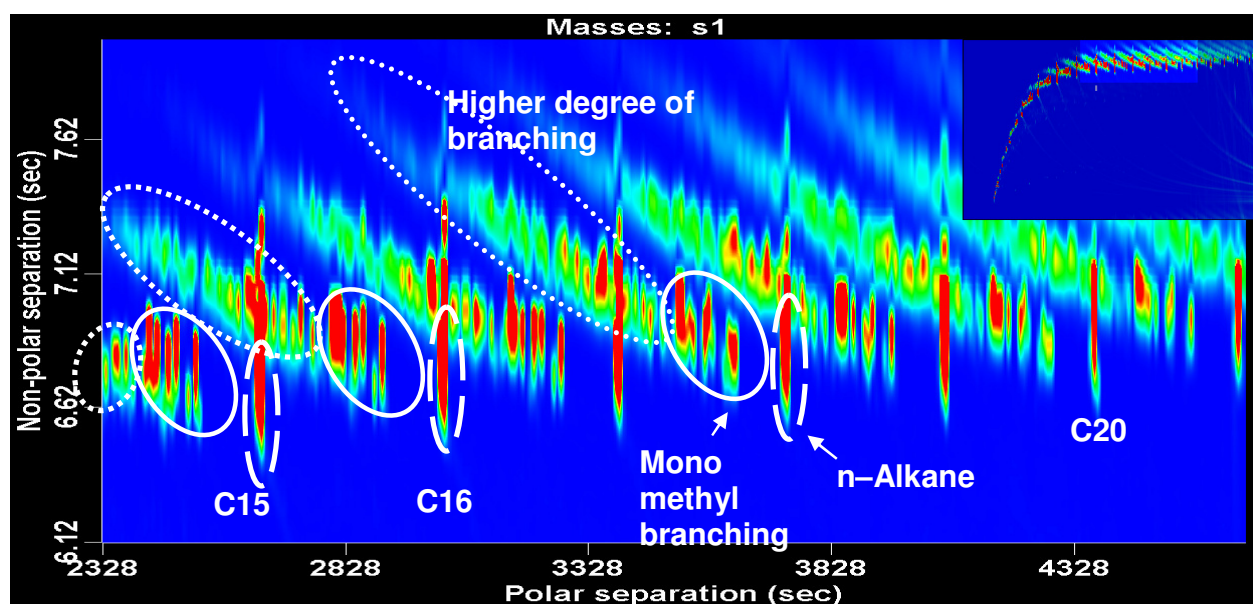


Figure 1. The GCxGC-FID contour plot obtained for a LT-FT diesel shows the elution of the 1) C<sub>18</sub> mono methyl branched alkanes being distinguished from the multi-branched alkanes. The C<sub>18</sub> branched alkanes stretch over three carbon numbers.

## Chapter 5: The use of GCxGC for fuel analysis

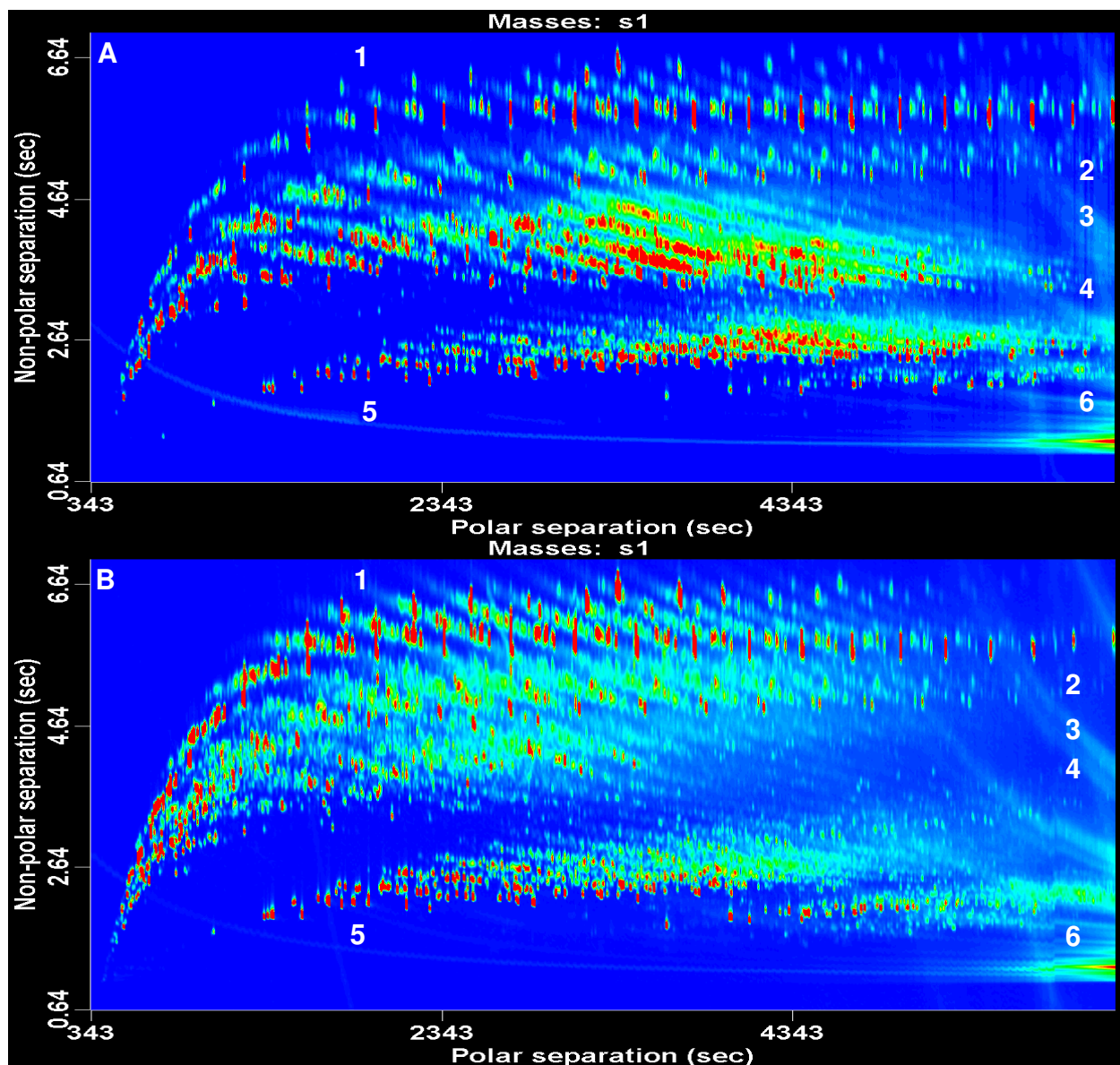


Figure 2. Comparison of A) HT-FT and B) crude-derived diesels. GCxGC-FID contour plots show excellent separation of the various compound classes of 1) linear and branched alkanes, 2) monocyclic alkanes, 3) bicyclic and 4) polycyclic alkanes as well as 5) mononuclear and 6) bi-nuclear and polynuclear aromatics.

### 5.1.3.1 Distillation range

A large variety of fuel products are produced from FT and crude oil, such as gasoline, jet fuel, diesel fuel and liquefied gasoline gas.

## Chapter 5: The use of GCxGC for fuel analysis

The difference between each of these fuels is mainly in terms of distillation range of products (i.e. the difference between initial and final boiling points of the oil). The distillation ranges in a typical refinery process are tabulated in Table 1.

**Table 1: Distillation ranges of products in a typical refinery [7]**

Product	Boiling range (°C)
LPG	-40-0
Gasoline	30-200
Gasoline jet fuel	100-250
Kerosene, jet fuel, light diesel	170-270
Diesel, furnace oil	180-340
Lube oils	340-540
Residual fuels	340-650
Asphalt	> 540
Gasoline coke	Solid

Gasoline is a light hydrocarbon oil used in internal combustion engines such as motor vehicles. Kerosene is of intermediate volatility between gasoline and diesel oils, with an oil distillation range between 170–270°C. Gasoline type jet fuel comprises a gasoline – kerosene blend of light hydrocarbon oils with a distillation range between 100°C and 250°C and a total aromatic content of < 25 vol %. The aromatic content is reduced to decrease the smoke point. Kerosene type jet fuel is a middle distillate with the same distillation range and flashpoint as kerosene, but has particular specifications on freezing point (as established by the International Air Transport Association). Special properties are required such as a high flash point for safe refueling, low freezing point for high altitude flying, and good water separation characteristics. Diesel fuel oils are obtained from the lowest fraction of atmospheric distillation, while heavy gas oils are obtained by vacuum re-distillation of the residual from atmospheric distillation. Diesel oil for diesel compression ignition engines typically distills between 180 and 340°C. Furnace oil is just another name for fuel oil, a general term used for oil used for the generation of power or heat.

## Chapter 5: The use of GCxGC for fuel analysis

---

The distillation range affects most of the properties of fuels because more branched and cyclic isomers are possible for components of higher carbon numbers, and also more aromatics. Because LT–FT fuels do not contain aromatics or cyclics, valuable information could be obtained regarding the effect of distillation range on cetane numbers (cetane numbers are a measure of the combustion quality of diesel during compression ignition).

GC techniques are ideally suited for the determination of the distillation range of a fuel because the GC separation on a non–polar column, such as the distillation process, is based on volatility (boiling point) differences of components. The distillation range of a mixture can be considered to be the range of boiling points from that of the first eluting compound to that of the last eluting compound. For example, ASTM D2887 describes a GC method to obtain simulated distillation curves. GC provides simple, consistent and reproducible distillation data [7, 8]. GCxGC using a non–polar x polar column combination can similarly be used to determine the distillation range of a fuel.

GCxGC contour plots for two LT–FT diesels with cetane numbers of 80 and 72, respectively, (Figure 3 A & B) show that while the two fuels have similar normal alkane to branched alkane (n–: i) ratios of around 0.5, the distillation range for LT–FT1 is much wider, to include five more carbon numbers. The alkane–rich heavier tail of LT–FT1 provides an increase in cetane number of eight units compared to the LT–FT2 fuel. The cetane number is also affected by other factors such as the linearity of the molecules. Comparing the contour plots of LT–FT 2 fuel with another one e.g. LT–FT3, (Figure 3B+C), it can be seen that the two products are of the same distillation range, but branching is much higher in LT–FT3. The fuel with the higher n:i ratio (0.54) has a cetane number which is five units higher than that of the fuel with the lower n:i ratio of 0.05.

### 5.1.3.2 Cold flow properties

Fuel cold flow properties are important if vehicles are used in cold weather conditions. Aircraft in particular are subjected to excessively cold temperatures when in the air.

## Chapter 5: The use of GCxGC for fuel analysis

---

The distillation range, hydrocarbon composition and use of cold flow additives dictate the cold flow properties of the fuel.

Cloud point, the temperature at which wax crystals start to appear in the fuel, and the cold filter plugging point (CFPP–value), the temperature at which a fuel will start to block filters, are used to measure cold flow properties.

At room temperature the fuel is a homogeneous fluid, but on cooling phase separation occurs between an alkane–rich solid phase and the liquid phase. Heavier n–alkanes, with the lowest  $K_{sp}$  values (the solubility product constant for saturated solutions), become insoluble and precipitate as waxy crystals. These crystals are typically flat, rhombic-shaped crystals, formed at temperatures close to the cloud point and block fuel system filters. At slightly lower temperatures an interlocking wax crystal is formed, which totally prevents flow from the fuel system, with resulting engine failure.

The addition of cold flow additives modifies the size and shapes of the wax crystals and reduces the fuels' tendency to block filters and lines. It also extends the temperature range over which a vehicle can operate. Cold flow additives are more soluble in aromatics than in hydrocarbons.

## Chapter 5: The use of GCxGC for fuel analysis

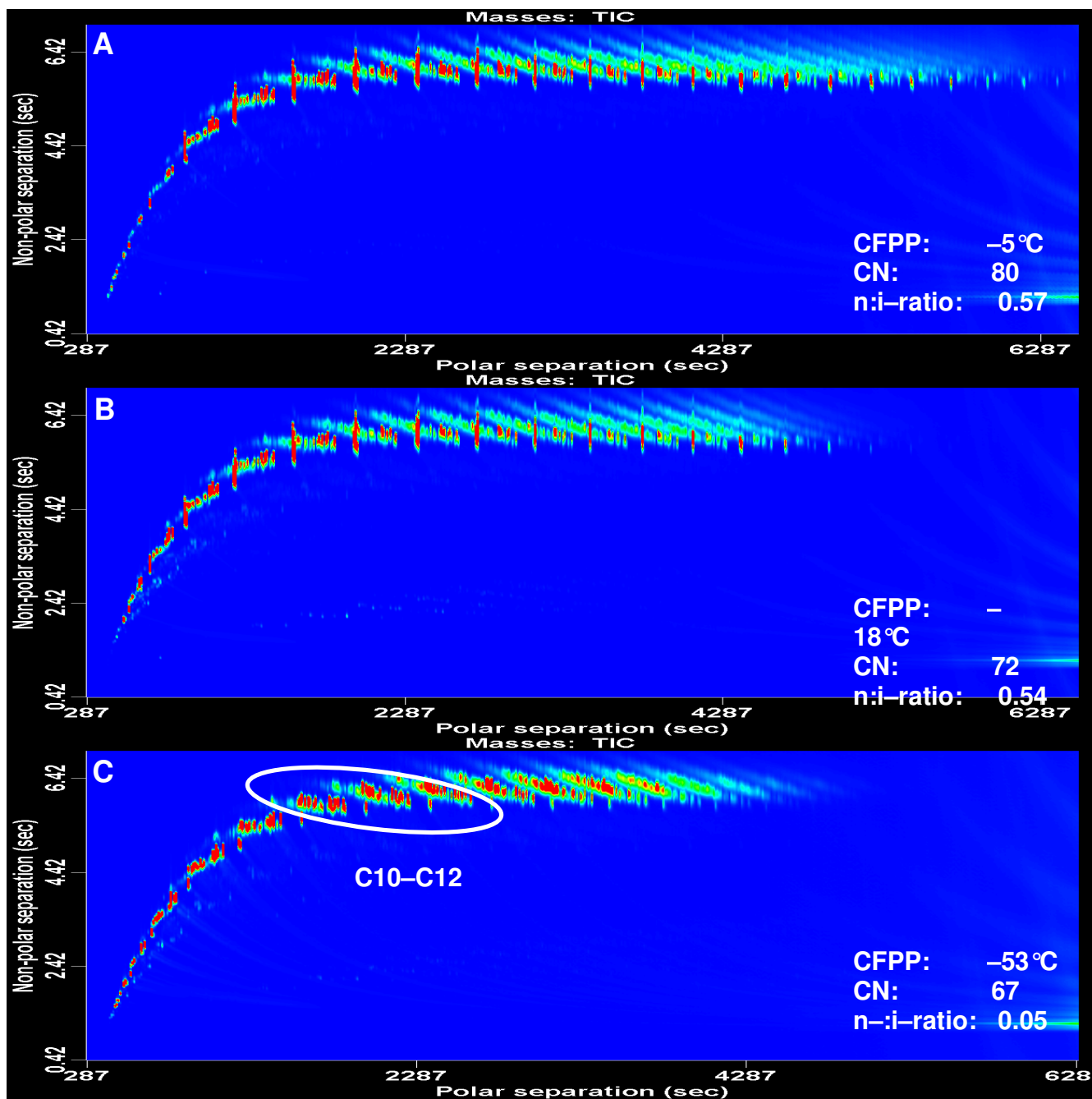


Figure 3. GCxGC-TOF-MS contour plots of three LT-FT diesels demonstrate how the distillation range and normal to branched alkane (n-i) ratios affect cetane numbers and cold flow properties of the fuels.

## Chapter 5: The use of GCxGC for fuel analysis

The cold flow properties of a fuel are improved by the presence of shorter chain hydrocarbons. For example, kerosene has excellent cold flow properties because of its relatively low boiling point range. The cold flow properties of diesel can therefore be enhanced by blending with kerosene, by removal of the heavy hydrocarbons, or by using catalytic dewaxing or isomerisation to increase the degree of branching. This is evident from Figures 3B and C, where the LT–FT fuel with the higher degree of branching ( $n: i$  ratio = 0.05) has a CFPP value of  $-53^{\circ}\text{C}$ , compared to fuel with a lower degree of branching ( $n: i = 0.54$ ), which has a CFPP value of  $-18^{\circ}\text{C}$ . The different compositional requirements for good cold flow properties and good cetane numbers therefore need to be carefully balanced to obtain optimum fuel qualities.

GCxGC also provides valuable information on the waxy crystals that cause fuel filter blockages at temperatures close to the cloud point of the fuel. GCxGC–FID analysis of the dissolved crystals obtained by cooling a small amount of fuel to  $\approx -20^{\circ}\text{C}$  and filtering the liquid crystals, shows the presence of mainly heavy  $n$ -alkanes of carbon numbers  $\text{C}_{16}$  and higher (Figure 4). These heavy  $n$ -alkanes are responsible for the formation of waxy crystals in cold weather conditions.

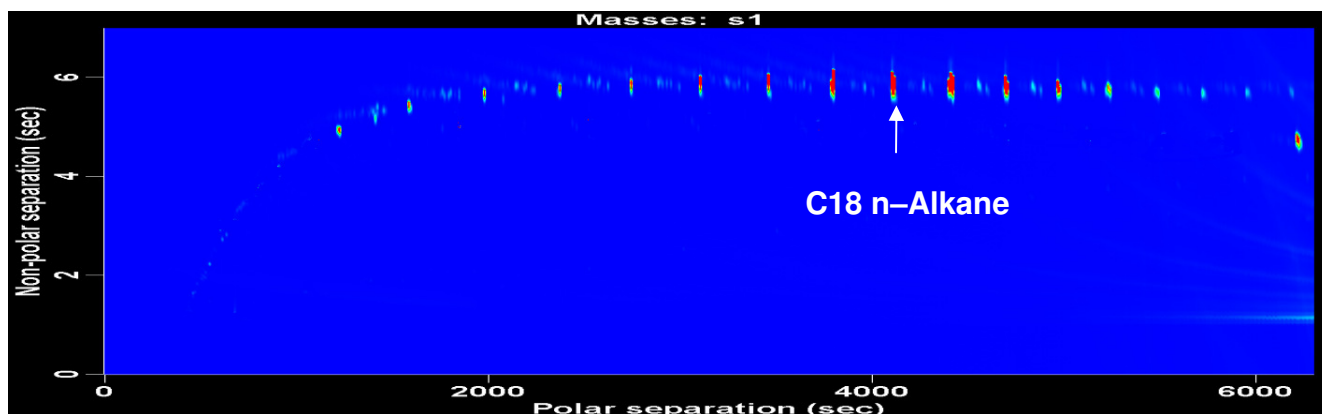


Figure 4. GCxGC–FID contour plot of the dissolved waxy crystals extracted from fuel at  $\approx -20^{\circ}\text{C}$  shows high concentrations of heavy alkanes which are the cause of fuel filter blockages at temperatures close to the cloud point.

## Chapter 5: The use of GCxGC for fuel analysis

---

### 5.1.3.3 Combining GCxGC and NMR to determine branching in fuels

By combining GCxGC and NMR data, valuable information can be obtained on the branching patterns that affect the cold flow properties of a fuel [9]. In this study, GCxGC and NMR analyses were combined for the analysis of LT–FT diesel with a CFPP value of  $-53\text{ }^{\circ}\text{C}$  (Figure 3C). GCxGC was used to determine that the diesel was highly branched, with an n: i ratio of around 0.05. The distribution of carbon numbers peaked at around  $\text{C}_{10}\text{--}\text{C}_{12}$ . This information aided with calculations used in the NMR studies. In addition, GCxGC–FID analysis enabled the calculation of the average carbon number of the product from the relative mass % for each carbon number. However, it was difficult to identify the types of branching, apart from mono–methyl branching, especially for highly branched products, based on GCxGC data. NMR data, on the other hand, provided more information regarding the types of branching per molecule.

$^{13}\text{C}$  NMR spectra were referenced to the terminal methyl group of a  $-\text{CH}_3$  of a long-chain alkane resonating at 14.0 ppm. It was found that the  $-\text{CH}_2-$  resonances of the product were very crowded and that it was better to analyse the  $-\text{CH}-$  and  $-\text{CH}_3$  regions of the spectra for the branching analysis of diesel samples. The DEPT spectrum allowed unambiguous assignment of  $-\text{CH}-$ ,  $-\text{CH}_2-$  and  $-\text{CH}_3$   $^{13}\text{C}$  NMR resonances. No quaternary carbons were present, therefore dialkyl substitution on the same carbon could be ruled out. However, using these data, multiple branching on the molecule could not be excluded.

Another way of looking at the branching is by observing the number of methyl groups present in the full  $^{13}\text{C}$  NMR spectrum. For a linear chain, only the terminal  $-\text{CH}_3$  was observed and the rest of the resonances were due to  $-\text{CH}_2-$  groups. For every additional alkyl branch (regardless of the type, methyl, ethyl etc) present along the chain, a new  $-\text{CH}_3$  peak appeared with a unique resonance. Associated with this  $-\text{CH}_3$  resonance was a  $-\text{CH}-$  resonance at the point of branching. It is for this reason that the CH and  $\text{CH}_3$  resonances were much easier to work with. Figure 5 shows the major branched structures as well as their respective characteristic  $-\text{CH}-$  and  $-\text{CH}_3$  resonances, marked with (\*), determined by means of  $^{13}\text{C}$  NMR and DEPT experiments, and with the aid of ACDLabs  $^{13}\text{C}$  NMR prediction software.

## Chapter 5: The use of GCxGC for fuel analysis

Figure 6 shows the section of the  $^{13}\text{C}$  NMR spectrum of the diesel sample with the methyl groups (identified by DEPT) used to identify the classes of branching present in the fuel. From the average carbon number and the classes of branched isomers, the mol % of each class (methyl, ethyl, propyl, etc.) could be determined. For instance, the propyl branching was determined by the integral for the  $-\text{CH}_3$  resonance at 14.4 ppm. The mol % of branching was then calculated from the integrated  $^{13}\text{C}$  NMR spectrum as follows:

$$\text{mol \% propyl branching} = \frac{\text{integral at 14.4 ppm}}{\text{sum of all integrals}} \times \text{average carbon number} \times 100\%$$

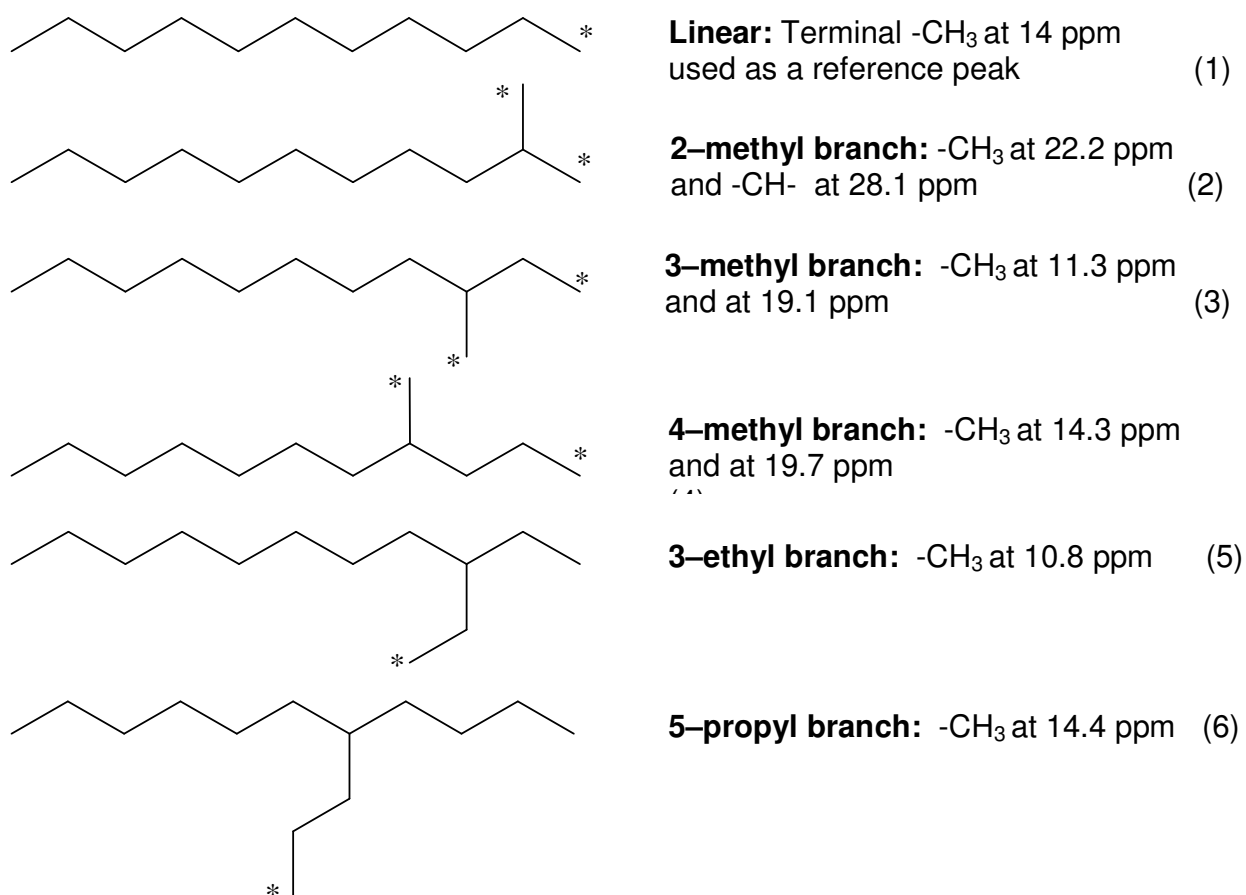


Figure 5: The major branched structures with their respective characteristic  $-\text{CH}-$  and  $-\text{CH}_3$  resonances, marked with (\*), as determined by using  $^{13}\text{C}$  NMR and DEPT experiments.

## Chapter 5: The use of GCxGC for fuel analysis

Other classes of branches could be determined in the same manner. Once all the classes of branching were identified and amounts calculated, the remainder was assumed to be due to linear alkanes. This was confirmed by quantitative GCxGC–FID analysis.

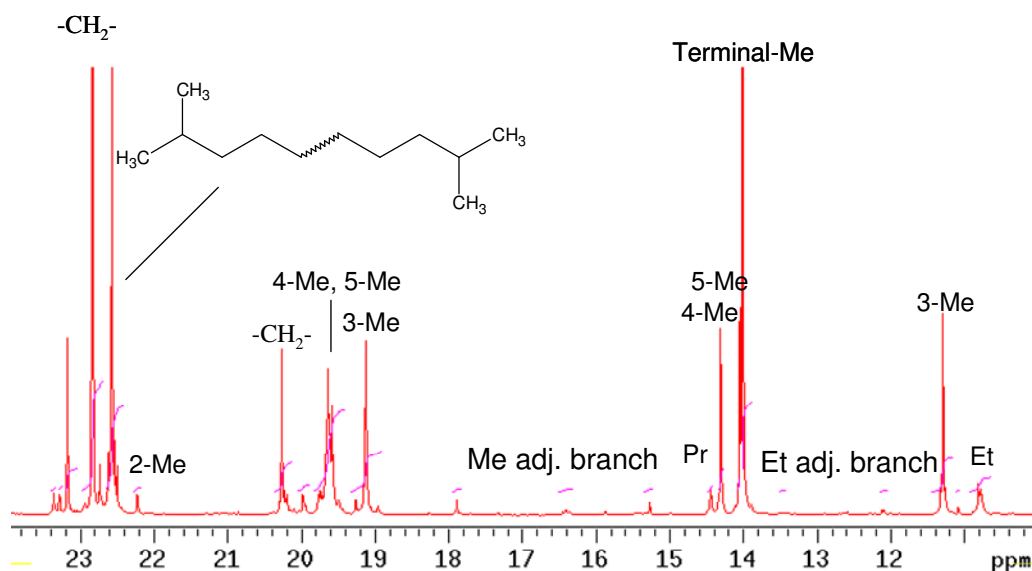


Figure 6. A section of the  $^{13}\text{C}$  NMR spectrum of a diesel sample showing the methyl groups (identified by DEPT experiment) used to identify the class of branching present in the fuel.

In the case where a branching class was identified by two sets of  $-\text{CH}_3$ 's, e.g. 3-methyl branching with  $\text{CH}_3$  resonances at 11.3 and 19.1 ppm, an average integral value of these resonances was considered for the calculation. Another special case was for 2-methyl branching with the  $\text{CH}_3$  resonances at 22.2 ppm representing two methyl groups. This integral value had to be divided by 2 to account for the mol % of this class of branching. Besides the major classes of branching shown above, other branches could also be identified, such as a methyl branch adjacent to an undefined branch (region ca 15–16 ppm) and an ethyl branch adjacent to an undefined branch (region 12–13 ppm). From these data we were able to conclude that the product was largely composed of chains with methyl branching in the 3 to 5 positions.

## Chapter 5: The use of GCxGC for fuel analysis

---

Branching in the middle of the chain is thought to have a greater positive influence on the cold flow properties as this would prevent wax crystallisation much better than if the branching was towards the end of the chain. The high amount of internal branching, relative to the low amount of linear molecules, is thought to be responsible for the very low CFPP value of this sample.

In this study,  $^{13}\text{C}$  NMR and DEPT proved to be valuable techniques for obtaining detailed information about the types of branching in the diesel sample. Moreover, NMR and GCxGC were found to be complimentary techniques for a detailed investigation of this aspect.

### 5.1.3.4 Density

Fuel density is important to achieve optimal air-to-fuel ratios in fuel injection systems. Increasing the density of a diesel fuel increases the power output of an engine per unit volume of fuel consumed. High viscosity can cause poor injector spray atomisation, which may lead to excessive coking and oil dilution. A reduction in density, on the other hand, reduces particulate matter and  $\text{NO}_x$  emissions in older technology engines, although this does not influence the emissions from more modern engines with electronic injection and computer controls [8]. A balance between optimal performance with the minimum engine fouling and environmental pollution is therefore important. Diesel engines are developed and calibrated for a narrow density band of between 820 and 845  $\text{kg/m}^3$ . Density specifications for jet fuel are between 775 and 840  $\text{kg/m}^3$  and for gasoline between 710 and 770  $\text{kg/m}^3$ .

Fuel density generally increases with increasing molecular weight of the constituent molecules, as well as with increasing numbers of aliphatic and aromatic ring structures. Increased cyclic and aromatic content can also lead to an increase in viscosity. FT fuels have a relatively low density compared to crude-derived fuels because of their relatively high aliphatic and low aromatic content, and sometimes do not conform to the international density specification. Ways of achieving higher densities are therefore important. This can be done by blending FT fuels with products of higher density, such as crude-derived fuels or tar fractions, or by subjecting the fuel to aromatisation processes.

## Chapter 5: The use of GCxGC for fuel analysis

Crude-derived fuels, on the other hand, often have too high a density and benefit from blending with FT fuels. When comparing the densities of various C<sub>10</sub> hydrocarbons in Table 2 [10], it is obvious that the density of a compound increases with an increasing number of aliphatic ring structures, and furthermore with an increasing numbers of aromatic rings. Bulkier molecules have higher density. Cyclic and bicyclic alkanes such as decalin have higher density than non-cyclics, but their contribution to the density will not be sufficient to improve the density of a FT diesel (for example the density of a FT diesel may range between 760 and 770 kg/m<sup>3</sup> [11], compared to the required specification of 820 – 845 kg/m<sup>3</sup>). The easiest way to increase the density would therefore be to increase the aromatic content. In this instance, the specifications on the total aromatic content as well as the polynuclear aromatic content should be considered.

**Table 2: Comparison of densities of some C<sub>10</sub> hydrocarbons [10]**

Compound	Density (kg/m <sup>3</sup> ) at 20 °C
Decane	735
Pentylcyclopentane	790
Butylcyclohexane	818
Decalin	896
Tetrahydronaphthalene	973
Naphthalene	990

Aromatics are responsible for large amounts of CO and hydrocarbon exhaust emissions, and poor smoke point properties of fuels. But their presence in fuels also offers some advantages. They cause beneficial swelling of elastomers in the fuel system, which provides better sealing of O-rings. The amount of aromatics permitted in fuels is regulated, and even stricter specifications will be enforced in the near future for environmental reasons. LT-FT processes produce no aromatics, and even in HT-FT processes, relatively small amounts of aromatics are produced, when compared with crude-oils. Blending FT fuels with aromatic-rich crude-derived fuels increases the density of FT fuels and provides better volumetric fuel efficiency. Blending FT fuel components with crude-derived fuels that have too high density, on the other hand, decreases the density of the crude-derived fuel and decreases undesirable

## Chapter 5: The use of GCxGC for fuel analysis

---

emissions. For environmental purposes, it would be preferable to increase the amount of cyclic and bicyclic alkylbenzenes rather than the binuclear or polynuclear aromatics. The compositions of four diesel samples with different densities are compared in Table 3. These data were calculated from normalised GCxGC–FID data (the relevant contour plots are shown in Figure 7). It is clear that, in general, fuels with higher aromatic and polycyclic content have higher density compared to fuels with a high n-alkane and branched alkane content.

**Table 3: Comparison of the chemical composition (determined by GCxGC–FID) and densities of various of diesel samples**

Fuel	Density	n-alkanes	Branched alkanes	Monocyclic alkanes	Bicyclic alkanes	Tricyclic alkanes	Alkyl benzenes	Cyclic alkyl benzenes	Bicyclic alkyl benzenes	Naphthalenes
	<i>kg/m<sup>3</sup></i>	<i>Mass %</i>	<i>Mass %</i>	<i>Mass %</i>	<i>Mass %</i>	<i>Mass %</i>	<i>Mass %</i>	<i>Mass %</i>	<i>Mass %</i>	<i>Mass %</i>
HT-FT heavy diesel	874	13.13	6.00	12.58	17.53	25.22	2.90	15.39	5.59	1.66
Standard European diesel	828	21.44	24.31	19.51	11.65	0.18	9.07	7.35	1.36	4.91
HT-FT diesel	808	31.05	29.64	12.62	1.71	0.00	10.75	11.91	0.69	1.58
LT-FT diesel	747	35.98	63.48	0.50	0.01	0.00	0.03	0.01	0.00	0.00

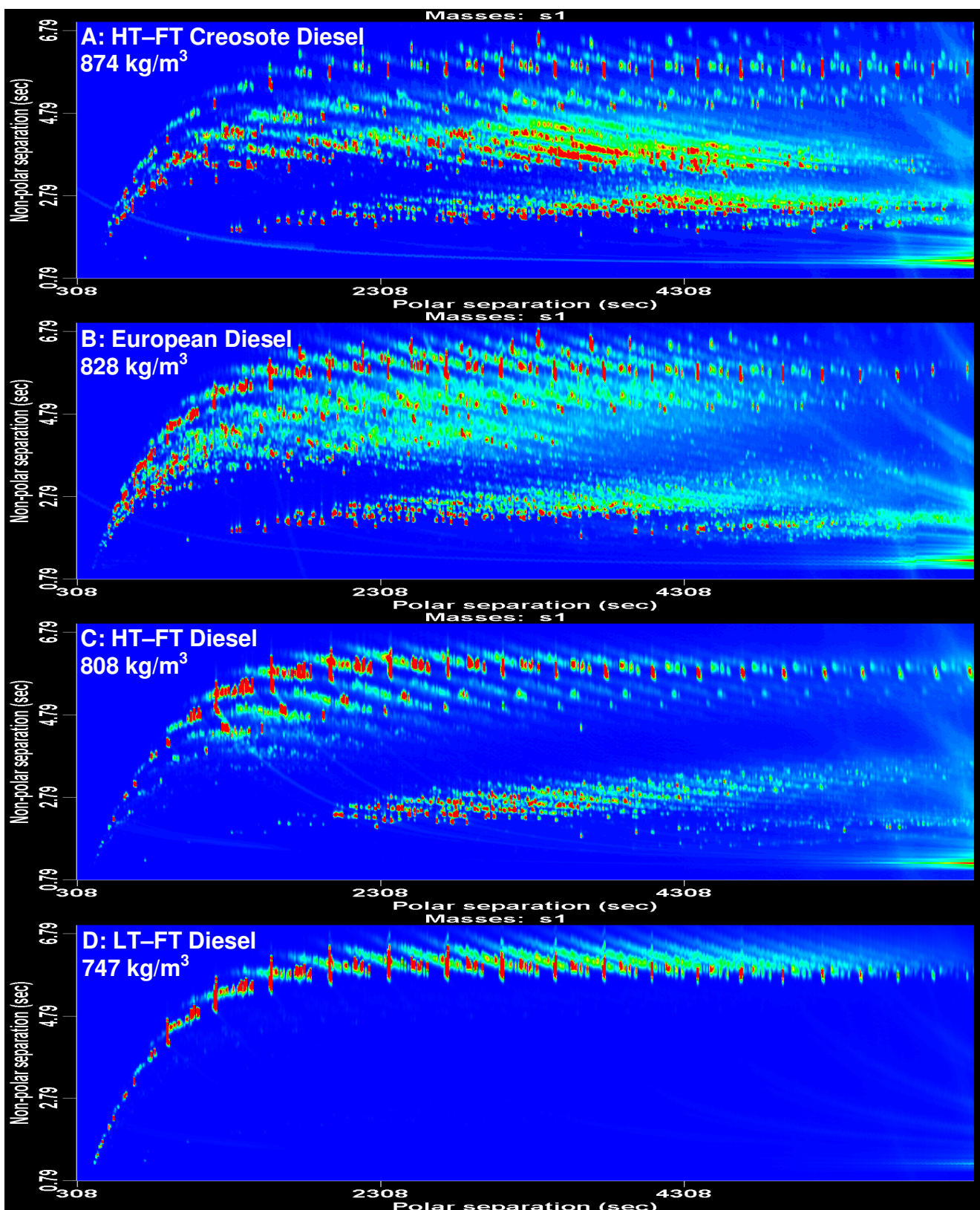


Figure 7. GCxGC-FID contour plots showing the variation in diesel composition with increasing density. Heavy aromatics contribute more towards density than aliphatics.

## Chapter 5: The Use of GCxGC for Fuel Analysis

---

### 5.1.3.5 Octane and cetane numbers

The octane rating of gasoline is a measure of a fuel's tendency to auto-ignite [8]. Knocking or pinking is caused by self-ignition in the cylinders and happens when the gasoline/air vapour mixture in the engine ignites before a spark is passed by the spark plug. The premature ignition pushes against the crankshaft instead of with it, producing a knocking or pinking sound. Knocking is avoided by using gasoline with a sufficiently high octane number. The higher the octane number the more resistant the gasoline is to self-ignition that causes knocking.

The octane rating scale is an arbitrary one based on the use of n-heptane and 2,2,4-trimethylpentane as reference compounds. N-Heptane has a high tendency to auto-ignite (octane number of 0), while 2,2,4-trimethylpentane has a low tendency to auto-ignite (octane number of 100). A mixture of these two components containing 95% 2,2,4-trimethylpentane has an octane number of 95. If a gasoline engine is run on a fuel with an octane number < 82–88, knocking will occur. Gasoline feed products are often subjected to isomerisation, dehydrocyclisation and catalytic cracking to increase the octane rating. Knocking can also be prevented by adding high-octane compounds to the gasoline.

Additives such as lead compounds (e.g. tetraethyl lead) have been banned in many countries because lead compounds in exhaust fumes are toxic. Alcohols or ethers increase the octane number of a fuel and produce lower levels of CO and less pollution when they burn. Methyl tertiary butyl ether (MTBE) is used most often; it has an octane rating of 118. Compounds with high octane ratings typically have a high degree of branching and ring structures with short chain lengths. Ghosh et al. [12] developed a method to calculate octane numbers from structural data obtained from GC analysis with a standard error of 1. This method can be modified for GCxGC analysis.

Diesel fuel has a boiling range between approximately 180–370 °C. As diesel engines do not have spark plugs, octane numbers are not relevant. Diesel depends on the fuel igniting itself by compression.

## Chapter 5: The Use of GCxGC for Fuel Analysis

---

The measure of a diesel fuel's ignition quality is called the cetane number (CN), which indicates the fuel's readiness to ignite spontaneously under the temperature and pressure conditions in the combustion chamber of the engine. The cetane number actually measures the fuel's ignition delay (the time period between the start of injection and the start of ignition), - an indication of the ability of a diesel fuel to ignite quickly after being injected into the cylinder. A fuel with a higher cetane number will have a shorter ignition delay period than a fuel with a low cetane number. Increasing cetane numbers correlate with improved fuel combustion and reduced NO<sub>x</sub> emissions, and to a lesser extent, also reduced particulate emissions.

To measure cetane number properly requires burning the fuel in a special diesel engine, called a Cooperative Fuel Research (SFR<sup>TM</sup>) engine under standard test conditions. The ignition delay of the fuel is measured and resulting cetane number is calculated by determining which mixture of cetane (hexadecane) and isocetane (2,2,4,4,6,8,8-heptamethylnonane) will result in the same ignition delay (optical test method ASTM D-613). Because ASTM D-613 is very time consuming and relatively large sample volumes are required, alternative calculation methods have been developed to determine CNs. For example, ASTM-D-986 or ASTM D-4737 calculate the cetane number from a fuel's density and boiling range. ASTM D-4734 correlates the American Petroleum Institute (API) gravity (a measure of how heavy a petroleum liquid is compared to water) and the T<sub>10</sub>, T<sub>50</sub> and T<sub>90</sub> points on the boiling curve (where T<sub>x</sub> is the temperature in °C at which x vol % of the sample has distilled off), to the CN of the fuel. However, calculation methods cannot be applied to fuels that contain additives that increase cetane number because the additives do not change the fuel density or distillation profile, - only the cetane number.

Normal alkanes have high cetane numbers, which increase with molecular weight. Branched alkanes have lower cetane numbers than n-alkanes, followed by monocyclic alkanes, alkylbenzenes, polycyclic alkanes and polycyclic aromatics. Isomers with several short side chains have lower cetane numbers than those with long side chains. Aromatics have low cetane ratings and therefore long ignition delays.

## Chapter 5: The Use of GCxGC for Fuel Analysis

---

It is therefore possible to use the molecular composition of the fuel as determined by GC [13–16], Fourier transform infrared spectroscopy [17], NMR [18–19], etc. to calculate the cetane number. Ladommatos and Goacher [13] tested 22 equations for predicting the cetane number of diesel fuels, by comparing the predicted values for more than 500 fuels with measured values. They found some of the equations to have a high predictive capability and several of them could predict cetane number with a standard error of  $< 2$ . They also found that the aniline point, the temperature at which equal volumes of aniline and diesel are completely miscible, is correlated very highly to the cetane number. Ghosh and Jaffe [20] developed a detailed composition-based model for predicting the cetane number of diesel fuels by using a combination of SFC, GC and MS data. They considered more than 200 diesel fuels and commercial blends in the study, and could predict cetane number with a standard error of 1.25. Ghosh further developed a model for predicting the effect of cetane improvers on cetane number [21].

Conventional diesel should have a cetane number  $> 51$  (according to European standards), while premium diesel fuels can have cetane numbers as high as 60. All components of a fuel affect its cetane number. As mentioned previously, longer linear hydrocarbon chains provide higher cetane numbers. An improvement in cetane number should thus be weighed against the poorer cold flow properties caused by an increase in heavy *n*-alkanes.

Compared to LT-FT diesels, HT-FT diesels have lower cetane numbers, closer to those of crude-derived diesels because of their higher cyclic and aromatic content. The effect of these compounds on cetane number is much more difficult to study because of the complexity of the diesels and because the carbon distributions for each of the compound classes also need to be taken into account. Figure 8 shows the relationship between cetane numbers and composition (as determined by normalised GCxGC-FID data) for six FT- and crude-derived fuels. From Figure 8, the increase in cetane number with linear and branched aliphatics is clear, but there seem to be some conflicting data for the cyclic aliphatics and the aromatics. This is the result of the effect of sub-classes and chain lengths on cetane number.

## Chapter 5: The Use of GCxGC for Fuel Analysis

For example, a tricyclic aliphatic compound of a higher carbon number will be less beneficial to the total cetane number of the fuel than a short-chain alkylbenzene, while naphthalene will be less beneficial than a monocyclic alkane. The separation of these compounds by GCxGC is invaluable and assists greatly in a better understanding of the relation between fuel properties and their chemical composition.

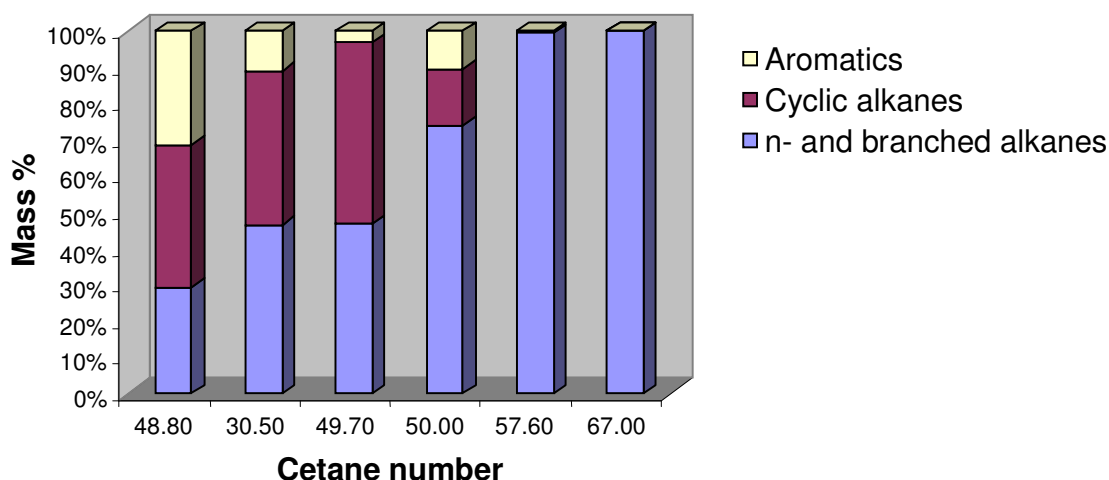


Figure 8. Graph showing the correlation between cetane number and composition for six FT diesels, as determined by GCxGC–FID. The structures of the individual compounds, as well as the chain lengths, contribute to the cetane number.

### 5.1.4 Conclusions

Detailed data analysis of the fuel compound classes obtained by GCxGC enables the determination of fuel properties such as density, octane number, cetane number, cold flow properties, etc. Both FT- and crude-derived fuels are highly complex mixtures that contain various hydrocarbon classes such as alkanes, naphthenes and aromatics. Each of these classes can have sub-classes of non-cyclic, monocyclic or higher cyclic structures. All of these components may affect the properties of the fuel in different ways.

## Chapter 5: The Use of GCxGC for Fuel Analysis

---

More branched alkanes relative to n-alkanes will increase the cold flow properties of a fuel but will decrease its cetane number. N-Alkanes are beneficial for cetane numbers but will cause the formation of waxy crystals at cold temperatures, which again causes blockage of fuel filters and eventually engine failure. Cyclic alkanes will increase the octane number of gasoline but will decrease the cetane number.

Aromatics are important for keeping the fuel density within specifications, but they reduce cetane numbers and causes smoke and particulate emissions. A very delicate balance needs to be maintained to ensure that the fuel performance is optimal for its application, with the least possible environmental pollution.

This study demonstrated how the excellent separation power of comprehensive multidimensional GC (GCxGC) with TOF-MS and FID detection can be used to correlate a fuel's physical properties such as its distillation range, density, cetane numbers and cold flow properties with its chemical composition. The results showed that FT-derived synthetic fuels are ideal for blending with crude-derived fuels because their high alkane content, low aromatic content and virtual absence of S- and N- components will increase the cetane numbers, lowers the density and improve the environmental impact of most crude-derived fuels.

## Chapter 5: The Use of GCxGC for Fuel Analysis

---

### 5.1.5 References

- [1] A. Steynberg, A., M.E. Dry, Fischer Tropsch Technology (Studies in Surface Science and Catalysis), Elsevier Science, Amsterdam, 2004.
- [2] J. Collings. Mind over Matter – The Sasol Story: A half–Century of Technology Innovation, Sasol, 2002.
- [3] J. Beens, J. Blomberg, P.J. Schoenmakers. J. High Resolut. Chromatogr. 23 (2000) 182.
- [4] J. Beens, P.J. Schoenmakers, U.A.Th. Brinkman, J. Chromatogr. A 972 (2002) 137.
- [5] J. Dalluge, J. Beens, U.A.Th. Brinkman, J. Chromatogr. A 1000 (2003) 69.
- [6] P.J. Marriott, R. Shellie, TrAC 21 (2002) 573.
- [7] G.K. Schmidt, E.J. Forster, Modern refining for today's fuels and lubricants, SAE International Technical Papers 861176, Canada, U.S., 1986.
- [8] W. Dabelstein, A. Reglitzky, A. Schütze, K. Reders, Handbook of Fuels: Automotive Fuels, Wiley–VCH, Weinheim, Germany, 2007.
- [9] Z. Dyolisi, K. Mokheseng, S. Mtongana, R. van der Westhuizen, unpublished results.
- [10] W.M. Haynes, CRC Handbook of Chemistry and Physics, 91<sup>st</sup> ed, CRC Press, 2010.
- [11] R.A. Maund, D.L. Smith, K.H. Lawson, Blending for Density Specifications using Fischer–Tropsch Diesel Fuel, US Patent 7345210, 2008.
- [12] P. Ghosh, J.H. Hickey, S.B. Jaffe, Ind. Eng. Chem. Res. 45 (2006) 337.
- [13] N. Ladommatos, J. Goacher, Fuel 74 (1995)1083.
- [14] T. Shigeaki, K. Takeshi, Y. Masayuli, Method and Instrument for Measuring Cetane Value or Cetane Index. JP Patent 03–100463, 1989.
- [15] H. Yang, Z. Ring, Y. Briker, N. McLean, W. Friesen, C. Fairbridge, Fuel 81 (2002) 65.
- [16] D.J. Cookson, C.P. Lloyd, B.E. Smith, Energy Fuels 2 (1988) 854.
- [17] L. Ramirez–Arizmendi, D.H. Hamje, US Patent 7420170; ExxonMobil: Annandale, NJ, USA, 2007.
- [18] T.H. de Fries, D. Indtriz, R. Kastrup, Ind. Eng. Chem. Res. 26 (1987) 188.
- [19] B. Basu, G.S. Kapur, A.S. Sarpal, R. Meusinger, Energy Fuels 17 (2003) 1570.
- [20] P. Ghosh, S.B. Jaffe, Ind. Eng. Chem. Res. 45 (2006) 346.
- [21] P. Ghosh, Energy Fuels 22 (2008) 1073.

## Chapter 5: The Use of GCxGC for Fuel Analysis

---

### 5.2 Fractionation by LC combined with GCxGC–TOF–MS for analysis of cyclics in oligomerisation products of Fischer–Tropsch derived light alkenes<sup>2</sup>

#### 5.2.1 Introduction

Synthetic crude oil derived during High Temperature Fischer–Tropsch (HT–FT) synthesis is rich in highly valuable alkenes and oxygenates, unlike conventional crude oil, which only contains these compounds at trace levels. During refining, some of these alkenes and oxygenates are extracted or converted to higher value fuels and chemicals. The rest of the synthetic crude is refined to transportation fuels.

In order to address the increasing demand for jet fuel and diesel, the gaseous alkenes ( $\approx C_3$ – $C_5$ ) are oligomerized with a solid phosphoric acid (SPA) catalyst to produce higher molecular weight oligomers. The oligomerisation products are then hydrogenated and distilled into gasoline, kerosene and diesel cuts. The oligomerisation of  $C_3$ – $C_5$  alkenes over SPA to produce heavier alkenes has been practiced commercially in crude–oil refineries since the 1930's [1]. The oligomerisation process is not only of value in fuel production e.g. kerosene and high octane gasoline, but also for the production of chemical starting materials such as alcohols, acids, esters and detergents. Alkene oligomerisation is especially suited for tuning the gasoline/kerosene/diesel ratio according to market requirements during HT–FT refining because of the abundance of  $C_3$ – $C_5$  alkenes in the primary FT product [2]. Another advantage is the conversion of short chain hydrocarbons (that have relatively good octane numbers but whose presence in gasoline is limited by the vapour pressure specification of the fuel) to molecules with higher molecular mass and excellent fuel properties. Moreover, the catalyst SPA is relatively inexpensive and the spent catalyst can be used as fertilizer, which makes the process environmentally friendly and cost effective [3, 4].

---

<sup>2</sup> R. van der Westhuizen, H. Potgieter, N. Prinsloo, A. de Villiers, P. Sandra, J. Chromatog. A 1218 (2011) 3173.

## Chapter 5: The Use of GCxGC for Fuel Analysis

---

Little is known regarding the exact composition of the complex mixture produced by SPA catalysts.

Bekker et al. [5] identified the principal alkenes in the C<sub>8</sub> fractions of four butene oligomerisation experiments performed with liquid phosphoric acid and SPA catalysts by gas chromatography–mass spectrometry (GC–MS). Of the 93 possible butene dimeric (C<sub>8</sub>) isomers, 38 were identified, despite a large degree of peak overlap in the one–dimensional GC analysis. Co–elution, combined with a lack of alkene reference materials, hampered further identification of oligomeric products. In addition, different isomers frequently yielded similar mass spectra and, as a result, the authors had to rely on Kovats retention index data, which were often found to be contradictory and difficult to reproduce.

The number of isomers increases exponentially with each additional carbon number (for example for C<sub>12</sub> products the number of isomers is 3,226. Considering that the peak capacity for a conventional 30 m high resolution capillary GC column is ca. 500 – 600 [6], it is clear that separation of all of these compounds by one–dimensional GC is impossible. Comprehensive multidimensional GC (GCxGC) provides a powerful method for the separation of complex mixtures and is therefore extensively applied for petrochemical analysis [7–10]. In combination with time–of–flight mass spectrometry (TOF–MS), providing data acquisition rates of up to 500 spectra per s, closely–eluting peaks can be deconvoluted by differentiating between unique fragments in the mass spectra [11–16].

Preliminary GCxGC–TOF–MS experiments with hydrogenated fuels indicated the possible presence of 3 to 10% cyclic alkanes. A clear differentiation of cyclic alkane and alkene classes could, however, not be achieved by GCxGC. The presence of low levels of alkenic hydrocarbons was confirmed by bromine number analysis [17]. (Note that the residual alkene content for HT–FT–derived fuels is limited to a bromine number of 10 g Br<sub>2</sub>/100g by the South African Department of Minerals and Energy (DME)). Components with cyclic structures are commonly detected in both crude–derived and conventional FT fuels. The presence of cyclics in oligomerized products, on the other hand, cannot be explained by the accepted oligomerisation reaction mechanism.

## Chapter 5: The Use of GCxGC for Fuel Analysis

---

No previous reports on the presence of cyclics in these products can be found. As the chemical and physical properties of fuels and their blends can directly be correlated to their chemical composition, it is of utmost importance to confirm the presence of cyclics in the oligomerisation products. For example, cyclics increase the density and viscosity of a fuel and affect distillation profiles.

Other properties such as cetane numbers, combustion quality, seal swell, cold flow properties, etc. are also affected. Moreover, the cyclics could be aromatic precursors that are formed in secondary reactions similar to what is observed for the reaction with mordenite and skeletal isomerisation [18], or could be part of a carbonaceous deposit formation [19] that is responsible for catalyst deactivation.

Identifying complex cyclic alkane profiles in the presence of alkenes by one-dimensional GC-MS is impossible due to the fact that these compounds have identical molecular masses and similar fragmentation patterns as the corresponding alkenes, as well as similar GC retention times. For these same reasons, even GCxGC-TOF-MS is unable to unambiguously differentiate between these classes. A way of improving the separation is to apply a fractionation step prior to GCxGC analysis [20–22].

The goal of this work was therefore to evaluate and optimise a fractionation method that would separate the cyclic alkanes from the alkenes. It is known that silver ions interact with double bonds of alkenic compounds by complexation [23]. In light of this, an LC fractionation procedure was developed using a silver-ion modified column to separate the oligomerisation product (hydrogenated) into saturated and unsaturated fractions [23,24]. Each of these fractions was analysed by GCxGC-TOF-MS to distinguish between non-cyclic and cyclic alkanes in the saturated fraction, and the non-cyclic and cyclic alkenes in the unsaturated fraction. GCxGC-FID was then used to quantify the cyclics and alkenes in gasoline, kerosene and diesel HT-FT fuels.

## Chapter 5: The Use of GCxGC for Fuel Analysis

---

### 5.2.2. Experimental

#### 5.2.2.1 Oligomerisation reactions

Alkene oligomerisation was performed using a SPA catalyst similar to the patented UOP SPA catalyst described in references [1,25] and consisting of phosphoric acid supported on silica [26]. The feed was obtained from three FT condensate streams which were fractionated in a feed debutaniser column. The C<sub>3</sub> and C<sub>4</sub> overheads fraction (distilled between 130°C and 160°C) was used as feed for the oligomerisation unit. Feed water content was adjusted to control the SPA catalyst hydration level. Oligomerisation of the light alkenes occurred via condensation reactions to form dimers, trimers, tetramers and their mixtures. The oligomer mixture was subsequently hydrogenated to a bromine number of 4.0 g Br<sub>2</sub>/100g, resulting in almost complete saturation of the alkenes.

The final product was distilled at atmospheric pressure into three cuts namely gasoline (< 150°C), kerosene (150–170°C) and diesel (>170°C). Standard mixtures containing 1–octene (Sigma–Aldrich, Johannesburg, SA, Fluka ≥ 99.5) and n–dodecane (Sigma–Aldrich, Fluka, ≥ 99.8 %) were used as internal standards for alkenes and cyclic alkanes, respectively. The standards were selected because no linear 1–alkene or n–alkane molecules were found in the oligomerisation products (based on retention times and mass spectral information) for both the unhydrogenated and hydrogenated products. The standards were added to the samples before fractionation. Quantification was performed from GCxGC–FID data using the Classifications function in the Leco ChromaTOF software (Version 4.21).

The final hydrogenated oligomerisation product as well as the distillation cuts, were analysed neat and after LC fractionation using both GCxGC–TOF–MS and GCxGC–FID. The final product was also brominated to confirm the LC fractionation. It may be difficult to correlate the bromine number of a compound directly with the degree of unsaturation (e.g. a product can undergo extensive hydrogenation but still give a bromine number).

## Chapter 5: The Use of GCxGC for Fuel Analysis

---

By using products with different bromine numbers, the decreasing amount of alkenes could be monitored by GCxGC. Therefore, to further aid with the identification, two oligomerisation products were hydrogenated to bromine numbers of 0.7 (low alkene sample) and 30g Br<sub>2</sub>/100g (high alkene sample), respectively. These samples were subjected to the same analyses.

### 5.2.2.2. Bromination

The standard test method ISO 3839 for the determination of unsaturates in petroleum [17] was used for determination of bromine number. Following the initial analysis of the brominated product (Figure 5 below), brominated products were removed by elution through a silica gel column prior to GCxGC analysis to prevent contamination of columns and syringes. Silica gel, 60–100 mesh and activated overnight at 250 °C (Sigma–Aldrich) was slurry–packed with n–hexane in a 1 m x 15 mm ID glass column. 1 g of sample was applied to 40 g of silica gel. The non–brominated solutes were eluted with 100 mL hexane (Chromasolv, Sigma–Aldrich). Brominated compounds were retained on the column and visible as a yellow band.

### 5.2.2.3 LC fractionation

Optimisation of the LC fractionation was performed using a standard mixture consisting of 1 % (v/v) of each of the components listed in Table 1 in n–hexane. A Dionex Ultimate 3000 HPLC system, equipped with autosampler, degasser, dual gradient pumping system and column compartment was used for the fractionation (Dionex, Sunnyvale, USA). Detection was performed by a corona charged aerosol detector (CAD) supplied by ESA Biosciences (Chelmsford, USA), operated with a total nitrogen gas flow of 4 L/min and a temperature of 30 °C. A sulphonic silica–based strong cation–exchange column (Nucleosil 100–5 SA, 25 cm L x 4.6 mm ID, 5 µm d<sub>p</sub> from Macherey–Nagel, Düren, Germany) was used. The column was loaded with silver–ions according to the procedure described by Sandra *et al.* [24]. The injection volume was 15 µL and an analysis temperature of 30 °C was used throughout. During the first 6 min 100% n–hexane (Chromasolv, Sigma–Aldrich) was used to elute the saturated hydrocarbons.

## Chapter 5: The Use of GCxGC for Fuel Analysis

**Table 1: Composition of the standard mixture used for optimisation of the LC fractionation procedure.**

<b>Nr</b>	<b>Alkanes</b>
1	n-Nonane
2	3,3-Dimethyloctane
3	3-Methylnonane
4	Dodecane
	<b>Cyclo-alkanes</b>
5	1-Methyl-2-propylcyclohexane,
6	1,2,4-Trimethylcyclohexane (c&t)
	<b>Alkenes</b>
7	3-Dodecene
8	2-Methyl-3-heptene
9	2,5-Dimethyl-2-hexene
	<b>Cyclic alkenes</b>
10	1,2,3-Trimethylcyclopentene
11	4-Methylcyclohexene
	<b>Dienes</b>
12	2,4-Dimethyl-1,3-pentadiene
13	1,3-Cyclooctadiene
	<b>Aromatics</b>
14	4-tert-Butyltoluene
15	Indane
16	1,2,3-Trimethylbenzene

At 6 min the mobile phase was changed to 100 % acetone (Chromasolv, Sigma-Aldrich) to elute the unsaturated hydrocarbons. A flow rate of 1 mL/min was applied and the column was conditioned with n-hexane for 15 min before the next injection. After the retention times were determined by CAD, the detector was disconnected and the eluent was collected manually. The n-hexane fraction was collected between 2.5–4 min and the acetone fraction between 10–10.75 min corresponding to 1.5 mL and 0.75 mL volumes, respectively.

## Chapter 5: The Use of GCxGC for Fuel Analysis

---

### 5.2.2.4. GCxGC–TOF–MS and FID analyses

The GCxGC instrument was a Pegasus 4D from Leco Corporation (St. Joseph, USA) equipped with a 7683B auto injector system (Agilent Technologies, Little Falls, USA). FID was used for quantification purposes due to the wide linear range and universal detection of hydrocarbons. In all other cases, TOF–MS was used. The reversed phase column set described in ref [27] was used: in the first dimension a 60 m x 0.25 mm ID, 0.25  $\mu\text{m}$   $d_f$  DB Wax column (J&W Scientific, Folsom, USA) and in the second dimension a 2 m x 0.1 mm ID, 0.1  $\mu\text{m}$   $d_f$  RTX–5 column (Restek, Bellefonte, USA). Helium was the carrier gas at a constant flow rate of 1.2 mL/min. A split ratio of 400:1 and injection volume of 0.05  $\mu\text{L}$  were used for the analysis of the fuels while for the LC fractions the split ratio was 20:1 and the injection 1  $\mu\text{L}$  to compensate for the dilution. The first oven was programmed from 40°C (0.2 min) to 240°C at 2°C/min. The second oven and modulator followed the first temperature program but started at 50°C and 70°C, respectively. TOF–MS and FID data were collected at 100 spectra/s and 100 Hz, respectively

### 5.2.3 Results and discussion

#### 5.2.3.1 Optimisation of the LC fractionation procedure

Using a silver–modified column, the saturated hydrocarbons were not retained and passed through with *n*–hexane. After 6 min the mobile phase was changed to acetone and all retained unsaturated compounds were eluted as a single peak. The GCxGC contour plots (Figure 1) obtained for the analysis of the *n*–hexane and acetone fractions of the standard mixture confirm that the LC fractionation procedure successfully separated the non–cyclic and cyclic saturated hydrocarbons (*n*–nonane, 3,3–dimethyloctane, 3–methylnonane, *n*–dodecane, 1–methyl–2–propylcyclohexane and 1,2,4–trimethylcyclohexane) from the unsaturated non–cyclic and cyclic hydrocarbons and from the aromatics (3–dodecene, 2–methyl–3–heptene, 2,5–dimethyl–2–hexene, 1,2,3–trimethylcyclopentene, 4–methylcyclohexene, 2,4–dimethyl–1,3–pentadiene, 1,3–cyclooctadiene, 4–tert–butyltoluene, indane and 1,2,3–trimethylbenzene).

## Chapter 5: The Use of GCxGC for Fuel Analysis

---

### 5.2.3.2 LC fractionation combined with GCxGC–TOF–MS analysis of the final oligomerisation product

The oligomerisation products of a selected fuel ranged in carbon numbers from C<sub>3</sub> to around C<sub>18</sub> (Figure 2). The hydrogenated product contained mainly alkanes but the bromine number was 4g Br<sub>2</sub>/100 g indicating the presence of low levels of remaining alkenes. This is confirmed by the mass spectral data as several components had molecular masses –2 units lower than expected for saturated hydrocarbons e.g. m/z 142 for C<sub>10</sub> alkanes. However, m/z 140 corresponds to C<sub>10</sub> alkenes or C<sub>10</sub> cyclic alkanes. In addition, some of the components had molecular masses –4 units lower than expected for saturated hydrocarbons i.e. for the C<sub>10</sub> domain m/z 138 which can correspond to cyclic alkenes, dienes or bicyclic alkanes. Based on ion extraction, these m/z values form 3 separate bands in the GCxGC plot (see insert). Trace levels ( $\approx$  0.2 mass %) of aromatic compounds were also observed (data not shown).

The complexity could be drastically reduced by fractionation with silver–ion chromatography. The hexane fraction (A) and for the acetone fraction (B). Figure 3 shows the C<sub>10</sub> part of the GCxGC–TOF–MS contour plots at m/z 142, 140 and 138 for the hexane fraction (A) and for the acetone fraction (B). In the hexane fraction only the non–cyclic, cyclic and bicyclic alkanes are detected while in the acetone fraction the alkenes and cyclic alkenes are recovered. As dienes are unstable and would have been hydrogenated before the mono–alkenes and cyclic alkenes, it was assumed that no dienes remained in the product. Note that the elution areas for the cyclic alkanes and alkenes overlap in the contour plot, making their differentiation, even with TOF–MS without pre-fractionation, very difficult. Similar trends were observed for the other carbon numbers and in the different distillates.

The GCxGC contour plots of the gasoline, kerosene and diesel distillation cuts as well their respective LC fractions (Figure 4) confirm that the LC fractionation procedure is equally successful for each of these samples (note that the peaks visible at low 2D retention times in the inserts are from the HPLC solvents used).

## Chapter 5: The Use of GCxGC for Fuel Analysis

---

As an alternative to the LC fractionation procedure, the bromination reaction can lead to similar results. Figure 5 illustrates the contour plots obtained for the analysis of the oligomerisation product before (A) and after bromination (B). The alkenes reacted with the bromine to form high molecular mass bromine derivatives while the alkanes and cyclic alkanes were not affected.

Disadvantages of this approach are that MS interpretation of the brominated alkene spectra is difficult, but above all that injection of the brominated sample contaminates the autosampler and the column. Fractionation by chromatography on silica gel could overcome this problem as the brominated species are retained (section 2.2) but the procedure is more time-consuming and samples have to be enriched increasing the risks of contamination.

Literature reports on reactions similar to SPA oligomerisation provide possible explanations for the presence of cyclics in the SPA product. Tabak *et al.* [18] reported a kinetic and modelling study of *n*-butene oligomerisation over H-mordenite. The authors proposed a simplified kinetic mechanism for the mordenite reaction and suggested that the newly formed molecules undergo secondary reactions such as isomerisation, cracking, aromatisation, etc.

It is possible that the cyclics from the SPA oligomerized product are formed during similar secondary reactions, for example as aromatic precursors.

## Chapter 5: The Use of GCxGC for Fuel Analysis

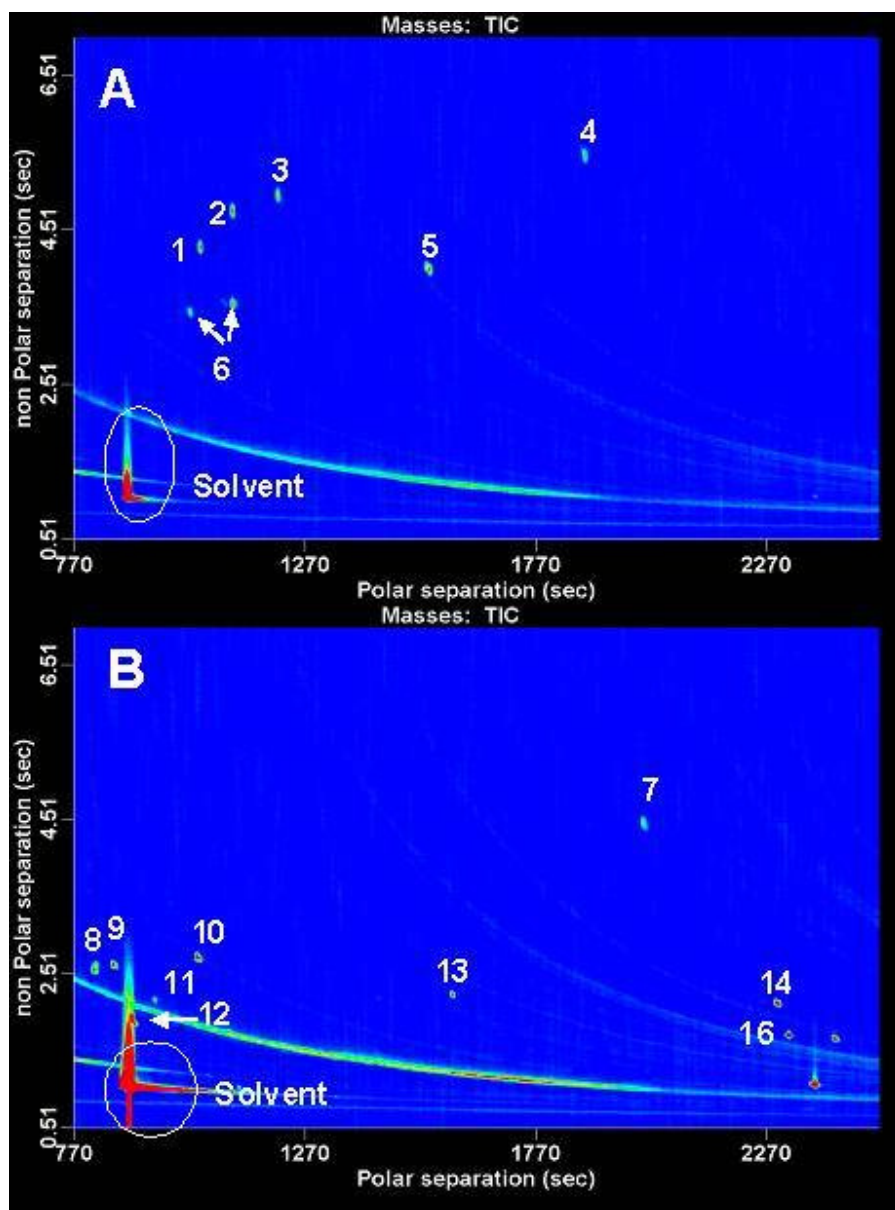


Figure 1. Contour plots obtained for the GCxGC-TOF-MS analysis of the *n*-hexane (A) and acetone (B) LC fractions of the standard mixture showing the separation of alkanes and cyclic alkanes from the alkenes, cyclic alkenes and aromatics in the standard mixture. Peak numbers correspond to Table 1.

In another study, Van Donk *et al.* [19] described the effects of carbonaceous deposit formation on the deactivation of zeolites used for butene skeletal isomerisation.

## Chapter 5: The Use of GCxGC for Fuel Analysis

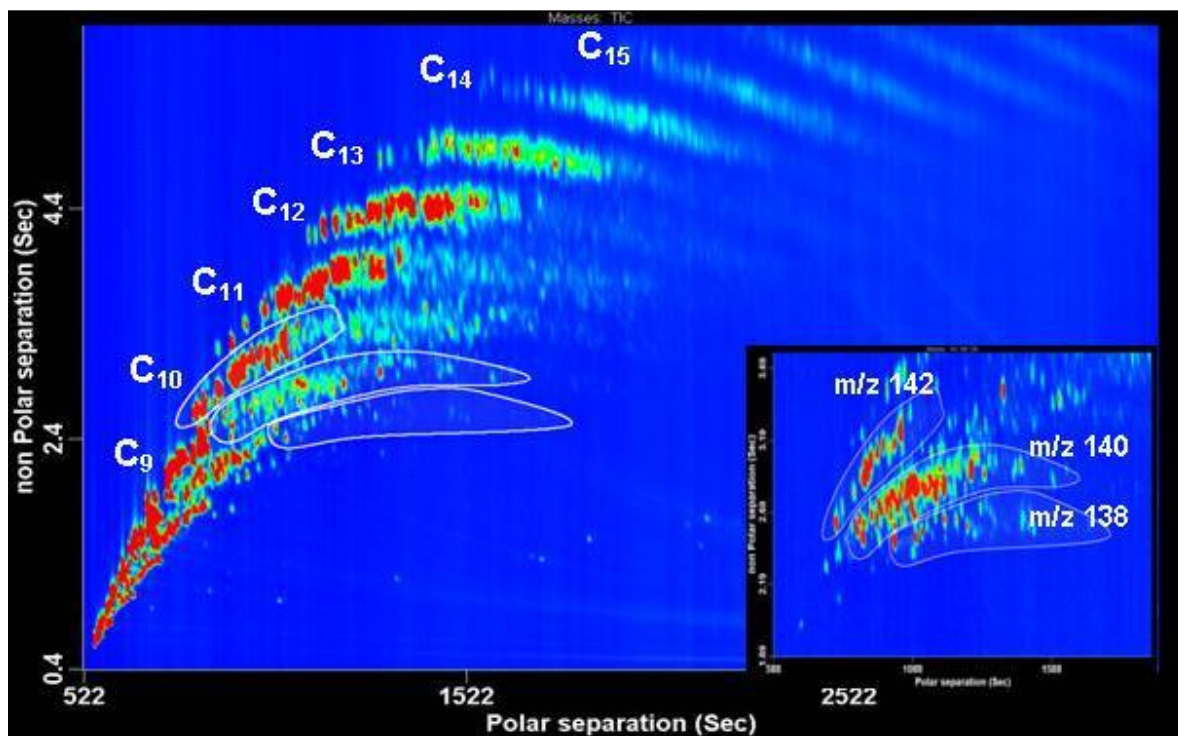


Figure 2. GCxGC–TOF–MS contour plot for the analysis of the total oligomerised product after hydrogenation and prior to LC fractionation (bromine number 4 g Br<sub>2</sub>/100 g). Extracted ion plots for m/z 142, 140 and 138 (insert) show the C<sub>10</sub> non–cyclic alkanes, cyclic alkanes and/or alkenes and the cyclic alkenes/dienes/bicyclic alkanes.

Skeletal isomerisation over microporous material is generally performed at high temperatures ( $\approx 350^\circ\text{C}$ ), where aliphatic coke is initially formed and subsequently slowly transformed to aromatics. Carbonaceous deposit formation was also observed on SPA catalysts used for skeletal isomerisation [28]. Although the temperatures used during SPA oligomerisation are not as high ( $140\text{--}230^\circ\text{C}$ ) as for skeletal isomerisation, the presence of cyclics could be an indication of the initial stages of carbonaceous deposit formation that will lead to the formation of aromatics and eventually to catalyst deactivation.

## Chapter 5: The Use of GCxGC for Fuel Analysis

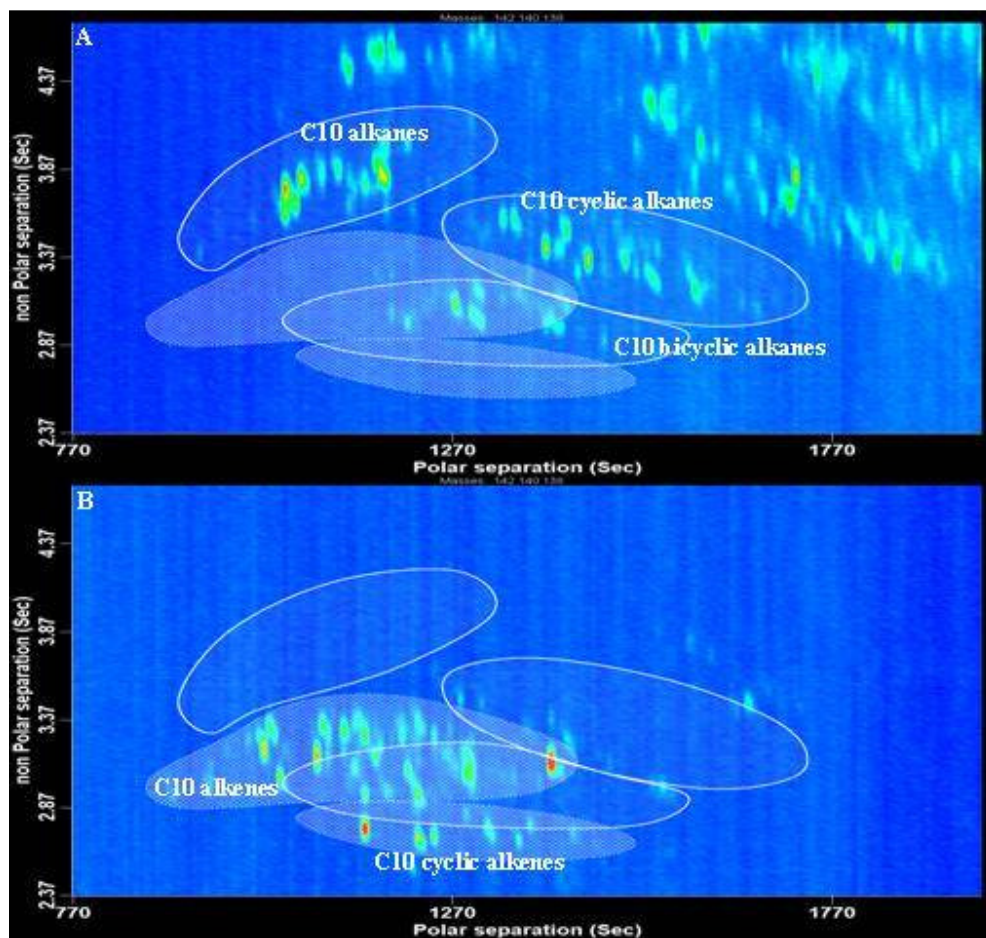


Figure 3. Extracted ion GCxGC-TOF-MS contour plots of  $m/z$  142, 140 and 138 of the LC fractions of the oligomerisation product (bromine number 4 g  $Br_2/100$  g). (A) The  $n$ -hexane fraction shows the presence of  $C_{10}$  non-cyclic, cyclic and bicyclic alkanes, (B) the acetone fraction shows the presence of  $C_{10}$  alkenes and cyclic alkenes.

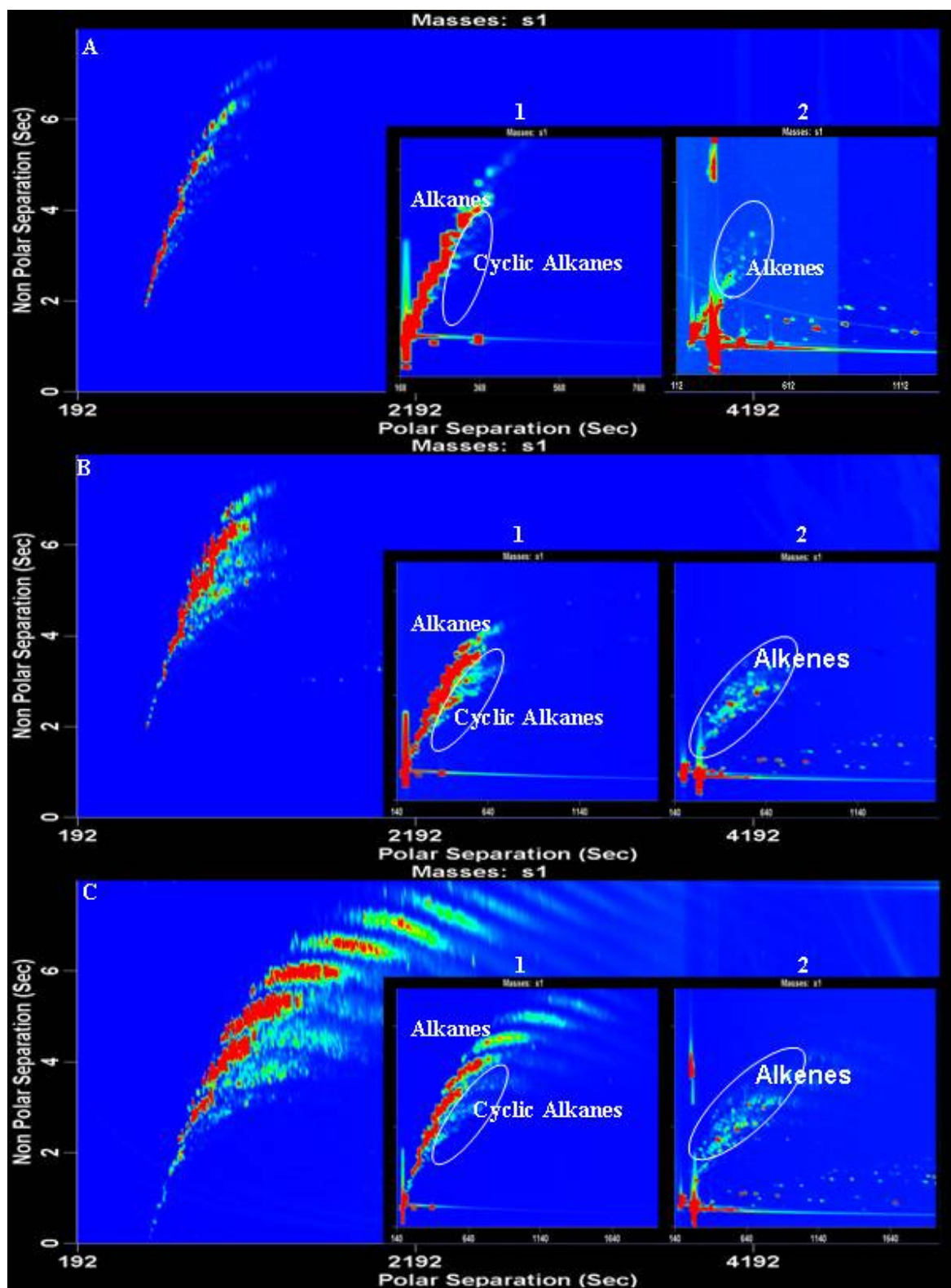


Figure 4. GCxGC-TOF-MS TIC contour plots for A) gasoline, B) kerosene and C) diesel distillation samples. Inserts show the fractionation of the alkanes and cyclic alkanes (1) and alkenes and cyclic alkenes (2) for each of the samples.

## Chapter 5: The Use of GCxGC for Fuel Analysis

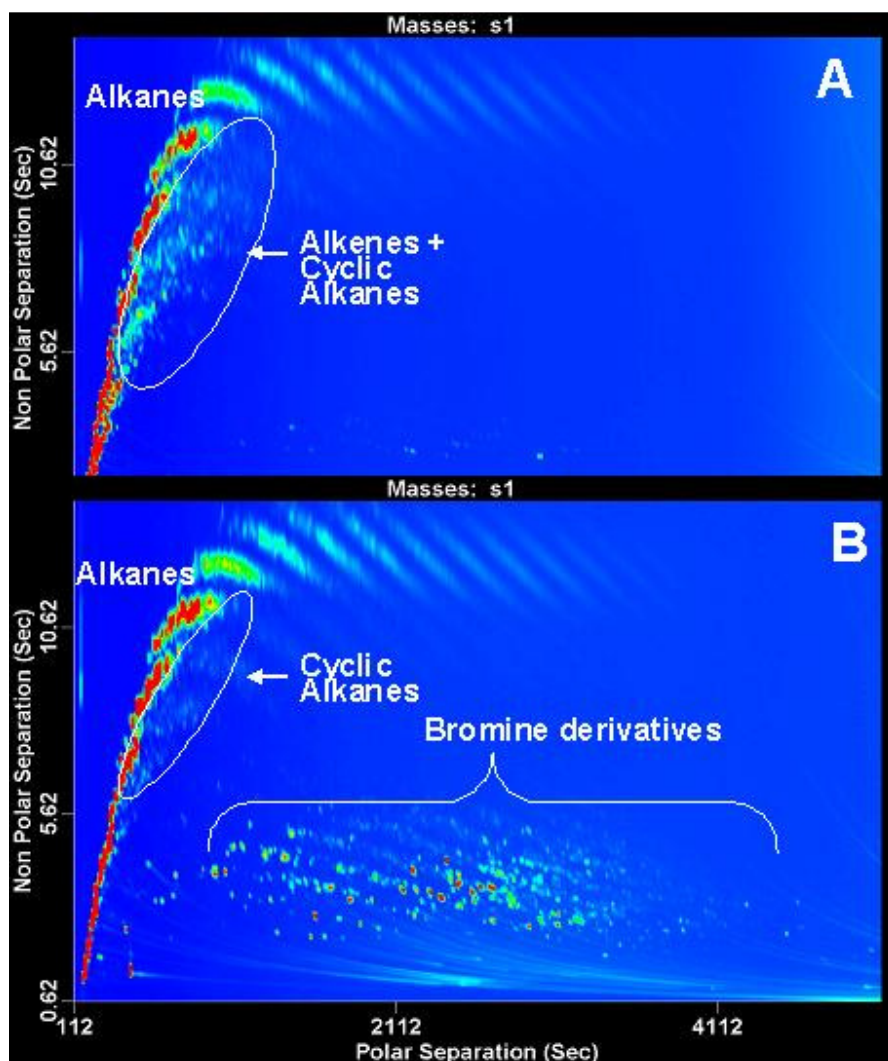


Figure 5. GCxGC–TOF–MS contour plots indicating the oligomerisation product A) before (bromine number 4 g Br<sub>2</sub>/100g) and B) after bromine derivatisation.

### 5.2.3.3 Determination of the cyclic/alkene distribution in oligomerisation products

GCxGC–TOF–MS plots of the oligomerisation products with bromine numbers 30 and 0.7 g Br<sub>2</sub>/100 g were compared using the described methodologies and the following conclusions could be drawn. For the product with the lower bromine number, where the alkene/cyclics fraction contained mostly cyclics and very few alkenes, the highest concentration was distributed in the C<sub>9</sub>–C<sub>10</sub> carbon number range.

## Chapter 5: The Use of GCxGC for Fuel Analysis

On the other hand, for the product with the higher bromine number, containing more alkenes than cyclics, the highest concentration was distributed in the C<sub>3</sub>–C<sub>7</sub> region.

Using GCxGC–FID, the cyclic and alkene distributions for the oligomerisation products could be quantified. Figure 6 shows the data for the oligomerisation product with bromine number 0.7 g Br<sub>2</sub>/100 g. The cyclic alkane and alkene content in the distillation fractions of gasoline, kerosene and diesel of the 0.7 g Br<sub>2</sub>/100 g product obtained by GCxGC–FID are summarised in Table 2.

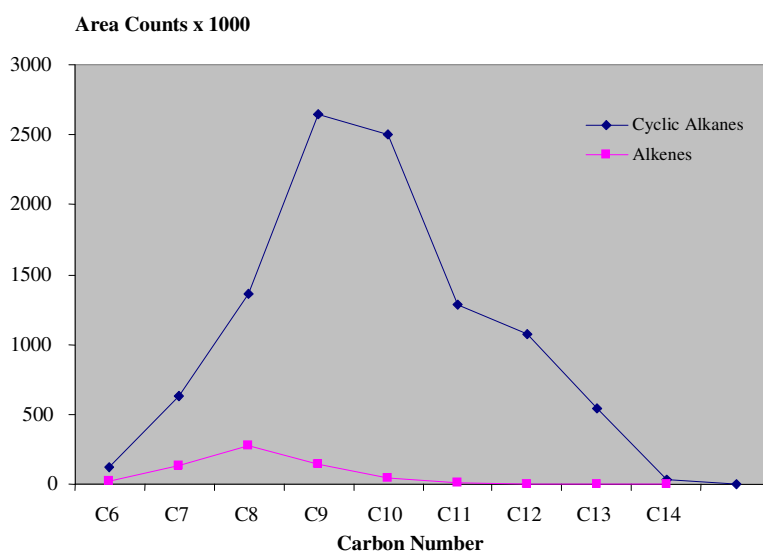


Figure 6. Graphic illustration of the distribution of alkenes and cyclic alkanes for the oligomerisation product with a bromine number of 0.7 mg Br<sub>2</sub>/100g.

The total amount of cyclics in this product is ca. 2.5%. As they are mainly distributed over the C<sub>9</sub>–C<sub>10</sub> carbon numbers, they will have the highest concentration in the kerosene (2.38%) and diesel (3.64%) cuts. The boiling points of C<sub>9</sub>–C<sub>10</sub> cyclic alkanes are in the region of 150°C–170°C (for example isopropylcyclohexane 154.5°C, isobutylcyclohexane 169°C). The gasoline fraction showed the highest fraction alkene concentration (refer Figure 4). Slight variations in distillation conditions could shift the majority of the cyclics to either the kerosene or the diesel cut.

## Chapter 5: The Use of GCxGC for Fuel Analysis

**Table 2: Quantitative results obtained by GCxGC–FID for the cyclic alkanes and alkenes in the LC fractions of the hydrogenated oligomerisation product (0.7 g Br<sub>2</sub>/100 g) and its distillation cuts.**

	Distillation temperatures	Distillation mass balance		Cyclic alkanes	Alkenes
		g	Mass %	Total mass %	Total mass %
	°C				
Oligomerisation product		2.956		2.52	0.69
Gasoline Cut	< 150	1.538	52.03	0.17	1.90
Kerosene Cut	150 – 170	0.412	13.94	2.38	0.34
Diesel Cut	> 170	0.879	29.74	3.64	0.29
			95.70		

### 5.2.3.4 Comparison of the alkene composition in oligomerisation products versus in conventional FT products.

Alkenes in the oligomerised product contain mostly internal double bonds. This is contrary to what is observed in the HT–FT synthetic crude, that are known to contain predominantly  $\alpha$ -alkenes [27,29]. Figure 7 compares the GCxGC–TOF–MS profiles for a standard HT–FT (A) and the oligomerisation product with a bromine number of 30 g Br<sub>2</sub>/100 g (B). The inserts of the figure show the selected ion plots at  $m/z$  140 for the fractionated acetone fractions. The HT–FT condensate contains high levels of C<sub>10</sub>  $\alpha$ -alkenes, identified by mass spectra and retention times ( $m/z$  140). The C<sub>10</sub> alkene peaks in the oligomerised product elute in a region adjacent to that of the  $\alpha$ -alkenes. Similarly, a comparison of the  $m/z$  138 extracted ion contour plots show a shift of the elution window for cyclic alkenes with internal double bonds on the side chain relative to those with  $\alpha$ -double bonds (results not shown). The same trend was observed for the product with bromine number of 4.0 mg Br<sub>2</sub>/100g, thereby eliminating the possibility that the linear  $\alpha$ -alkene was hydrogenated preferentially.

## Chapter 5: The Use of GCxGC for Fuel Analysis

No dienes were expected in either of these two samples because the second double bond of the diene would be hydrogenated before the mono-alkenes or cyclic alkenes. Neither was any n-alkanes observed in the hydrogenated products.

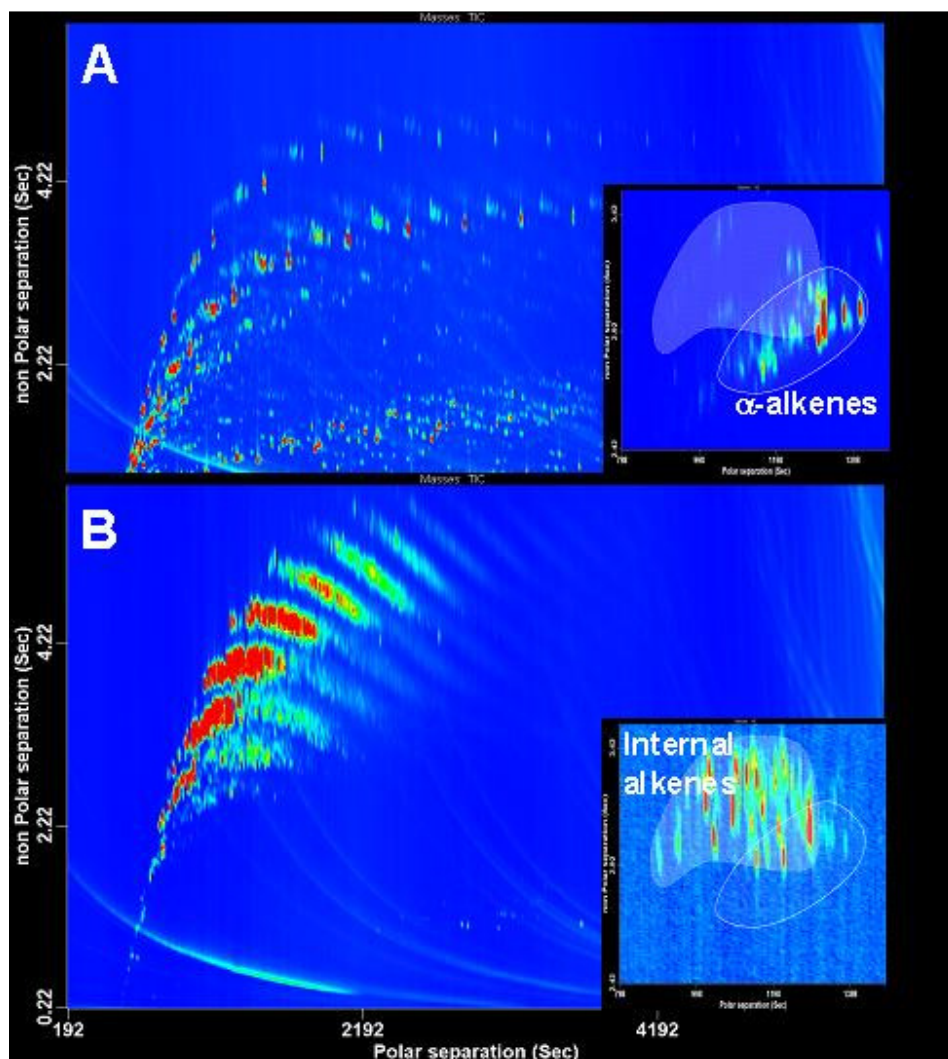


Figure 7. A comparison of the GCxGC plots for a highly alkenic HT-FT condensate (A) and an oligomerised product (B). Inserts show selected ion contour plots ( $m/z$  140) for the acetone fractions of these samples, demonstrating the difference in elution positions of  $\alpha$ -alkenes and internal alkenes.

## Chapter 5: The Use of GCxGC for Fuel Analysis

---

### 5.2.4 Conclusions

The analysis of cyclic alkanes and internal alkenes in SPA catalyzed oligomerisation products of FT derived alkenes is problematic as co-elution of peaks occurs, even when using GCxGC. Mass spectrometry is also not of much help because of similar molecular masses and very similar mass fragmentation patterns for these component classes.

An LC fractionation procedure utilising a silver–modified column was developed to separate saturated and unsaturated components in oligomerised products. Combined with GCxGC–TOF–MS, the separation of alkanes and alkenes into non-cyclic, mono-cyclic and bicyclics component classes could be obtained. This allowed us to confirm that cyclics are present in SPA catalyzed oligomerisation products of FT derived alkenes. The developed procedure could be applied to (i) determine the concentration of alkanes, cyclic alkanes and alkenes in oligomerised products and (ii) to tune the distillation conditions to shift the cyclic alkanes either in the kerosene or diesel cuts. The study made also clear that contrary to standard HT–FT condensates, SPA catalyzed oligomerisation products of FT derived alkenes contain internal alkenes and very little  $\alpha$ –alkenes.

## Chapter 5: The Use of GCxGC for Fuel Analysis

---

### 5.2.5. References

- [1] J.C. Morell, Polymerisation Catalyst Comprising Phosphoric Acid and Siliceous Material. US Patent Nr. 3, 132, 108 B1 (1964).
- [2] N.M. Prinsloo, Fuel Process. Technol. 87 (2005) 437.
- [3] R. Schwarzer, E. du Toit, W. Nicol, Applied Catalysis A: General 369 (2009) 83.
- [4] D. Leckel, Energy & Fuels 23 (2009) 2342.
- [5] R. Bekker, N.M. Prinsloo, Ind. Eng. Res. 48 (2009) 10156.
- [6] L.M. Blumberg, W.H. Wilson, M.S. Klee, J. Chromatogr. A 894 (1999) 15.
- [7] Z. Y. Lui, J. B. Philips, J. Chromatogr. Sci. 29 (1991) 227.
- [8] J. Beens, U. A.Th. Brinkman, Analyst 130 (2005) 123.
- [9] M. Abahcour, J. Beens, R.J.J. Vreuls, U. A. Th. Brinkman, Trends Anal. Chem. 25 (2006) 540.
- [10] P. Marriott, R. Shellie, Trends Anal Chem. 21 (2002) 573.
- [11] J. B. Philips, J. Xu, J. Chromatogr. A. 703 (1995) 327.
- [12] J. B Philips, J. Beens, J. Chromatogr. A 856 (1999) 331.
- [13] J. Blomberg, P.J. Schoenmakers, J. Beens, R. Tijssen, J. High Resolut. Chromatogr. 20 (1997) 539.
- [14] J. Beens, J. Blomberg, P.J. Schoenmakers, J. High Resolut. Chromatogr. 23 (2000) 182.
- [15] J. Dalluge, J. Beens, U. A. Th. Brinkman, J. Chromatogr. A 1000 (2003) 69.
- [16] M. van Deursen, J. Beens, J Reijenga, P. Lipman, C. Cramers, J. Blomberg, J. High. Resolut. Chromatogr. 23 (2000) 5.
- [17] Standard Test Method: ISO 3839, Petroleum products – Determination of bromine number of distillates and aliphatic olefins – Electrometric method, second edition, 01/01/1996.
- [18] S.A. Tabak, F. J. Krambeck, W.E Garwood, AIChE J. 32 (1986) 1526.
- [19] S. van Donk, J.H. Bitter, K. P. De Jong, Applied Catalysis A: General 212 (2001) 97.
- [20] G. S Frysinger, R.B. Gaines, L. Xu, C.M. Reddy, Environ. Sci. Technol. 37 (2003) 1653.
- [21] R. Edam, J. Blomberg, H.–G Janssen, P.J. Schoenmakers, J. Chromatogr. A. 1086 (2005) 1200.

## Chapter 5: The Use of GCxGC for Fuel Analysis

---

- [22] C. Vendeure, F. Bertoncini, D. Espinat, D. Thiebaut, M.–C. Hennion, *J. Chromatogr. A* 1090 (2005) 116.
- [23] D. Mao, H. v.d. Weghe, L. Diels, N. De Brucker, R. Lookman, G. Vanermen, *J. Chromatogr. A* 1179 (2008) 33.
- [24] P. Sandra, A. Medvedovici, Y. Zhao, F. David, *J. Chromatogr. A* 974 (2002) 231.
- [25] A. de Klerk, “Fischer–Tropsch Refining”, Ph.D. Thesis, University of Pretoria, February 2008.
- [26] A. de Klerk, *Energy & Fuels* 20 (2006) 439.
- [27] R. Van der Westhuizen, A. Crouch, P. Sandra, *J. Sep. Sci.* 31 (2008) 3423.
- [28] J. Houžvička, V. Ponec, *Applied Catalysis: A General* 145 (1996) 95.
- [29] A. Steynberg, M. Dry, (Eds) *Fischer–Tropsch Technology*, Elsevier, Amsterdam (2004).

## Chapter 5: The Use of GCxGC for Fuel Analysis

---

### 5.3 The use of GCxGC with time-of-flight mass spectrometry to investigate dienes and Diels–Alder polymerisation products in high temperature Fischer–Tropsch based fuels<sup>3</sup>

#### 5.3.1 Introduction

The Fischer–Tropsch (FT) process is a catalyzed chemical process in which carbon monoxide and hydrogen are converted into liquid mixtures mainly composed of hydrocarbons of various forms. Typical catalysts used are based on iron and cobalt. The principal purpose of this process is to produce synthetic fuels and chemicals from coal, natural gas or biomass. The FT process is a stepwise polymerisation reaction that produces a complex mixture of components [1]. Valuable products such as the  $\alpha$ -olefin monomers and various solvents are extracted during the product work-up step and purified. About two thirds of FT products are converted into fuels.

Besides the catalyst, an important variable in the FT process is the temperature. The operating temperature in the high temperature Fischer–Tropsch (HT-FT) process for coal is around 330°C–350°C. At these high temperatures, a more complex product spectrum is obtained than during low temperature FT (LT-FT) processes (220°C–250°C) using Fe- and Co- catalysts. In HT-FT, an increased degree of branching is noted together with the formation of aromatics. Blending LT-FT and HT-FT could unlock potential performance synergies in the fuel properties of the individual fuels [2]. Cyclic olefins, dienes and cyclic dienes, resulting from the dehydrogenation of paraffins and olefins, are also present at trace- and ultra-trace level in HT-FT fuels, and especially conjugated dienes have been associated with gum formation in fuels [3]. Gums can build up in a car's carburettors, fuel injection valves and near intake valves. It makes operation difficult and may result in inappropriate mixing and deficient fuel burn. Gasoline with a high diene content has been reported to be prone to high residue formation [4–6]. Dienes are highly reactive components that can undergo Diels–Alder and Retro–Diels–Alder reactions.

---

<sup>3</sup> R. Van der Westhuizen, A. Crouch, P. Sandra, J. Sep. Sci. 31 (2008) 3423.

## Chapter 5: The Use of GCxGC for Fuel Analysis

---

The Diels–Alder reaction is thought to be partially responsible for gum formation in HT-FT derived fuels. Dienes can be removed from FT fuels by selective hydrogenation to olefins. This ensures that no valuable products are lost from the process. Extensive research is being done in developing more selective catalysts for the hydrogenation of dienes to olefins. Group VIII metals such as Pd–, Pt–, or Ni–based catalysts are among the most promising transition metals for this process. Pd catalysts have been shown to be very active and selective [7–9]. Ideally the catalyst should convert the diene to valuable olefins and should not lead to further hydrogenation to paraffins or produce significant isomerisation of the 1–octene to the internal olefins. A Pt/ Al catalyst was used in this study.

Few methods exist for the determination of trace levels of dienes in complex fuel matrices. These determinations are very challenging for several reasons. Because the boiling points and polarities of dienes are very similar to those of olefins, conventional techniques such as distillation, column separations or selective extraction, are not effective. One–dimensional capillary gas chromatography (CGC) is also not appropriate as the diene components present at ppm levels are obscured by the high concentrations of paraffins, olefins, aromatics and oxygenates. Moreover, the mass spectra (MS) of dienes are very similar to those of the corresponding cyclic olefins. For the same carbon number, both classes have the same molecular mass and similar mass fragmentation patterns. To make structure elucidation even more difficult, in one–dimensional GC–MS eventual mass spectra of the suspected dienes cannot be interpreted because of the high degree of peak co–elution.

At present, the maleic anhydride method based on derivatisation and titration is the method of choice for the determination of the total conjugated diene content in fuels [10]. Briefly, the sample is refluxed with maleic anhydride to form the Diels–Alder product. Unreacted anhydride is extracted, hydrolyzed and back–titrated with a strong base such as NaOH. The method is tedious and susceptible to interferences. In a recent NMR study, it was shown that in the maleic anhydride method hindered dienes do not react, while some dienes form Diels Alder adducts with other dienes and some aromatics such as anthracene also react with maleic anhydride [11].

## Chapter 5: The Use of GCxGC for Fuel Analysis

---

On the other hand, the determination of the gum content in fuels is a standard method [12]. The test involves evaporation of the fuel under controlled conditions of temperature (232–246°C) and flow of steam ( $1000 \pm 150$  mL/s). Gum is expressed in mg/100 mL.

Comprehensive GC has received much interest in recent years and especially for the characterisation of petroleum derivatives. Pioneering work was performed by J.B. Phillips, the inventor of GCxGC, and co-workers [13,14] and at the Shell Research and Technology Centre, Amsterdam, The Netherlands by J. Beens, J. Blomberg and co-workers [15–17]. Main features are the structured profiles, the high peak capacity and the increased sensitivity for trace analysis compared to one-dimensional GC. Combined with Time-of-Flight mass spectrometry (TOF-MS) and MS deconvolution, it is one of the most powerful analytical techniques available today for the analysis of complex mixtures.

The use of GCxGC/TOF-MS for differentiation and quantification of cyclic olefins, dienes and cyclic dienes as well as of the Diels-Alder dimers and trimers in HT-FT derived fuels is described.

### 5.3.2 Experimental

#### 5.3.2.1 Samples

A HT-FT sample with a low gum value (4.1 mg/100mL) was used to generate a total GCxGC profile. The dienes, cyclic dienes, cyclic olefins, and dimer and trimer Diels Alder products were analysed in a HT-FT sample with a relatively high gum value (22.1 mg/100 mL) before and after selective hydrogenation. The gum value was determined according to ref [12].

#### 5.3.2.2 Instrumentation

Analyses were performed on a Leco Pegasus 4D GCxGC-TOF-MS system (LECO Corporation, St. Joseph, MI, USA).

## Chapter 5: The Use of GCxGC for Fuel Analysis

---

The main column was a 60 m x 250 mm ID x 0.25  $\mu\text{m}$   $d_f$  polyethylene glycol (DB-Wax) from (Agilent Technologies, Little Falls, DE, USA, and the secondary column a 2 m x 100 mm ID x 0.1  $\mu\text{m}$   $d_f$  5% phenyl, 95% methyl polysiloxane (TRB-5) from Teknokroma, Cataluna, Spain. For the total profile and the analysis of the dienes, cyclic olefins and cyclic dienes the main oven temperature was programmed from 35°C (1 min) to 230°C at 3°C/min. The second oven started at 40°C (1 min) and was programmed to 235°C at 3°C/min. The modulation time was 10 s. For the analysis of the Diels–Alder products the main oven temperature was programmed from 25°C (0.2 min) to 260°C at 2°C/min. The second oven started at 35°C (0.2 min) and was programmed to 300°C at 2°C/min while the modulation time was 14 s. In all cases, a split ratio of 1/400 was used for an injection volume of 0.1  $\mu\text{L}$ . Helium was the carrier gas at a constant flow of 1 mL/min. The TOF–MS was acquiring data at 200 spectra/s.

### 5.3.3 Results and discussion

GCxGC profiling of fuels is commonly performed on an apolar column as main column and a polar column as secondary column. For FT profiling we experienced, however, that in the reversed polarity mode i.e. a polar column first followed by an apolar column the best group type separation was obtained. This is illustrated in Figure 1 showing the total GCxGC profile of the HT-FT low gum sample. An excellent structured separation using the complete  $^2\text{D}$  space is noted. Some cyclic olefins, dienes and cyclic dienes can be elucidated directly from the plot but in order to detect their traces, ion extraction was applied.

## Chapter 5: The Use of GCxGC for Fuel Analysis

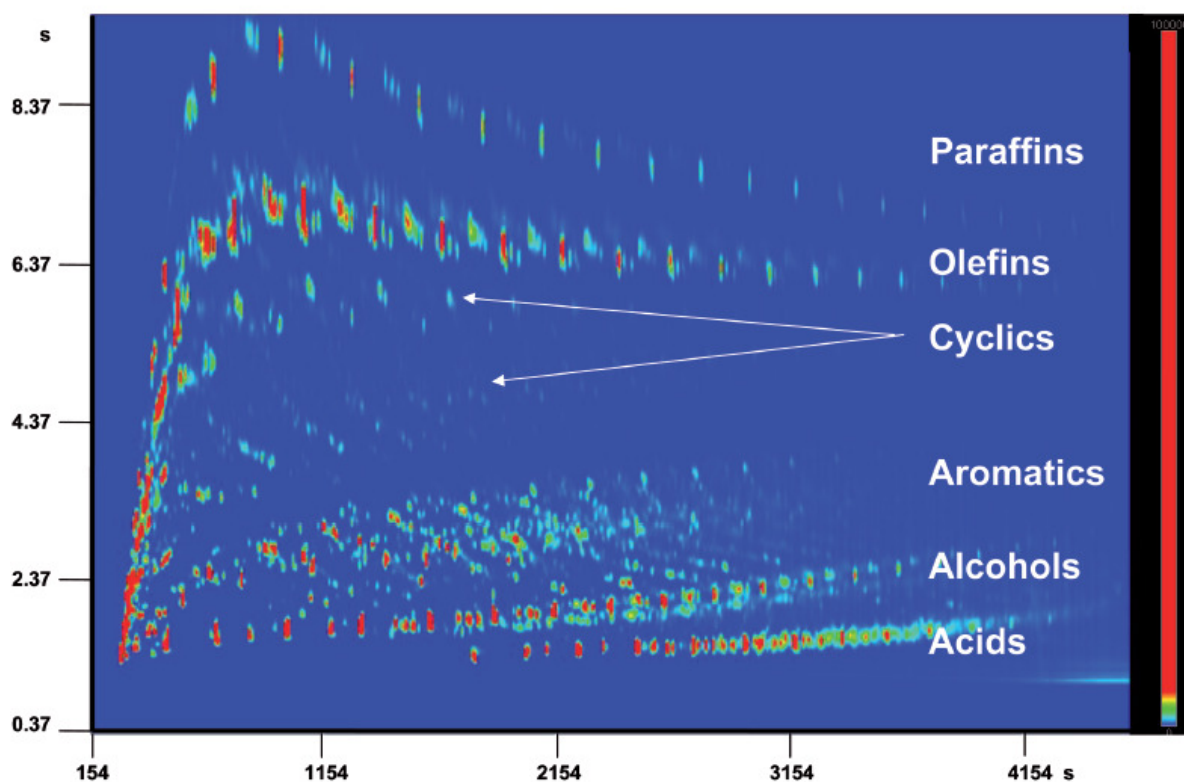


Figure 1. Total GCxGC profile of a HT-FT sample with low gum content.

Cyclic olefins and dienes have the same molecular mass and very similar mass fragmentation patterns e.g. 3-methyl-cyclohexene and 1,3-hexadiene. On the other hand, cyclic dienes have a molecular weight  $-2$  compared to their cyclic olefin and diene analogues. The plot of the  $m/z$  values 66 (C5 cyclic diene), 68 (C5 cyclic olefin and diene), 80 (C6 cyclic diene), 82 (C6 cyclic olefin and diene), 94 (C7 cyclic diene) and 96 (C7 cyclic olefin and diene) is shown in Figure 2. The 3 groups are nicely separated. Ion extraction can be extended with 14 amu for higher homologues.

The quantitative composition of the high gum fuel before and after hydrogenation was studied by using absolute MS abundances. For example, C<sub>6</sub> dienes decreased in quantity by 6.3% of the original content while this value was 12.0% for C<sub>6</sub> cyclic dienes.

## Chapter 5: The Use of GCxGC for Fuel Analysis

As cyclic dienes are hydrogenated to cyclic olefins, an equivalent increase was observed for the cyclic olefin content.

The higher the residual diene and cyclic diene content is after hydrogenation, the higher the expected formation of polycyclic olefins and polycyclic dienes by Diels–Alder reactions. This polymeric material is thought to be, at least partly, responsible for gum formation.

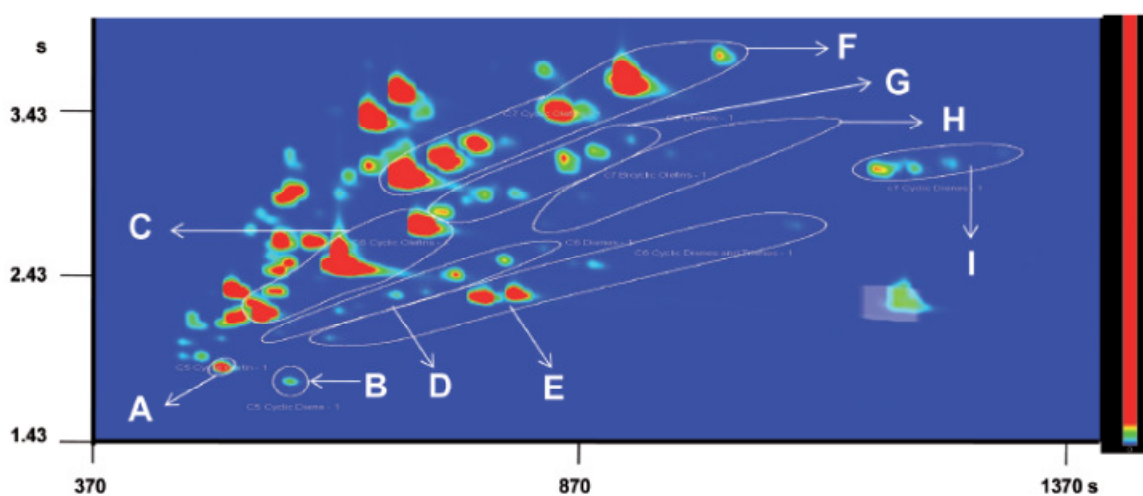
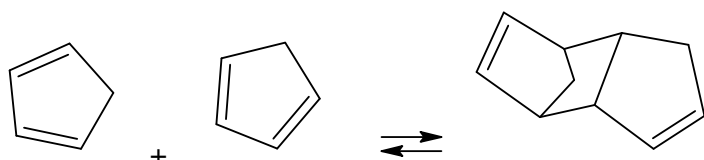


Figure 2. The plot of the  $m/z$  values 68 (A– $C_5$ –cyclic alkene), 66 (B– $C_5$  cyclic diene), 82 (C– $C_6$  cyclic alkenes, 82 (D– $C_6$  dienes), 80 (E– $C_6$  cyclic diene), 96 (F– $C_7$  cyclic alkene), 96 (G– $C_7$  dienes), 94 (H– $C_7$  bicyclic alkene, and 94 (I– $C_7$  cyclic diene).

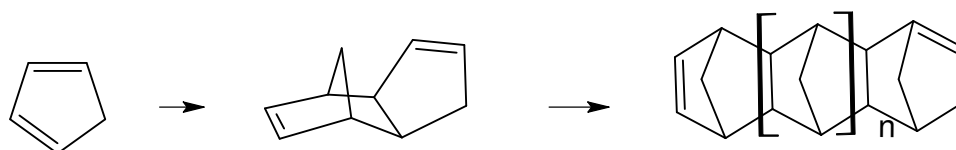
The Diels–Alder pericyclic process is a cyclic redistribution of bonding electrons between two reactants: a conjugated diene (in the *s-cis* conformation) and a dienophile that involves the 4  $\pi$ -electrons of the diene and the 2  $\pi$ -electrons of the dienophile. New  $\sigma$ -bonds are formed that are energetically more stable than  $\pi$ -bonds. For an overview we refer the reader to ref [18]. Diels–Alder reactions can be reversible and this is called the Retro–Diels–Alder. Products of the reverse reaction are not always the same as the mother molecules. Considering the presence of olefins, cyclic olefins, dienes, cyclic dienes, etc. in HT-FT samples, the number of formed Diels–Alder and Retro–Diels–Alder products can be very high. Moreover dienes can react as conjugated diene as well as dienophilic reactants.

## Chapter 5: The Use of GCxGC for Fuel Analysis

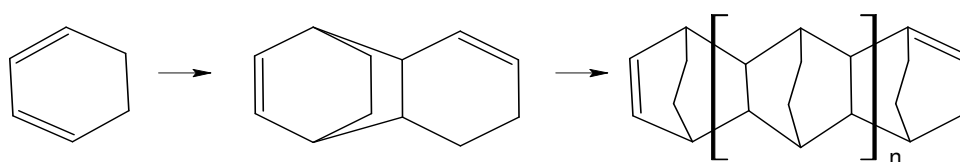
Cyclic dienes react particularly rapidly because they are "locked" in the s-cis conformation. The Diels–Alder polymerisation reaction for C<sub>5</sub> cyclic dienes was described by Stille in 1961 [19]. Cyclopentadiene slowly undergoes cycloaddition with itself giving bicyclopentadiene as illustrated below.



Once cyclopentadiene has served its role as diene, the adduct becomes a dienophile for the addition to the next diene molecule. In this polymerisation process dimers, trimers, tetramers, etc. are formed by the successive Diels–Alder additions of cyclopentadiene to the dienophilic oligomers.



Similar polymeric structures are observed for C<sub>6</sub> cyclic dienes in Fischer–Tropsch derived fuels.



FT fuels are subjected to a number of processes where heat and pressure, both influencing Diels–Alder and Retro-Diels–Alder reactions, are applied. Considering the number of candidates in FT fuels that can undergo those reactions, a huge amount of new structures are expected. In order to tune FT conditions, a highly powerful analytical technique is required and GC×GC presently is the most performant technique to look at these structures. Under the conditions applied here, only dimers and trimers could be analysed. Other column combinations are required for the analysis of higher molecular weight oligomers.

## Chapter 5: The Use of GCxGC for Fuel Analysis

Table 1 shows some possible Diels–Alder products in HT-FT samples. Based on this, molecular weights of dimers and trimers can be selected for ion extraction analysis.

As an example, Figure 3A shows the ion extraction plot at  $m/z$  132, 134, 160, 162, 198, 200 and 240. These ions are highlighted in Table 1. Several aromatics are detected as well because of the presence of C10 and C12 alkylbenzenes and alkenylbenzenes giving similar molecular masses. Further differentiation can be made based on the specific fragment ions from the Diels–Alder products as illustrated by extracting ions  $m/z$  80, 94 and 108 (Figure 3B). The mass spectra of specific blobs can be recalled and some examples are given in Figure 4 for dimers and trimers.

**Table 1. Molecular masses of some Diels–Alder products**

Carbon Number	Dienes	Cyclic Dienes	Cyclic Diene + Cyclic Olefin Dimers	Cyclic Diene Dimers	Cyclic Diene + Cyclic Olefin Trimers	Cyclic Diene Trimers
<b>C10</b>	138	136	<u>134</u>	<u>132</u>	130	128
<b>C12</b>	166	164	<u>162</u>	<u>160</u>	158	156
<b>C15</b>	208	206	204	202	<u>200</u>	<u>198</u>
<b>C18</b>	250	248	246	244	242	<u>240</u>
<b>C20</b>	278	276	274	272	270	268

Most mass spectra cannot be identified by library search but the interpretation of some of them is straightforward. Figure 4A is the dimer of cyclopentadiene with molecular mass at  $m/z$  132 and most important fragment ion at 66 representing the monomer; Figure 4B is the spectrum of the dimer of conjugated cyclohexadiene (MW 146) with the monomeric structure as most important fragment ion. If interested in the determination of substituted dimers, the specific ion of the dimer is selected for ion extraction and the spectrum is called up. Figure 4C shows this procedure for the elucidation of the methyl substituted conjugated cyclopentadiene. The most dominant fragment corresponds to its monomer. In the same way, trimers can be identified as illustrated in Figure 4D and 4E for the trimers of cyclopentadiene and cyclohexadiene, respectively.

## Chapter 5: The Use of GCxGC for Fuel Analysis

The complete elucidation of all blobs in the contour plot shown in Figure 3 is a time-consuming task. However, this is not really required to improve and further develop the catalytic hydrogenation process after HT-FT. Specific markers as those shown in Figure 4 can be monitored.

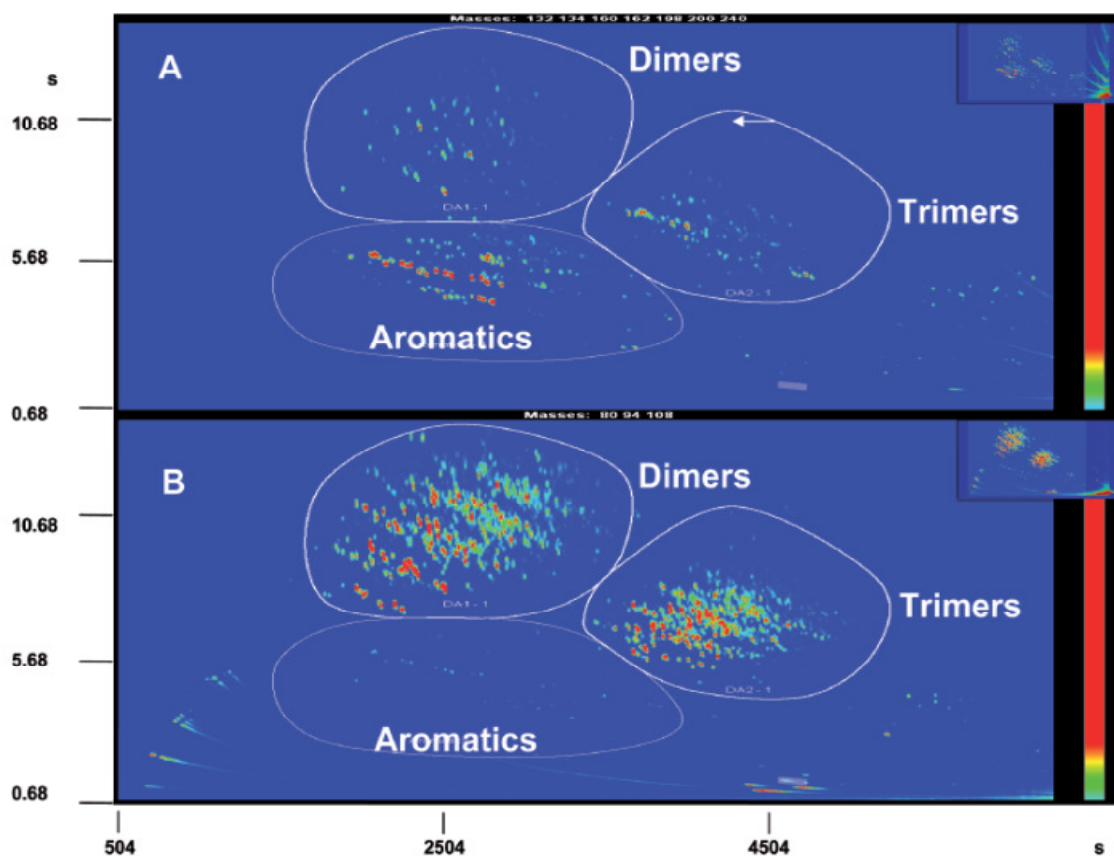


Figure 3. Diels–Alder dimers and trimers in a HT–FT sample.

A. Ion extraction on  $m/z$  132, 134, 160, 162, 198, 200 and 240 and

B. Ion extraction on fragments  $m/z$  80, 94 and 108.

## Chapter 5: The Use of GCxGC for Fuel Analysis

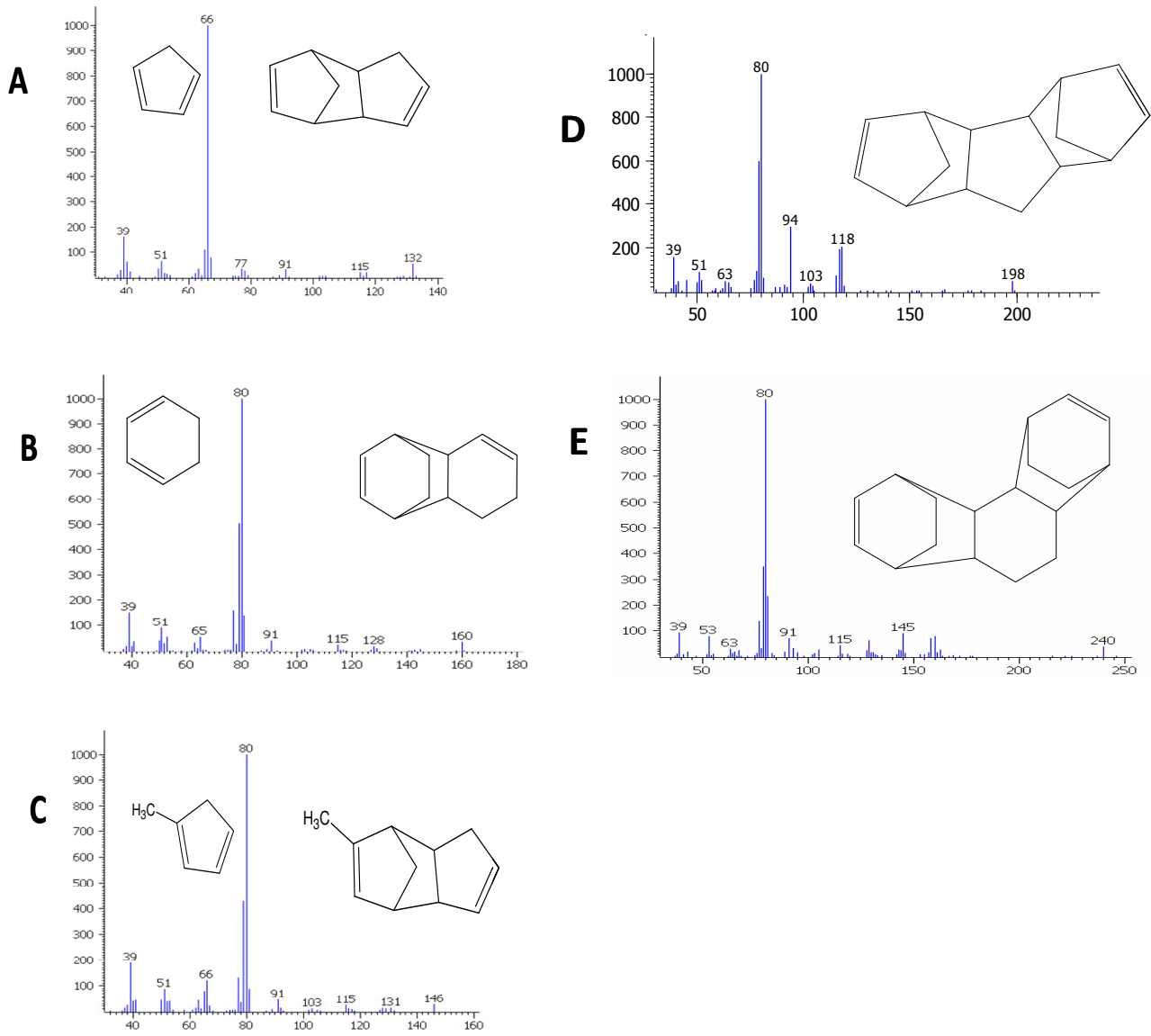


Figure 4. Examples of mass spectra of recorded dimers and trimers.

## Chapter 5: The Use of GCxGC for Fuel Analysis

---

### 5.3.4 Conclusion

GCxGC/TOF-MS has proven to be an invaluable tool in the profiling of Fischer-Tropsch fuels and derived products. Highly structured chromatograms are obtained in which specific groups can be studied in detail.

This has been illustrated for the determination of cyclic olefins, dienes and cyclic dienes in high temperature Fischer-Tropsch based fuels. Moreover, Diels-Alder dimer and trimer polymerisation products that contribute to gum formation could be determined.

*The authors are indebted to Dr. Debby Yoell of Sasol Fuels Research and Ms Jeanine Williams of Sasol Technology R&D for providing the samples, information and for facilitating the gum formation tests. We thank Prof. Frank David, RIC, Belgium, for valuable comments*

## Chapter 5: The Use of GCxGC for Fuel Analysis

---

### 5.3.5. References

- [1] A. Steynberg, M. Dry, (Eds) Fischer–Tropsch Technology, Elsevier, Amsterdam 2004.
- [2] D. Lamprecht, L.P. Dancuart, K. Harillal, *Energy Fuels* 21 (2007) 2846.
- [3] R.C.C. Pereira, V.M.D Pasa, *Fuel* 85 (2006) 1860.
- [4] J.M. Nagpal, G.C. Joshi, J. Singh, *Fuel Sci. Technol. Int.* 12 (1994) 873.
- [5] J.M. Nagpal, G.C. Joshi, S.N. Rastogi, *Fuel* 74 (1995) 714.
- [6] J.M. Nagpal, G.C. Joshi, S.N. Rastogi, *Fuel* 74 (1995) 720.
- [7] A.J. Den Hartog, M. Deng, F. Jongorius, V. Ponec, *J. Mol. Catal.* 60 (1990) 99.
- [8] J.C. Bertolini, Y. Jugnet, in: D. P. Woodruff, (Ed), *Alloy Surfaces and Surface Alloys*, Elsevier, Amsterdam Vol. 10, 2002, 404.
- [9] C. Yoon, M.X. Yang, G.A Somorjai, *Journal of Catalysis* 176 (1998) 35.
- [10] Universal Oil Products Company test method: UOP 326, Diene value by maleic anhydride addition reaction, Des Plaines, IL, 1982.
- [11] S. Jones, I. Wilson, *Tetrahedron Letters*, 47 (2006) 4377.
- [12] Standard Test Method: ASTM D381–04, Standard test method for gum content in fuels by jet evaporation, ASTM International, West Conshohocken, PA, 2004.
- [13] C. J. Venkatramani, J.B. Phillips, *J. Microcol. Sep.* 5 (1993) 511.
- [14] J. Xu, J.B. Phillips, *J. Chromatogr. A* 703 (1995), 327.
- [15] J. Blomberg, P.J. Schoenmakers, J. Beens, R. Tijssen, *J. High Resol. Chromatogr* 20 (1997) 539.
- [16] P.J. Schoenmakers, J.L.M.M. Oomen, J. Blomberg, W. Genuit, G. van Velzen, *J. Chromatogr. A* 892 (2000) 29.
- [17] J. Dallüge, J. Beens, U.A.Th. Brinkman, *J. Chromatogr. A* 1000 (2003) 69.
- [18] K.C Nicolaou, *Angew. Chem. Int. Ed.* 41 (2002) 1668.
- [19] J. K. Stille, *Fortscr. Hochpolym.–Forsch.* 3 (1961) 48.

## Chapter 5: The Use of GCxGC for Fuel Analysis

---

### 5.4 Comprehensive two-dimensional gas chromatography for the analysis of synthetic and crude-derived jet fuels<sup>4</sup>

#### 5.4.1 Introduction

The increased interest in the production of synthetic fuels via Fischer–Tropsch (FT) technology as an alternative to crude-derived fuels is driven mostly by unstable crude oil prices, the need for energy security, greater strategic flexibility and the need for cleaner (green) transportation fuels. Sasol (the South African Coal, Oil and Gas Corporation), the world's leading producer of synthetic fuels, has been blending a synthetic component known as Synthetic Paraffinic Kerosene (SPK) with a crude-derived, straight run Merox (mercaptan oxidation) kerosene stream to produce a semi-synthetic jet fuel (SSJF) since 1999. Approved SSJF blends may contain a maximum of 50% synthetic product blended with kerosene from conventional crude-derived sources. The ASTM standard specification D7566 [1] that was approved in September 2009, implied that kerosene, produced by either coal-to-liquid (CTL) or gas-to-liquid (GTL) processes and meeting the specification, can be used to blend SSJF for commercial use in the USA.

Sasol's fully synthetic jet fuel (FSJF) has been approved for commercial use in April 2008, as published in the British Ministry of Defense Standard (DEF STAN 91–91) [2]. ASTM International has also been working closely with the British Ministry of Defense and the writing of Sasol's FSJF into ASTM D1655, as a specific approval, was completed in June 2009 [3]. Sasol's FSJF meets all commercial Jet A–1 specifications as stipulated by the reference method DEF STAN 91–91 [2].

In modern aircraft, the aviation turbine fuel is increasingly used as the primary coolant, thereby increasing the thermal stress that the jet fuel is exposed to.

---

<sup>4</sup> R.van der Westhuizen, M. Ajam, P. de Coning, J. Beens, A. de Villiers, P. Sandra, J. Chromatogr. A, 1218 (2011) 4478.

## Chapter 5: The Use of GCxGC for Fuel Analysis

---

Thermal stability demands on jet fuel are anticipated to become even more stringent as military aircraft approach extreme speeds of Mach 2 to 4. At such high speeds, jet fuels are expected to withstand temperatures up to 500 °C for short residence times [4]. Considerable improvement in jet fuel thermal stability is therefore required to ensure optimum performance for next generation jet engines.

Fuel stability relates to the resistance of the fuel to changes in physical and/or chemical properties which could hinder the aircraft performance or operation. Two types of instability are distinguished: storage stability refers to the effect of long-term ambient-temperature storage conditions on fuel properties, whereas thermal and oxidative instability refers to the effect of short-term high-temperature stress conditions on the fuel properties. The long-term storage stability involves oxidation leading to hydroperoxide intermediates, oxygenates and eventually gums. Peroxides cause significant deterioration of nitrile rubber, neoprene and Buna-N O-rings in jet engine fuel pumps, which could result in the leakage of fuel [5]. Thermal and oxidative stability, on the other hand, involves the formation of insoluble deposits which could result in reduced heat transfer efficiency, plugged fuel nozzles and filters, restricted fuel flow and degraded valve performance. These factors could eventually lead to engine malfunction and catastrophic engine failure. Jet fuel used in modern aircraft fuel systems is required to be free of water, dirt and other foreign contaminants and is sent through multi-stage filtration systems to ensure a good quality fuel. Clay treatment is used to remove polar species from jet fuel [6] that may cause deposit formation and contribute to thermal oxidative instability [7].

Accurate analysis methods for these fuels are essential. Because of limited international experience with the use of synthetic fuels, test requirements were identified specifically for these fuels and blends. The DEF STAN 91-91 standard stipulates various tests to ensure suitability of the fuel, e.g. the analysis of aromatics by fluorescent indicator absorption (FIA) [8] and high performance liquid chromatography (HPLC) [9], total sulphur and mercaptans by X-ray fluorescence [10] and potentiometry [11,12], naphthalene content by ultraviolet spectroscopy [13] and fatty acid methyl ester (FAME) content by gas chromatography-mass

## Chapter 5: The Use of GCxGC for Fuel Analysis

---

spectrometry (GC–MS) (Method IP PM–DY/09) [14] or GCxGC [15]. FAMEs originate from contamination by biodiesel that is transported in the same pipelines as aviation fuels.

Detailed information on the content of individual chemical species is mandatory in predicting fuel performance, stability, emissions, etc.

Method ASTM D2425 is based on MS and is commonly used for hydrocarbon type analysis of middle distillates [16]. According to this method mass fragments and molecular ions of a hydrocarbon family are summed and used to calculate concentrations from coefficient matrices depending on carbon number. An HPLC separation (ASTM D2549) is performed prior to MS analysis to obtain separation of different chemical families of identical mass [17]. A method without HPLC pre–separation was proposed by Bernabei et al. [18] for the determination of total and polycyclic aromatics in jet fuels.

The most accurate way to obtain detailed compositional information for highly complex petrochemical mixtures is, however, by means of comprehensive two–dimensional gas chromatography [19–26]. GCxGC offers high peak capacity, structured separations and high sensitivity. GCxGC in the reversed mode i.e. a polar × non–polar column combination, was used for the qualitative and quantitative analysis of individual hydrocarbon and hetero–atomic compounds that might affect fuel properties in FSJF and Merox kerosene. Structure elucidation was performed by time–of–flight mass spectrometry (TOF–MS) and quantification by flame ionisation detection (FID). GCxGC was further applied for the analysis of products during Jet Fuel Thermal Oxidation Testing (JFTOT), which measures deposit formation of a fuel under simulated engine conditions.

### 5.4.2 Experimental

#### 5.4.2.1 Samples

The Merox process is a licensed refinery process that converts mercaptans to disulphides. Merox is a straight run kerosene stream originating from the crude oil distillation (CDU) column.

## Chapter 5: The Use of GCxGC for Fuel Analysis

---

After the Merox unit, the kerosene was passed through an Attapulugus clay filter to remove colour bodies, impurities and surfactant type molecules. The Sasol Secunda refinery utilizes a high temperature Fischer–Tropsch (HT-FT) process with an iron–based catalyst to produce a hydrocarbon product. Synthetic Paraffinic Kerosene (SPK) was produced in the CTL (coal–to–liquid) facility by catalytic polymerisation of the C<sub>3</sub> and C<sub>4</sub> olefins in the synthetic crude product.

Samples were kept refrigerated at all times to prevent loss of volatile material and ensure sample integrity. Samples were injected neat and GC–vials were recapped after each injection.

### 5.4.2.2 Chromatographic conditions

A Pegasus 4D GCxGC system (Leco Co., St. Joseph, MI, USA) equipped with FID and TOF–MS was used. Conditions for the reversed GCxGC mode were as follows. The primary column was a 60 m StabilWax capillary column (0.25 mm i.d and 0.25 µm d<sub>f</sub>). The secondary column was a 2 m Rxi–5ms column (0.1 mm i.d. and 0.1 µm d<sub>f</sub>). Both columns were supplied by Restek (Bellefonte, PA, USA). The primary oven was programmed from 40°C (0.2 min) at 2°C/min to 240°C. The second oven followed the first oven program with a 10°C offset. A dual jet thermal modulation system was used with an 8 s modulation period. Helium carrier gas was used at a constant flow of 1.2 mL/min. Conditions for the normal GCxGC mode were as follows. The primary column was a 60 m Rxi–5ms capillary column (0.25 mm i.d and 0.25 µm d<sub>f</sub>). The secondary column was a 2 m Rtx–wax (0.1 mm i.d. and 0.1 µm d<sub>f</sub>); both from (Restek (Bellefonte, PA, USA). The primary oven was programmed from 40°C (0.2 min) at 2°C/min to 240°C. The second oven followed the first oven program with a 10°C offset. The modulation period was 4 s. Helium carrier gas was used at a constant flow of 1.2 mL/min. 0.1 µL was injected using an Agilent Technologies 7683 auto injector. The split ratio was 400:1 for normal injections and 20:1 for hetero–atom analysis. Data collection for the TOF–MS and FID was at 100 spectra/s and 100 Hz, respectively.

## Chapter 5: The Use of GCxGC for Fuel Analysis

### 5.4.2.3 Analytical procedure

GCxGC–FID was used for quantification using the standard addition method. Three standards were used for hydrocarbon analysis to compensate for differences in response factors between different chemical classes. Standards of iso–octane (anhydrous, ≥99.8 %, Sigma–Aldrich, Midrand, South Africa), xylene (standard for GC, ≥ 99.5 %, Fluka, Midrand, South Africa) and decalin (cis+trans, ≥98.0%, Fluka) were weighed (see masses in **Table 1**) and diluted to 50 mL with n–hexane (BDH, HiPerSolv, 97%, VWR International, Arlington Heights, IL, USA). Solutions were prepared by diluting 1 mL of the standard solution and 10 mL jet fuel to 50 mL hexane.

**Table 1: Solutions used for quantification by standard addition.**

Standard Addition Method								
SOL.	Iso–octane	Xylene	Decalin	Volume sample	Total volume (hexane added)	Iso–octane	Xylene	Decalin
	Mass weighed (g)	Mass weighed (g)	Mass weighed (g)	(mL)	(mL)	Concentration $\mu\text{g/mL}$	Concentration $\mu\text{g/mL}$	Concentration $\mu\text{g/mL}$
1	0.0166	0.0133	0.0694	10.00	50.00	6.6	5.3	27.8
2	0.0238	0.0190	0.1591	10.00	50.00	9.5	7.6	63.6
3	0.0738	0.0590	0.3095	10.00	50.00	29.5	23.6	123.8
4	0.1692	0.1352	0.4973	10.00	50.00	67.7	54.1	198.9
5	0.3291	0.2629	1.4166	10.00	50.00	131.6	105.2	566.6
6	0.5289	0.4226	2.9432	10.00	50.00	211.6	169.0	1177.3
7	1.5066	1.2037	10.4420	10.00	50.00	602.6	481.5	4176.8
8	3.1303	2.5009	14.3585	10.00	50.00	1252.1	1000.4	5743.4

Three–point standard addition procedures were done using iso–octane, cis/trans–decalins and a mixture of m, p and o–xylenes for the quantification of non–cyclic aliphatic hydrocarbons, cyclic aliphatic and aromatic species, respectively. The peak areas for the standards (the isomers m–, o–, p–xylene and cis/trans–decalin were grouped together) were determined using the classifications in the ChromaTOF–GC software (Leco, V4.21).

## Chapter 5: The Use of GCxGC for Fuel Analysis

---

Standard addition calibration curves were used to determine the concentration of each of the three standard compounds in the sample. Sample compounds were labeled as non-cyclic aliphatic, cyclic aliphatic or aromatic and this elucidation determined which standard to use for quantification (for example the concentrations of aromatic compounds were calculated by comparing the peak areas and concentration of the xylenes with the peak areas of the sample peaks). It was assumed that compounds of the same class have the same FID response factors.

The eight standard mixtures as well as the samples were each analysed five times to obtain repeatability data. Recoveries were determined by summing the concentrations for all the peaks in a sample and averaging for the five repeated analyses.

Hetero-atomic species, present at low  $\mu\text{g/mL}$  levels in the Mercox kerosene, could not be observed in the FID-trace because of the detector's lack of response. Analysis of these compounds was therefore performed by GCxGC-TOF-MS. To increase on detectability, the split ratio was decreased to 20:1 for these analyses. This led to overloading of the hydrocarbons, but the hetero-atomic species could be identified by using extracted ion chromatography. Poor repeatability resulting from column overloading necessitated the use of internal standards for semi-quantification of hetero-atomic species. Thiophene (Sigma-Aldrich) and o-cresol (Sigma-Aldrich), spiked at  $5 \mu\text{g/mL}$  each, were used as internal standards for sulphur compounds and oxygenated compounds, respectively. Semi-quantification was done by adding the peak areas of the compounds and comparing with that of the internal standards assuming a similar detector response.

### 5.4.2.4 Stability tests

Thermal stability tests were performed by evaluating the break point temperatures of fresh fuels using the JFTOT procedure according to ASTM D3241 [27]. JFTOT was measured at  $10^\circ\text{C}$  intervals from  $260\text{--}360^\circ\text{C}$  until the break point temperature of the fuel was reached. Test fuels were also clay treated before stability analysis to remove polar species, water and colour bodies.

## Chapter 5: The Use of GCxGC for Fuel Analysis

---

Dry Attapulugus clay (500 g) was loaded into a glass vessel and 5 L test fuel was subsequently loaded and allowed to pass through the clay at a rate of 100 mL/hour. JFTOT and GCxGC analyses were performed on the fresh and clay-treated jet fuels.

### 5.4.3 Results and discussion

#### 5.4.3.1 GCxGC optimisation

GCxGC analysis of fuels is commonly performed in the normal GCxGC mode i.e. a non-polar column in the first dimension and a polar column in the second dimension [19]. The reversed mode i.e. a polar  $\times$  non-polar column combination is considered 'less orthogonal [28] but has shown to be advantageous to extend the separation space for the characterization of the aromatic fraction in petroleum middle-distillates [29], to provide improved resolution of FAMES from hydrocarbons in biodiesels [30] and for the characterization of Fischer-Tropsch fuels [31–33]. Contour plots comparing the class separations for an FSJF by reversed and normal mode GCxGC are shown in Figure 1A and B, respectively.

## Chapter 5: The Use of GCxGC for Fuel Analysis

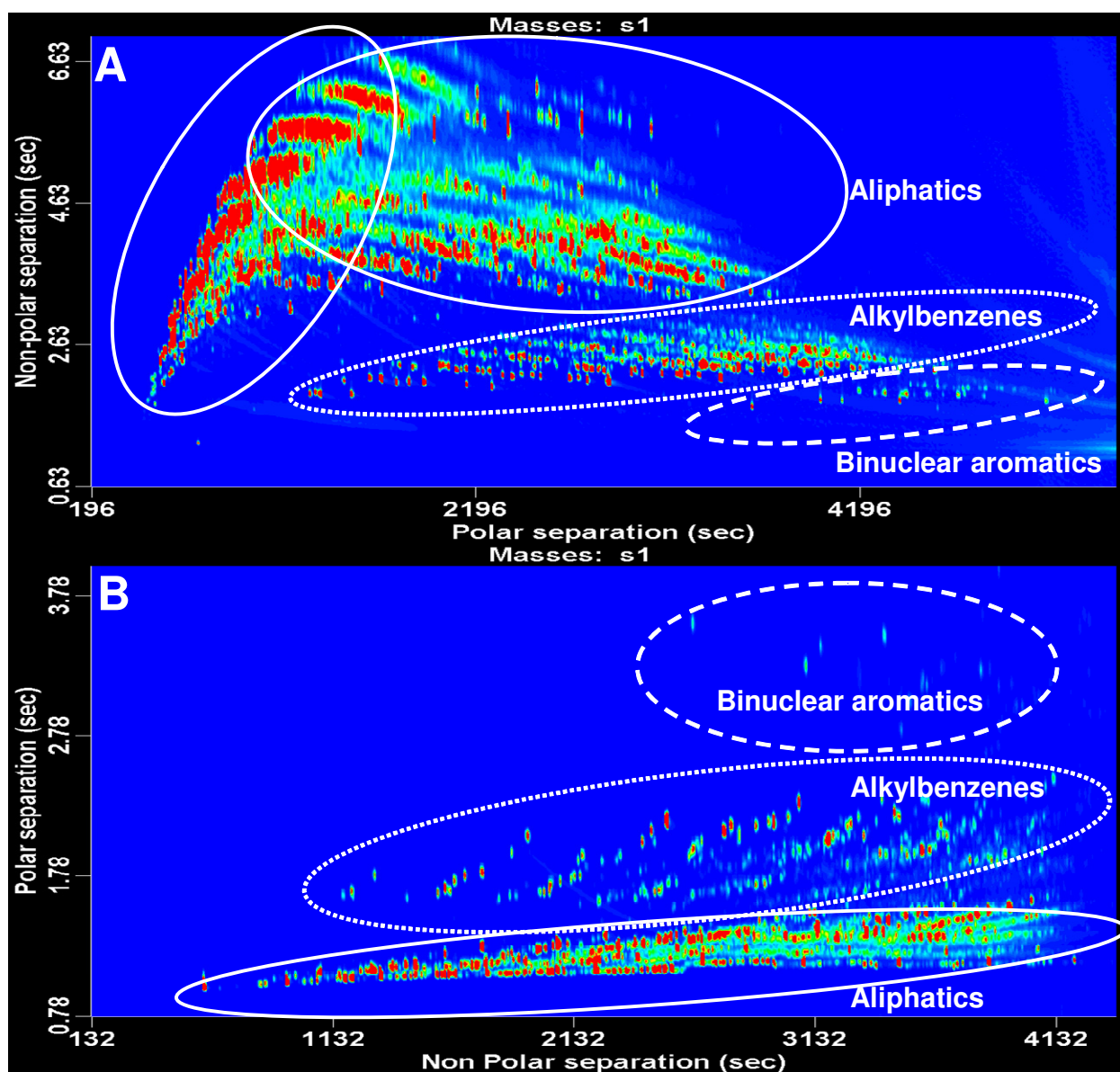


Figure 1: GCxGC separation of FSJF with the polar  $\times$  non-polar column configuration (A) and the non-polar  $\times$  polar column configuration (B). For experimental details, refer to the Experimental section.

The improved separation space for the aliphatic compounds is obvious, while a similar separation space is noted for the alkylbenzenes and a worse one for the binuclear aromatics.

## Chapter 5: The Use of GCxGC for Fuel Analysis

---

The selected column combination provides excellent separation of individual components as well as of the different aliphatic classes and between aliphatics and hetero-atom compounds for both synthetic and crude-derived jet fuels. All of these factors are especially advantageous for the analysis of FT fuels that are relatively high in aliphatic content, low in aromatics and do not contain significant amounts of hetero-atomic species.

TOF-MS is the preferred detector for GCxGC because this detector provides structural information. In addition, the high data acquisition rate prevents spectral skewing and deconvolution software can locate and identify closely eluting analytes based on unique ions. However, in petrochemical products that consist of thousands of compounds, determining the TOF-MS response factor for every compound for quantitative analysis is unrealistic. Moreover, another disadvantage of TOF-MS is that the data files are very large and as a result, data processing can be very time-consuming, which is especially problematic in routine applications. In contrast, use of FID significantly reduces data processing time. TOF-MS was therefore used initially to identify the hydrocarbon peaks, and subsequently FID was used for quantification of the identified compounds. On the other hand, FID failed to detect hetero-atomic species in the fuels at trace levels. TOF-MS in the ion-extraction mode was used for elucidation of the hetero-atom containing compounds but accurate quantification was hampered by the very low levels (sub- $\mu\text{g/mL}$ ) of the individual compounds and the large differences in mass spectral intensity of the compounds of the same class (see further).

Calibration details used for the quantification of the hydrocarbons in the FSJF samples by FID are summarized in Table 2. Small changes in the calibration graphs have a relatively large effect on quantitative results and therefore it was found that sufficient calibration data points were required to decrease the standard deviation.

## Chapter 5: The Use of GCxGC for Fuel Analysis

**Table 2: Summary of calibration results.**

Standard	Slope	y-intercept	Sample concentration ( $\mu\text{g/mL}$ )	Linear range ( $\mu\text{g/mL}$ )	$R^2$	% RSD
Iso-octane	284.97	14446.89	50.70	50.7–1302.8	0.9999	2.35
Xylene	409.81	517175.20	1261.99	1261.99–2262.37	0.9946	1.68
decalin	320.37	1228019.09	3833.17	3833.17–9576.55	0.9990	0.90

The hydrocarbon compounds were classified using the classification software available in ChromaTOF software. Eight compound classes (n-alkanes, branched alkanes, monocyclic-, bicyclic- and polycyclic alkanes, alkylbenzenes, cyclic alkylbenzenes and naphthalenes) were identified in FSJF and Mercox kerosene, with each of these classes ranging in carbon numbers from  $C_6 - C_{20}$ . Boundaries of the classes in the contour plots are elucidated via the TOF-MS data through ion extraction of the molecular masses of the compound classes. These boundaries are then matched with the FID separation. As an example, for the  $C_{12}$  alkane classes,  $m/z$  170 is selected for the n- and branched dodecanes. The n- $C_{12}$  is completely separated from the pre-eluting branched  $C_{12}$  alkanes and both solute groups can be quantified. In a similar way,  $m/z$  168 is selected for the monocyclic  $C_{12}$  alkanes,  $m/z$  166 for the bicyclic  $C_{12}$  alkanes,  $m/z$  164 for the tricyclic  $C_{12}$  alkanes, etc. The alkylbenzenes and binuclear aromatics can easily be distinguished from the contour plots. The quantitative data are summarized in Table 3.

**Table 3: Quantitative data for FSJF and Merox kerosene obtained by GCxGC–FID**

<b>Fully Synthetic Jet Fuel</b>									
<b>Carbon Number</b>	<b>n-Paraffins</b>	<b>Branched Paraffins</b>	<b>Mono Cyclic Paraffins</b>	<b>Bicyclic Paraffins</b>	<b>Polycyclic Paraffins</b>	<b>Alkyl Benzenes</b>	<b>Cyclic Alkyl Benzenes</b>	<b>Naphthalenes &amp; Other Binuclear Aromatics</b>	<b>Total</b>
	<i>Mass %</i>	<i>Mass %</i>	<i>Mass %</i>	<i>Mass %</i>	<i>Mass %</i>	<i>Mass %</i>	<i>Mass %</i>	<i>Mass %</i>	<i>Mass %</i>
C5	0.00	0.00	0.00	0.00	0.00	0.00	0.00	0.00	0.00
C6	0.00	0.00	0.00	0.00	0.00	0.00	0.00	0.00	0.00
C7	0.00	0.01	0.00	0.00	0.00	0.00	0.00	0.00	0.01
C8	0.00	0.90	0.34	0.00	0.00	0.12	0.00	0.00	1.36
C9	0.14	7.52	2.36	0.49	0.01	0.55	0.00	0.00	11.07
C10	0.34	11.00	3.14	3.70	0.01	0.59	1.09	0.02	19.89
C11	0.36	11.86	2.45	4.65	0.02	0.41	1.86	0.08	21.69
C12	0.56	5.96	2.38	4.85	0.51	0.38	2.12	0.14	16.90
C13	0.65	3.35	1.47	4.02	2.32	0.33	1.96	0.10	14.20
C14	0.59	1.63	1.05	1.92	3.82	0.24	1.21	0.00	10.46
C15	0.07	0.49	0.52	0.69	1.62	0.11	0.27	0.00	3.77
C16	0.00	0.05	0.10	0.08	0.38	0.00	0.00	0.00	0.61
C17	0.00	0.00	0.00	0.00	0.00	0.00	0.00	0.00	0.00
C18	0.00	0.00	0.00	0.00	0.00	0.00	0.00	0.00	0.00
C19	0.00	0.00	0.00	0.00	0.00	0.00	0.00	0.00	0.00
C20	0.00	0.00	0.00	0.00	0.00	0.00	0.00	0.00	0.00
<b>Total</b>	<b>2.71</b>	<b>42.77</b>	<b>13.84</b>	<b>20.39</b>	<b>8.68</b>	<b>2.73</b>	<b>8.48</b>	<b>0.35</b>	<b>99.95</b>
<b>Merox Kerosene</b>									
<b>Carbon Number</b>	<b>n-Paraffins</b>	<b>Branched Paraffins</b>	<b>Mono Cyclic Paraffins</b>	<b>Bicyclic Paraffins</b>	<b>Polycyclic Paraffins</b>	<b>Alkyl Benzenes</b>	<b>Cyclic Alkyl Benzenes</b>	<b>Naphthalenes &amp; Other Binuclear Aromatics</b>	<b>Total</b>
	<i>Mass %</i>	<i>Mass %</i>	<i>Mass %</i>	<i>Mass %</i>	<i>Mass %</i>	<i>Mass %</i>	<i>Mass %</i>	<i>Mass %</i>	<i>Mass %</i>
C5	0.00	0.00	0.01	0.00	0.00	0.00	0.00	0.00	0.01
C6	0.01	0.01	0.18	0.00	0.00	0.01	0.00	0.00	0.20
C7	0.11	0.08	0.52	0.00	0.00	0.11	0.00	0.00	0.83
C8	0.40	0.33	3.56	0.04	0.00	0.97	0.00	0.00	5.30
C9	2.18	1.55	4.04	0.52	0.00	4.43	0.00	0.00	12.72
C10	3.64	5.67	3.55	0.52	0.00	3.44	0.52	0.22	17.57
C11	3.65	5.42	2.95	1.75	0.11	1.97	1.12	0.86	17.82
C12	3.16	4.87	2.50	1.45	0.16	1.27	1.22	1.37	16.00
C13	2.74	4.25	1.70	1.39	0.06	0.78	1.18	0.99	13.08
C14	2.12	3.50	1.02	0.76	0.20	0.63	0.73	0.19	9.15
C15	1.27	2.46	0.28	0.29	0.00	0.37	0.23	0.03	4.93
C16	0.35	1.39	0.02	0.01	0.00	0.08	0.00	0.00	1.85
C17	0.06	0.32	0.00	0.00	0.00	0.00	0.00	0.00	0.38
C18	0.01	0.07	0.00	0.00	0.00	0.00	0.00	0.00	0.08
C19	0.00	0.02	0.00	0.00	0.00	0.00	0.00	0.00	0.03
C20	0.00	0.00	0.00	0.00	0.00	0.00	0.00	0.00	0.00
<b>Total</b>	<b>19.69</b>	<b>29.94</b>	<b>20.34</b>	<b>6.73</b>	<b>0.53</b>	<b>14.05</b>	<b>5.01</b>	<b>3.66</b>	<b>99.95</b>

## Chapter 5: The Use of GCxGC for Fuel Analysis

---

### 5.4.3.2 Chemical composition of fully synthetic and crude-derived jet fuels.

A comparison of the FSJF and Merox kerosene was performed to investigate whether the synthetic fuel contains components not present in crude-derived products that may potentially affect fuel properties and/or pose an environmental threat.

For the hydrocarbons, a high degree of similarity in terms of chemical content is observed between both fuels. All hydrocarbons present in the synthetic fuel are also observed in the crude-derived product, although present at different ratios (Figure 2 and Table 3). The synthetic product is characterised by more aliphatic compounds with a higher degree of branching and relatively higher amounts of bi- and polycyclic aliphatics. Moreover, the FSJF contains significantly less aromatic species, especially naphthalenes and their derivatives. This difference in hydrocarbon composition of the FSJF is expected to affect jet fuel characteristics such as cold flow properties, while the absence of any “new molecules” ensures that the fuel is suitable for use in commercial aircraft. Moreover, the lower aromatic content ensures a cleaner-burning fuel with less soot and smoke pollution.

Hetero-atomic species were observed in the crude-derived kerosene even after clay-treatment. These species are absent in the FT fuel. The total amounts of these compounds were at low  $\mu\text{g/mL}$  (ppm) levels and individual compounds could only be observed by decreasing the split ratio to 20:1 and using extracted ion chromatograms.

Acidic pollution, arising from the emission of sulphur and nitrogen oxides, has been implicated in acidification of water resources, damage to trees and buildings and also in some respiratory diseases. Typical sulphur components that are found in crude-derived fuels are mercaptans, sulphides, disulphides, and thiophene derivatives [34,35]. The Merox process is a sweetening process that converts sulfur species and mercaptans (thiols) to disulfides in the presence of oxygen under alkaline conditions (NaOH).

## Chapter 5: The Use of GCxGC for Fuel Analysis

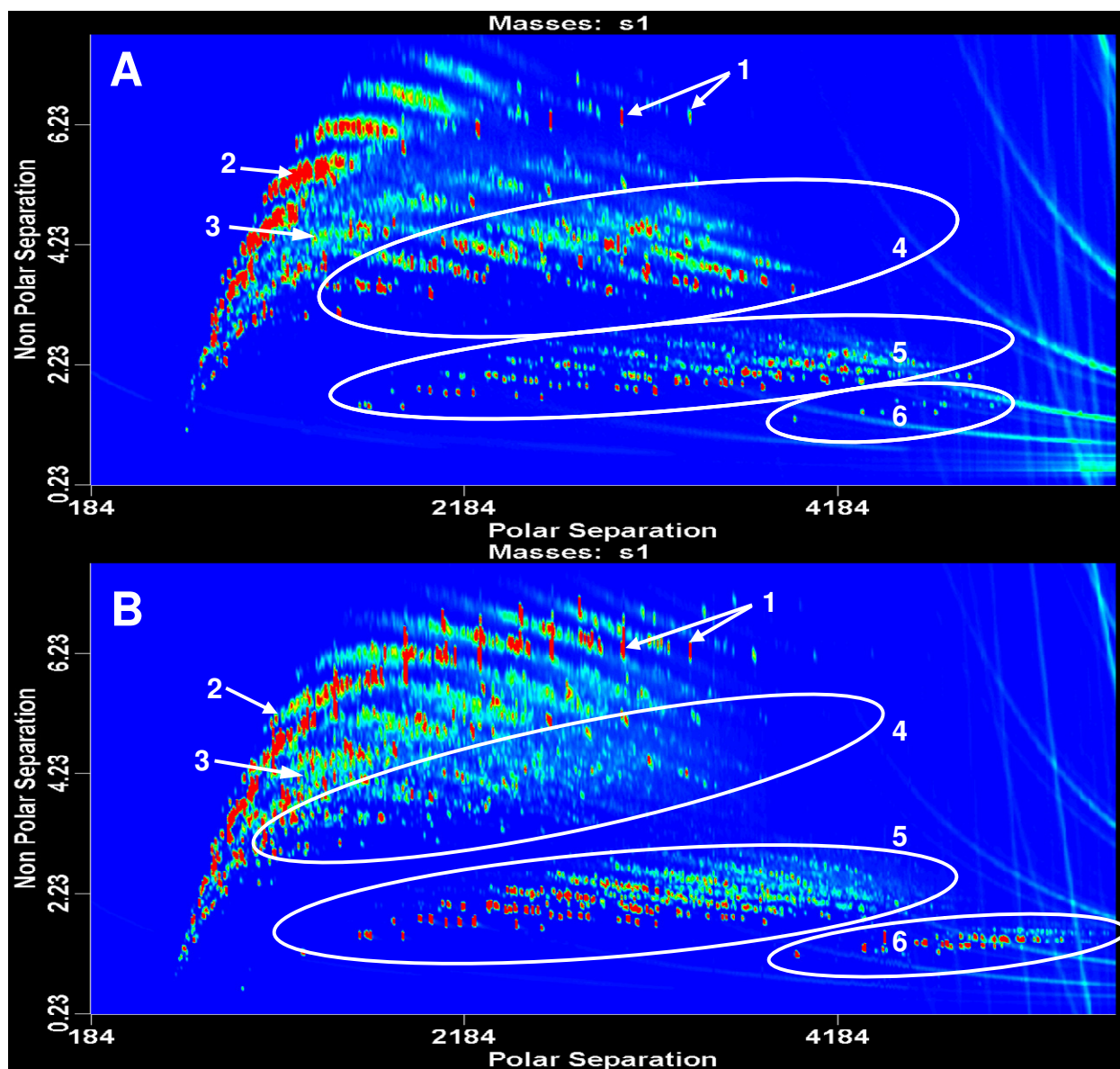


Figure 2: GCxGC analysis of (A) FSJF and (B) crude-derived jet fuel using a polar  $\times$  non-polar column combination. Numbering: 1. *n*-paraffins, 2. branched paraffins, 3. monocyclic aliphatics, 4. bi- and polycyclic aliphatics, 5. mononuclear aromatics and 6. binuclear aromatics.

The mercaptans, such as the disulfides, are undesirable species because they are corrosive and have an offensive odor.

## Chapter 5: The Use of GCxGC for Fuel Analysis

---

In this chemical sweetening process, the total sulphur content of the fuel remains unchanged. Most of the sulphur species can be removed easily [36,37], although the heterocyclic thiophene derivatives are less reactive and more difficult to remove.

In the clay-treated Merox kerosene, the presence of more than 50 sulphur-containing compounds was noted. It was not possible to obtain standards for each of these. The internal standard, thiophene, was therefore used for semi-quantification of S-compounds and above all for comparison with the S-compounds in the FT fuel. Assuming that the TOF-MS detector has the same response for all sulphur compounds as for the internal standard, a total of 0.13% S-compounds was measured in the clay-treated Merox kerosene. The main sulphur-containing classes were the thiophenes, hydro-thiophenes, thianes, thiophanes, benzothiophenes and hydro benzothiophenes.

As an illustration, the ion extracted plots at  $m/z$  84, 101 and 115, typical for thiophene and, thiane and thiolane derivatives for FSJF and Merox kerosene, without addition of the thiophene as internal standard, are presented in Figure 3. Thiophene is not present in the samples and can thus be used as internal standard. Notwithstanding the overloading of the plots with the alkylbenzenes (dotted lines) that contains similar ions in their spectra, the thiolanes (C6) and thianes (C7) together with C8 and C9 homologues can be observed in the crude-derived fuel and not in the FT fuel. The high degree of peak co-elution, in this case thianes-thiolanes and the alkylbenzenes, makes correct quantification very difficult. The use of a sulphur-selective detector, the sulphur chemiluminescence detector (SCD), is currently being investigated for accurate quantification of sulphur species in crude-derived fuels after several treatments e.g. the Merox process and clay-treatment.

## Chapter 5: The Use of GCxGC for Fuel Analysis

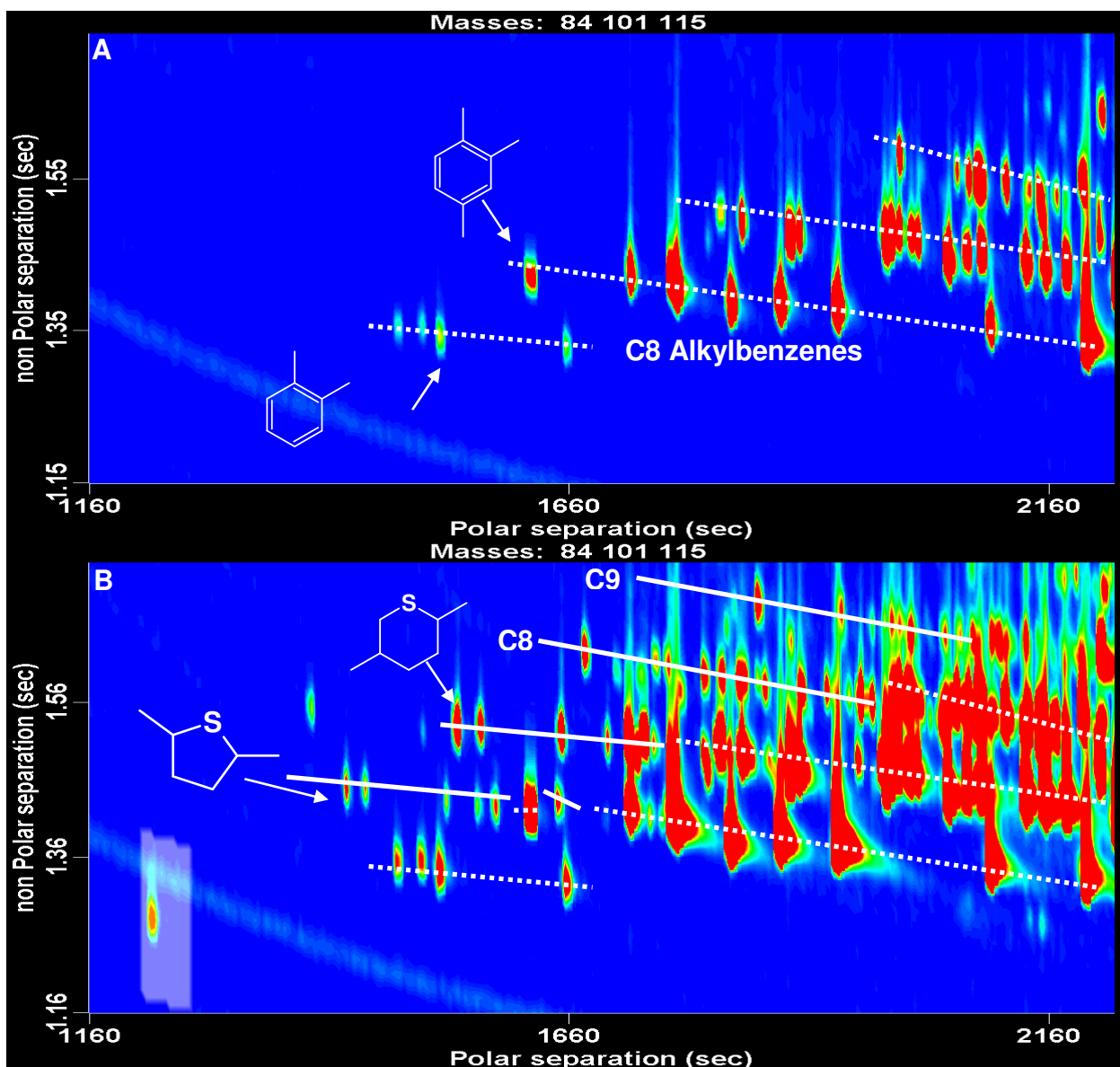


Figure 3: Extracted ion contour plots of  $m/z$  84 (thiophene), 101 (thiophanes) and 115 (thianes) in (A) FSJF and (B) crude-derive jet fuels.

Nitrogen-containing species, especially with a basic character, also have a negative environmental impact. Moreover, these compounds cause deactivation of the acidic catalysts used in catalytic conversion. Typical nitrogen compounds found in crude-derived fuels are the neutral indoles, carbazoles and tetrahydrocarbazoles as well as basic nitrogen compounds such as anilines, quinolines, acridines, cinnolines and aminoindanes [38].

## Chapter 5: The Use of GCxGC for Fuel Analysis

---

None of these compounds could be observed in the clay-treated crude-derived or synthetic jet fuels by selective ion extraction.

Hydrotreated fuels tend to form significant quantities of peroxides during storage. Phenolic antioxidants are generally added to jet fuel in the range of 17–24  $\mu\text{g/mL}$  to prevent peroxide formation. Antioxidants are naturally found in crude-derived fuels but are removed from synthetic fuels during severe hydro-processing. The clay-treated crude-derived fuel still contained trace levels ( $\approx 30 \mu\text{g/mL}$ ) of phenols and other benzene alcohols as well as benzofurans and indanones. By decreasing the split ratio to 20:1 and using extracted ions of  $m/z$  94, 108, 122, 131, 136, 150 and 164, which are typical for phenols and other aromatic oxygenates (e.g.  $m/z$  131 for ethylbenzofuran), the presence of some of these oxygenates in the Merox kerosene and their absence in FSJF could be observed (Figure 4).

The last class of compounds that is of interest to investigate in jet fuels is the olefins. While crude-derived fuels contain negligible amounts of olefins, FT fuels are hydrotreated to remove olefinic material that might cause fuel instability and gum formation. For fuels with negligible amounts of olefins, the presented GCxGC method can be used directly. If olefins are expected (as indicated by the bromine number [39] or FIA analysis [6]), fractionation using silver ion chromatography prior to the GCxGC separation is required [40,32]. These fractionation methods use a silver modified column for fractionation of unsaturates from saturates. The fractions can then be analysed separately by GCxGC and the results consolidated. Data on olefins in jet fuels will be presented elsewhere.

We have to note that synthetic fuels exhibit borderline lubricity compared to crude-derived fuels and that corrosion inhibitor/lubricity additives (LIA) are required to improve fuel lubricity. The DEF-STAN 91–91 [2] standard provides a list of the type and concentration of LIA's allowed in jet fuels.

## Chapter 5: The Use of GCxGC for Fuel Analysis

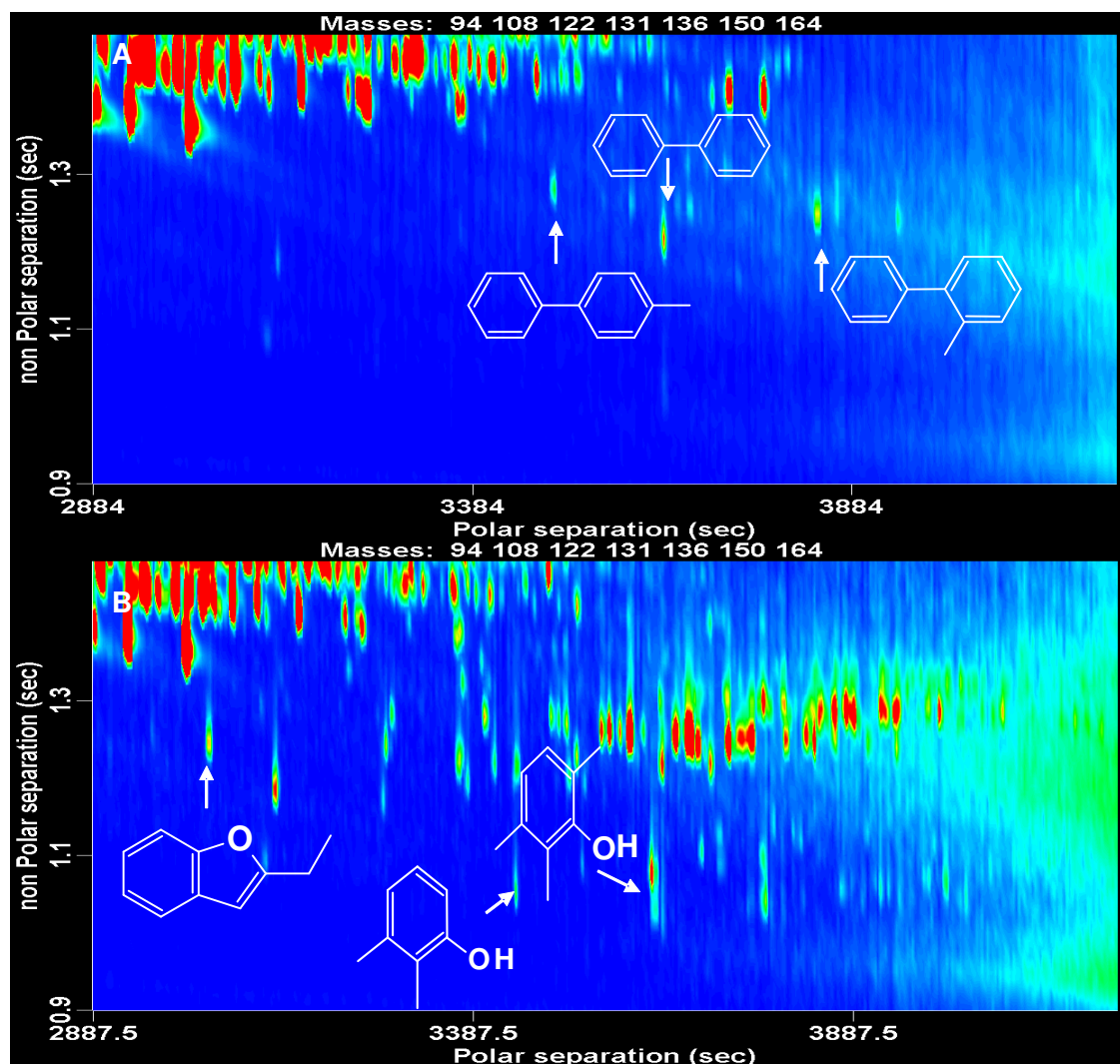


Figure 4: Extracted ion contour plots of  $m/z$  94, 108, 122, 131, 136, 150 and 164 showing the presence of oxygenates in the crude-derived fuel (B) and their absence in the synthetic fuel (A).

#### 5.4.3.3 Fuel stability

Current Jet A-1 specification requires the fuel to pass the JFTOT procedure at a test temperature of 260°C. JFTOT is used as a qualitative pass/fail rating instrument for thermal oxidative stability at this temperature. The JFTOT procedure measures the deposit formation tendencies of jet fuel in the presence of oxygen and a metal surface.

## Chapter 5: The Use of GCxGC for Fuel Analysis

---

The degree of fuel degradation due to thermal oxidation is determined by the amount of deposit formation, rated using a tube deposit ratio (TDR) on a scale from 0 (no deposit) to 4 (heavy deposit). The “break point temperature” can be evaluated by operating the JFTOT apparatus at the highest temperatures at which a fuel still passes the specification rating criteria. The thermal stability of the fuels studied here was investigated according to ASTM D3241 [27].

FSJF exhibited excellent thermal oxidative stability characteristics with a JFTOT break point temperature above 360 °C, while the crude oil–derived Merox kerosene which had been clay–treated once, exhibited a JFTOT break point temperature at 280 °C. This observation points to the presence of problematic species causing jet fuel instability. After a second clay treatment, the JFTOT break point temperatures of the Merox kerosene improved to 290 °C, confirming that clay treatment has a positive effect on the JFTOT break point temperatures.

GCxGC–TOF–MS extracted ion contour plots for ions  $m/z$  94, 108, 122 and 136 (phenols) and 134, 147, 161, 176 (benzothiophenes) of FSJF and crude–derived fuel before and after clay–treatment (Figure 5), show the removal of trace levels of phenols from the crude–derived fuel, while the benzothiophene content remains unchanged. No benzothiophenes or phenols were observed in the FSJF. Benzothiophenes and other components with cyclic sulphur structures could be responsible for the lower JFTOT break temperatures of the crude–derived fuel.

### 5.4.4 Conclusions

A GCxGC method utilizing a polar  $\times$  non–polar column combination which demonstrated excellent separation for the various compound classes in jet fuel was developed. The increase in available separation space for aliphatic compounds was especially advantageous for the analysis of synthetic fuels because of their relatively high aliphatic to aromatic ratio. The degree of peak co–elution that was observed for some of the sulphur–containing species and alkylbenzenes did not significantly affect the analysis of aromatics but prevented accurate quantification of the sulphur species.

## Chapter 5: The Use of GCxGC for Fuel Analysis

---

A detailed comparison of FSJF with crude-derived Merox kerosene showed that the fuels have very similar hydrocarbon compositions, although compounds were present at different ratios. Significantly, this implies that synthetic fuels do not introduce “new” molecules into aircraft’s fuel systems that might negatively affect the fuel’s properties. The presence of hetero-atomic species in the Merox kerosene and their absence in the FSJF was confirmed. The effect of clay treatment on JFTOT break point temperatures for the test fuels was investigated and the hetero-atomic content of the fuels was compared before and after clay treatment.

The proposed method proved to be suitable for quantification of the hydrocarbon compound classes in both synthetic and crude-derived jet fuels and to provide valuable information regarding the hetero-atomic species that affect fuel stability.

## Chapter 5: The Use of GCxGC for Fuel Analysis

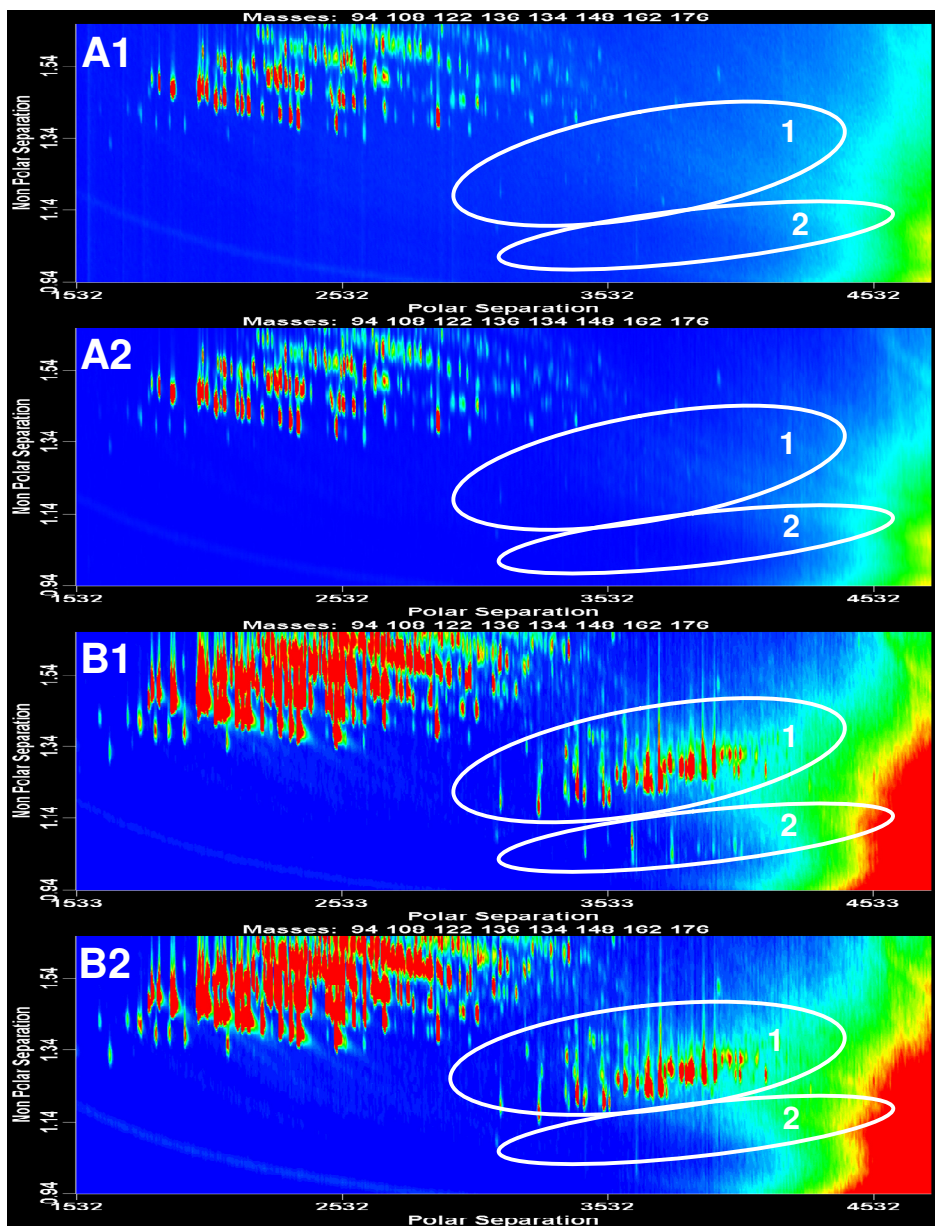


Figure 5: Comparison of extracted ion GCxGC plots of FSJF (A1) before and (A2) after clay treatment, and Mercox kerosene (B1) before and (B2) after clay treatment. Numbering: 1. benzothiophenes, 2. phenols.

## Chapter 5: The Use of GCxGC for Fuel Analysis

---

### 5.4.5 References

- [1] Standard Test Method: ASTM D7566, Standard specification for aviation turbine fuel containing synthesized hydrocarbons, ASTM International, D02.JO.06, West Conshohocken, USA, 2009.
- [2] British Ministry of Defense Standard 91–91, 7, 2011.
- [3] Standard Test Method: ASTM D1655, Standard test specification for aviation turbine fuels, ASTM International, West Conshohocken, USA 2009.
- [4] R.N. Hazlett, Thermal Oxidative Stability of Aviation Turbine Fuels; ASTM Monograph 1; ASTM: Philadelphia, 1991, 163.
- [5] G.E. Fodor, D.W. Naegeli, K.B. Kohl, Energy Fuels 2 (1988) 729.
- [6] M.O. Adebajo, R.L.Frost, J.T. Kloprogge, O. Carmody, J. Porous Material 10 (2003) 159.
- [7] B. Beaver, L. Gao, C. Burgess–Clifford, M. Sobkowiak, Energy Fuels 19 (2005) 1574.
- [8] Standard Test Method: ASTM D1319, Standard test method for hydrocarbon types in liquid petroleum products by fluorescent indicator adsorption, ASTM International, West Conshohocken, USA, 05.01 2008.
- [9] Standard Test Method: ASTM D6379, Determination of aromatic hydrocarbon types in aviation fuels and petroleum distillates – High Performance Liquid Chromatography method with refractive index detection, ASTM International, West Conshohocken, USA, 436/01 2004.
- [10] Standard Test Method: IP336, Petroleum products– determination of sulphur content – energy dispersive X–ray fluorescence spectrometry, the Energy Institute, London, UK, 04 2004.
- [11] Standard Test Method: IP342, Petroleum products – Determination of thiol (mercaptan) in light and middle distillate fuels – Potentiometric method, the Energy Institute, London, UK, 2000.
- [12] Standard Test Method: ASTM D3227, Standard test method for sulphur in gasoline, kerosene, aviation turbine and distillate fuels (Potentiometric method), ASTM International, West Conshohocken, USA, 2000.

## Chapter 5: The Use of GCxGC for Fuel Analysis

---

- [13] Standard Test Method: ASTM D1840, Standard test method for naphthalene hydrocarbons in aviation turbine fuels by ultraviolet spectrophotometry, ASTM International, West Conshohocken, USA, D02.04 2007.
- [14] IP PM DY/09 "Determination of fatty acid methyl esters (FAME), derived from biodiesel, in aviation turbine fuel – GC–MS with selective ion monitoring/scan detection method," the Energy Institute, London, UK.
- [15] J. Blomberg, P.J. Schoenmakers, U.A.Th. Brinkman, *J. Chromatogr. A* 972 (2002) 137.
- [16] ASTM D2425 – 04(2009) Standard Test Method for Hydrocarbon Types in Middle Distillates by Mass Spectrometry.
- [17] ASTM D2549 – 02(2007) Standard Test Method for Separation of Representative Aromatics and Nonaromatics Fractions of High–Boiling Oils by Elution Chromatography.
- [18] M. Bernabei, R. Reda, R. Galiero, G. Bocchinfuso, *J. Chromatogr. A* 985 (2003) 197.
- [19] M. Adahchour, J. Beens, R.J.J. Vreuls, U.A.Th. Brinkman, *TrAC* 25 (2006) 726.
- [20] J. Blomberg, P.J. Schoenmakers, J. Beens, R. Tijssen, *J. High Resolut. Chromatogr.* 20 (1997) 539.
- [21] J. B. Philips, J. Beens, *J. Chromatogr. A* 856 (1999) 331.
- [22] A.C. Lewis, N. Carslaw, P.J. Marriott, R.M. Kinghorn, P.D. Morrison, A.L. Lee, K.D. Bartle, M.J. Pilling, *Nature* 405 (2000) 778.
- [23] J. Beens, J. Blomberg, P.J. Schoenmakers. *J. High Resolut. Chromatogr.* 23 (2000) 182.
- [24] J. Beens, P.J. Schoenmakers, U.A. Th. Brinkman, *J. Chromatogr. A* 972 (2002) 137.
- [25] C. Vendeuvre, F. Bertoncini, L. Duval, J.L. Duplan, D. Thiebaut, M.C.Hennion, *J. Chromatogr. A* 1056 (2004) 155
- [26] C. von Mühlen, C.A. Zini, E.B. Caramao, P.J. Marriott, *J. Chromatogr. A* 1105 (2006) 39.
- [27] Standard Test Method: ASTM D3241, Thermal Oxidation Stability of Aviation Turbine Fuels (JFTOT Procedure), ASTM International, Philadelphia, PA, 08 2008.
- [28] J–M.D. Dimandja, G.C. Clouden, I. Colón, J–F. Focant, W.V. Cabey, R.C. Parry, *J. Chromatogr. A* 1019 (2003) 261.

## Chapter 5: The Use of GCxGC for Fuel Analysis

---

- [29] C. Vendeuvre, R. Ruiz–Guerrero, F. Bertoncini, L. Duval, D. Thiébaud, M–C. Hennion, *J. Chromatogr. A* 1086 (2005) 21.
- [30] F. Adam, F. Bertoncini, V. Coupard, N. Charon, D. Thiebaut, D. Espinat, M.C. Hennion, *J. Chromatogr. A* 1186 (2008) 236.
- [31] R. van der Westhuizen, A. Crouch, P. Sandra, *J. Sep. Sci.* 31 (2008) 3423.
- [32] R. van der Westhuizen, H. Potgieter, N. Prinsloo, A. de Villiers, P. Sandra, *J. Chromatogr. A* 1218 (2011) 3173.
- [33] R. van der Westhuizen, R. Crous, A. de Villiers, P. Sandra, *J. Chromatogr. A* 1217 (2010) 8334.
- [34] J.A. Valla, A.A. Lappas, I.A. Vasalos, *Appl. Catal. A*, 276 (2004) 75.
- [35] C. Yin, D. Xia, *Fuel*, 80 (2001) 607.
- [36] J. Diao, *Petrol Refin. Eng.* 29 (1999) 24–31.
- [37] L. Lin, G. Wang, H. Qu, *J. Membrane Sci.* 280 (2006) 651.
- [38] F. Adam, F. Bertoncini, N. Brodusch, E. Durand, D. Thiébaud, D. Espinat, M–C. Hennion, *J. Chromatogr. A* 1148 (2007) 55.
- [39] Standard test method: ASTM D1159, Standard test method for bromine numbers of petroleum distillates and commercial aliphatic olefins by electrometric titration, ASTM International, West Conshohocken, USA, 2007.
- [40] D. Mao, H. v.d. Weghe, L. Diels, N. De Brucker, R. Lookman, G. Vanermen, *J. Chromatogr. A* 1179 (2008) 33.

# **Chapter 6**

## **Current Projects and Future Challenges**

## Chapter 6: Current Projects and Future Challenges

---

### 6.1 On-line GCxGC for High temperature Fischer–Tropsch product analysis

#### 6.1.1 Introduction

As part of the research and development on FT synthesis, laboratory– and pilot plant scale experiments were performed to optimise processes for current and future plants. New processes, next generation catalysts and the effects of promoters and of changes in reaction variables such as temperature, pressure and feed gas ratios on the product spectrum are some of the aspects that have been investigated in the laboratory. Successful experimentation on laboratory scale may lead to larger pilot plant scale operations, and eventually new or improved industrial plants.

Accuracy of analysis is very important in the development of kinetic and selectivity models that are used in plant optimisation. HT–FT products are distributed over three phases at room temperature: a gaseous phase that contains  $C_1$ – $C_6$  hydrocarbons and some light oxygenates, a highly complex oil phase with hydrocarbons and oxygenates ranging in carbon numbers from  $C_1$  to  $\approx C_{30}$ , and an aqueous phase in which some oxygenates are dissolved. A good understanding of the HT–FT product spectrum has been obtained through various studies, some of which were discussed in this dissertation. The emphasis of this research has largely been on the analysis of the oil phase products, because products from this phase are predominantly used in chemical and fuels production. However, products in the gas phase and the organics dissolved in the aqueous phase also have to be quantified, because these products can be very valuable; examples include ethylene and propylene, which are basic chemicals widely used in the industry. Quantitative analysis of the feed and unreacted gases is also important to determine conversion rates of the various FT reactions, for economic reasons.

At Sasol, and as has been reported in literature, the feed gases, unconsumed reactants and non–condensable products such as the gaseous hydrocarbons are analysed using on–line GC–FID, GC–TCD and MS.

## Chapter 6: Current Projects and Future Challenges

---

On the other hand, condensable products containing higher carbon number hydrocarbons ( $>C_6$ ) and heavier oxygenates, are collected and analysed off-line. The product has to be cooled down before being separated into organic and aqueous phases, and then weighed to determine mass balances. The two phases then need to be analysed separately. Analysis results for all phases subsequently have to be combined to obtain an overall result [1–5].

Off-line sampling has a number of disadvantages, including the evaporation of low-boiling species and contamination and oxidation that occurs during cooling, storage and handling. Moreover, components usually appear in more than one phase and analysis results for the different phases then need to be recombined to obtain the full product spectrum. Relatively large amounts of sample are needed, which is not always feasible for laboratory-scale experiments. Finally, the various analyses may take several hours, which is very inconvenient when following the dynamics of the catalyst or reaction condition changes.

Different experimental conditions are needed to obtain optimal separation for the three phases. Gases have high vapour pressures and elute very early from conventional GC columns. They therefore require longer columns with thicker phases to ensure sufficient retention for optimal resolution. High-boiling components, on the other hand, are strongly retained on these columns. For oils of higher carbon numbers, shorter, narrow-bore columns with less stationary phase need to be used to ensure elution of the heavier compounds. Organics dissolved in the water phase need to be extracted prior to GC analysis, or a column that can handle water has to be used.

On-line analysis can overcome some of the problems with quantification and sample handling [6–9], but has its own challenges; the greatest being the ability to transfer representative samples from the reactor to the GC instrument. Heavy products tend to condense and adsorb in the sample lines, leading to blocked flow and under-representation of certain species. The development of an on-line GCxGC-system was previously investigated in Sasol Technology R&D in collaboration with Scientific Supply Services (Johannesburg, South Africa) for the analysis of LT-FT products [10–12].

## Chapter 6: Current Projects and Future Challenges

---

However, problems with condensation of high-boiling compounds in the sample lines have been found to occur and, as a result, sample lines have to be purged periodically. Because the condensation occurs gradually, it may not be detected early enough and may affect quantitative results.

The current study investigates the development of an improved on-line GCxGC system that will enable the analysis of all HT-FT feed gases and products obtained during micro-reactor experiments in the laboratory. The sampling system has to deliver a representative sample to the GC without condensation of heavy products, while the analytical system has to provide accurate, quantitative analysis for a product that may range in carbon numbers from  $C_1$  to  $\approx C_{30}$  and that also contains some reaction water, as well as the permanent feed and tail gases.

### 6.1.2 Experimental

#### 6.1.2.1 Sampling system

The micro-reactor was typically operated at 2000–3000 kPa and 300–380°C. Sample transfer from the reactor to the sampling system was done by opening a valve (computer controlled) on the reactor. A small sample stream flowed through a narrow orifice to the analytical system via sample lines that were steam-heated to 220°C and thermally isolated with heat-resistant tape. The sample flow was 30 mL/min (determined by an Aalborg flowmeter, Randburg, South Africa) and gas dilution was done by the addition of helium at 300 mL/min to the sample lines at the reactor interface. The product was drained daily from a heated sample collection point after completion of the on-line analysis.

#### 6.1.2.2 Analytical system and conditions

The analytical system consisted of two 6890 GC (Agilent Technologies, Little Falls, DE, USA) instruments.

## Chapter 6: Current Projects and Future Challenges

---

The first GC was equipped with two split/splitless injectors and FID detectors and connected to a micro-reactor via heated sample lines. The front channel of this GC was converted to a GCxGC–FID (Zoex Corporation, Houston, TX, USA) with a ZX1 2–stage loop modulator. The first dimension column was a 50 m x 200  $\mu\text{m}$  i.d. x 0.30  $\mu\text{m}$  HP–FFAP (Agilent Technologies), while the second dimension column was a 1.5 m x 100  $\mu\text{m}$  x 0.1  $\mu\text{m}$  RTX–5 (Restek). The second channel of the GC was set up for 1D–GC–FID analysis of light boiling gases using a 50 m x 200  $\mu\text{m}$  i.d. x 0.5  $\mu\text{m}$  HP–PONA (Agilent Technologies) column. Hydrogen was used as carrier gas on both columns at a constant flow of 1.4 mL/min.

The GC oven employed a temperature program of 40°C (0.1 min), ramped at 3°C/min to 240°C (shared by both channels). No secondary oven was used for GCxGC, and the modulation period was 8 s. FID data were collected at 100 points/s for GCxGC and 20 points/s for the 1D–GC. Both injectors were kept at a temperature of 240°C.

Sample was injected into the split/splitless injectors (splitless mode) of the GCxGC–FID and GC–FID via guard columns (1 m x 250  $\mu\text{m}$  i.d., Rxi-5, Restek) and ten–port sample valves with 100  $\mu\text{L}$  loop volume. The valves were programmed to inject selected fractions of the eluent from the guard columns. Fraction selection was controlled by selecting suitable “valve load time” and “inject time” settings in the Agilent Chemstation (Ref. B.03.01, Agilent Technologies) software. These time settings could be varied, depending on the specific sample fraction which was targeted for analysis. The heavy fraction of the sample was vented to prevent heavy boiling compounds from contaminating the columns. The sampling valve injected 100  $\mu\text{L}$  of the gas–diluted sample into the split/splitless inlet (splitless mode). GCxGC–FID data interpretation was done using GC Image software (Version 1.8b6, Zoex Corporation).

The permanent gases  $\text{H}_2$ ,  $\text{CO}$ ,  $\text{CH}_4$ ,  $\text{CO}_2$  and  $\text{N}_2$  (air peak) were analysed on the second GC containing a column switching system with two ten–port valves, a six–port valve and two thermal conductivity detectors (TCDs). A sample volume of 100  $\mu\text{L}$  was injected via the two ten–port valves.

## Chapter 6: Current Projects and Future Challenges

---

After injection, hydrogen was passed through the first molecular sieve 5A plot column (80/100 mesh, 1 m x 1/8 inch. x 2 mm i.d., Restek), and the rest of the product was back-flushed and vented.

Hydrogen was then passed through the second molecular sieve column and detected on TCD1. Argon was used as carrier gas for hydrogen analysis. After 1.8 min, the first detector was switched off and the second detector was switched on. After injection onto the second ten-port valve, Ar, N<sub>2</sub>, CO, CH<sub>4</sub> and CO<sub>2</sub> were eluted from the first Shincarbon ST packed column (2 m x 2 mm i.d., 80/100 mesh, Agilent Technologies) using helium as carrier gas, while the heavier boiling compounds were back-flushed and vented. Ar, N<sub>2</sub>, CO, CH<sub>4</sub> were then passed through the second Shincarbon column and separated further on the third molecular sieve column, and then analysed on the second TCD. The sequence was reversed at 5.5 min, before the CO<sub>2</sub> could elute from the second Shincarbon column. The compound was moved back through this column and detected on TCD 2. Sequence reversal was necessary because CO<sub>2</sub> adsorbs on molecular sieve columns. Using an isothermal oven temperature of 100°C, analysis is completed within 8 min. All Shincarbon columns and all molecular sieve columns had the same dimensions. A constant flow of 22.5 mL/min was used for H<sub>2</sub> analysis and a constant flow of 25.8 mL/min was used for the second channel separation.

### 6.1.2.3 Identification and quantification

Identification of peaks was done by off-line GCxGC-TOF-MS analyses in 1D and 2D modes (Pegasus 4D, Leco Corporation, St. Joseph, MI, USA) using the same columns as for quantification. A standard gas mixture, consisting of 55.0% H<sub>2</sub>, 20.0 % Ar, 15.0% CO, 5% CO<sub>2</sub>, 0.9% N<sub>2</sub> and 4.0% CH<sub>4</sub> (Afrox Scientific, Johannesburg, SA), was connected on-line to the GC system, and used for quantification of compounds analysed on the GC-TCD. CH<sub>4</sub> was used to quantify compounds separated by the GC-FID while the 1-pentene peak, quantified in the GC-FID data, was used to tie the GC-FID and GCxGC-FID data.

## Chapter 6: Current Projects and Future Challenges

---

### 6.1.3 Results and discussion

The on-line analytical system enabled simultaneous on-line analysis of all the HT-FT products. These products included a mixture of permanent feed gases, H<sub>2</sub>, CO, CO<sub>2</sub>, Ar and N<sub>2</sub>, hydrocarbon product gases from C<sub>1</sub>-C<sub>6</sub>, an oil fraction that contained a highly complex mixture of hydrocarbons and oxygenates from C<sub>1</sub>-C<sub>30</sub>, and a water fraction that contained oxygenates. To keep all of these products in the gas phase during sampling and to prevent condensation of heavy products in the sample lines, the lines were steam-heated to 220°C and the product eluting from the reactor was diluted by addition of helium to the sample lines. Helium addition was done at the reactor / sample line interface. The gas dilution was found to provide a significant improvement compared to the previous on-line system. By using gas dilution, the partial pressures of individual compounds were lowered.

The second-dimension columns used in GCxGC are typically very short, narrow bore columns, with a very thin film of stationary phase for ultra fast analysis, and are therefore not optimal for the analysis of highly volatile gases. While the GCxGC experimental conditions can be optimised to enable separation of light gases, these conditions will then not be optimal for oil analysis, where the carbon numbers can be as high as C<sub>30</sub>. The front channel of the first GC was therefore optimised for the GCxGC separation of the hydrocarbon products from C<sub>5</sub> to C<sub>30</sub>. The complexity of the C<sub>1</sub>-C<sub>6</sub> fraction of the HT-FT product is not as high as that of the oil phase product because only a limited number of isomers are possible for lower carbon numbers. For these light gases 1D-GC provides sufficient resolution for most of the isomers if the correct column and operating conditions are selected. The back channel of the first GC was therefore optimised for 1D-GC-FID separation for the light (C<sub>1</sub>-C<sub>6</sub>) hydrocarbons.

The instrumental configuration used for GCxGC-FID and GC-FID separations is presented in Figure 1. An example of the separation of the light hydrocarbon gases on the 1D-GC-FID is shown in Figure 2. The FID detector only detects hydrocarbons and, for this reason, the use of TCD detectors is necessary for the analysis of permanent gases. The second GC was set up with two TCD detectors for analysis of the feed and un-reacted permanent gases Ar (reference gas), H<sub>2</sub>, CO and CO<sub>2</sub> (feed gases) as well as CH<sub>4</sub> (product) (Figure 3).

## Chapter 6: Current Projects and Future Challenges

This set-up provided excellent separation of all these gases as well as for the standard gas mixture in an analysis time of 8 min (Figure 4).

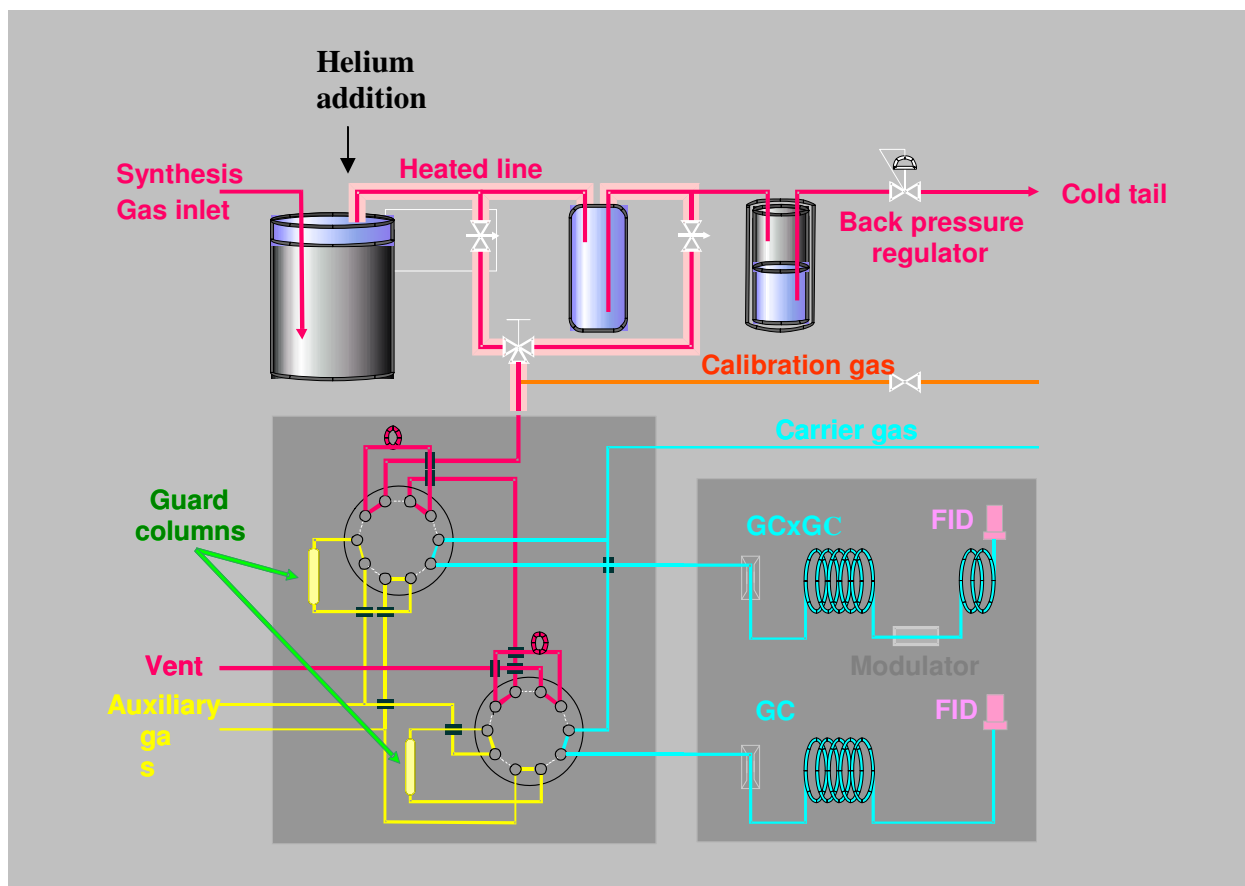


Figure 1. Schematic diagram illustrating the GCxGC-FID/GC-FID system configuration used for analysis of the  $C_1$ - $C_{30}$  hydrocarbons in HT-FT products.

Chapter 6: Current Projects and Future Challenges

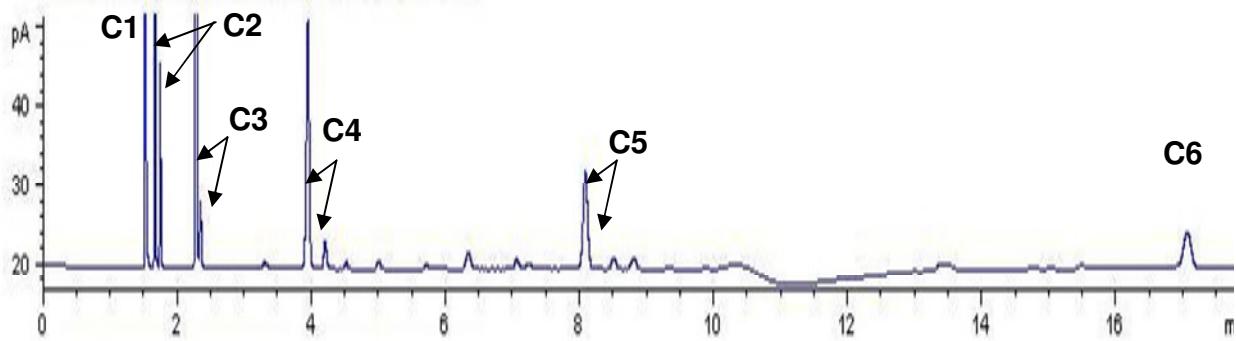


Figure 2. Example of the on-line GC-FID analysis of light ( $C_1$ – $C_6$ ) hydrocarbon gases from the thick-phase column using the experimental configuration presented in Figure 1. The 1-alkenes and  $n$ -alkanes are shown for the carbon numbers  $C_2$ – $C_5$ .

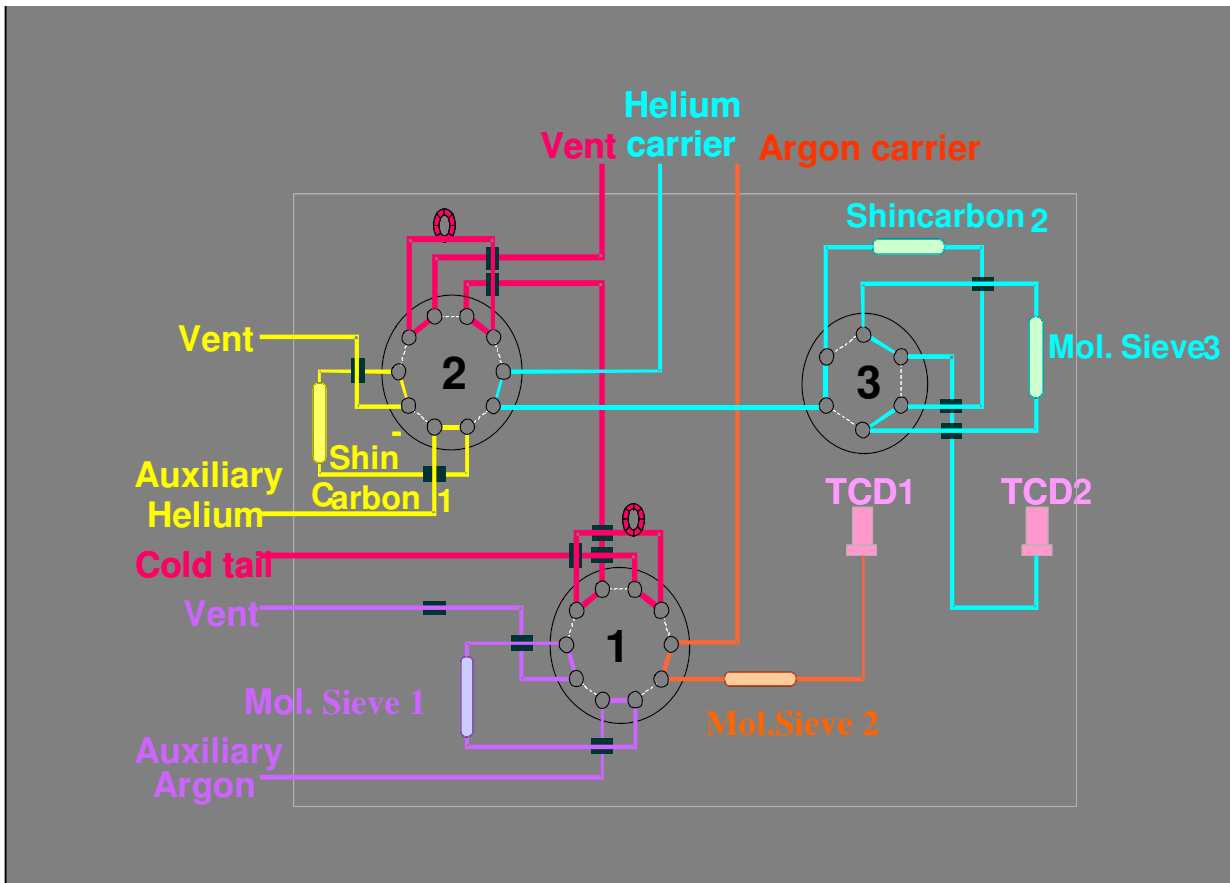


Figure 3. Schematic configuration of the GC-TCD configuration used for the analyses of permanent gases. Two ten-port and one six-port valve are used to regulate flow to two TCD detectors for the analysis of the permanent gases  $H_2$ , Ar,  $N_2$ , CO,  $CH_4$  and  $CO_2$ .

## Chapter 6: Current Projects and Future Challenges

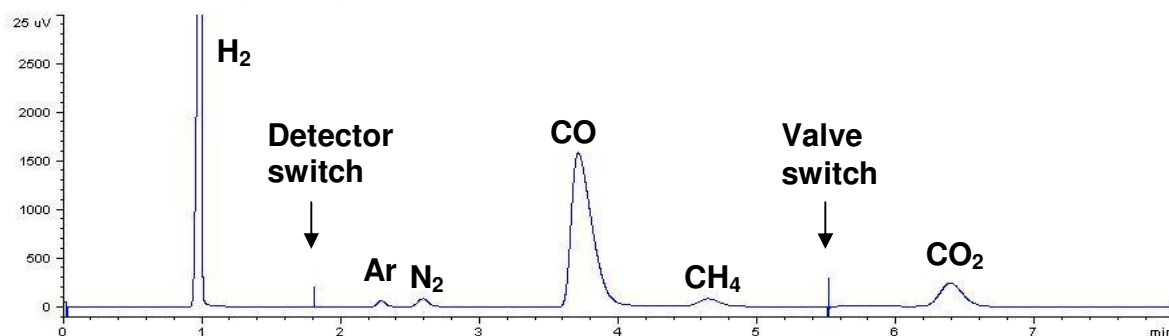


Figure 4. Example of the GC–TCD separation of permanent gases and CH<sub>4</sub> from a feed gas sample using the experimental configuration presented in Figure 3.

The standard mixture contained mostly permanent gases and was used as an external standard to quantify these gases on the GC–TCD system. Only CH<sub>4</sub> was detected by FID and is used to quantify compounds separated by the 1D–GC–FID. The separation of CH<sub>4</sub> on the GCxGC–FID was not sufficient for quantification purposes and the 1–pentene peak, quantified in the GC–FID data, was used to tie the GC–FID and GCxGC–FID data. It is therefore essential for quantification purposes that no co-elution with 1–pentene occurs in both the 1D–GC–FID and GCxGC–FID separations. The concentration of the 1–pentene injected into the GC–FID and GCxGC–FID was the same, even though different fractions of the sample were sent to the two separations systems. The on–line GCxGC–FID separation of the combined HT–FT hydrocarbon and oxygenated products is shown in Figure 5.

Initial results achieved on the on–line GCxGC system were very promising. Before helium was added into the sample lines, heavy boiling compounds from the numerous trial runs were condensed in the sample lines, preventing accurate sample delivery and quantification. After the helium installation, heavy boiling compounds were still observed as a result of the residual condensation products from previous runs, but, following purging of the lines and valves with acetone, no evidence of the condensation could be found in any of the subsequent runs. Condensation products can be recognised as a group of heavy–boiling compound peaks that do not fit in with the HT–FT product profile. More than a hundred analyses were performed on this system, and to date, no evidence of condensation has been observed.

## Chapter 6: Current Projects and Future Challenges

In the event of condensation observed in future for specific products, electrical heating will be considered to further improve the heating of transfer lines.

We are currently investigating the repeatability of the sample delivery to the GCxGC-system and improving on the quantification. Currently, only the gas standard containing six components is available on-line, which hampers accurate quantification. These compounds are all detected by the TCD but only CH<sub>4</sub> is detected by the GC-FID. We are obtaining more standards for GC-FID and also some heavier standards for the GCxGC-FID. The heavy standards will enable the monitoring of any possible condensation in the sample lines. We are also investigating the use of a multi-point gas-calibration system for more accurate quantification.

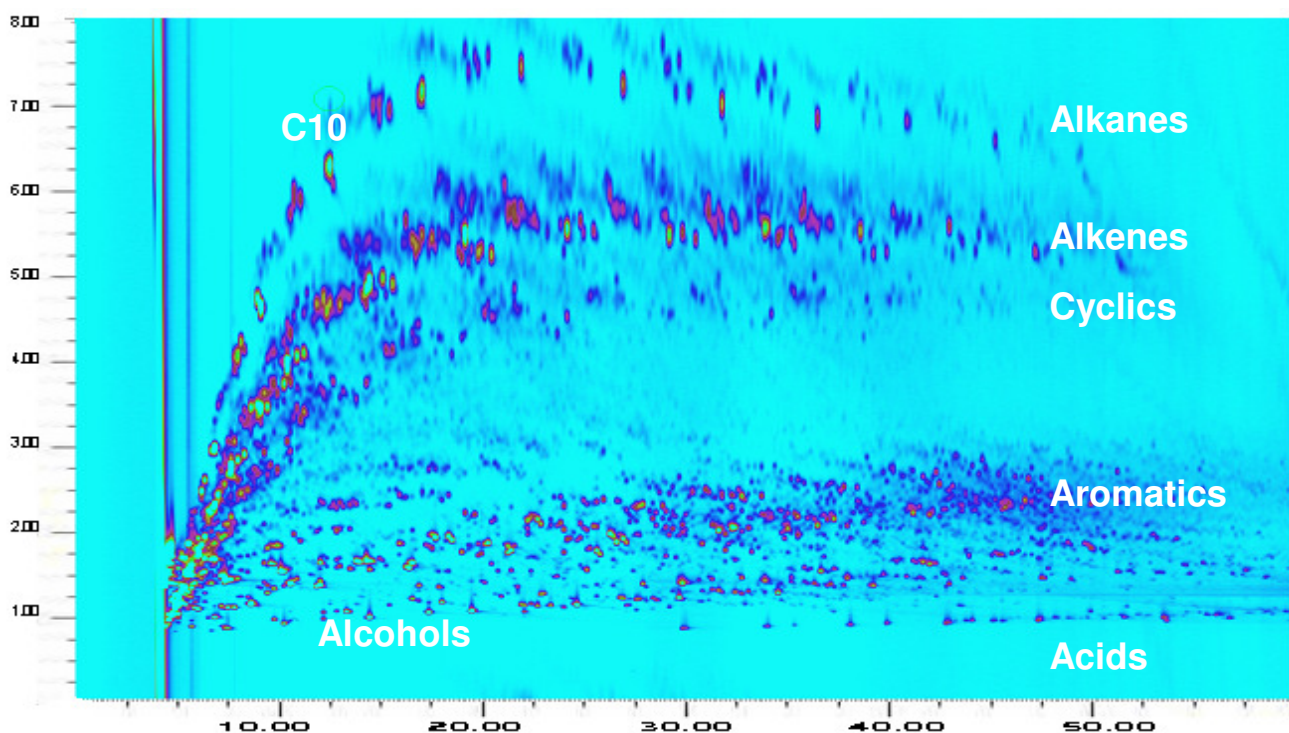


Figure 5. On-line GCxGC-FID contour plot obtained for the analysis of the combined HT-FT product.

## Chapter 6: Current Projects and Future Challenges

---

### 6.1.4 Summary

The developed sampling system enables accurate sampling of the HT–FT products by preventing the condensation of heavy compounds in the mixture. This is obtained by heating sample lines and by diluting the product with helium. The helium dilution provides a significant improvement to the previous on–line system as it dilutes the product and keeps it in the gas phase.

The analytical system provides simultaneous analysis of the various product fractions using optimal separation conditions for the different fractions. Further optimisation will be done by the addition of more hydrocarbon standards and a multipoint calibration system.

## 6.2 On–line SFC–GCxGC for the analysis of FT products

### 6.2.1 Introduction

GCxGC provides exceptional separation power for the analysis of highly complex products but, even with this technique, co–elution is still observed in certain applications. In order to overcome these limitations, HPLC and GCxGC have been combined off–line (Chapter 5.2) to enable the distinction between cyclic alkanes and residual internal alkenes in the hydrogenated oligomerisation products of C<sub>3</sub>–C<sub>4</sub> alkenes. GC inlet hydrogenation has also been used to assist in the distinction between cyclic and non–cyclic alkenes in highly complex oligomerisation products of pure 1–hexene (Chapter 4.3.5).

By combining HPLC and GCxGC off–line it is possible that solute loss, contamination and/or oxidation may occur during sample collection and re–concentration. On–line hyphenation, on the other hand, is challenging because of the large volumes of HPLC solvents that require special interfaces such as retention gaps and solvent evaporation techniques.

Supercritical fluid chromatography (SFC) provides similar, but faster, hydrocarbon group–type separation than HPLC, but it is more compatible with hyphenation to GC or GCxGC due to

## Chapter 6: Current Projects and Future Challenges

---

the use of carbon dioxide-based mobile phase [13–15]. For example, Adam et al. [16] separated middle distillates into saturated and unsaturated fractions by SFC in a first step towards achieving separation of classes of alkanes, iso-alkanes, alkenes, naphthenes and aromatics. These authors transferred the SFC effluent to a split/splitless injector through restrictors that were inserted directly in the injector. The injectors were operated in splitless mode to prevent precipitation of analytes. The on-line coupling of SFC and GCxGC is currently being investigated by Sasol, in collaboration with the University of Pretoria, in order to obtain separation of compound classes in FT products that cannot be separated by GCxGC alone. Some of the preliminary results are discussed in this chapter.

### 6.2.2 Experimental

A Series 4000 SFC (Selerity Technologies, Salt Lake City, Utah, US) was equipped with two six-port valves and three SFC columns, using CO<sub>2</sub> as mobile phase, at a pressure of 20.265 MPa and a temperature of 41°C. An FID detector was used at 400°C, with an air pressure of 21 kPa and hydrogen pressure of 23 kPa. The three columns, packed by Selerity Technologies, were connected in series. The first column was 5 cm long, with a 1 mm internal diameter (i.d.) and was packed with polyvinyl alcohol (PVA). The second column was 50 cm long with a 1 mm i.d. and was packed with high-surface-area silicagel, having an average diameter of 5 µm, 600 nm pores and a surface area ≥ 350 m<sup>2</sup>/g. The third column, packed with strong cation exchange silica material and loaded with silver ions, was 5 cm long, with a 1 mm i.d. The particles had an average diameter of 5 µm.

For on-line analysis, the SFC restrictor at the GCxGC interface was modified in order to maintain a constant flow of the CO<sub>2</sub> mobile phase to the GCxGC as described by Guthrie and Schwartz [17] and placed directly into the split/splitless inlet of the GC. The injector temperature was 260°C (splitless mode). The oven was kept at –50°C to trap and focus the analyte molecules, after which the GCxGC run was started and the first fraction analysed. This injection procedure was followed for all analyte fractions.

## Chapter 6: Current Projects and Future Challenges

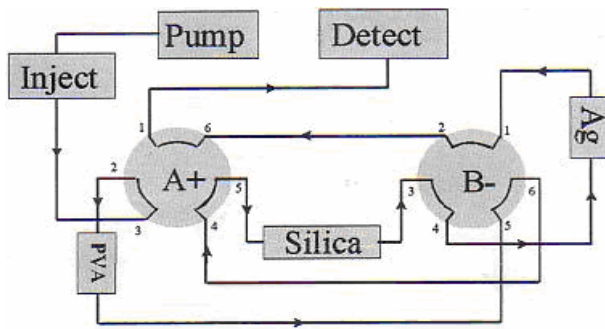
---

GCxGC was performed using a Pegasus 4D instrument equipped with a FID detector (Leco Corporation, St. Joseph, MI, USA). The first-dimension column was a 30 m x 250  $\mu\text{m}$  i.d. x 0.25  $\mu\text{m}$  RTX–Wax (Restek) with a temperature program of 40°C (0.2 min), ramped at 3°C/min to 245°C. The second-dimension column was a 1.8 m x 100  $\mu\text{m}$  x 0.1  $\mu\text{m}$  RTX–5 (Restek), and the second oven followed the first oven with a lead of 25°C. The modulation period was 7 s. The carrier gas was hydrogen at a constant flow of 1.4 mL/min. A splitless injection was done via the 1  $\mu\text{l}$  samples valve. FID data were collected at 100 points/s.

### 6.2.3 Initial results and future work

The configurations of the SFC valves are illustrated in Figure 6. In forward-flow mode (valves position 1), oxygenates were retained on the PVA column, aromatics were retained on the silica column and alkenes on the Ag column. The alkanes were eluted from all three columns to the detector. After elution of the alkanes, valve A was switched (valves position 2), and the oxygenates were back-flushed to the detector. With the valves in this position, the silica and Ag columns were not in the flow path. Valve B was now switched (valves position 3) to place the Ag and PVA columns in series in back-flush mode to elute the alkenes from the Ag column to the detector. In this mode, the silica column was not in the flow path.

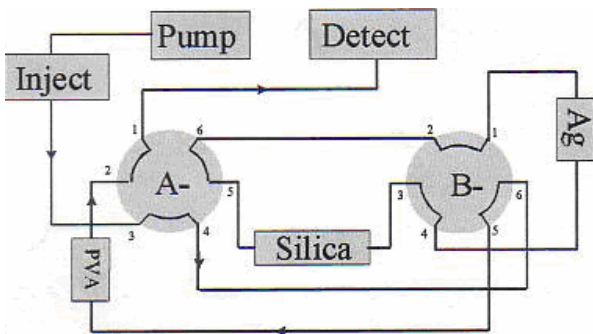
## Chapter 6: Current Projects and Future Challenges



### Valves in position 1

PVA column: forward flush  
 Silica column: forward flush  
 Ag column: forward flush

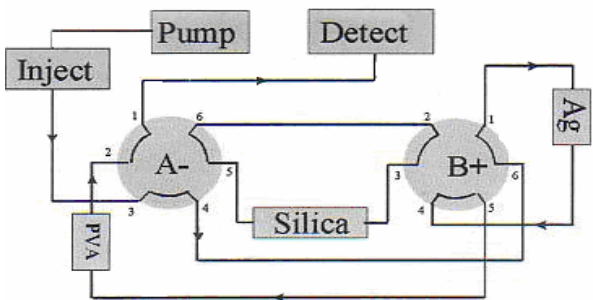
Columns connected in series  
Alkanes elute



### Valves in position 2

PVA column: back-flush to detector

Silica and Ag columns not in flow path  
Oxygenates elute

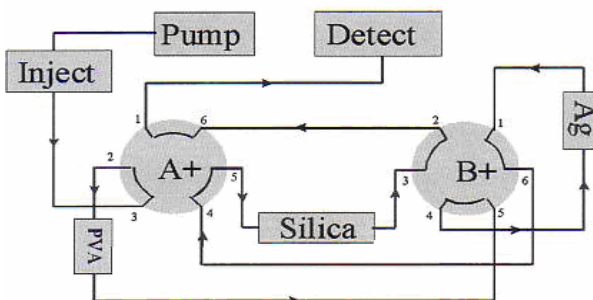


### Valves in position 3

PVA column: back-flush  
 Ag column: back-flush

PVA and Ag columns connected in series in back-flush mode.

Silica column not in flow path  
Alkenes elute



### Valves in position 4

PVA column: forward flush  
 Ag column: forward flush  
 Silica column: forward flush

Silica column now last in series connection  
Aromatics elute

Figure 6. Schematic diagrams illustrating the configuration of the columns and valves used for the SFC-FID separation of alkanes, oxygenates, alkenes and aromatics.

## Chapter 6: Current Projects and Future Challenges

Finally, valve A is switched back so that the silica column is the last in the series and aromatics can be eluted to the detector (valve position 4).

The off-line separation of the four compound classes (alkanes, alkenes, aromatics and oxygenates) for a HT-FT oil by using the SFC configuration described above is demonstrated in Figure 7 [18]. These fractions were analysed individually using GCxGC-FID (results not shown).

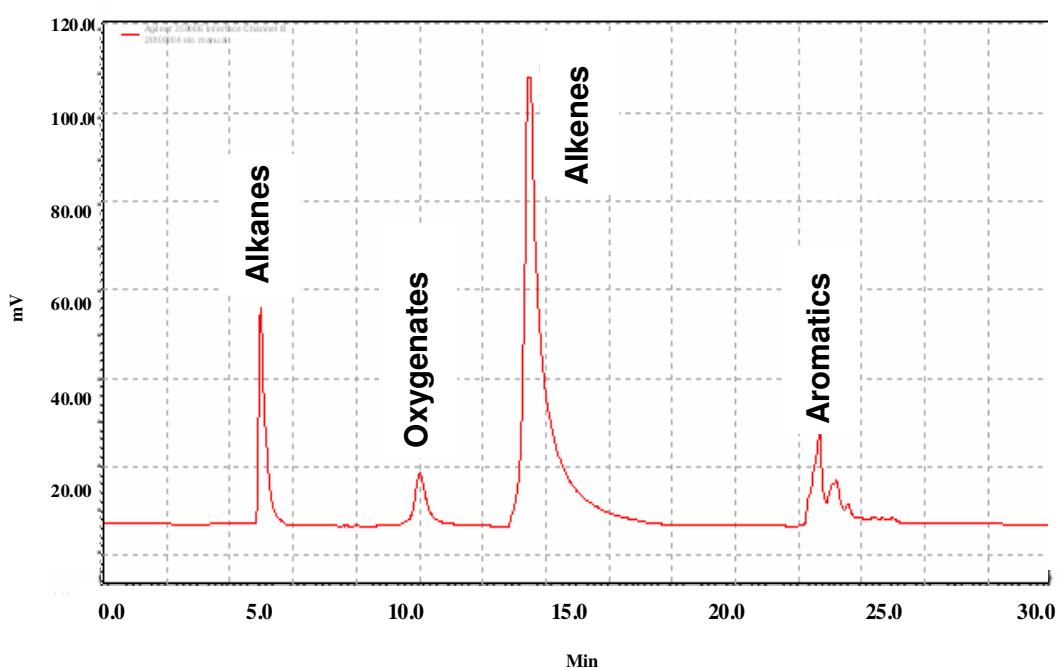


Figure 7: The separation of the alkanes, oxygenates, alkenes and aromatics in a HT-FT oil, obtained by the SFC configuration described above.

Off-line SFC-GCxGC analysis proved to be problematic. A solvent had to be used to collect the very small volumes eluting from the SFC restrictor, and solvent removal then became a problem similar to HPLC sampling. The sensitivity for the analysis was reduced because of the relatively large volumes of residual solvent, while solvent peaks co-elute with those of light boiling analytes on the GCxGC contour plot. On-line SFC-GCxGC will eliminate the problems encountered with off-line sampling because no solvents are required to collect fractions.

## Chapter 6: Current Projects and Future Challenges

---

The on-line coupling of the SFC with GCxGC is currently in progress. For this system, the SFC restrictor is placed directly into the split/splitless inlet of the GCxGC. After elution of the first SFC fraction, it is transferred to the GCxGC for analysis, while the separation on the SFC is paused. Following completion of the GCxGC separation, flow on the SFC is commenced and the next fraction is transferred to the GCxGC. This process is repeated for all four fractions. We will also be looking at automating the process by controlling the GCxGC instrument via the SFC software. TOF-MS and FID detectors will be selected depending on the application. A six-port valve has been installed between the SFC and GCxGC that will bypass the FID on the SFC during on-line analysis. When the valve is open the on-line connection is enabled, and when closed the SFC and GCxGC can be used separately in the normal off-line fashion.

Other on-line SFC-GCxGC applications, like distinguishing between the various alkenic classes, will also be attempted.

### 6.2.4 Summary

The development of the on-line SFC-GCxGC for FT applications shows great promise. The SFC separation of alkane, oxygenate, alkene and aromatic compound classes of a HT-FT oil has already been demonstrated, and the on-line coupling of SFC with GC is feasible. This coupling will enable the separation of compound classes that cannot be obtained with GCxGC only, and will eliminate the problems associated with off-line sampling because no solvents are required.

## Chapter 6: Current Projects and Future Challenges

---

### 6.3 GCxGC–SCD, GCxGC–NCD

#### 6.3.1 Introduction

It is known that sulphur- and nitrogen-containing compounds adversely affect fuel stability during storage and are precursors to  $\text{NO}_x$  and  $\text{SO}_x$  emissions which are released after combustion of the fuel and which are responsible for acid rain [19,20]. Knowledge about the contribution of individual species to fuel stability and environmental pollution could be useful when considering methods for the removal of these compounds from the fuel.

Accurate quantification of the total sulphur and total nitrogen species is normally done by using Antek analysers that use sulphur (SCD) and nitrogen (NCD) chemiluminescence detectors (for example, test methods EN20846, UOP971, UOP936, ENV12260, ASTM D7359, D5453, etc.). SCD and NCD detectors convert sulphur- and nitrogen species to their respective chemiluminescent ion species, which can then be accurately quantified. These detectors are characterised by equimolar responses to sulphur and nitrogen components, an absence of quenching effects, and excellent selectivity and sensitivity.

FT products do not contain significant amounts of sulphur- and nitrogen-containing compounds because these species are removed from the synthesis gas prior to FT synthesis. Heteroatomic species are, however, present at trace levels in crude-derived fuels and because these fuels are often blended with FT fuels and sold as semi-synthetic fuels, it is important to understand the effect of these compounds on the properties of a fuel. The blending with tar distillates, a by-product of high-temperature coal gasification, could also be investigated as a means to increase the density of FT-derived fuels. The tar fractions may also contain some heteroatom-containing compounds.

GCxGC–TOF–MS is an excellent method for identification of the heteroatomic species but quantification is complex due to the large number of possible isomers, and differences in detector responses for these isomers. Pure reference standards for each compound are therefore necessary for accurate quantification, which complicates analysis.

## Chapter 6: Current Projects and Future Challenges

---

SCD and NCD detectors have been combined with GCxGC in petrochemical laboratories with great success [21–25] and will also be implemented in the Sasol research laboratories in the near future. GCxGC is highly sensitive and provides group-type separation that aids in peak identification, while the SCD and NCD detectors are highly sensitive and selective to enable accurate quantification of sulphur and nitrogen species. By combining GCxGC–TOF–MS, GCxGC–SCD and GCxGC–NCD it should be possible to accurately quantify trace levels of sulphur and nitrogen species in semi-synthetic fuels.

### 6.4 Further challenges

The application of GCxGC to Fischer–Tropsch products has opened a wide range of opportunities in Sasol’s research and development laboratories and can be applied in most of the research areas. One of the main priorities, resulting in part from the research presented in this thesis, is to extend the use of GCxGC to Sasol’s routine analytical laboratories. To enable this, standard test methods are now being developed and validated for implementation in the near future. We are also investigating the use of chemometrics to facilitate the handling of assist in handling the huge amounts of data generated by GCxGC.

## Chapter 6: Current Projects and Future Challenges

---

### 6.5 References

- [1] J.V. Bauer, P.N. Dyer, *Chem. Eng. Prog.* 51 (1982) 51.
- [2] W.D. Deckwer, Y. Serpemen, M. Ralek, B. Schmidt, *Ind. Eng. Chem. Process Des. Dev.* 21 (1982) 222.
- [3] G.A. Huff, C.N. Satterfield, M.H. Wolf, *Ind. Eng. Chem. Fundam.* 22 (1983) 258.
- [4] J.L. Feimer, P.L. Silveston, R.R. Hudgins, *Ind. Eng. Chem. Prod. Res. Dev.* 20 (1981) 609.
- [5] H.E. Atwood, C.O. Bennet, *Ind. Eng. Chem. Process Des. Dev.* 18 (1979) 163.
- [6] R.C. Everson, E.T. Woodburn, R.M. Kirk, *J. Catal.* 53 (1978) 186.
- [7] H.H. Nils, P.A. Jacobs, *J. Chromatogr. Sci.* 19 (1981) 40.
- [8] H. Schultz, B. Gregor, R. Lochmiller, *San Min, S. Erdöl Kohle, DGMK Compendium* 78/79, 1978.
- [9] R.A. Dictor, A.T. Bell, *Ind. Eng. Chem. Fundam.* 23 (1984) 252.
- [10] R. van der Westhuizen, S. Mahabir, R. Bekker, R. Griffiths, The use of comprehensive multidimensional GC (GCxGC) for the analysis of Fischer–Tropsch products. Paper presented at Analitika 2006 Conference, Kwa Maritane Bush Lodge, Pilanesberg Nature Reserve, South Africa, September 10–13, 2006.
- [11] R. Bekker, M.J. Janse van Vuuren, T. Grobler, The on–line analysis of Fischer–Tropsch product streams. Paper presented at 30<sup>th</sup> International Symposium on Capillary Chromatography and 4<sup>th</sup> GCxGC symposium, Dalain, China, June 4–7, 2007.
- [12] T. Grobler, M. Claeys, E. van Steen, M.J. Janse van Vuuren, *Catalysis Commun.* 10 (2009) 1674.
- [13] P.E. Anderson, M. Demirbüker, L.G. Blomberg, *J. Chromatogr.* 595 (1992) 301.
- [14] J.M. Levy, *J. High Resolut. Chromatogr.* 17 (1994) 212.
- [15] A. Venter, E.R. Rohwer, A.E. Laubscher, *J. Chromatogr. A* 847 (1999) 309.
- [16] F. Adam, D. Thiebaut, M. Courtiade, M–C. Hennion, *J. Chromatogr. A* 1217 (2010) 1386.
- [17] E.J. Guthrie, H.E. Schwartz, *J. Chromatogr. Sci.* 22 (1986) 236.
- [18] H. Potgieter, R. van der Westhuizen, N. Malan, unpublished results, October 2010.
- [19] M. Dorbon, C. Bernasconi, *Fuel* 68 (1989) 1067.

- [20] J. Mao, C.R. Pacheco, D.D. Traficante, W. Rosen, *Fuel*, 74 (1995) 880.
- [21] J. Blomberg, Triemersma, M. van Zuijlen, H. Chaabani, *J. Chromatogr. A* 1050 (2004) 77.
- [22] C. Vendeuvre, R. Ruiz–Guerrero F. Bertoncini, L. Duval, D. Thiébaud, M–C. Hennon, *J. Chromatogr. A* 1086 (2005) 21.
- [23] R. Hau, Y. Li, W. Liu, J. Zheng, H. Wei, J. Wang, X. Lu, G. Xu, *J. Chromatogr. A* 1019 (2003) 101.
- [24] F. Adam, F. Bertoncini, N. Brodusch, E. Durand, D. Thiébaud, D. Espinat, M–C. Hennon, *J. Chromatogr. A* 1148 (2007) 55.
- [25] D. Dutriez, J. Borrás, M. Courtiade, D. Thiébaud, H. Dulot, F. Bertoncini, M–C. Hennon, *J. Chromatogr. A* 1218 (2001) 3190.

# **Chapter 7**

# **Conclusions**

## Chapter 7: Conclusions

The primary goal of the study was to evaluate the use of GCxGC for the analysis of FT products. It was found that GCxGC is an essential analytical tool for the analysis of the highly complex FT products, especially HT–FT products that may contain tens–of–thousands of compounds. The exceptionally high peak capacity of GCxGC enables the separation of these highly complex products, while the highly structured chromatograms separate compounds according to chemical classes, which greatly assists in peak identification. An added advantage is the high sensitivity that results from the very narrow second-dimension peaks, which again enabled the analysis of trace level compounds in the complex sample matrix.

TOF–MS was found to be essential for the identification of the very narrow peaks generated by GCxGC and also assisted in deconvolution of closely eluting peaks. Extracted ion chromatography proved to be of exceptional value in displaying peaks of specific masses and mass fragments, e.g. for the dehydration of oxygenates to alkenes, where the completeness of the dehydration reaction could clearly be deduced from the contour plots. The availability of GCxGC–FID, on the other hand, was very convenient for quantification purposes. Similar separation patterns were observed for GCxGC–TOF–MS and GCxGC–FID. The identification of one sample by TOF–MS can be used to set up templates for quick identification of peaks in similar samples by FID. The data files generated with GCxGC–FID are much smaller than GCxGC–TOF–MS files and data interpretation could therefore be completed in seconds. The FID has a universal response for hydrocarbons which further aided in accurate quantification.

A comparison was made between GCxGC with 1D–GC. It was found that even the best 1D–GC columns, providing peak capacities of five to six hundred, were completely inadequate for separation of the highly complex FT mixtures. Even for less complex products such as LT–FT condensates a degree of peak co–elution was observed, although the number of peaks in the sample was less than the peak capacity of the column used.

GCxGC enabled the investigation of trends in FT product formation with increasing reaction temperature.

## Chapter 7: Conclusions

---

This was especially valuable to investigate secondary product formation, e.g. trends in the formation of aromatic precursors and sub-classes, with increasing reaction temperatures. Two maxima in the total aromatic distribution were detected for the first time as a result of sub-group distributions formed within the mononuclear aromatic class. This would have been impossible to detect without the high peak capacity of GCxGC. The trends in oxygenate formation with increasing temperature could also be studied accurately for the first time.

It was further shown that  $\alpha$  values traditionally used for HT-FT selectivity models and based on 1D-GC data are incorrect. Deviations from linearity of ASF plots, previously reported by various authors, can at least in part be attributed to analytical error caused by the high degree of peak co-elution in the 1D-GC methods that were used in the past. The information obtained from GCxGC analyses allows the optimisation of plant conditions to produce more high-value fuels and chemicals.

GCxGC is also very valuable in FT refining, and a number of applications were discussed. The separation of the  $C_4$ - $C_8$  alkenic compound classes of mono-alkenes, cyclic alkenes, dienes and cyclic dienes could be distinguished for the Superflex<sup>TM</sup> catalytic cracker (SCC) feed and products during the selective hydrogenation of dienes to mono-alkenes. This information is very valuable to optimise the process. The degree of hydrogenation is visible at a glance of the extracted ion contour plots.

For some applications such as the oligomerisation of light alkenes ( $C_3$ - $C_4$ ), the product is of such complexity that even GCxGC does not provide sufficient resolving power to separate all of the highly branched isomers in the product. By off-line hyphenation of HPLC and GCxGC, the separation of residual alkenes and cyclic alkanes in the hydrogenated fuel products could be obtained. These compound classes have similar mass spectra and elute in adjacent regions on the contour plot, and overlap to a degree. By using HPLC-GCxGC, the presence of compounds with cyclic structures in the oligomerisation product could be confirmed.

## Chapter 7: Conclusions

---

It was also shown that the double bonds of the alkenes are predominantly internal double bonds, and that the highest distribution of cyclic compounds was in the kerosene and diesel fractions.

Experiments on the oligomerisation of pure 1-hexene at two temperatures (100 °C and 250 °C) showed that cyclics and aromatics were formed in increasing quantities at higher reaction temperatures. However, the complexity of these products was such that compound classes could not be distinguished by the GCxGC group-type separations only, and some method to simplify the analysis was therefore required. Hydrogenation of the alkenic product was done in the inlet liner of the GCxGC and, by comparing the product before and after hydrogenation; it was possible to distinguish between cyclic and non-cyclic alkenes. This technique is especially valuable when only small quantities of sample are available.

For most of the applications in this study a polar x non-polar column combination was used. This column configuration provides the largest separation space on the GCxGC separation plane for aliphatic hydrocarbons and, because FT products typically contain more than 75% aliphatic hydrocarbons, this configuration is the obvious choice. For PAHs and aromatics in general, a larger separation space is available when using a non-polar x polar-column combination. In this study, GCxGC with such a column combination was used to investigate the effect of the addition of a tar fraction (120–360 °C distillation cut) on the PAH content of a FT-derived diesel fuel. It was found that the tar fraction addition did not increase the PAH content of the fuel significantly, but the density of the fuel was improved. This is valuable information because FT fuels typically have lower density than diesel fuel specifications because of their high aliphatic content. Tar is readily available but contains significant amounts of PAHs. By careful selection of the tar fraction, the density of a fuel can be increased without a significant increase in PAH content.

The physical and chemical properties of a fuel can be directly correlated to its composition. GCxGC is able to provide detailed profiles of components in a fuel, even at trace levels, and is therefore particularly well suited to investigate such correlations.

## Chapter 7: Conclusions

---

Properties such as cold flow, cetane number and distillation range have been linked to fuel composition in this study.

Alkenes, and especially dienes, are linked with gum formation in gasoline. Dienes are highly reactive components that can undergo Diels–Alder and retro-Diels–Alder reactions. These products are thought to be partially responsible for gum formation in SCC-derived fuels. GCxGC was used to demonstrate an increase in the formation of Diels–Alder polymerisation products in gasoline during ageing studies. GCxGC was able to separate the compound classes of cyclic alkenes, dienes and cyclic dienes and also the Diels–Alder dimer and trimer polymerisation products, thereby providing valuable information on gum formation in gasoline.

Aircraft refuelling at Johannesburg's O.R. Tambo International Airport have been using semi-synthetic jet fuel (SSJF) for more than a decade already, although the use of fully synthetic jet fuel (FSJF) has only recently been approved. Sasol Synfuels in Secunda produces the first fully synthetic jet fuel worldwide. It has been approved for commercial use as Jet–A1 fuel. This is a great milestone for Sasol. Before approval could be given, the fuel had to be subjected to rigorous testing and GCxGC proved to be highly beneficial during these tests. A quantitative GCxGC–FID method was developed to provide a detailed breakdown of components of the fuel. The method can also be used equally successfully for crude–derived jet fuel analysis, and was applied to compare FSJF to a standard crude–derived fuel. It was shown that the fuels have very similar hydrocarbon compositions, although compounds were present at different ratios. It was found that FSJF did not introduce any molecules into aircraft's fuel systems that might negatively affect the fuel's properties, and it had better storage stability than crude–derived jet because of the absence of nitrogen and sulphur species.

Other exciting projects involving GCxGC are in progress or are being planned at Sasol. To investigate optimal FT plant conditions and to plan for new plants, a GCxGC–system has been connected on–line to laboratory-scale micro-reactors. On-line sampling ensures that representative samples are delivered to the GCxGC and prevents problems such as loss of volatiles, contamination and oxidation.

## Chapter 7: Conclusions

---

Sample lines from the reactor to the GCxGC are steam-heated and isolated with heat-resistant tape and helium is used as diluent to keep the product in the sample lines in the gaseous phase and prevent condensation.

The on-line instrument consists of a GC in which the first channel was converted to GCxGC-FID, while the second channel was used as a GC-FID for the analysis of light gases. A standard mixture was used for on-line quantification. Initial results obtained using this system are promising, although some method development still needs to be done before the system can be operated quantitatively in a routine laboratory environment.

For some applications where even GCxGC does not provide sufficient separation power, fractionation of compound classes prior to GCxGC is of great assistance. SFC is especially well suited for on-line coupling with GCxGC because this technique does not require large volumes of solvents, and the CO<sub>2</sub> used as mobile phase can easily be vaporised in the GC inlet. In this study a three-column configuration was developed for the SFC separation of the alkane, alkene, aromatic and oxygenated compound classes in synthetic crude. The SFC is currently being coupled on-line to GCxGC with the aid of a six-port valve system. The separated compound classes will then be analysed by GCxGC without interference from solvents or other impurities.

The acquisition of selective detectors such as SCD, NCD and PFPD will further enhance the usefulness of GCxGC. This is currently being investigated. GCxGC combined with these detectors will be especially useful for analysis of sulphur and nitrogen species in FT fuels blends, where heteroatoms may be introduced into the fuel by blending with crude-derived fuel components.

In order to introduce GCxGC in routine analytical laboratories, standard test methods need to be developed and validated for numerous applications. Conventional 1D-GC methods need to be scrutinised for possible inaccuracies that result from peak co-elution and lack of sensitivity, and then these methods need to be replaced with more efficient GCxGC methods.

## Chapter 7: Conclusions

---

The use of chemometrics, to assist with the handling of the huge amount of data generated with GCxGC, also has to be investigated.

The potential of GCxGC for the analysis of FT products has been highlighted in this study. However, only a few selected applications have been discussed.

Endless further opportunities still need to be explored where the benefits of GCxGC can be exploited to improve existing analytical methods.

In conclusion, GCxGC is nowadays an essential analytical tool that should replace conventional 1D–GC for analysis of highly complex petrochemical products.